I, Elizabeth Erasmus, declare that the dissertation hereby submitted by me for the Magister Scientiae degree at the University of the Free State is my own independent work and has not previously been submitted by me at another university/facility. I therefore cede copyright of the dissertation in favour of the University of the Free State.

Signed …….. Date ……...

Synthesis, substitution kinetics and electrochemistry of betadiketonato titanium and titanocene complexes with biomedical applications

A dissertation submitted in accordance with the requirements of the degree

Magister Scientiae

in the

Department of Chemistry

Faculty of Science

at the

University of the Free State

by

Elizabeth Erasmus

Supervisor

Dr. J Conradie

Co-supervisor

Prof. J.C. Swarts

November 2003

Dankbetuigings

Aan God Almagtig, dankie vir die groot genade en voorreg om 'n baie klein deeltjie van U skepping te kon bestudeer. Verder dank ek U ook vir U krag en wysheid wat my deur hierdie studie gedra het. Aan U alleen kom al die eer toe!

Ek wil graag my promotor, Dr. J. Conradie, bedank vir haar uitstekende leiding, ondersteuning en al haar kosbare tyd wat sy afgestaan het gedurende die verloop van die studie. Aan my mede-promotor, Prof. J.C. Swarts, dankie vir al die waardevolle insette en bereidwilligheid om altyd te help. Die entoesiasme van beide word opreg waardeer.

Die skrywer bedank Prof. C.E.J. Medlen van die Departement Farmakologie, Universiteit van Pretoria, vir die uitvoer van die sitotoksiese toetse en die opstel van die oorlewingsgrafieke.

My dank gaan ook aan al my vriende, die studente en personeel van die Chemie Departement vir al hulle bystand, belangstelling en hulp hoe gering dit ook al was.

Aan my familie, in besonder my ouers, dankie vir al die liefde, gebede en ondersteuning. Sonder julle was dit nie moontlik nie.

Die skrywer erken die NRF vir finasiële bystand.

Elizabeth (Lizette) Erasmus

2003

Contents

List of Abbreviations

A	absorbance
Å	angstrom
$acac^-$	2,4-pentanedionato, acetylacetonato
$biphen^{2-}$	2,2-biphenyldiolato
bipy	2,2-bipyridine
$bzac^-$	1-phenyl-1,3-butanedionato, benzoylacetonato
cat^{2-}	1,2-benzenediolato (catecholato)
CH_3CN	acetonitrile
CH_3OH	methanol
cisplatin	*cis*-diamminedichlororplatinum(II)
CO	carbon monoxide or carbonyl
CoLo	human colorectral cell line
Cp	cyclopentadienyl $(C_5H_5)^-$
CV	cyclic voltammetry
δ	chemical shift
Hdbm	dibenzoylmethane
DCM	dichloromethane
DMSO	dimethyl sulfoxide
D_O	diffusion coefficient of the oxidized specie
D_R	diffusion coefficient of the reduced specie
ε	molecular extinction coefficient
E	applied potential
E^{01}	formal reduction potential
E_a	energy of activation
E_{pa}	peak anodic potential
E_{pc}	peak cathodic potential
ΔE_p	separation of peak anodic and peak cathodic potentials
Et	ethyl
F	Faraday constant (96485.3 C mol^{-1})
Fc	ferrocene or ferrocenyl (Note: strictly ferrocene should be Hfc and fc ferrocenyl, but it is customary in electrochemistry to abbreviate the ferrocene/ferrocenium couple as Fc/Fc^+. In this document this notation will be accepted as the current form.)

LIST OF ABBREVIATIONS

fca^-	1-ferrocenoyl-1,3-butanedionato, ferrocenoylacetonato
ΔG^*	free energy of activation
h	Planck's constant (6.626×10^{-34} J s)
ΔH^*	enthalpy of activation
Hacac	2,4-pentanedinel, acetylacetone
H_2biphen	2,2-biphenyldiol
Hbzac	1-phenyl-1,3-butanedione, benzoylacetone
H_2cat	1,2-benzenediol (catechol)
Hc	hafnocenyl, biscyclopentadienylhafnium(IV), $(C_5H_5)_2Hf^{2+}$
$HcCl_2$	hafnocene dichloride, dichlorobiscyclopentadienylhafnium(IV)
HeLa	human cervix epitheloid cancer cell line
$hfaa^-$	1,1,1,5,5,5-hexafluoro-2,4-pentanedionato, hexafluoroacetylacetonato
Hfca	1-ferrocenoyl-1,3-butanedione, ferrocenoylacetone
Hmaa	1-methoxy-1,3-butanedione, methyl acetoacetone
HSacac	4-thioxopenatan-2-one, thioacetylacetone
Htfaa	1,1,1-trifluoro-2,4-pentanedione, trifluoroacetylacetone
Htfba	1-phenyl-3-trifluorobutanedione, trifluorobenzoylacetone
IC_{50}	mean drug concentration causing 50% cell death
i_{pa}	peak anodic current
i_{pc}	peak cathodic current
k_2	second-order rate constant
k_b	Boltzmann constant (1.381×10^{-23} J K^{-1})
k_{obs}	observed rate constant
k_s	rate constant of solvation
L	ligand
LDA	lithium diisopropylamide
λ_{exp}	wavelength at maximum absorbance
M	central metal atom
maa^-	1-methoxy-1,3-butanediolato, methyl acetoacetonato
Mc	metallocenyl, $(C_5H_5)_2M^{2+}$
$McCl_2$	metallocene dichloride
Me	methyl
n	number of electrons
NHE	normal hydrogen electrode
^{1}H NMR	nuclear magnetic resonance spectroscopy

LIST OF ABBREVIATIONS

o	ortho
Ph	phenyl (C_6H_5)
phen	1,10-phenanthroline
pK_a	-log K_a, K_a = acid dissociation constant
ppm	parts per million
Pr^i	isopropyl
R	gas constant (8.134 J K^{-1} mol^{-1})
S	solvent
ΔS^*	entropy of activation
$Sacac^-$	4-thio-2-pentanto, thioacetylacetonato
$Scat^{2-}$	1,2-benzenedithiolato (dithiocatchole)
SCE	standard calomel electrode
SHE	standard hydrogen electrode
T	temperature
$TBAFP_6$	tetrabuthylammonium hexafluorophosphate
Tc	titanocenyl, biscyclopentadienyltitanium(IV), $(C_5H_5)_2Ti^{2+}$
$TcCl_2$	titanocene dichloride, dichlorobiscyclopentadienyltitanium(IV)
$tfaa^-$	1,1,1-trifluoro-2,4-pentanediolato, trifluoroacetylacetonato
$tfba^-$	1-phenyl-3,3,3-trifluorobutanediolato, trifluorobenzoylacetonato
THF	tetrahydrofuran
UV/Vis	ultraviolet/visible spectroscopy
ΔV^*	volume of activation
Vc	vanadocenyl, biscyclopentadienylvanadium(IV), $(C_5H_5)_2V^{2+}$
$VcCl_2$	vanadocene dichloride, dichlorobiscyclopentadienylvanadium(IV)
ν(C=O)	infrared carbonyl stretching frequency
X	halogen
χ_R	group electronegativity (Gordy scale) of R group
Zc	zirconocenyl, biscyclopentadienylzirconium(IV), $(C_5H_5)_2Zr^{2+}$
$ZcCl_2$	zirconocene dichloride, dichlorobiscyclopentadienylzirconium(IV)

List of Structures

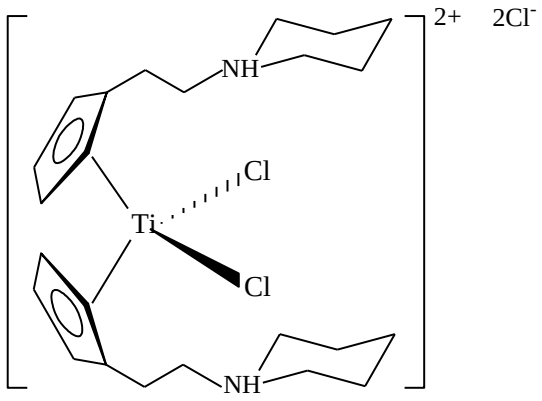

[1]

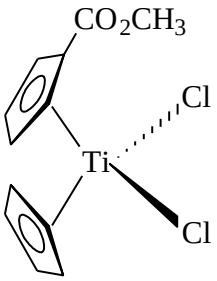

[2]

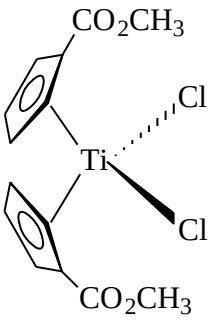

[3]

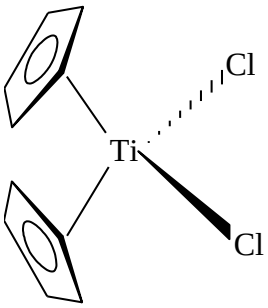

[4]

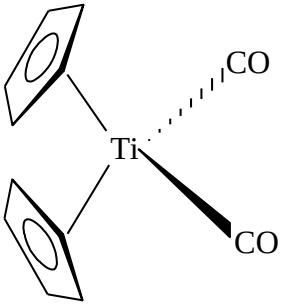

[5]

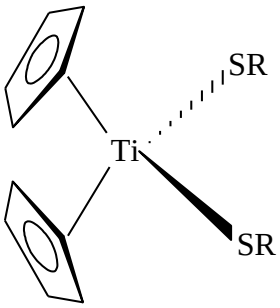

[6]

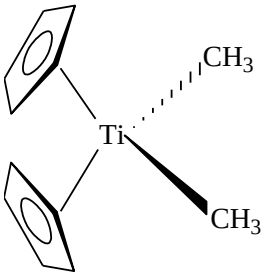

[7]

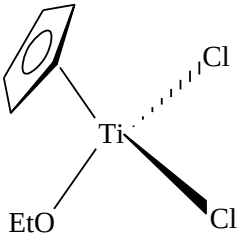

[8]

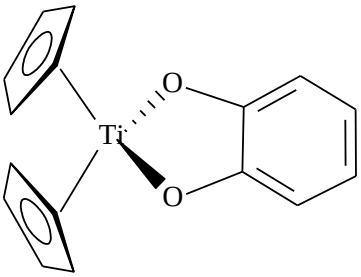

[9]

LIST OF STRUCTURES

LIST OF STRUCTURES

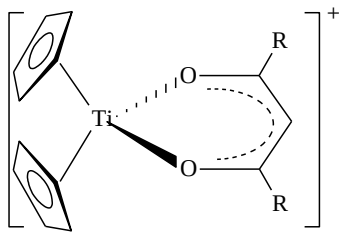

[10]

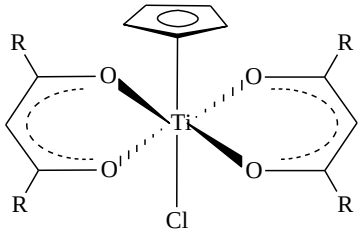

[11]

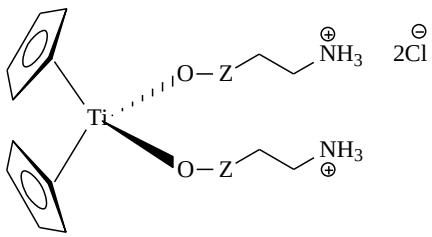

[12]

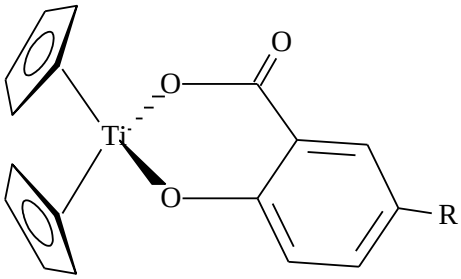

[13]

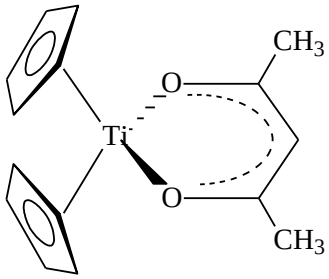

[14]

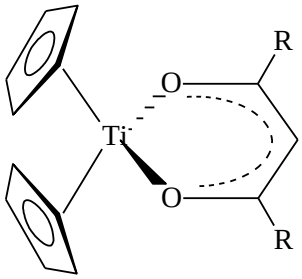

[15]

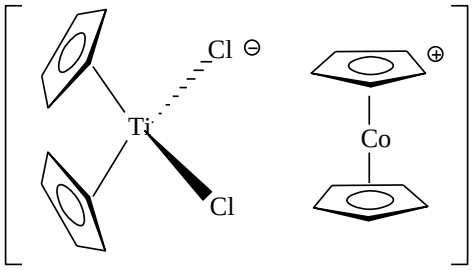

[16]

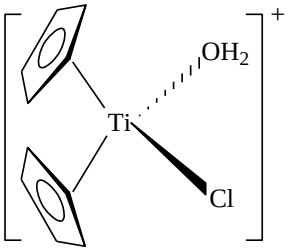

[17]

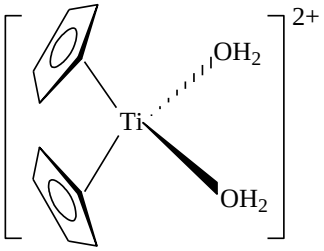

[18]

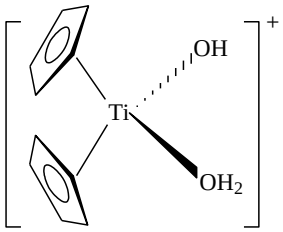

[19]

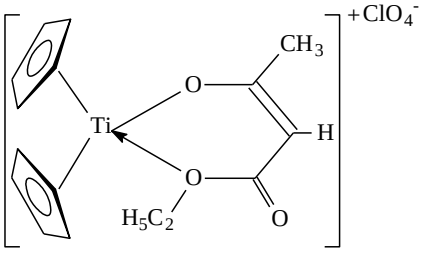

[20]

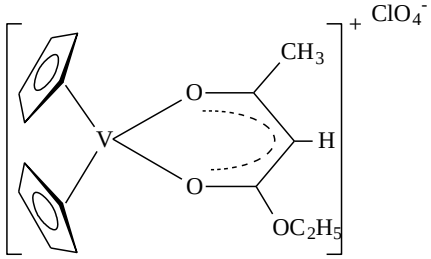

[21]

LIST OF STRUCTURES

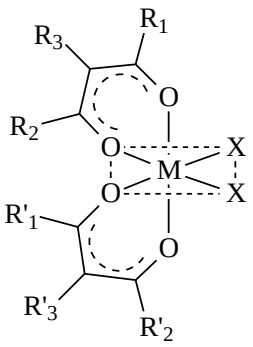

[22]

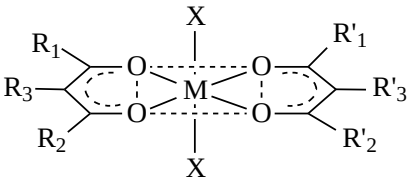

[23]

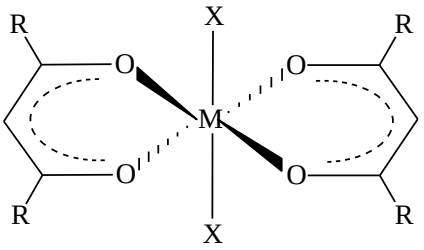

[24]

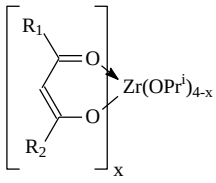

[25]

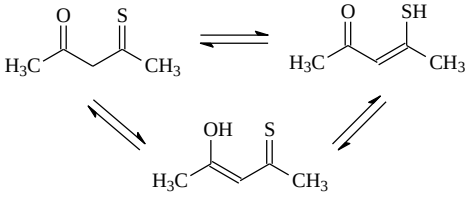

[26]

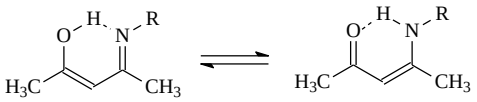

[27]

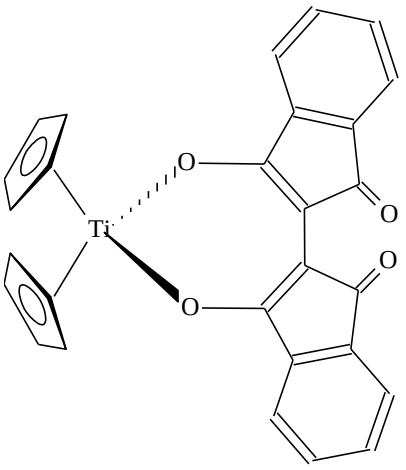

[28]

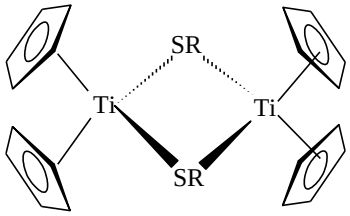

[29]

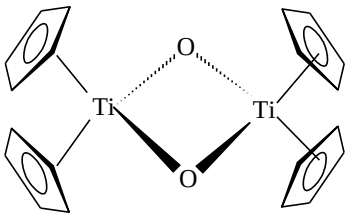

[30]

LIST OF STRUCTURES

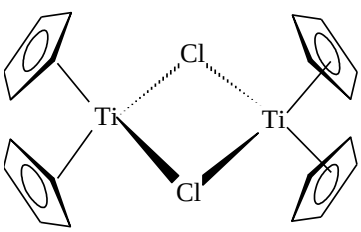

[31]

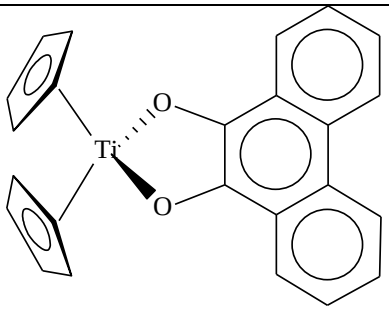

[32]

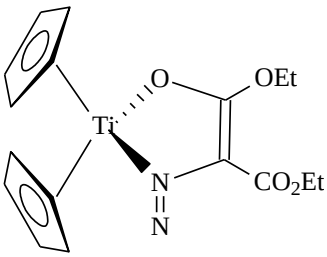

[33]

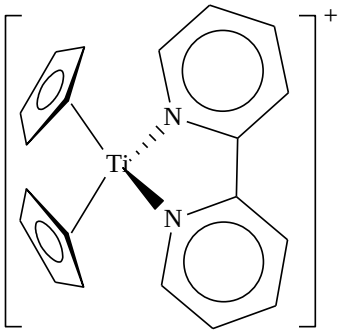

[34]

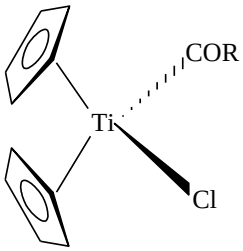

[35]

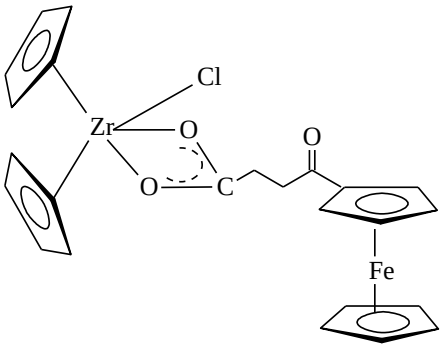

[36]

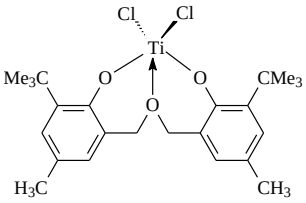

[37]

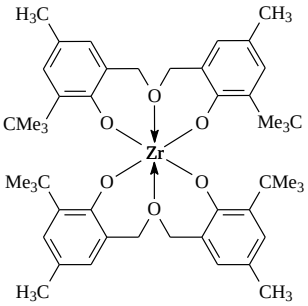

[38]

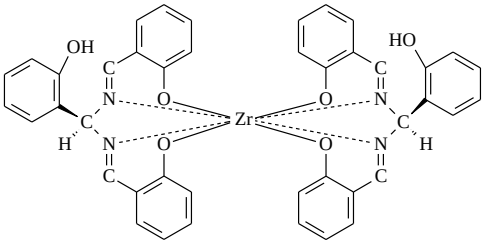

[39]

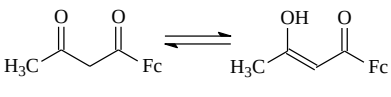

[40]

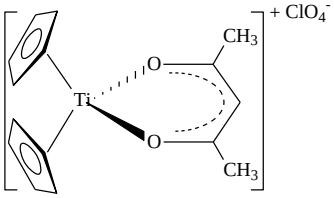

[41]

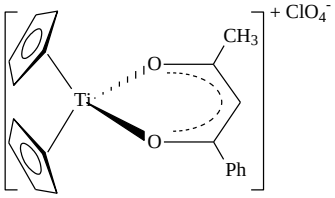

[42]

LIST OF STRUCTURES

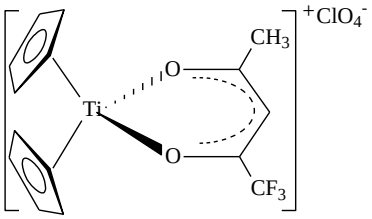

[43]

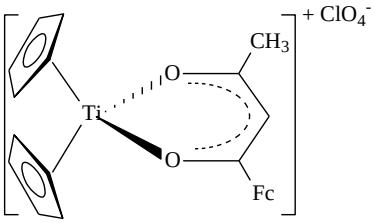

[44]

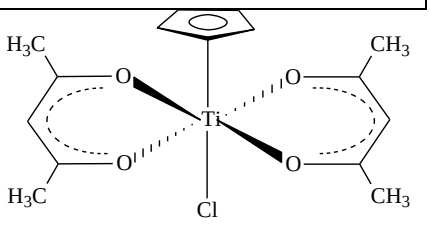

[45]

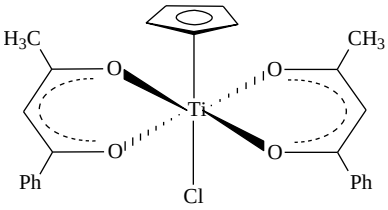

[46]

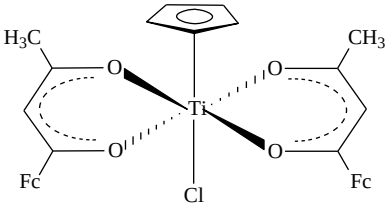

[47]

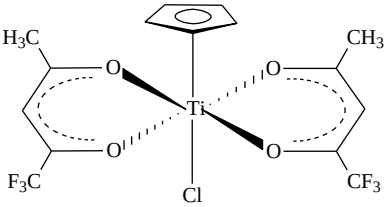

[48]

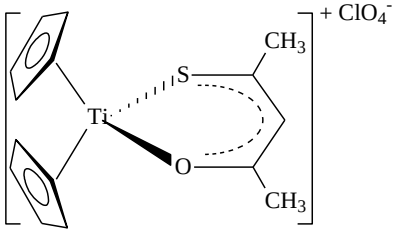

[49]

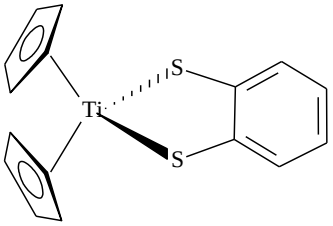

[50]

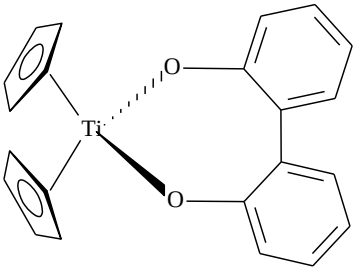

[51]

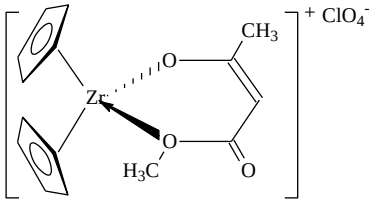

[52]

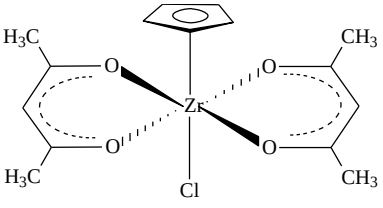

[53]

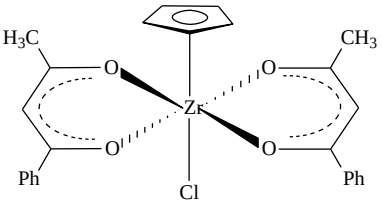

[54]

LIST OF STRUCTURES

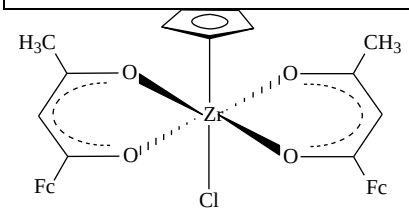

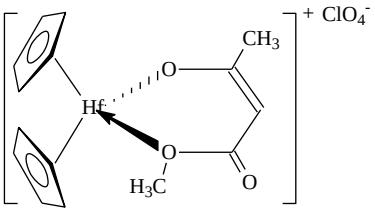

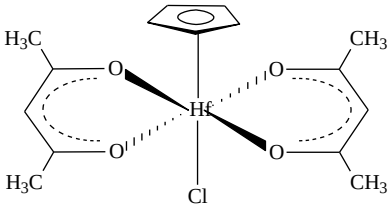

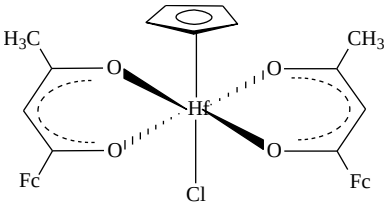

[58]

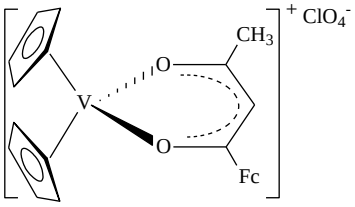

[59]

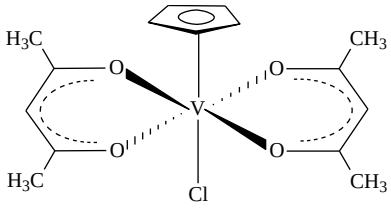

[60]

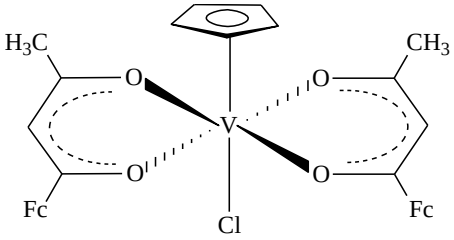

[61]

Chapter 1

Introduction and aim of study

1.1. Introduction

There is currently many different areas of study involving the chemistry of metallocenes, such as organic synthesis,[1] as catalysts or catalytic components in a variety of reactions,[2] as flame-retardants,[3] or smoke suppressants and in medical applications.[4, 5, 6, 7, 8]

Biscyclopentadienyl metal dihalides (metallocene dihalides) are ideal starting materials for ligand exchange and redox reactions.[9] Titanocene dichloride is a convenient starting material for preparation of many other organometallic compounds of titanium,[10] and has found application as a catalyst or catalyst component for a wide variety of hydrometalation and carbometalation reactions as well as other transformations involving Grignard reagents.[11] In organic synthesis a titanocene derivative, "Tebbe's reagent" has proven to be useful, particularly as an alternative to classical Wittig reagents.[12] In the field of Ziegler-Natta catalysis, metallocenes have proved to be a useful polymerisation catalyst system for various alkenes (ethylene, butadiene-styrene),[13] and random and super-random copolymerisation of olefins (elastomer manufacturing).[14] The mixed biscyclopentadienyl metal chloride hydride $[(C_5H_5)_2ZrCl(H)]$, known as the 'Schwartz's reagent', is used in organic synthesis to form substituted alkanes from alkenes.[15]

In the medical field, the metallocene ferrocene for example, acts as a mediator in the biosensoring of glucose.[16] When *cis*-diamminedichloroplatinum(II) was introduced as a chemotherapeutic drug in 1979, it led the way for the development of new and improved metal-containing chemotherapeutic agents.[17] One of these new antineoplastic drugs is titanocene dichloride. It shows impressive cancerostatic activity,[18] and is currently in phase II clinical trial.[19] Many derivatives of titanocene were also found to have antitumor properties.[19] In 1984 Köpf-Maier reported on the antineoplastic activity of another metallocene, ferrocenium salts, against Ehrlich Ascites tumour cell lines. These cell lines are resistant to classical anti-tumour agents.[20, 21, 22, 23] Compounds that are constructed from more than one antineoplastic moiety, such as a titanocenyl and a ferrocenyl fragment, within the same molecule, hold the promise of displaying synergistic effects in chemotherapy without the need for administering two or more types of antineoplastic drugs simultaneously.[24, 25, 26, 27]

1.2. Aims of the study

With this background the following goals were set for this study:

(i) The synthesis and characterisation of new complexes containing a titanocenyl or related titanium(IV) centre coordinated to a β-diketonato or related bi-chelating ligand. These complexes will have the general formula $[(C_5H_5)_2Ti(CH_3COCHCOR)]^+$ or $[(C_5H_5)Ti(Cl)(CH_3COCHCOR)_2]$.

(ii) An electrochemical study utilising cyclic voltammetry and bulk electrolysis on all the synthesised complexes to determine the electrochemical reversibility and the formal reduction potentials of the redox active centre(s) of the complexes synthesized.

(iii) A kinetic study of the substitution of the β-diketonato or bi-chelating ligand from selected synthesised titanium complexes with acetylacetone, thioacetylacetone and 2,2-biphenyldiol.

(iv) Quantification of the relationships from (ii) between many physical properties of the new complexes of this study. This will include quantities such as second order substitution rate constants from (iii), formal reduction potentials from (ii), group electronegativity of each R group in compounds of (i), IR stretching frequency and ^1H NMR shift positions of characteristic peaks of compounds of (i).

(v) A cytotoxic study to determine if some of the new titanium complexes exhibit antineoplastic activity against human colorectral cell line (CoLo) and human cervix epitheloid cancer cell line (HeLa) cells.

---

[1] G. Wilkinson, Editor, *Comprehensive Organometallic Chemistry*, vol. 3, Pergamon Press, Oxford, 1982, p. 273-278 and references therein.

[2] G. Wilkinson, Editor, *Comprehensive Organometallic Chemistry*, vol. 3, Pergamon Press, Oxford, 1982, p. 475-545 and references therein.

[3] E.W. Neuse, J.R. Woodhouse, G. Montaudo and S. Puglisi, *Appl. Organomet. Chem.*, 1988, **2**, 53.

[4] E.W. Neuse and F. Kanzawa, *Appl. Organomet. Chem.*, 1990, **4**, 19.

[5] P. Köpf-Maier, M. Leitner and H. Köpf, *J. Inorg. Nucl. Chem.*, 1980, **42**, 1789.

[6] P. Köpf-Maier, M. Leitner, R. Voigtlander and H. Köpf, *Z. Naturforsch.*, 1979, **34C**, 1174.

[7] P. Köpf-Maier, S. Grabowski, J. Liegener and H. Köpf, *Inorg. Chim. Acta*, 1985, **108**, 99.

[8] E. Meléndez, *Crit. Rev. Oncol.*, 2002, **42**, 309.

[9] N.J. Long, *Metallocenes: An introduction to sandwich complexes*, Blackwell Science, London, 1998, p. 148-154.

[10] G. Wilkinson, Editor, *Comprehensive Organometallic Chemistry*, vol. 3, Pergamon Press, Oxford, 1992, p. 331-426 and references therein.

[11] N.J. Long, *Metallocenes: An introduction to sandwich complexes*, Blackwell Science, London, 1998, p. 23.

[12] F.N. Tebbe, G.W. Parshall and G.S. Reddy, *J. Am. Chem. Soc.*,1978, **100**, 3611.

[13] V.A.E. Barrios, A. Petit, F. Pla and R.H. Najera, *Eur. Polym. J.*, 2003, **39**, 1151.

[14] S. Gambarotta, *Coord. Chem. Rev.*, 2003, **237**, 229.

[15] J. Schwartz and J.A. Labinger, *Angew. Chem.*, 1976, **88**, 402.

[16] N.J. Long, *Metallocenes: An introduction to sandwich complexes*, Blackwell Science, London, 1998, p. 258.

[17] J.A. Gotlieb and B. Drewinko, *Cancer Chemother. Rep. Part I*, 1973, **59**, 621.

[18] H. Köpf and P. Köpf-Maier, *Angew. Chem.*, 1979, **18**, 477.

[19] J.R. Boyles, M.C. Baird, B.G. Campling and N. Jain, *J. Inorg. Biochem.*, 2001, **84**, 159.

[20] P. Köpf-Maier, H. Köpf and E.W. Neuse, *Cancer Res. Clin. Oncol.*, 1984, **108**, 336.

[21] P. Köpf, *Naturforsch. C. Biochem. Biophys. Biol. Virol.*, 1985, **40C**, 843.

[22] D. Osella, M. Ferrali, P. Zanello, F. Laschi, M. Fontani, C. Nervi and G. Caviviolio, *Inorg. Chim. Acta*, 2000, **306**, 42.

[23] P. Yang and M. Guo, *Coord. Chem. Rev.*, 1999, **185**, 189.

[24] M. D'Incalci, T. Colombo, P. Ubezio, I. Nicoletti, R. Giavazzi, E. Erba, L. Ferrarese, D. Mece, R. Riccardi, C. Sessa, E. Cavallini, J. Jimeno and G.T. Faircloth, *Eur. J. Cancer*, 2003, **39**, 1920.

[25] G.R. Gale and L.M. Atkins, *Cancer*, 1978, **41**, 1230.

[26] G.R. Gale and L.M. Atkins, *Cancer Treat. Rep.*, 1977, **61**, 817.

[27] G.R. Gale and L.M. Atkins, *Bioinorg. Chem.*, 1978, **8**, 445.

Chapter 2

Literature Survey

2.1. Metallocenes

2.1.1. Introduction

Many early-transition metal complexes (of the metals indicated in Table 2.1) that possess anti-tumour activity are metallocenes, which have a distorted tetrahedral structure.[1] A few octahedral complexes possesing anti-tumour activity, for example budotitane, are also known.[2]

As far as the tetrahedral metallocene complexes are concerned, metallocene dichlorides possess a unique chemical structure where substituents or replacements at three different positions can be made to tailor diverse physical, chemical and biological properties (Figure 2.1). While still maintaining a tetrahedral structure the central metal atom (position A) can be varied using the metal ions Ti, Zr, Hf, V, Nb, Ta, Mo and W. Various substituents can be introduced into the cyclopentadienyl ring prior to forming the metallocene dihalide (position B) and different ligands can replace the two Cl^- ions coordinated to the central metal atom (position C).

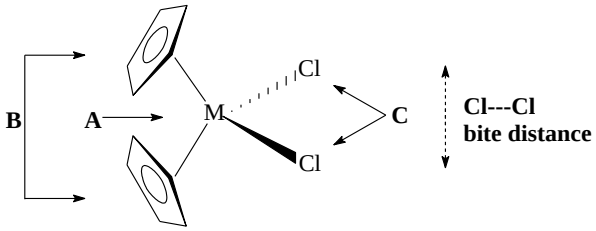

Figure 2.1. Structural flexibility of metallocene dichlorides for chemical design.

Table 2.1. $Cl^{---}Cl$ bite distance for various types of metallocene dichlorides and *cis*-platin.

M	Ti	Zr	Hf	V	Nb	Ta	Mo	W	*cis*-platin
$Cl^{---}Cl$ / Å	3.470[3]	3.660[3]	3.664[4]	3.420[5]	3.569[6]	3.670[7]	3.242[6]	3.198[8]	3.349[9]

2.1.2. Variation of the central metal atom

Variation of the central metal atom leads to variations in the chemical and physical properties of the complexes. The reactivity of the various metallocenes is governed by the central metal atom and attainment of 18 valence electron (VE) coordination spheres. After rehybridisation of the frontier orbitals group 6 Mo and W metallocene dihalides use only two of the available three *d* orbitals to bind the halides, leaving the third *d* orbital as a lone pair pointing between the two substituents. It can also take part in back donation. On the other hand, group 4 Ti, Zr and Hf metallocenes often bind only two monodentate ligands and have only four valence electrons. Their maximum oxidation state is M(IV). This leaves the 16-electron metallocene dihalide with an empty *d* orbital rather than a filled one. The differences in the chemistry of the group 4 and 6 metallocene compounds can therefore be accounted for. The former act as Lewis acids and tend to bind to π-basic ligands such as –OR but the latter act as Lewis bases and bind π-acceptor ligands such as ethylene. π-Bonding can be either stabilising, if the ligand carries low-lying acceptor orbitals, or destabilising, if the ligand is composed of relatively high-lying donor orbitals.

The variation of the metal also leads to a dramatic change in the antineoplastic activity against cancer. Of the eight sited transition metals (Table 2.1), only the first and second rows show good activity (Ti, V, Nb and Mo).[1] Tungsten and tantalum show small chemotherapeutic activity,[10] while zirconium and hafnium shows alomost no tumour inhibiting properties.[11]

When considering the fact that $ZcCl_2$ and $HcCl_2$ does not posses cancerostatic properties and the Cr analogue is not yet known, a diagonal relation (Figure 2.2.) in the periodic table of those central atoms which effect strong cancerostatic properties in their metallocene complexes becomes evident.[10] This may correspond to the similarity of the atomic radii within a diagonal pair of elements, leading to similar Cl---Cl bite distances (Figure 2.1), which has been correlated with antitumor activity.[11]

Also, the electron configuration of the central metal atom may influence toxicity but does not directly govern anticancer activity of the metallocene derivative.[10]

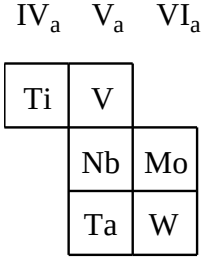

Figure 2.2. Position of early transition metal in the periodic table.

2.1.3. Alterations on the cyclopentadienyl ring

The cyclopentadienyl ring can be modified in a virtually unlimited number of ways in order to influence the electronic properties, steric and coordination environment of the metal by a static intramolecular coordination of the side chain. Seeing as the alteration of the cyclopentadienyl ring is not a major part of this study, only a short discussion will be given on each topic.

2.1.3.1. Cyclopentadienyl ring substitution to improve water solubility

Recent studies done on amino-functionalised metallocenes showed that the neutral amino function can be reversibly coordinated to the metal centre. The quaternisation of the pendant amino group can result in water-soluble species.[12] The reaction of a novel, high yield one-step synthesis of water stable and soluble titanocene dichloride dihydrochloride salts [1] from the direct reaction of neutral amino-substituted cyclopentadienes with $TiCl_4$ is shown in Scheme 2.1.[13]

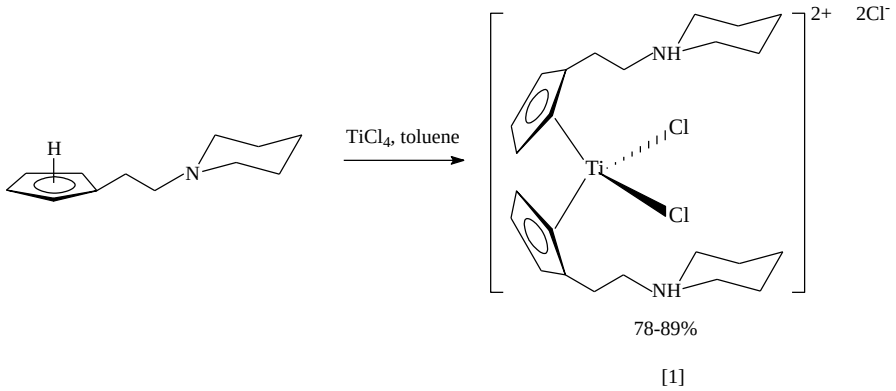

Scheme 2.1. Reagents and conditions for the synthesis of titanocene dichloride dihydrochloride salt [1].

2.1.3.2. Cyclopentadienyl ring substitution to influence biological activity

Many investigations involving ring functionalising by electron donating groups such as methyl, ethyl, trialkylsilyl and trialkylgermyl have resulted in a decrease in antineoplastic activity.[14] However, cyclopentadienyl ring derivatives containing polar, electron-withdrawing groups such as carboxylic acids and esters have shown to be more effective than titanocene dichloride as an antineoplastic agent.[15] The compounds used for these tests were the carbometoxycyclopentadienyl derivatives of titanocene dichloride: the monosubstituted

$(C_5H_5)(C_5H_4CO_2CH_3)TiCl_2$ [2] and the disubstituted $(C_5H_4CO_2CH_3)_2TiCl_2$ [3]. The substitution of the carbomethoxy moiety to the cyclopentadienyl ring is introduced prior to formation of titanocene dichloride.[16, 17] This is achieved *via* a multi-step synthesis according to Scheme 2.2.

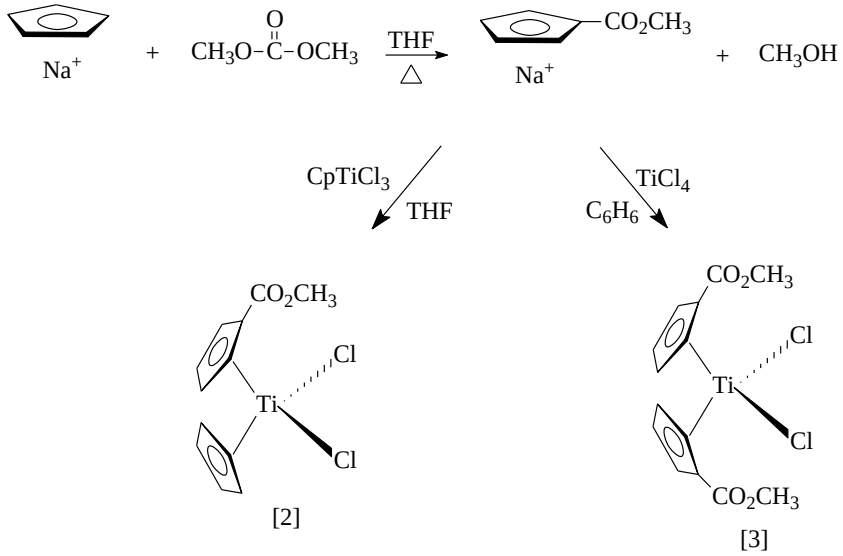

Scheme 2.2. Multi-step synthesis of the monosubstituted (η^5-C_5H_5) (η^5-$C_5H_4CO_2CH_3$)$TiCl_2$ [2] and the disubstituted (η^5-$C_5H_4CO_2CH_3$)$_2TiCl_2$ [3].

2.1.3.3. Bridged cyclopentadienyl rings

Another way in modifying the cyclopentadienyl ring is the introduction of a linking group between the two cyclopentadienyl rings of the metallocene. This linkage is called an interannular bridge. Complexes with interannular bridges were originally called metallocenophanes. This term still applies to group 8 metal dicyclopentadienyl complexes. The bent-metallocene complexes of the early transition metals, lanthanide and main group metals are commonly referred to as *ansa*-metallocenes.[18] The multiple functions that the *ansa*-bridge serve include:[19]

- preventing free rotation, thus fixing the symmetry of the metallocene complexes;
- controlling the stereochemistry of metallocene formation by directing the orientation of the rings upon metalation;
- enforcing a bent-sandwich geometry between the rings thereby influencing the reactivity of the metal;
- increasing the electrophilicity of the metal and increasing the tilt of the rings on the metal causing an increase in the access of substrates to the equatorial wedge of the complex;
- providing an active site at which reversible metal ion binding, reversible bridge formation, ligand substitution and ring opening polymerisation chemistry can occur.

2.1.4. Halide replacement by different ligands

The chloride ligands on the central metal atom of the titanocene dichloride can be exchanged for any other halide or pseudohalide ligand without the loss of any anti-tumour activity.[20] From a medical point of view, this is therefore the preferred site of molecular modification.

Many well-documented reviews on the chemistry of titanocenes are available.[21] Only a few relevant points will therefore, be mentioned.

Reduction of titanocene(IV) dichloride [4] to dicarbonyldi(cyclopentadienyl)titanium(II) [5] can occur *via* several methods including the aid of an activated magnesium amalgam in a carbon monoxide atmosphere.[22] A more recent method of reductive carbonylation, which is currently used in catalytic process, is the exposure of Ti(IV) to CO in an ionic liquid like $AlCl_3$ and 1-ethyl-3-methylimidazolium chloride ($AlCl_3$-EMIC) melt.[23] It should be mentioned that the titanium in [5] is in the II oxidation state and the rest of the complexes discussed are in the IV oxidation state, and that titanium(III) dicarbonyl complexes are known and have a formula of $[Tc(CO)_2]^+$.[23] Further reactions of [5] will be discussed in paragraph 2.2.2.6.

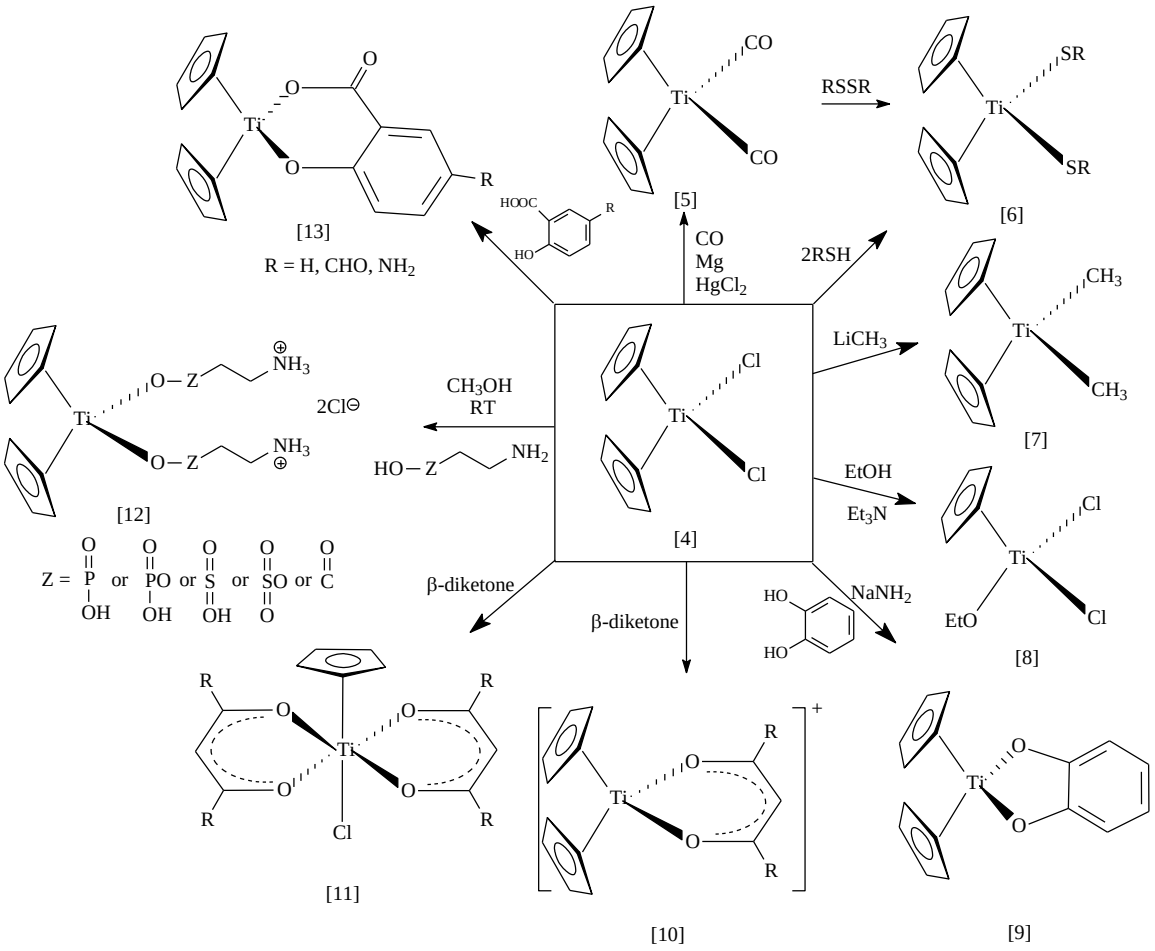

Scheme 2.3. Common reactions of titanocene dichloride.

Compound [6], the dithio titanocene complex, can be obtained by reaction of [4] with 2 RSH ([4] has a marked tendency to react with thiols).[24, 25] The same type of compound [6] can be prepared by oxidative addition of alkyl and aryl disulphides to [5].[26]

Reaction of methyl lithium with [4] yields bis(cyclopentadienyl)dimethyltitanium(IV) [7],[27] which is a very useful precursor to a large variety of different titanium(IV) complexes.

Equimolar amounts of most alcohols react with [4], resulting in the cleavage of the cyclopentadienyl ring in preference over the chloride ligand to yield the monoalkoxide [8].[28] More forcing conditions yield the di- and tetraalkoxides.[28] Dialcohols (such as 1,2-benzenediol) normally react by splitting off one Cp-ring and one Cl^- ion,[29] but under the right conditions, such as in the presence of sodamide, $NaNH_2$, displacement of both Cl^- ions is achieved to yield [9] as the product.[30]

Depending on reaction conditions, two types of titanium(IV) β-diketonates can be formed, [10] and [11]. Titanium(IV) β-diketonates will be discussed in paragraph 2.2.2.

Air-stable titanocene(IV) salt complexes [12] were synthesized by reacting [4] with phosphorous- or sulphur-based β-amino acid complexes in atmospheric conditions.[31] Each complex of [12] contains two identical ligands with a terminal ammonium chloride group and either the phosphorous- or sulphur-based ester groups bonded directly to the titanium centre.

Complex [13] was synthesised to functionalise the titanium complex to have a suitable site (R) to anchor a monomeric or polymeric drug carrier.[32]

2.1.5. Synthesis of metallocene

There are three main routes that are normally employed in the formation of metallocenes.

2.1.5.1. Using a metal salt and cyclopentadienyl reagents

The normal starting point for metallocene synthesis is the ‘cracking’ of dicyclopentadiene. This involves a retro Diels-Alder reaction to produce the monomeric and fairly unstable C_5H_6. Because it is a weak acid (pK_a = 15), it can be deprotonated by alkali metals. Sodium cyclopentadienide (NaCp) is the preferred reagent for metallocene synthesis. In the final step of metallocene synthesis, the Cp from NaCp is reacted with a metal salt or metal halide (Scheme 2.4).

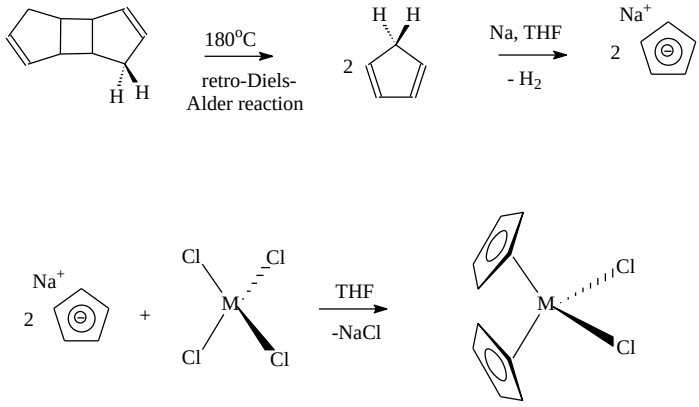

Scheme 2.4. Synthesis of metallocenes using a metal salt and cyclopentadienyl reagents.

2.1.5.2. Using a metal and cyclopentadiene

In this type of metallocene synthesis, the 'co-condensation method' is employed. It is possible to use vapours of transition metals as routine reagents in synthesis and catalysis.[33] The highly reactive metal or molecules are generated at high temperatures in a vacuum and then brought together with the chosen co-reactants on a cold surface. Complexes are then formed on warming the system to room temperature. The use of metal atoms in the vapour phase rather than the solid metal provides synthetic advantages. Scheme 2.5 shows this reaction to form a metallocene.

$$M + 2C_5H_6 \xrightarrow{500^oC} [(C_5H_5)_2M] + H_2$$

Scheme 2.5. Synthesis of metallocenes *via* the co-condensation method, M = Fe, Ru and Os.

2.1.5.3. Using a metal salt and cyclopentadiene

If the salt anion, such as Cl^- in $FeCl_2$, has poor basicity and cannot deprotonate cyclopentadiene, an auxiliary base can be utilised to generate the cyclopentadienyl anions *in situ*, which can sometimes be more convenient (Scheme 2.6).[34] Alternatively, a reducing agent is required.

$$FeCl_2 + 2C_5H_6 + 2C_2H_5NH \longrightarrow [(C_5H_5)_2Fe] + 2[(C_2H_5)_2NH_2]Cl$$

Reaction with reducing agent

$$Ru^{III}Cl_3(H_2O)_x + 3C_5H_6 + 3/2\ Zn \longrightarrow [(C_5H_5)_2Ru^{II}] + C_5H_8 + 3/2\ Zn^{2+}$$

Scheme 2.6. Synthesis of metallocenes using a metal salt and cyclopentadiene.

2.2. Synthesis of various early transition metal complexes (with the focus on Ti, V, Hf and Zr)

2.2.1. Synthesis of β-diketones

As this study is concerned with the synthesis of titanium β-diketonato complexes, a brief discussion of β-diketone synthesis is appropriate.

A general method of synthesis of a wide range of β-diketones, is the Claisen-condensation reactions.[35] In these reactions a ketone, which possesses an α-hydrogen, reacts with a suitable acylation reagent (ester, acid anhydride, acid chloride) in the presence of an appropriate base (Scheme 2.7). The mechanism is as indicated in Scheme 2.8. For this illustration the base lithium diisopropylamide (LDA) and the ester R^2COOEt is used.

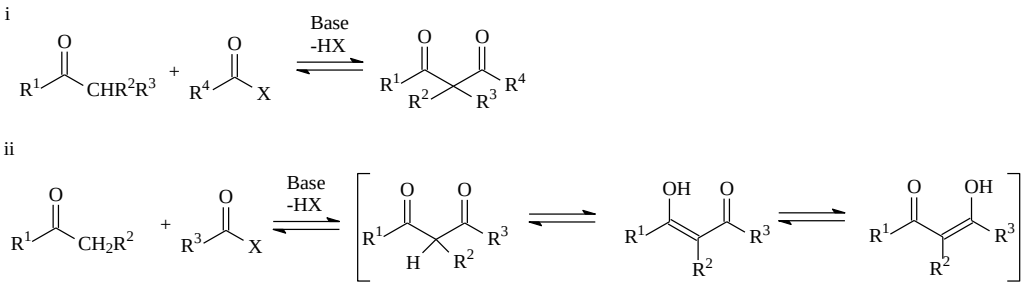

Scheme 2.7. The synthesis of β-diketones.

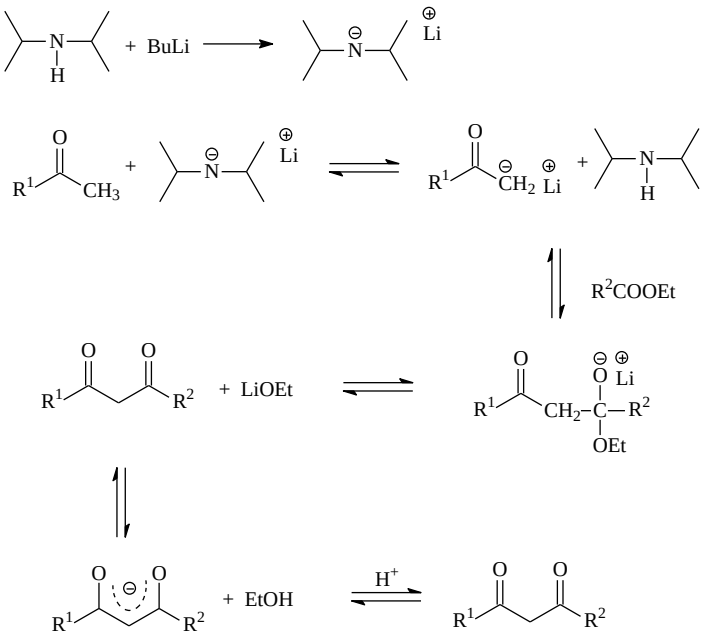

Scheme 2.8. Mechanism for the formation of a β-diketone.

Most β-diketones exist in solution in an equilibrium involving keto- and enol forms provided that there is at least one methine hydrogen present. In the solid state, however, the enol form is often the sole form observed. The methine proton in the keto form and the hydroxyl proton in the enol form of the β-diketones are acidic and their removal generates 1,3-diketonate anions, which are the source of an extremely broad class of coordination compounds.

2.2.2. Synthesis of metal of β-diketonato complexes

Under appropriate conditions the enolic hydrogen atom of a β-diketonato ligand can be replaced by a metal cation to produce a six-membered pseudo-aromatic chelating ring (six-membered metallocyclic ring), see Scheme 2.9.

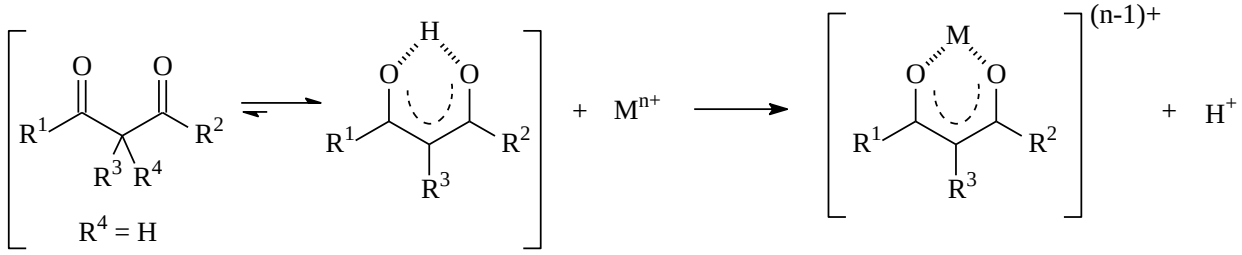

Scheme 2.9. Formation of a six-membered pseudo-aromatic chelating ring of metal β-diketonates.

It should be noted that metal coordination is not possible if both hydrogen atoms of the methine carbon in β-diketones are replaced by an allyl or another group, (R^3 and $R^4 \neq H$), because such β-diketones cannot exist in the enol form. Mono, bis, tris and even tetrakis β-diketonato metal complexes are known.[36]

2.2.2.1. Mono-β-diketonato metal(III) complexes

In mono-β-diketonato metal complexes, the β-diketonato ligands are bidentate with the configuration about the metal (Ti, V, Zr and Hf for this study) approximately tetrahedral.[37] Acetylacetonatobis(cyclopentadienyl)titanium(III) [14] can be obtained *via* a few methods, one of which involves the vigorous stirring of a fourfold excess acetylacetone in a solution of $Cp_2Ti^{III}Cl$ in air-free water (Scheme 2.10).[38] Not all titanium are in the III oxidation state; some of the titanium are oxidized to titanium(IV) that was brought about by the protonation of the titanium(III) species by the hydrochloric acid produced in the initial step.

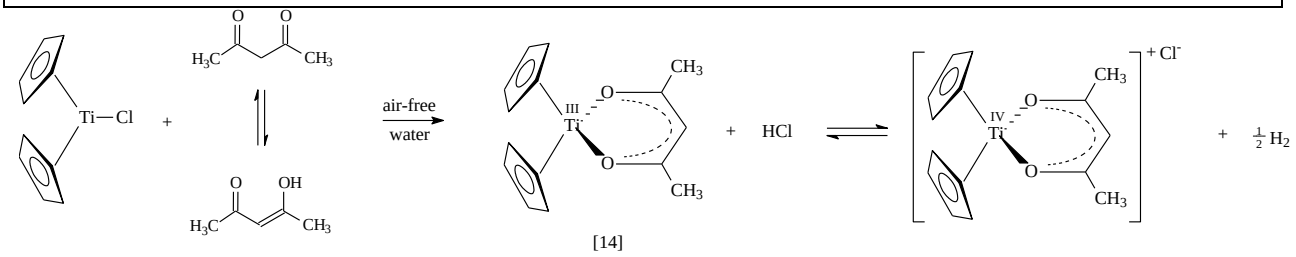

[14]

Scheme 2.10. Synthesis of acetylacetonedi(cyclopentadienyl)titanium(III) [14].

An alternative approach in producing titanium(III) β-diketonato complexes [15], involves the effective replacement of one chloride ligand in $[Ti(C_5H_5)_2Cl_2]$ by the β-diketone leading to the neutral paramagnetic titanocene(II)-β-diketonato complex.[39] A more efficient method of the above mentioned procedure is to start with titanocene dichloride and to reduce it with cobaltocene to form $[Co(C_5H_5)_2][Ti(C_5H_5)_2Cl_2]$ [16], which reacts readily with the β-diketone and triethyl amine (Scheme 2.11).

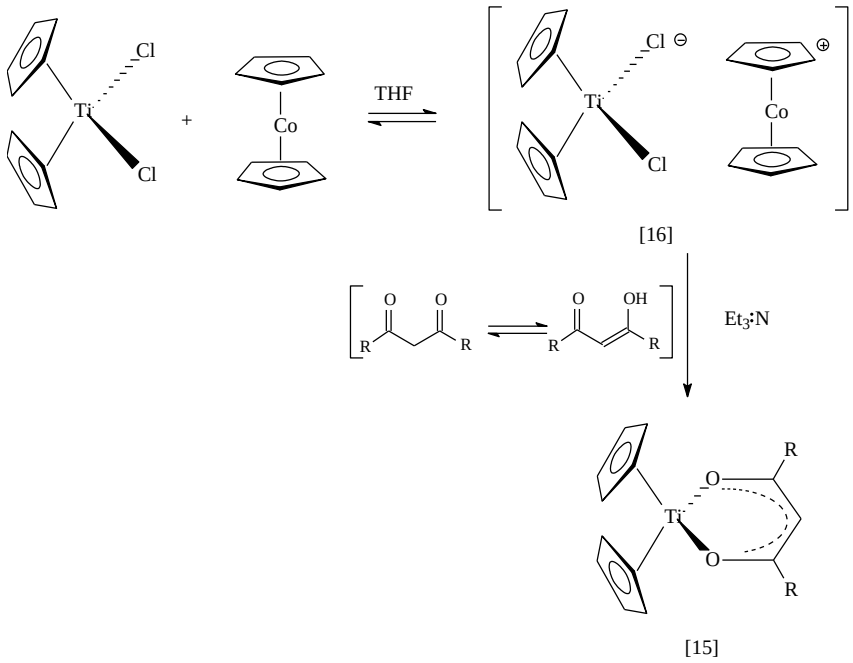

[16]

[15]

Scheme 2.11. Synthesis of titanium(III) β-diketonato complexes [15] by reduction with cobaltocene.

Crystallographic data obtained for the acetylacetonatobis(cyclopentadienyl)titanium(III) [14],[39] shows it has a monoclinic lattice with a $P2_1/c$ space group, since the two cyclopentadienide ligands are asymmetrically bounded. The structure was found to be slightly distorted, but the average Ti-C bond length of 2.37Å as well as the Cp-Ti-Cp angle of 134.4° are similar to values found for other titanocene(III),[40] and titanocene(IV) complexes.[41] The Ti-O bond length (2.07Å) and the O-Ti-O angle (84.3˚) are in agreement with similar complexes.

2.2.2.2. Mono-β-diketonato metal(IV) complexes

The synthesis of titanium(IV) complexes is usually based on an anion metathesis reaction, which is driven by precipitation of one of the products. Doyle and Tobias prepared titanocene(IV)-β-diketonato complexes *via* this procedure.[42] Titanocene dichloride dissolves in water with aquation to give cationic species and some polynuclear complexes also exist (Scheme 2.12). Either one of the cationic species [17], [18] or [19] can react with $AgClO_4$ to form the perchlorate chelate. Addition of the β-diketonate displaces the perchlorate ligand to produce the titanocene(IV)-β-diketonato complexes (Scheme 2.13). It is important to note that even with very high concentrations of the chelating ligand it is impossible to obtain the bis chelate.

Indication that the β-diketonato ligand is chelating comes from both the infrared and NMR spectra, the complexes undoubtedly have a wedge-like sandwich structure with tetrahedral coordination about the titanium centre, which is the same coordination as for the titanocene dichloride.[43] The same synthesis was used to synthesize vanadium(IV)-β-diketonato complexes.[44] It was found that the structural details of the vanadium and titanium β-diketonates are essentially the same. The infrared of the two compounds are almost identical and X-ray studies show that they are isomorphous.[44] The ease of preparation of these mono-β-diketonate complexes results from the very low solvation energy of the complex cation.

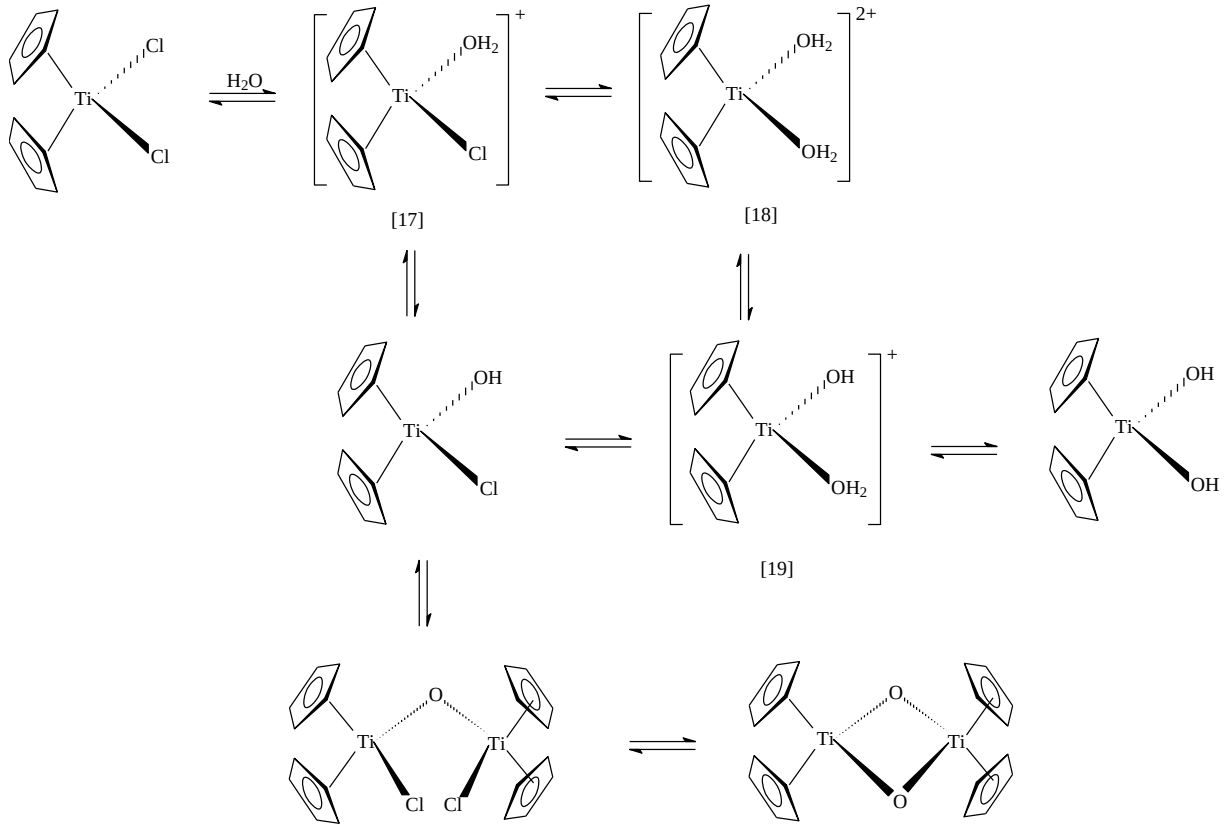

Scheme 2.12. Aqueous chemistry of titanocene dichloride.

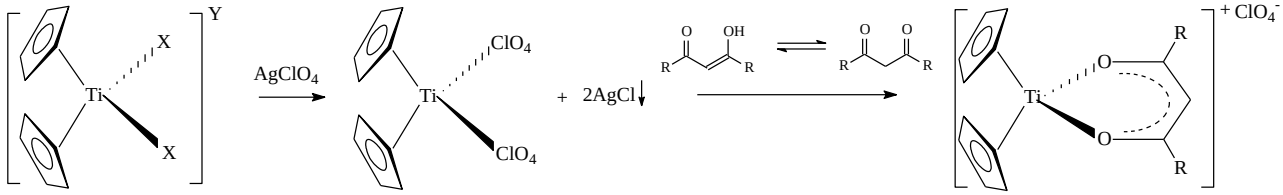

[17], [18] or [19]

[10]

X = Cl, OH or H_2O

Y = + or 2+

Scheme 2.13. Reaction and formation of the titanocene(IV)-β-diketonato complexes.

Metallocene(IV) complexes with various β-diketonates (Figure 2.3),[45] and different counterions like F_3CSO_3, BF_4 and RR'NCS_2 with R = Me, Et and *i*-Pr are known.[42, 46, 47]

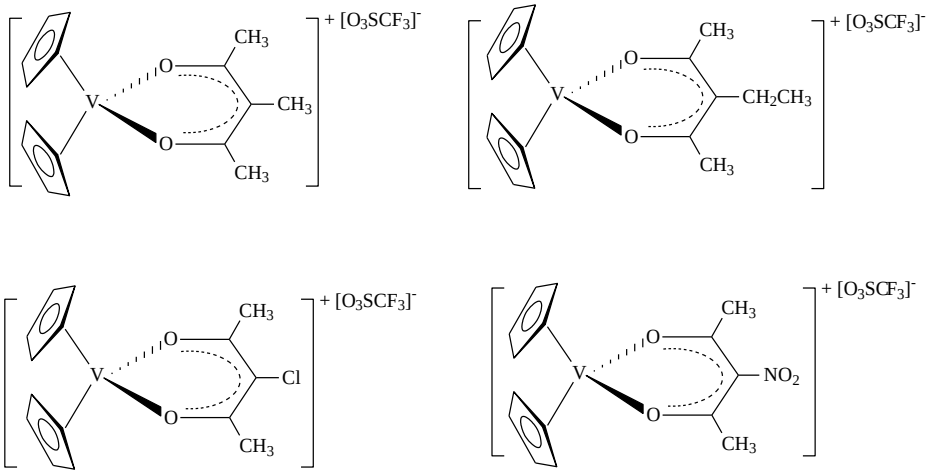

Figure 2.3. Chemical structure of vanadocene(IV) complexes with various β-diketones.

Although there is a very close parallel between the analogous bis(cyclopentadienyl)titanium(IV) [20] and –vanadium(IV) [21] compounds, the reaction with ethyl acetoacetate is one case where different products (Figure 2.4) are obtained. Conclusive evidence for this comes from comparing their infrared spectra.[48]

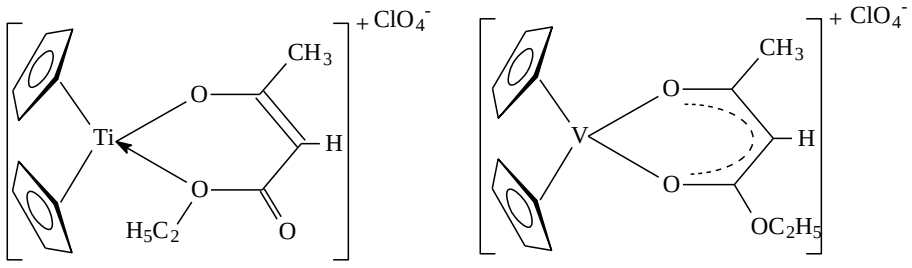

[20] [21]

Figure 2.4. Different structures of titanocene(IV)- [20] and vanadium(IV) ethyl acetoacetate [21].

2.2.2.3. Bis-β-diketonato metal complexes

The bis-β-diketonato complexes have an octahedral-coordination and can occur both in the *trans*- and *cis*-configuration (Figure 2.5). The *cis*-configuration is the most stable isomer for most cases, even though the *trans*-configuration may sometimes be preferred due to steric reasons. The higher stability of the *cis*-configuration is attributed to the π-back donation into the three metal *d*-orbitals (d_{xy}, d_{xz} and d_z^2), whereas for the *trans*-configuration only two *d*-orbitals (d_{xy} and d_{xz}) are occupied.[49]

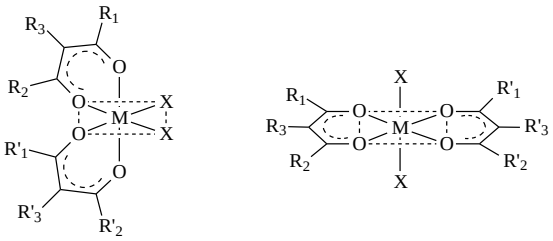

[22] [23]

Figure 2.5. Structure of the bis-β-diketonato metal complexes, [M(bis-β-diketonato)$_2$X$_2$], in the *cis*- [22] and *trans*-conformations [23], X = OR, Cl or $(C_5H_5)^-$.

Reaction of metallocene(IV) dichlorides (Ti, Zr) with β-diketonates in the presence of a hydrogen acceptor such as triethyl amine yields chlorocyclopentadienylbis(β-diketonato)metal(IV) and triethylammonium chloride (Scheme 2.14).[50] The titanium complex and the amine can be separated by extraction with benzene (or toluene). The chlorocyclopentadienylbis(β-diketonato)metal(IV) with metal = Ti, Zr and Hf are very susceptible to atmospheric moisture and can be readily hydrolysed (see Scheme 2.16 for products).

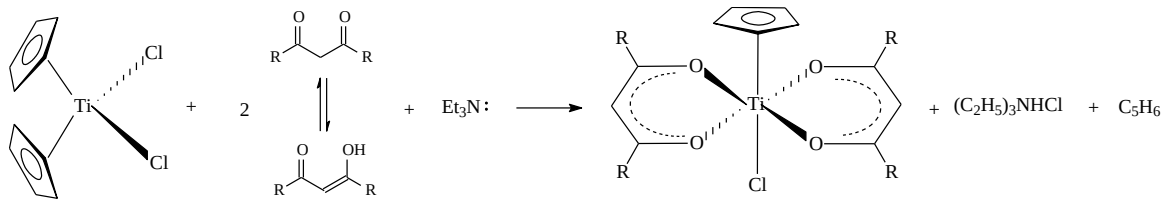

[4] [11]

Scheme 2.14. Reaction and formation of the bis-β-diketonato titanium(IV) complexes.

Another type of bis-β-diketonato metal complex [24] (M = Ti, Zr, Hf, Ge and Sn) can be synthesized from the corresponding metal tetrahalogenides and the β-diketone in an organic solvent,[51] according to the Scheme 2.15. An exception to the rule is the corresponding molybdenum complexes, which have molybdenum pentachloride as its starting material.

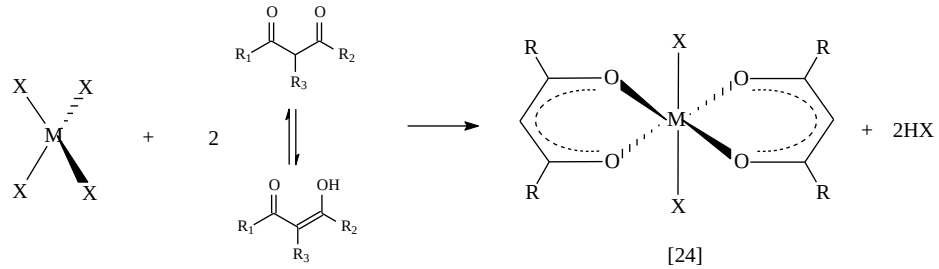

[24]

Scheme 2.15. General synthesis of [M(β-diketonato)$_2$X$_2$] complexes [24], M = Ti, Zr, Hf, Ge and Sn, X = halogen or alkoxide.

The bis-β-diketonato metal complexes [24] hydrolyse according to Scheme 2.16.[2] The easily replaceable group, X, which is usually an alcohol or a halogen, is substituted for the β-diketonato ligand. Substitution of the group X occurs at a relatively rapid rate. The order of stability against hydrolysis, which depends on the hydrolysable group X; is:

$$OEt > F > Cl > Br > I$$

$$[M(\beta\text{-diketonato})_2X_2] \overset{H_2O}{\rightleftharpoons} [M(H_2O)(\beta\text{-diketonato})_2X]^+X^- \rightleftharpoons$$

$$[M(OH)(\beta\text{-diketonato})_2X] + HX \overset{H_2O}{\rightleftharpoons} [M(OH)(H_2O)(\beta\text{-diketonato})_2]^+X^- \rightleftharpoons$$

$$[M(OH)_2(\beta\text{-diketonato})_2] + HX \overset{-H_2O}{\rightleftharpoons} \text{polymers} \longrightarrow\!\!\!\!\!\!\rightarrow MO_2$$

Scheme 2.16. Hydrolysis of bis-β-diketonato metal complexes [24].

2.2.2.4. Tris- and tetrakis- β-diketonato metal complexes

Although β-diketonato complexes are known for every early transition metal, zirconium and hafnium are unique in that in the Ti, Zr and Hf group, they are the only metals reported to form β-diketonates in which the metal exhibit six, seven and eight coordination numbers. The known compounds for the seven and eight coordinated species are of the type [M(β-diketonato)$_3$Cl],[52] and [M(β-diketonato)$_4$],[52] with M = Zr, Hf and β-diketonato = dibenzoylmethanato, (PhCOCHCOPh)$^-$. Zirconium(IV) and hafnium (IV) chlorides and bromides react with a β-diketone under anhydrous conditions to yield substitution products plus hydrogen halide. In diethyl ether, the di-substituted products [M(β-diketonato)$_2$X$_2$] are obtained.[36] At higher temperatures, in refluxing benzene the reaction gives the tri-substituted product [M(β-diketonato)$_3$X].[36] The tetra-substituted product [M(β-diketonato)$_4$] cannot be prepared by reaction of M(IV) chloride with the access of β-diketone, even after prolonged

heating. However, heating of [M(β-diketonato)$_3$X] with the β-diketone (ratio 1:40) for 24 h at 80˚, yielded [M(β-diketonato)$_4$] in 20% yield.[36]

Depending on the ratio of zirconium isopropoxide to β-diketones or β-ketoesters, a mono-, di, tri or tetra-substituted zirconium β-diketonato or β-ketoester [25] can form according to Scheme 2.17.[53]

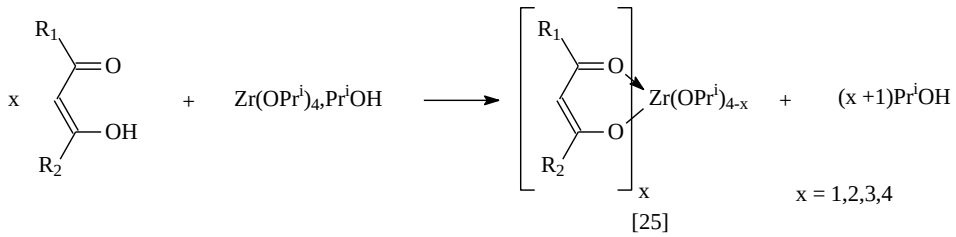

Scheme 2.17. The general synthesis of either a mono-, di, tri or tetra-substituted zirconium β-diketonato or β-ketoester [25].

2.2.2.5. Other bidentate ligand metal complexes

2.2.2.5.1. Synthesis of thio-β-diketonates and amine-β-diketonates and its derivatives

Thioacetylacetone [26] and enaminoketones [27], are related to acetylacetone in that one of the oxygen atoms are replaced by sulphur or an amine respectively (Figure 2.6).

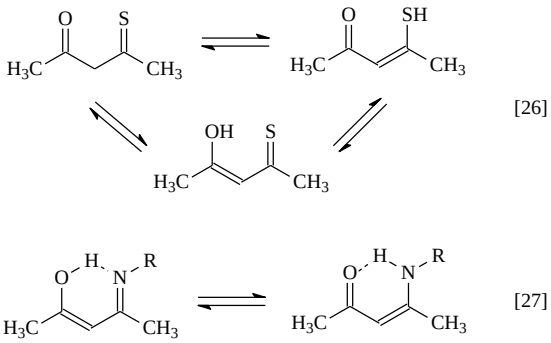

Figure 2.6. Structure of thioacetylacetone [26] and enaminoketone [27].

In synthesising β-thioketones such as thioacetylacetone, [26], the reaction temperature and the nature of the solvent used, are critical to obtain good yields. There is also a decisive dependence on the concentration of the catalyst (HCl). Treatment of acetylacetone in acetonitrile solution with excess of both H_2S gas and HCl gas at -40˚C leads to complete and exclusive formation of thioacetylacetone within 6h. The crude product is sufficiently pure for further, immediate synthetic use.

Thioacetylacetone is thermally unstable and high temperature distillation of the crude product inevitably leads to partial decomposition. Decomposition also takes place slowly at room temperature, but freshly distilled thioacetylacetone can be kept for months in a closed ampoule at -20˚C.

Coordination reactions of thioacetylacetone are very much the same as that found in acetylacetone. Tetrakis(thioacetylacetonato)zirconium(IV), [Zr(Sacac)$_4$], has been prepared by reaction of stoichiometric amounts of zirconium(IV) chloride and sodium thioacetylacetonate in DCM.[54] The complexes are thermally stable, unlike the free thioacetylacetone.

Thioacetylacetone can also react with [$Rh_2Cl_2(CO)_4$] to form [Rh(Sacac)$(CO)_2$], by refluxing $RhCl_3.3H_2O$ in DMF and the addition of equal amounts of Sacac.[55]

Dithio-β-diketones can only be obtained *in situ*, however the metal dithio-β-diketonato complexes can be isolated.[56]

Various methods exit for the preparation of enaminoketones such as reactions of α-metalated imines with esters,[57] reduction of β-amino ketones in the presence of triethyl amine promoted by Pd(II),[58] and a new method which starts from β-ketoesters or 1,3-diketones and primary amines in water to yield β-enamino ester or enaminoketones (Scheme 2.18).[59]

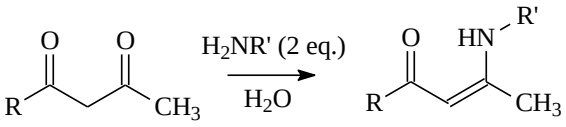

Scheme 2.18. Synthesis of β-enamino ester or enaminoketones.

Dinuclear molybdenum(V) complexes are prepared by reaction of [$Mo_2O_3(acac)_4$] with the polydentate ligand β'-hydroxy- β-enaminones in DCM.[60] Even though the β'-hydroxy-β-enaminones ligands are polydentate only the diketone part is chelating, not the amine part (Figure 2.7). There are, however, known rhodium complexes where the amine part is chelating. They are of the type [Rh(L,L')(CO)(PPh_3)] where L,L' = N-*o*-tolylsalicylaldiminato,[61] 8-hydroxyquinolinato,[62] and 2-carboxypyridinato.[63]

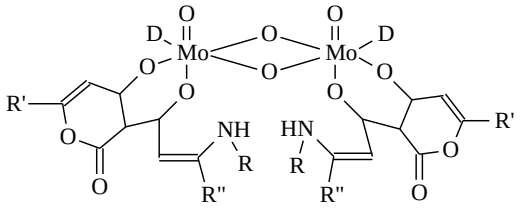

D = methanol, ethanol, i-propanol
R = *p*-$C_6H_4OCH_3$
R' = CH_3
R" = $CO_2C_2H_5$

Figure 2.7. Structure of the dinuclear molybdenum(V) complex.

2.2.2.5.2. Five- and seven membered metallocyclic complexes

The formation of five and seven membered metallocyclic compounds is achieved by reaction of either 1,2-benzenediol (for the five membered metallocyclic compound) or 2,2-biphenyldiol (for the seven membered metallocyclic compound) with titanocene dichloride in the presence of sodamide, $NaNH_2$.[30]

Another method to obtain a seven membered metallocyclic compound [28], involves the reaction of the bicyclic 2-diazoindane-1,3-dione with dicarbonyltitanocene [5] in toluene at 0˚C for 3 days.[64] An interesting feature of this reaction is that the reaction proceeds with a C-C coupling and the elimination of nitrogen (Scheme 2.19).

Phthalocyaninatotitanium(IV) oxide can undergo axial substitution to form a seven membered metallocyclic compound, just like [28]. This is a very simple reaction involving only the stirring of the two reagents phthalocyaninatotitanium(IV) oxide and 1,2-biphenyldiol for a few hours in DCM.[65]

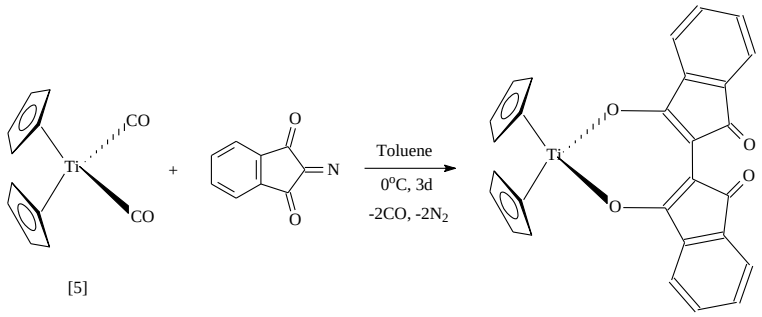

[5] [28]

Scheme 2.19. Formation of a seven membered metallolcyclic compound [28].

Phthalocyaninatotitanium(IV) oxide can also undergo axial substitution to give a five membered metallocyclic compound. The reaction is different than that for the formation of the seven membered metallocyclic compounds, in that it involves the refluxing of the two reagents phthalocyaninatotitanium(IV) oxide and 1,2-benzenediol or 1,2-benzenedithiol (this reaction also works for derivatives of 1,2-benzenediol and 1,2-benzenedithiol).[66] The driving force of the reaction is based on the electrophilic character of titanium(IV) and the nucleophilicity of oxygen and sulphur atoms in 1,2-benzenediol- or 1,2-benzenedithiol-based derivatives.

Tetrachlorobenzene-1,2-dithiolate can also react with titanocene dichloride [4] to form tetrachlorobenzene-1,2-dithiolato-di(cyclopentadienyl)titanium(IV).[67] This reaction proceeds in ethanol as the solvent and in the presence of triethyl amine. Ionic, five coordinated titanium complexes can also form with the 1,2-benzenedithiol-based derivatives, like the bis(dithiolene) chelate $[(C_5H_5)Ti(1,2,4\text{-}S_2C_6H_3CH_3)_2]^-[N(C_2H_5)_4]^+$.[68]

2.2.2.6. Related chemistry of early transition metals

Because the synthesis of dicarbonylbis(cyclopentadienyl)titanium(II) [5] has already been discussed in paragraph 2.1.4, only a few reactions of [5] will be referred to here (Scheme 2.20).

Depending on the ratio of RSSR, either the titanium (IV) complex [6] or the titanium(III) complex [29] can be formed.[26] Complex [5] is very moisture- and oxygen-sensitive, giving various decay products, [30] is just one of them.

[4] Reacts with [5] to give the titanium(III)chloro complex [31], which acts as a convenient precursor for many titanium(III) complexes.[69] One of these is the bipyridyl titanium(III) complex [34],[70] which may also be prepared by reaction of [5] with bipyridyl.[71] Titanocene dicarbonyl [5] reacts with diethyl diazomalonate (DEDM) by losing carbon monoxide and giving [Cp_2Ti(DEDM)] [33], in which the diazo ligand is η^3-N,N,O bonded to the metal through both nitrogen atoms and one oxygen of the ester groups.[72] The phenatrenediolate complex [32] is formed when [5] reacts with 9,10-phentraquinone.[73] Addition of acyl halides to [5] would result in the formation of [35],[74] this bond is greatly distorted owing to a bond interaction between titanium and the carbonyl oxygen.

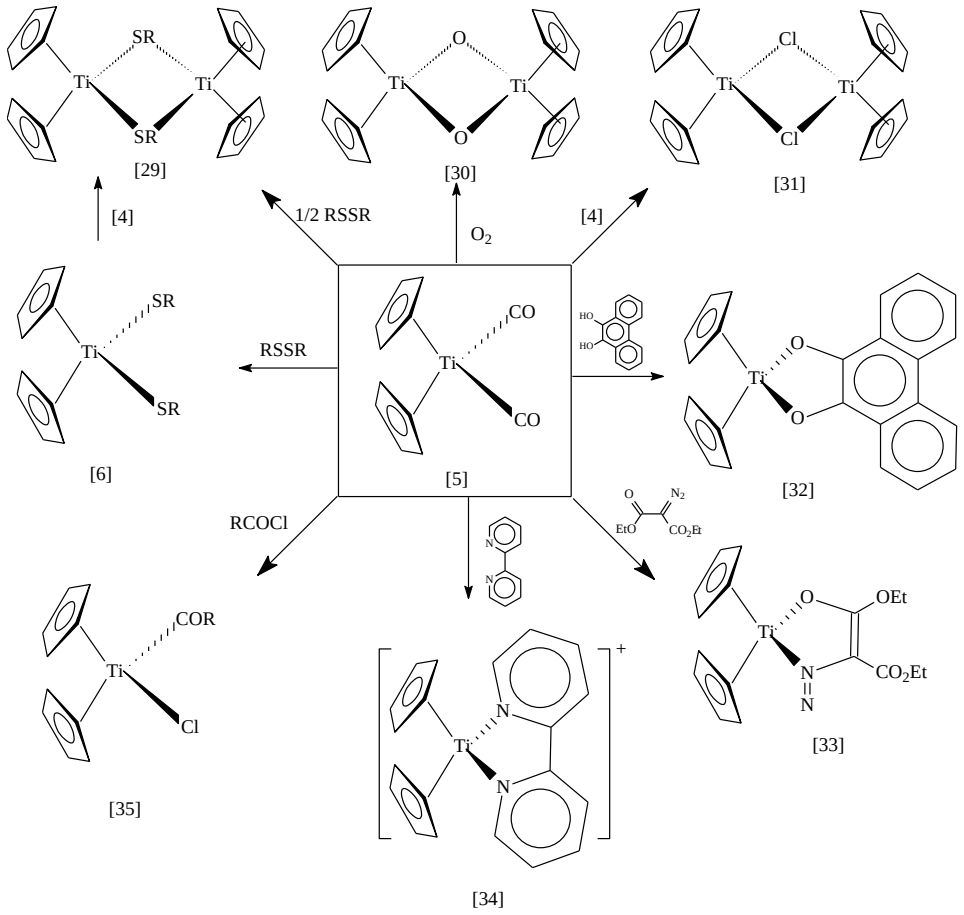

Scheme 2.20. Some general reaction of dicarbonyldi(cyclopentadienyl)titanium(II) [5].

There exists various ways in which ferrocene can be incorporated into a metallocene molecule, for example the direct binding of ferrocene to a metallocene dichloride (Ti, Zr and Hf):[75]

$$(C_5H_5)_2MCl_2 + 2FcLi \rightarrow (C_5H_5)_2MFc_2 + 2LiCl$$

Another method is linkage through a backbone of carbon and oxygen molecules, like the reaction of 4-oxoferrocenebutanoate with zirconocene dichloride yielding chlorobis(cyclopentadienyl)(4-oxoferrocenebutanoyloxy)zirconium(IV) [36] (Figure 2.8).[76]

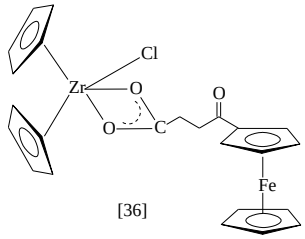

[36]

Figure 2.8. Structure of bis(cyclopentadienyl)chloro(4-oxoferrocenebutanoyloxy)zirconium(IV) [36].

Other than the β-diketonato ligands, there exists many polychelating ligands that binds *via* oxygen to Ti, Zr and Hf. Some of these are shown in Figure 2.9.

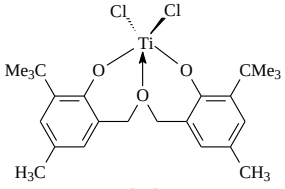

[37]

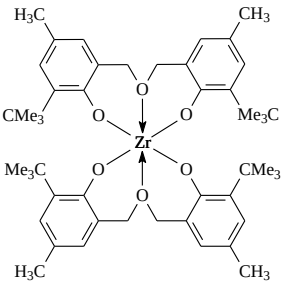

[38]

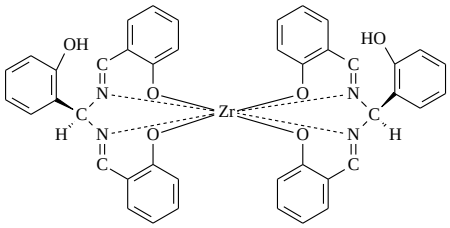

[39]

Figure 2.9. Structure of polydentate oxygen and nitrogen coordinated Ti and Zr complexes.

2.3. Electroanalytical chemistry

2.3.1. Introduction

Cyclic voltammetry (CV) is possibly the simplest and most versatile electroanalytical technique for the study of electro-active species. The effectiveness of CV is its ability to obtain the redox behaviour of electro-active species fast over a wide potential range.[77] Cyclic voltammetry is a simple and direct method for the measurement of the formal reduction potential

of a reaction when both oxidized and reduced forms are stable during the time when the voltammogram is taken.[78] Both thermodynamic and kinetic information is available in one experiment. Therefore both reduction potential and heterogeneous electron transfer rates can be measured. The rate and nature of a chemical reaction coupled to the electron transfer step can also be studied. Knowledge of the electrochemistry of a metal complex can be useful in the selection of the proper oxidizing agent to put the metal complex in an intermediate oxidation state.

2.3.2. The basic cyclic voltammetry experiment[77]

Cyclic voltammetry, CV, consists of oscillating of the potential of an electrode, in an unstirred solution and measuring the resulting current. The potential of the small, static, working electrode is controlled relative to a reference electrode. The reference electrode could be for example a saturated calomel electrode (SCE) or a silver/silverchloride electrode (Ag/AgCl). The controlled potential, which is applied over these two electrodes, can be viewed as an excitation signal. This excitation signal for the CV is a linear potential scanning with a triangular waveform, from an initial value, E_i, to a predetermined limit $E_{\lambda 1}$ (switching potential) where the direction of the scan is reversed (Figure 2.10). The scan can be stopped anywhere or a second cycle, as indicated by the broken line, can be initiated. Singular or multiple cycles can be measured. The scanning rate as indicated by the slope, can be anything between ± 15 mV s^{-1} to 40000 mV s^{-1}.

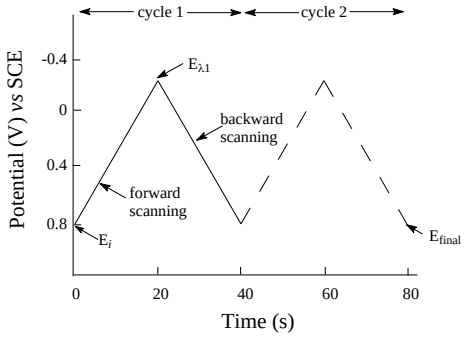

Figure 2.10. Typical excitation signal for cyclic voltammetry – a triangular potential waveform.

The current response on a cyclic voltammogram (vertical axis) is plotted as a function of the applied potential (horizontal axis). See Figure 2.11 for a typical CV. Often there is very little difference between the first and successive scans. However, the changes that do appear on repetitive cycles are important in obtaining and understanding information about reaction mechanisms.

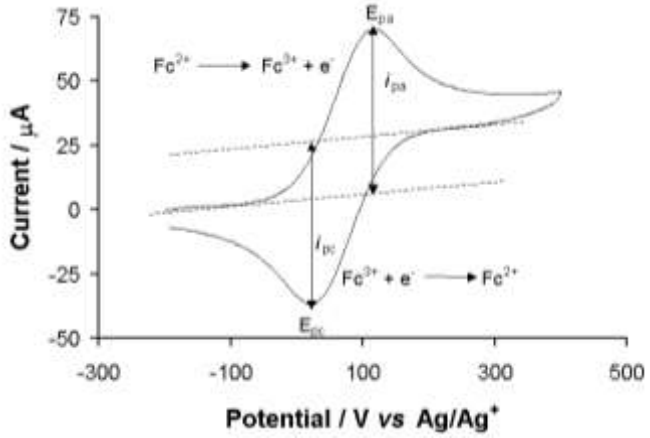

Figure 2.11. Cyclic voltammogram of a 3.0 mmol dm^{-3} ferrocene measured in 0.1 mol dm^{-3} tetrabutylammonium hexafluorophosphate/acetonitrile on a glassy carbon electrode at 25˚C, scan rate 100mV s^{-1}.

2.3.3. Important parameters of cyclic voltammetry [77, 79]

The most important parameters of cyclic voltammetry are the peak anodic potentials (E_{pa}), peak cathodic potential (E_{pc}) and the magnitudes of the peak anodic current (i_{pa}) and peak cathodic current (i_{pc}) (Figure 2.11). One method of measuring i_p is the extrapolation of a baseline. Establishing the correct baseline is essential for accurate measurement of the peak currents.

A redox couple may or may not be electrochemically reversible. By electrochemically reversibility, it is meant that the rate of electron transfer between the electrode and substrate is fast enough to maintain the concentration of the oxidised and reduced species in equilibrium at the electrode surface. The formal reduction potential for an electrochemically reversible redox couple is midway between the two peak potentials (Equation 2.1)

Equation 2.1.

$$E^{01} = (E_{pa} + E_{pc})/2$$

This E^{01} is an estimate of the polarographic $E_{1/2}$ value provided that the diffusion constants of the oxidised and reduced species are equal. The polarographic $E_{1/2}$ value can be calculated from E^{01} *via* Equation 2.2.

Equation 2.2.

$$E_{1/2} = E^{01} + (RT/nF) \ln (D_R/D_O)$$

Here D_R = diffusion coefficient of the reduced specie, D_O = diffusion coefficient of the oxidised specie. In cases where $D_R/D_O = 1$, $E_{1/2} \approx E^{01}$.

For electrochemical reversible couples the difference in peak potentials (ΔE_p) should be 59 mV at 25˚C for a one electron transfer process. The number of electrons (*n*) transferred in the electrode reaction for a reversible couple can be determined from the separation between the peak potentials from Equation 2.3.

Equation 2.3.

$$\Delta E_p = E_{pa} - E_{pc} \approx 59 \text{ mV}/n$$

This 59 mV/*n* separation of peak potentials is independent of the scan rate of the reversible couple, but slightly dependent on the switching potential and cycle number.[80] In practice, within the context of this research program, a redox couple with a ΔE_p value up to 90 mV will still be considered as electrochemically reversible. Peak separation increases due to slow electron transfer kinetics at the electrode surface.

The peak current, i_p, is dependent on a few variables and is described by the Randle-Sevcik equation for the first sweep of the cycle at 25˚C (Equation 2.4).

Equation 2.4.

$$i_p = (2.69 \times 10^5) n^{3/2} A D^{1/2} v^{1/2} C$$

i_p = peak current (A), *n* = amount of electrons per molecule, A = working electrode surface (cm^2), C = concentration (mol cm^{-3}), *v* = Scan rate (V s^{-1}) and D = Diffusion coefficient (cm^2 s^{-1}).

The values of i_{pa} and i_{pc} should be identical for a reversible redox couple, which is not followed by any chemical reaction (Equation 2.5).

Equation 2.5.

$$i_{pc}/i_{pa} = 1$$

Systems can also be quasi-reversible or irreversible (Figure 2.12). An electrochemically quasi-reversible couple is where both the oxidation and reduction processes takes place, but the electrochemical kinetics are slow and $\Delta E_p > 59$ mV (practically 90 mV $\leq \Delta E_p \geq \pm$ 150 mV). A complete chemical irreversible system is one where only oxidation or reduction is possible.[81] In cases where the system is quasi-reversible or irreversible, Equations 2.1, 2.3 and 2.4 are not applicable.

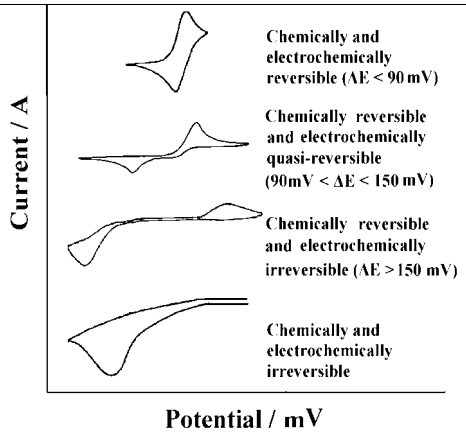

Figure 2.12. A schematic representation of the cyclic voltammogram expected from an electrochemical reversible, an electrochemical irreversible and a chemical irreversible system.

2.3.4. Solvents, supporting electrolytes and reference electrodes

A suitable medium is needed for electrochemical phenomena to occur. This medium generally consists of a solvent containing a supporting electrolyte. The most important requirement of a solvent is that the electrochemical specie under investigation must be soluble and stable in it.[82] The electrochemical specie under investigation must be soluble to the extent of at least 1 x 10^{-4} mol dm^{-3} and the electrolyte concentration must be at least 10 times that of the electrochemical specie under investigation. An ideal solvent should possess electrochemical and chemical inertness over a wide potential range, it should be a good solvent for both electrochemical species and electrolyte, and it should preferably be unable to solvate the electrochemical specie. Solvents that are often used are dipolar aprotic solvents, which have large dielectric constant (≥ 10) and low proton availability. Acetonitrile (CH_3CN) has a dielectric constant of 37 and is most commonly used in anodic studies. CH_3CN is an excellent solvent for both inorganic salts and organic compounds and is stable after purification. Dichloromethane (DCM) is used when a strictly non-coordinating solvent is required.

In the majority of electroanalytical and electrosynthetic experiments, a supporting electrolyte is used to increase the conductivity of the medium. Most of the current is carried by the ions of the supporting electrolyte. Tetrabutylammonium hexafluorophosphate, $TBAPF_6$, is the most widely used supporting electrolyte, in organic solvents. A $TBAPF_6$ solution in CH_3CN exhibits a wide potential range with positive (3.4 V) and negative decomposition potentials (–2.9 V) *vs* SCE.[83]

In nearly al experimental papers, potentials of a reference electrode is specified *vs* normal hydrogen electrode (NHE) or saturated calomel electrode (SCE). However, IUPAC now recommend that all electrochemical data are reported *vs* an internal standard. In organic media

the Fc/Fc^+ couple is a convenient internal standard.[84, 85] Fc/Fc^+ couple E^{01} = 0.400 V *vs* NHE.[86] NHE and SCE are used for measurements in aqueous solutions. However, in many instances electrochemical measurements in water are impossible due to insolubility or instability. With non-aqueous solvents, a system like Ag/Ag^+ (0.01 mol dm^{-3} $AgNO_3$ in CH_3CN) is preferred.

2.3.5. Bulk electrolysis

While cyclic voltammetry only considers electrochemistry at the surface of an electrode, the bulk electrolysis technique involves the electrolysis of the bulk solution. The total amount of coulombs consumed during electrolysis is used to determine the amount of substance electrolysed. Alternatively the number of electrons (*n*) transferred per molecule can be determined of a known amount of substance.

During the process of bulk electrolysis (controlled potential electrolysis) or coulometry, the analyte is completely electrolysed by applying a fixed potential to an electrode. The solution is stirred and an electrode with a large surface area is used to minimize electrolysis time. The total amount of coulombs (Q) consumed during the experiment is determined by the integration of the current (*i*) (Equation 2.6) during the course of the experiment (Figure 2.13).

Equation 2.6.

$$Q(t) = \int i(t) \partial t$$

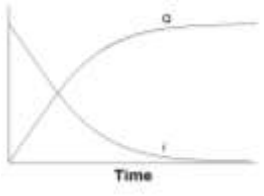

Figure 2.13. Current-time and charge-time response for controlled potential electrolysis.

When the electrolysis of the analyte is complete ($i \rightarrow 0$), the total charge is used to calculate the number of electrons (*n*) transferred per molecule for a known amount (N mol) of the analyte electrolysed by means of Faraday's law (Equation 2.7).

Equation 2.7.

$$Q = nFN$$

Q = the total amount of charge consumed during the experiment / C, F = Faraday's number = 96485 C eq^{-1}, *n* = the number of electrons transferred per molecule / eq mol^{-1} and N = amount of analyte / mol.

2.3.6. Electrochemistry of some metallocene complexes

2.3.6.1. Ferrocene

Ferrocene, with a formal reduction potential of 400 mV *vs* NHE,[86] can be used in CV experiments as an internal reference system in a wide range of non-aqueous solvents,[85] or when using different reference electrodes.[84] The Fc/Fc^+ couple is reversible and has a ΔE_p = 59 mV under ideal conditions. Different formal reduction potentials of Fc in solvents such as THF, DCM and CH_3CN referred to the same reference electrode have been measured (Table 2.4). Irrespective of the shift in E^{01} (Fc/Fc^+) in different solvents, the formal reduction potential of another compound (e.g. $[IrCl_2(fctfa)(COD)]$) *vs* Fc/Fc^+ as an internal standard, remains unchanged.[87] Complexes with two or three ferrocenyl ligands bounded to it, showed different oxidation and reduction peaks for the different Fc moieties (Figure 2.14).[88, 89, 90] The observed inequalities is due to the improbability of both ferrocenyl groups of the same molecule, coming simultaneously in reaction contact with the electrode to invoke two simultaneous one-electron transfer processes.[91, 92]

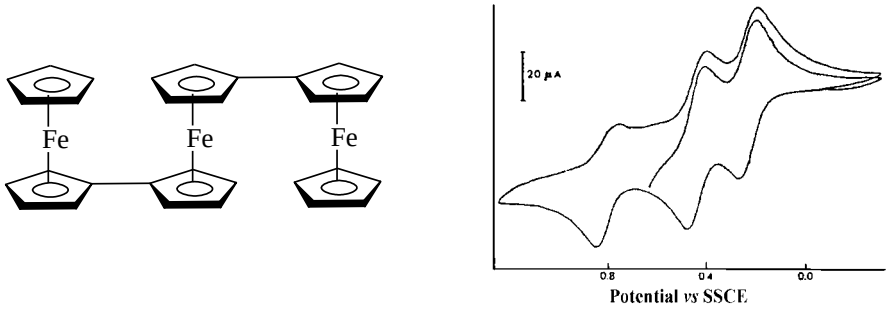

Figure 2.14. Left: Structure of 1,1'-terferrocene(1+). Right: Cyclic voltammogram of 1,1'-terferrocene(1+) in 1:1 CH_2Cl_2:CH_3CN containing 0.1 M TBAH at scan rate 200 mV/s.

In the complexes where two ferrocenyl ligands are bound, it could be either by one or two linkages (Figure 2.15).[93] This leads to quite a dramatic difference in their polarographic behaviour (Table 2.2), which can be related to electrochemical behaviour *via* Equation 2.2. In the bridged ferrocenes with two linkages, the Fe-atoms are kept very close to one another. Its CV data shows that the second oxidation step is more difficult than the first. Electron interaction can take place *via* two ways: 1) through the carbon skeleton of the ligands, 2) through direct metal-metal interaction (field effect). The CV results of the bridged ferrocenes with one linkage show that its second oxidation step is easier than that found for the bridged ferrocenes with two linkages, thus the potential of the two redox couples are closer to one another. This is attributed

to the direct electrostatic field interaction between the Fe atoms, because due to steric reasons the mono bridged ferrocenes derivative can adopt a conformation in which the two Fe atoms are pseudo-*trans* to one another.

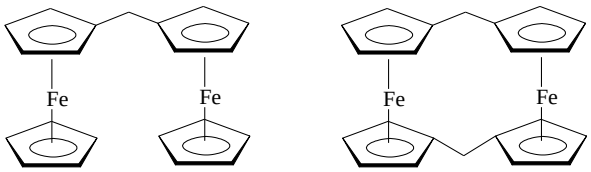

Figure 2.15. Ferrocene derivatives, which are either linked *via* one or two linkages.

Table 2.2. Polarographic half potentials of ferrocene derivatives, bridged ferrocenes that are either linked *via* one or two linkages.

Bridged ferrocenes	$E_{1/2}$ / V	$\Delta E_{1/2}$ / V *vs* Fc (0.34 V)
One linkage	0.30, 0.40	-0.04, 0.06
Two linkages	0.25, 0.44	-0.09, 0.10

When ferrocene is bounded in a complex like a β-diketone ($FcCOCH_2COR$), the E^{01} value of the Fc/Fc^+ couple is influenced by the group electronegativity of the R group (Figure 2.16, Table 2.3),[91] due to the good communication between the ferrocenyl ligand and the R group *via* the backbone of the pseudo-aromatic β-diketone core. With increasing electronegativity of the R group on the β-diketone, the E^{01} value of the Fc/Fc^+ couple also increases since electron-density is withdrawn from it by R. There is also a linear relationship between the pK_a of the β-diketone and the E^{01} value of the Fc/Fc^+ couple, and with increasing pK_a there is a decrease in the E^{01} value of the Fc/Fc^+ couple.

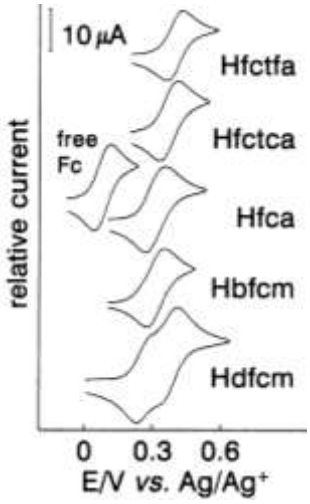

Figure 2.16. Cyclic voltammograms of 2 mmol dm^{-3} solutions of ferrocene (Fc) and ferrocene containing-β-diketones measured in 0.1 mol dm^{-3} $TBAPF_6/CH_3CN$ at a scan rate of 50 mV s^{-1} on a Pt working electrode at 25.0(1)°C *versus* Ag/Ag^+.

Table 2.3. E^{01} *vs* Ag/Ag^+, of the β-diketones of the type $FcCOCH_2COR$ R = CF_3, CCl_3, CH_3, Ph and Fc group electronegativities of the R groups on the β-diketones and pK_a values of the β-diketones.

β-diketones	R groups on the β-diketones	E^{01} *vs* Ag/Ag^+ / mV[91]	Group electronegativities of the R groups[91]	pK_a of the β-diketones[92]
Hfctfa	CF_3	0.394	3.01	6.53
Hfctca	CCl_3	0.370	2.76	7.15
Hfca	CH_3	0.313	2.34	10.01
Hbfcm	Ph	0.306	2.21	10.41
Hdfcm	Fc	0.265; 0.374	1.87	13.1

2.3.6.2. Early transition metal metallocenes

The redox properties of titanocene dichloride reveal a strong dependence on the solvent; in THF and DCM quasi-reversible redox character has been observed with i_{pa}/i_{pc} = 0.65-0.95 and ΔE_p = 90-100 mV, while in CH_3CN a small reoxidation peak, strongly shifted to the positive direction with ΔE_p = 400 mV, was observed (Table 2.4).[94] This can be interpreted within the framework of a 'square scheme' where the electrochemical reduction step is accompanied by the rapid substitution of one chloride ligand by the solvent molecule (Scheme 2.21). The back electron transfer follows the same reaction path for weakly coordinating media (THF, DCM) whereas this process is shifted to a more positive potential in the case of strong coordinating solvents (CH_3CN).

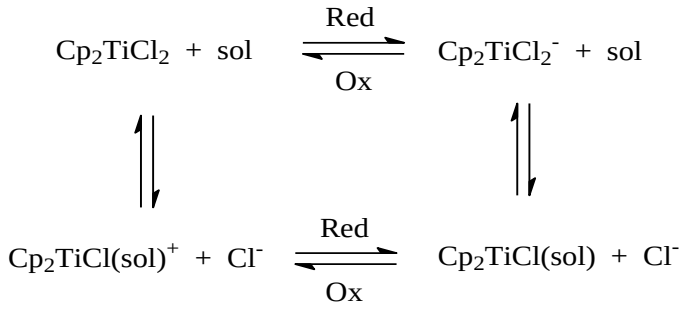

Scheme 2.21. The 'square scheme' illustrating the oxidation and reduction of titanocene dichloride.

The reported E^{01} for titanocene dichloride is similar to values reported elsewhere.[94, 95, 96] Electrochemical characterisation of a titanocene dichloride derivative, $[Cl_2TiCpC_5H_4(CH_2)_3NC_4H_4]$, (one of the cyclopentadienyl rings is functionalised with a pyrrolyl

ring (Py)), revealed that the reduction and oxidation resemble the behaviour of the unsubstituted titanocene dichloride or Py (Table 2.4).[97] Reduction of this complex demonstrates a dependence on the solvent complexation ability, which gives rise to the quasi-reversible behaviour found in THF and DCM. In CH_3CN, on the other hand, irreversibility was found. The Ti^{4+}/Ti^{3+} transition leads to the substitution of one of the Cl^- ions by the solvent molecule.

Table 2.4. Redox potentials in solutions *vs* Ag/Ag^+ and SCE (Pt electrode and supporting electrolyte 0.2 M *n*-Bu_4NPF_6) of Fc, $TcCl_2$ and $[Cl_2TiCpC_5H_4(CH_2)_3NC_4H_4]$ (Tc3Py).[97]

Substance	Solution	$E_{1/2}$ *vs* Ag/Ag^+ / V	$E_{1/2}$ *vs* SCE / V	$E_{1/2}$ *vs* Fc/Fc^+ / V	i_{pa}/i_{pc}	ΔE_p / V
Fc	THF	0.20	0.53	-	1.0	100
	DCM	0.21	0.43	-	1.0	100
	CH_3CN	0.10	0.43	-	1.0	80
$TcCl_2$	THF	-1.08	-0.76	-1.28	0.-90-0.95	90
	DCM	-0.95	-0.73	-1.16	0.65-0.75	100
	CH_3CN	-0.80	-0.47	-0.90	-	400
Tc3Py	THF	-1.12	-0.79	-1.32	0.7-0.9	95
	DCM	-0.98	-0.76	-1.19	0.65-0.8	115
	CH_3CN	-0.845	-0.525	-0.945	-	425

As can be seen from Table 2.4, the E^{01} values as well as the reversibility (ΔE_p) of the complexes are highly dependent on the nature of the solvent and the supporting electrolyte used.[98] This is also confirmed by electrochemical studies done on another titanocene derivative, di(propylthiotetramethylcyclopentadienyl)titanium dichloride,[98] $[(C_5Me_4SCH_2CH_2CH_3)_2TiCl_2]$, whose electrochemical behaviour is analogous to that of titanocene dichloride. The first reduction step of $[(C_5Me_4SCH_2CH_2CH_3)_2TiCl_2]$ depends strongly on the nature of the solvent and the supporting electrolyte.

Methyl-substituted titanocene dichlorides', $[(C_5H_{5-n}Me_n)_2TiCl_2]$ n = 0-5, CV data in THF revealed that the standard potential (E^0_1) shifts to more negative values proportionally to the number of methyl groups in the $[(C_5H_{5-n}Me_n)_2TiCl_2]$ n = 0-3, compounds, with an increment of 0.093 V per one methyl group.[99] A decline from this linear dependence is observed for $[(C_5HMe_4)_2TiCl_2]$ and a positive shift for $[(C_5Me_5)_2TiCl_2]$ (Table 2.5). These positive shifts can be brought about by a steric strain between the cyclopentadienyl ligands, which lower the dihedral angle between cyclopentadienyl ring planes.

Table 2.5. Cyclic voltammetry of titanocene dichloride complexes in THF, potentials were related to the standard redox potential of Fc/Fc^+ couple (0.203 V *vs* sat. Ag/AgCl in water).

Compound	ΔE_p / V	E^{01} *vs* Fc/Fc^+ / V
$(C_5H_5)_2TiCl_2$	0.090	-1.313
$(C_5H_4Me)_2TiCl_2$	0.083	-1.403
$(C_5H_3Me_2)_2TiCl_2$	0.093	-1.478
$(C_5H_2Me_3)_2TiCl_2$	0.079	-1.593
$(C_5HMe_4)_2TiCl_2$	0.081	-1.623
$(C_5Me_5)_2TiCl_2$	-	-1.573

Other metallocene of group IV (Zr, Hf) of the periodic table also displays reversibility or quasi-reversibility in THF and DCM, the same as was found for Ti (Table 2.6).[100, 101] The behaviour of these metallocenes are subsequently dependent on traces of moisture.[96]

Table 2.6. Cyclic voltammetry of $TcCl_2$, $ZcCl_2$ and $HcCl_2$ in THF and DCM *vs* SCE and Fc/Fc^+.

Metallocene		E^0_{red} *vs* SCE / mV	E^0_{red} *vs* Fc/Fc^+ / mV
$TcCl_2$	DCM	-730[95]	-1160[95]
	THF	-760[96]	-1280[94]
$ZcCl_2$	DCM	-1630[95]	-2060[95]
	THF	-1780[96]	-2158[95]
$HcCl_2$	DCM	-1930[95]	-2370[95]
	THF	-	-

Similar results to what was observed for the Tc derivatives, $[(C_5H_{5-n}Me_n)_2TiCl_2]$ n = 0-5, was found for the Zc derivatives, $[(C_5H_{5-n}Me_n)_2ZrCl_2]$ n = 0-5. In THF $[(C_5H_{5-n}Me_n)_2ZrCl_2]$ n = 0-5, it was revealed that for n = 0-4 E^{01} shifts 0.071 V more negative (than –2.158 V for Zc) for every methyl group were added (Table 2.7).[102] The E^{01} value for $[(C_5Me_5)_2ZrCl_2]$ does not follow the linear dependence, a less negative E^{01} value was observed (Table 2.7). This was attributed to the steric hindrance between the rotating C_5Me_5 ligands, which tends to decrease the angle between the Cp ring planes and consequently, the energy difference between MO frontier orbitals.

Table 2.7. Cyclic voltammetry of zirconocenes in THF, potentials were related to the standard redox potential of Fc/Fc^+ couple (0.203 V *vs* sat. Ag/AgCl in water).

Compound	ΔE_p / V	E^{01} *vs* Fc/Fc^+ / V
$(C_5H_5)_2ZrCl_2$	-0.078	-2.158
$(C_5H_4Me)_2ZrCl_2$	-0.085	-2.228
$(C_5H_3Me_2)_2ZrCl_2$	-0.114	-2.298
$(C_5H_2Me_3)_2ZrCl_2$	-0.114	-2.378
$(C_5HMe_4)_2ZrCl_2$	-	-2.438
$(C_5Me_5)_2ZrCl_2$	-	-2.418

2.3.6.3. Metallocene β-diketonato complexes

Electrochemical data obtained from the titanocene(III)-β-diketonato complex $[TiCp_2(LL')]$, where LL' = $acac^-$ or $bzac^-$, shows that both the metal as well as the β-diketonato ligand are electrochemically active (Figure 2.17).[39] The Ti(III) can be reversibly oxidized in a one electron process at a potential, which is apparently independent of the β-diketonato ligand. $[TiCp_2(acac)]$ E^{01} = -0.86 V and ($[TiCp_2(bzac)]$ E^{01} = -0.85 V *vs* Fc/Fc^+ in butyronitrile (0.2 M NBu_4PF_6). The author of this publication attributed the negligible influence of the β-diketonato ligand to the existence of a highly localized centred frontier orbital, which dominates the redox chemistry. The peaks at ± -2.5 V is attributed to the β-diketonato ligand.

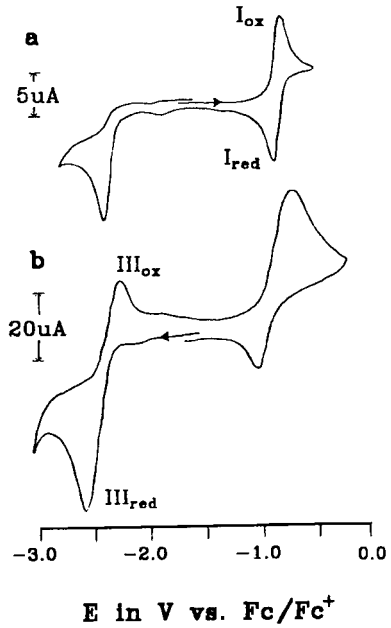

Figure 2.17. CV of $[TiCp_2(bzac)]$ (2 mM) obtained in butyronitrile (0.2 M NBu_4PF_6) at scan rate 200 mV/s with a) 1 mm Pt disk electrode at 22˚C and b) a 5 mm glassy carbon disk electrode at -50˚C.[39]

The cyclic voltammogram of $[VCp_2(acac)](CF_3SO_3)$ was examined both in acetonitrile and PBS solutions using a Pt working electrode.[103] The complex displayed a characteristic one electron quasi-reversible reductive couple for the V^{3+}/V^{4+} process with $E_{1/2}$ = -1.06 V (*vs* Fc/Fc^+). An oxidative quasi-reversible cyclic voltammogram, attributable to V^{4+}/V^{5+} heterogeneous electron transfer process, was observed at 0.987 V (*vs* Fc/Fc^+). The peak current ratio (i_{pa}/i_{pc} for oxidative and i_{pc}/i_{pa} for reductive couple) for both the redox processes is nearly one and the plots of i_p (peak current) *vs* $v^{1/2}$ (v = scan rate) for each redox process are linear implying a limited mass transfer of the one electron stoichiometric reaction:

$$[V^{V}Cp_2(acac)]^{2+} \leftrightarrow [V^{IV}Cp_2(acac)]^{+} \leftrightarrow [V^{III}Cp_2(acac)]^{0}$$

Conversely, the cyclic voltammetric response of $[VCp_2(acac)](CF_3SO_3)$ in PBS, using glassy carbon as the working electrode, showed only irreversible process at –0.768 V (*vs* Ag/AgCl), over a potential range of 1.0 to –1.0 V. From the i_{pc} value of the reverse scan of the CV, it was evident the reduced V^{III} species is undergoing a full chemical transformation in aqueous medium within the time scale of cyclic voltammetric measurements.

2.4. Substitution kinetics

2.4.1. Introduction

Substitution reactions or ligand exchange are usually divided into three main groups: nucleophillic substitution, electrophillic substitution and oxidative addition followed by reductive elimination.[104] These substitution reactions involve the interaction between 18-electron and 16-electron species.

2.4.2. Mechanism of substitution reactions

The two main mechanisms of ligand substitution that can be identified are the dissociative mechanism and the associative mechanism.

2.4.2.1. The dissociative mechanism

The dissociative mechanism resembles S_N1 substitution in organic chemistry. Firstly the leaving monodentate ligand dissociates from the coordination sphere of the metal. The number of monodentate ligands bonded to the central metal atom is thus reduced. Secondly, the incoming (entering) ligand reacts with the transition state to form the final product. The intermediate transition state, $[L_nM]$, is coordinatively unsaturated and very reactive.

$$\text{Slow step:} \quad [L_nM - X] \xrightarrow{k,\ \text{slow}} [L_nM] + X$$

$$\text{Fast step:} \quad [L_nM] + Y \xrightarrow{\text{fast}} [L_nM - Y]$$

The kinetic rate law take the form of: rate = $k[L_nM – X]$ and the entropy (ΔS) is positive because the transition state is less ordered than the starting materials. In a dissociative mechanism, the stereochemistry may be retained or racemization may take place. This depends on the rate at which the incoming ligand traps the intermediate.[105]

2.4.2.2. The associative mechanism

The associative mechanism resembles S_N2 substitution in organic chemistry. The incoming ligand initially binds to the metal centre, leading to an intermediated with an increased coordination number. This intermediate subsequently undergoes a further reaction, where the leaving group detaches to give the substituted product.

$$\text{Slow step:} \quad [L_nMX] + Y \xrightarrow{k,\ \text{slow}} [L_nMX - Y]$$

$$\text{Fast step:} \quad [L_nMX - Y] \xrightarrow{\text{fast}} [L_nM - Y] + X$$

A different kinetic rate law applies: rate = $k[L_nMX][Y]$. The entropy (ΔS) is negative, which implies that the transition state is more ordered than the starting materials. Electron-deficient complexes (*e.g.* 16 or 17 valence electron compounds) favour the associative mechanism, but some 18 electron compounds also follow the associative mechanism.[105] The associative mechanism often involves solvolysis (Scheme 2.22), especially if the solvent is polar or has a tendency to solvate. If solvolysis takes place the kinetic rate law changes to:

$$\text{rate} = (k_s + k_2[Y])[L_nM – X] = k_{obs}[L_nM – X]$$

where $k_{obs} = k_s + k_2[Y]$, k_s = rate constant of solvent pathway and k_2 = rate constant of the direct pathway.

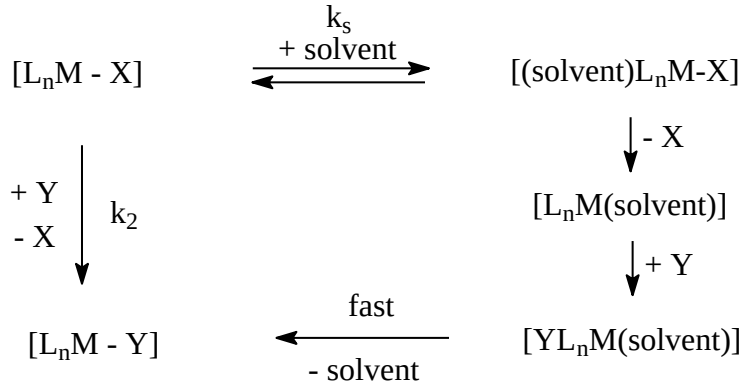

Scheme 2.22. Schematic representation of the direct and solvent pathway for the associative mechanism.

2.4.3. Factors influencing substitution reaction rates[106]

Factors that may influence the rate of substitution is the type and nature of all the ligands involved (entering, leaving and remaining), the central metal atom and the solvent.

2.4.3.1. Effect of the entering ligand

As expected for an associative mechanism, the entering ligand has a large influence on the rate of the reaction. The nucleophilicity of the incoming ligand is one of the most important factors that influence the reaction rate. Nucleophilicity is a measure of the ability of an incoming ligand to attack the positive metal centre or the ability to supply the electrons needed for the reaction to proceed. The ability of an incoming ligand to induce bond making and breaking processes, thus determines the rate of a substituted reaction. A strong nucleophile will attack the metal centre of a complex more readily than a weaker one and would hence form a more stable bond with the central metal atom. Consequently, the reaction rate will increase with increasing strength of the incoming ligand's nucleophilicity. This has been confirmed by the rate constants obtained for the substitution of Cl^- by a large variety of ligands from *trans*-$[Pt(py)_2(Cl)_2]$ (Scheme 2.23 and Table 2.8).[107, 108] These rate constants have been fitted to the Swain-Scott equation (Equation 2.9) and are used to set up a scale of nucleophilic power for ligand substitution.

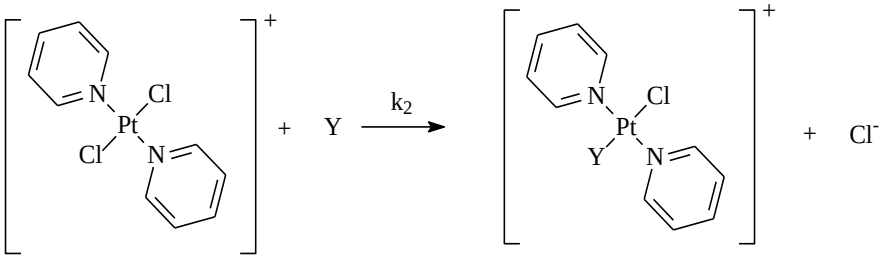

Scheme 2.23. Substitution reaction of Cl^- by a large variety of ligands (Y) from *trans*-$[Pt(py)_2(Cl)_2]$.

Table 2.8. Second order rate constants (k_2) of the substitution reaction of *trans*-$[Pt(py)_2(Cl)_2]$ with a number of nucleophiles in CH_3OH.

Nucleophile	10^3 k_2 / dm^3 mol^{-1} s^{-1}	n_{Pt}	pK_a*
CH_3OH	1 x 10^{-5}	0.0	-1.7
CH_3O^-	Very slow	<2.4	15.7
Cl^-	0.45	3.04	-5.7
NH_3	0.47	3.07	9.25
C_5H_5N	0.55	3.19	5.23
Br^-	3.7	3.7	-7.7
$(CH_3)_2S$	21.9	21.9	-5.3
I^-	107	5.46	-10.7
$AsPh_3$	2320	6.89	-
CN^-	4000	7.14	9.3
PPh_3	249000	8.93	2.73

*pK_a values in water.[107, 108]

Equation 2.9.

$$\log k_2 = s n_{Pt} + \log k_s$$

In equation 2.9 k_2 = second order rate constant of the substitution reaction of the nucleophile, k_s = rate constant for solvation reaction, *s* = nucleophilic discrimination factor (measure of the sensitivity of the substrate) and n_{Pt} = nucleophilic reactivity constant. The terms *s* and k_s depend only on the Pt complex and not the incoming ligand. The n_{Pt} value can be used to correlate kinetic data for other Pt(II) complexes. Values of n_M and *s* can be used to predict reaction rates.

Basicity, is a thermodynamic term and is defined by the pK_a of the conjugated acid of the Lewis base (a nucleophile), and differs significantly from nucleophilicity, which is a kinetic term. There is also no correlation between the pK_a and nucleophilicity of an incoming ligand. The basicity of the incoming ligand (in contrast to the nucleophilicity) has a rather small effect

on the rate of associative substitution reactions. This can be seen from the substitution reaction rates of [Rh(acac)(cod)] with derivatives of 1,10-phenanthroline and 2,2'-dipyridyl (Scheme 2.24 and Table 2.9).[109]

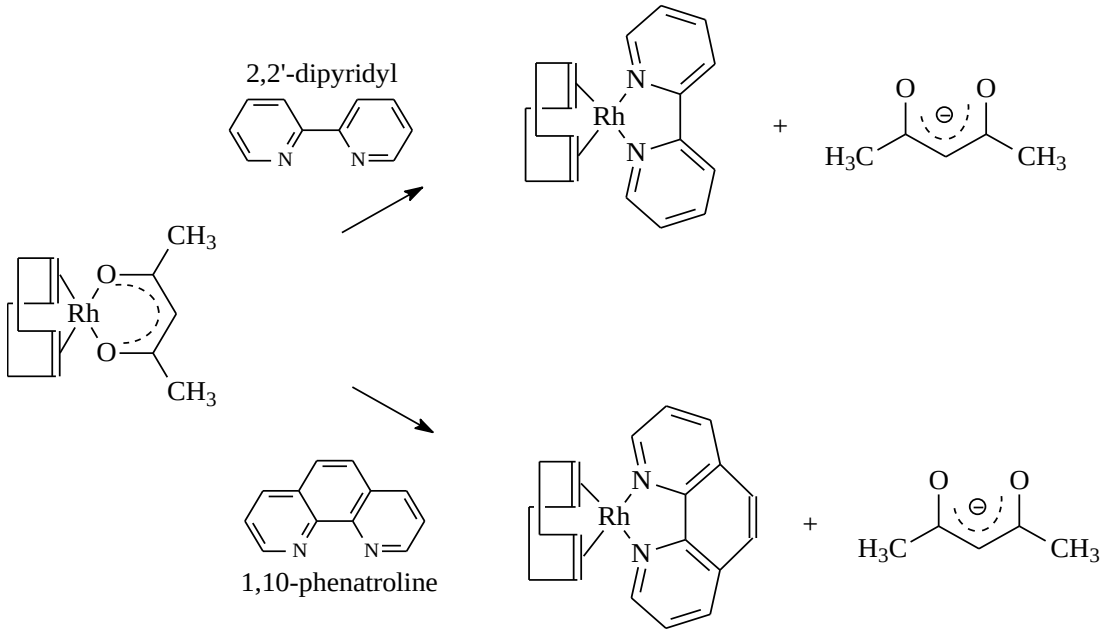

Scheme 2.24. Substitution reaction of β-diketonato ligand by various derivatives of 1,10-phenanthroline and 2,2'-dipyridyl from [Rh(acac)(cod)].

Table 2.9. Second order rate constants (k_2) and activation parameters for the substitution of β-diketonato ligand by various derivatives of 1,10-phenanthroline and 2,2'-dipyridyl from [Rh(acac)(cod)] in CH_3OH.

Incoming ligand	pK_a[#]	k_2 / dm^3 mol^{-1} s^{-1}	ΔH^* / kJ mol^{-1}	ΔS^* / kJ mol^{-1}
5- nitro-phenanthroline	3.57	12.4	30.8	-121
1,10-phenanthroline	4.96	29.00	32.6	-108
5,6-dimethyl-phenanthroline	5.20	19.9	38.7	-90
4,7-dimethyl-phenanthroline	5.97	18.8	36.7	-97
3,4,7,8-tetramethyl-phenanthroline	6.31	19.6	40.7	-84
2,2'-dipyridyl	4.30	124	36.8	-112

[#]pK_a values in water.[110]

2.4.3.2. Effect of the leaving group

In contrast to the incoming ligand, the second order rate constant (k_2) of the substitution reaction is influenced by the basicity (pK_a) of the leaving group. As the basicity of the leaving

group decreases the second order rate constant of substitution increases. This is illustrated by the substitution of the β-diketonato ligands from [Rh(β-diketonato)(cod)] with 1,10-phenantroline (see example Scheme 2.22 and Table 2.10).[111]

Table 2.10. Second order rate constants (k_2) and activation parameters for the reaction between [Rh(β-diketonato)(cod)] and 1,10-phenantroline in CH_3OH.

B-diketonato	$pK_a^{\#}$	k_2 / dm^3 mol^{-1} s^{-1}	ΔH^* / kJ mol^{-1}	ΔS^* / kJ mol^{-1}
$CH_3COCHCOCH_3$	8.95	29.0	32.6	-108
$CH_3COCHCOPh$	8.70	51.2	31.6	-106
PhCOCHCOPh	9.35	61.4	27.3	-119
$CH_3COCHCOCF_3$	6.30	1330	30.5	-83
$PhCOCHCOCF_3$	6.30	2420	26.2	-93
$CF_3COCHCOCF_3$	4.35	276000	23.2	-63

$^{\#}pK_a$ values in water.[109, 111]

The effect of the leaving group is often related to the strength of the M-X bond (metal-ligand bond, where X = the leaving group). A stronger M-X bond makes it more difficult for X to be substituted by another ligand, resulting in a decrease in the substitution rate. The opposite applies to the weaker M-X bond.

2.4.3.3. Effect of the remaining ligand

The remaining groups in the coordination sphere of the metal, *cis* and *trans* to the leaving group also play an important part in the rate of substitution. The *trans*-influence is a thermodynamic property, which can be defined as the influence a fixed ligand has on the metal-ligand bond *trans* to it, and it may influence the crystallography bond length. The *trans*-effect is a kinetic property, which is defined as the effect a fixed ligand has on the rate of substitution of a ligand *trans* to it.[112] The kinetic *cis*-effect of a coordinated ligand is defined the same as the *trans*-effect except that it is the effect a fixed ligand has on the rate of substitution for another ligand *cis* to it. The influence of the two groups *cis* to the leaving group is less pronounced than that found for the group *trans* to the leaving group. The similarity between the *cis*- and *trans*-effect stems from the direct communication between *cis*-ligands *via* the metal p_y and d_{x2-y2} orbitals. In cases where a relatively poor nucleophile acts as the entering group, the relative ability of ligands to act as *trans* labilizers is the same as their ability to act as *cis* labilizers. (Scheme 2.25).

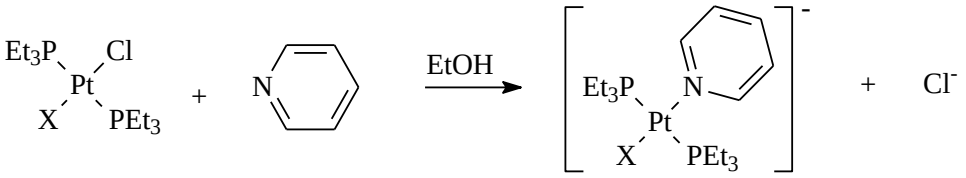

(A) [largest *trans*-effect] X = H^- (>10000) > CH_3^- (>170) > $C_6H_5^-$ (40) > Cl^- (1) [smallest *trans*-effect]

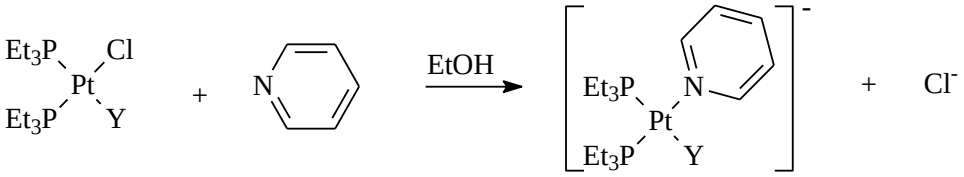

(B) [largest *cis*-effect] Y = CH_3^- (3.6) > $C_6H_5^-$ (2.3) > Cl^- (1) [smallest *cis*-effect]

Scheme 2.25. (A) Illustration of the *trans*-effect by measuring the kinetic substitution rate. X = ligand exerting the *trans*-effect. Rate constants, expressed as the ratio k(X)/k(Cl), are given in brackets after each X. (B) Illustration of the *cis*-effect by measuring the kinetic substitution rate. Y = ligand exerting the *cis*-effect. Rate constants, expressed as the ratio k(Y)/k(Cl), are given in brackets after each Y.

From molecular orbital calculations it is shown that ligands that weaken bonds *trans* to themselves also weaken bonds *cis* to them, but not by much.[113] In the transition state, bond breaking becomes somewhat easier for good *cis*-directors and the reaction rate increases, but not quite as much as it would have been if the *cis* ligand was in the *trans* position.

The sterically hindrance of bulky ligands coordinated to the metal centre also influence the rate of substitution. In sterically crowded complexes, bulky ligands shield the metal centre, thereby blocking the attack of the incoming ligand. An example of this is the hydrolysis of *cis*-[Pt(Cl)L(PEt_3)$_2$] where Cl^- is replaced,[114] and there is a decrease in reaction rate the more bulky the ligand becomes (Table 2.11).

Table 2.11. Rate constants (k) for the hydrolysis of *cis*-[Pt(Cl)L(PEt_3)$_2$].

Bulky ligand (L)	10^4 k / s^{-1}
Pyridine	800
2-methylpyridine	2.0
2,6-dimethylpyridine	0.01

These results indicate that increasing steric hindrance of ligands coordinated to a metal complex progressively retards the substitution rate of the incoming ligand. Also, *cis* hindrance is

more effective than *trans* hindrance, in [PtCl(2,6-dimethylpyridine)(PEt_3)$_2$] the *ortho*-CH_3 of 2,6-dimethylpyridine, blocks the positions above and below the plane of the complex, causing steric hindrance for the position *cis* to it. The group *trans* to the 2,6-dimethylpyridine is more susceptible for attack as can be see from Figure 2.18.

cis-isomer *trans*-isomer

Figure 2.18. Structure of *cis*- and *trans*-[PtCl(2,6-dimethylpyridine)(PEt_3)$_2$].

2.4.3.4. Effect of the central metal atom

The dependence of the rate of substitution on the central metal is based on the ability of the metal (with coordination sphere of four) to form a five coordinated transition state in an associative mechanism and the metal's ability to form a three coordinated transition state in a dissociative mechanism. The relative rate of substitution decreases in going from top to bottom in a given group of transition metals in the periodic table as well as going from right to left in a given row of the transition metals of the periodic table.[115]

2.4.3.5. Effect of the solvent

The influence of the solvent lies in its ability to solvate the metal, this influences the energetics of the activation process of the ground and activated states. It can also act as a nucleophile in the reaction (Scheme 2.22), to change the kinetic rate law to:

$$rate = (k_s + k_2[Y])[complex]$$

where k_s is the rate constant of the solvent pathway. A large k_s is observed for solvents which has a good ability to donate electrons to the metal and coordinates strongly to the metal. The general order of stronger solvation power by solvents is:

$$(CH_3)_2SO > CH_3NO_2, H_2O > ROH$$

Solvents like benzene and chloroform which coordinates very poorly to metals, have little or no influence on the reaction rate, seeing as $0 \approx k_s << k_2$.

2.4.4. Substitution kinetics of bidentate titanium-complexes with a bidentate ligand

The general rate law applicable to the substitution reaction between titanocenyl complexes of the type $[Tc(L_1L_2)]^x$ (x = 0, +1) and an incoming ligand L_3L_4 (L_1L_2 and L_3L_4 both bidentate ligands according to Scheme 2.26, is given by Equation 2.10.

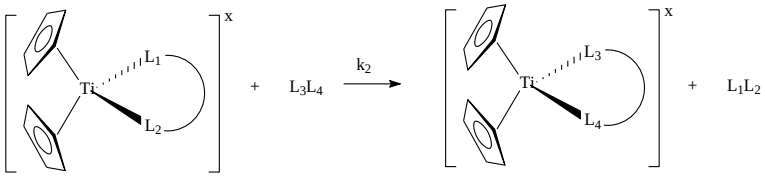

Scheme 2.26. General reaction scheme of the substitution reaction of titanocenyl complexes with a bidentate ligand, x = 0, +1, the charge of the titanocenyl complex.

Equation 2.10.

$$Rate = \{k_s + k_2[L_3L_4]\}[[Tc(L_1L_2)]^x]$$

with x = 0, +1, the charge of the titanocenyl complex. If $[L_3L_4] >> [[Tc(L_1L_2)]^x]$ then this rate simplifies to:

$$Rate = k_{obs}[[Tc(L_1L_2)]^x]$$

with the pseudo first-order rate constant $k_{obs} = k_s + k_2[L_3L_4]$. Here k_2 is the second order rate constant for the substitution process and k_s is the rate constant associated with the solvent (in this case acetone) taking part in the reaction. For the reactions studied, the plot of k_{obs} *vs* $[L_3L_4]$ passes through the origin, suggesting $k_s << k_2$ for acetone as the solvent. The observed zero intercept is to be expected because the displacement rate of the bidentate ligand (L_1L_2) by a monodentate solvent would be much slower or even approach zero, compared to L_1L_2 displacement by the bidentate ligand L_3L_4.

This reaction can occur *via* a dissociative (see Scheme 2.27.A), an interchange (see Scheme 2.27 B) or an associative (Scheme 2.27.C) mechanism.

Scheme 2.27.A

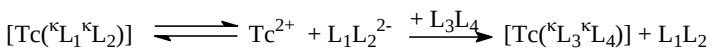

Scheme 2.27.B

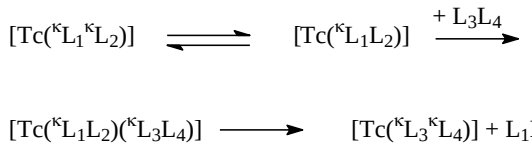

Scheme 2.27.C

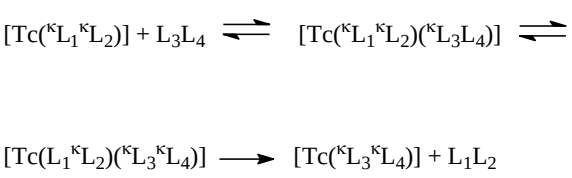

Scheme 2.27. Substitution reaction of titanocenyl complexes with a bidentate ligand *via* a dissociative (A), interchamge (B) or an associative (C) mechanism. (Note that only the mechanism of the neutral titanocenyl complex is used for demonstration in the Scheme.) The κ symbols indicate ligand coordination to the titanocenyl.

The dissociative or interchange mechanism (Scheme 2.27. A and B) is improbable due to reluctance of formation of $[(Cp)_2Ti]^{2+}$ or $[Tc(^{\kappa}L_1L_2)]$, a 14 and 16 electron species, whereas the associative mechanism is more probable due to the fact that Ti^{IV} can form a five coordinated 18 electron species.[116]

The activation enthalpy (ΔH^*) and activation entropy (ΔS^*) of substitution reaction according to Scheme 2.26 can be determined from a least-squares fit by a fitting program such as MINSQ,[117] of the reaction rate constants *vs* temperature data according to the Eyring relationship (Equation 2.11).[118]

Equation 2.11.

$$\ln (k/T) = \ln (k_b/h) - (\Delta H^*/RT) + (\Delta S^*/R)$$

Here k_b = Boltzmann's constant (1.38×10^{-23} J K^{-1}), h = Planck's constant (6.626×10^{-34} J s), R = Gas constant (8.314 J mol^{-1} K^{-1}). The linear free energy ΔG^* may be calculate from Equation 2.12.[119]

Equation 2.12.

$$\Delta G^* = \Delta H^* - T\Delta S^*$$

Large negative activation entropies (ΔS^*) imply that the mechanism of substitution is associative of nature, when a mechanism changes from associative to dissociative, ΔS^* values of the reaction would near zero. Large positive activation entropy ΔS^* implies that the mechanism

of substitution is dissociative of nature. It must, however, be kept in mind that ΔS^* values are not the absolute distinction between an associative and a dissociative mechanism. Activation volumes (ΔV^*), which are obtained during high-pressure kinetic studies, are a better measure for the mechanism. For a dissociative mechanism ΔV^* would be positive whereas it would be negative for an associative mechanism.

2.4.5. Activation parameters

The rate of chemical reactions increases with temperature. Generally, the dependence of the rate constant k on temperature follows the Arrhenius equation (Equation 2.13).[120]

Equation 2.13.

$$k = Ae^{(-Ea/RT)}$$

Here E_a is the activation energy and is useful in determining the mechanism of the reaction. The higher the activation energy the slower the reaction at any given temperature.

Other activation parameters include ΔH^*, ΔS^*, $\Delta G^*$and ΔV^*. The sign and magnitude of these thermodynamic parameters also often indicates the mechanism of a reaction. The transition state theory postulates that an activated complex is in equilibrium with the reagent before the reaction takes place and that the reaction rate is given by the rate of decomposition of the activated complex to form the products (Scheme 2.28) and the rate constant is given by Equation 2.14.

$$A + B \underset{}{\overset{K_c^*}{\rightleftharpoons}} [A\cdot B]^* \xrightarrow{k} \text{products}$$

Scheme 2.28. General scheme illustrating the transition state theory.

Equation 2.14.

$$k = (RT/Nh)K_c^*$$

Here K_c^* = equilibrium constant, R = gas constant, h = Planck's constant, N = Avogadro's number and T = absolute temperature.

The information of this activated complex is governed by thermodynamic considerations similar to those of ordinary chemical equilibria. The free energy of activation is thus defined thermodynamically as shown in Equation 2.15.

Equation 2.15.

$$\Delta G^* = -RT \ln K_c^*$$
$$= \Delta H^* - T\Delta S^*$$

Combination of Equations 2.14 and 2.15 gives Equation 2.16.

Equation 2.16.

$$\ln k = \ln [(RT)/(Nh)] + \Delta S^*/R - \Delta H^*/ RT$$

The magnitude of ΔS^*, can be used to determine whether the mechanism of substitution is associative or dissociative of nature. A small negative or positive ΔS^* value indicates a dissociative mechanism and a large negative ΔS^* value indicates an associative mechanism of substitution.

The volume of activation consists of two parts an intrinsic part ΔV^*_{intr} and a solvation part ΔV^*_{solv}, and is defined in Equation 2.17.

Equation 2.17.

$$\Delta V^* = \Delta V^*_{intr} + \Delta V^*_{solv}$$

The volume changes that arise during the formation of the transition state due to the vibrations in bond lengths and angles are represented by ΔV^*_{intr}, while the change in solvation is reflected by ΔV^*_{solv}. For a dissociative mechanism ΔV^*_{intr} is positive due to bond cleavage and ΔV^*_{solv} is negative due to electrostriction, thus $\Delta V^*$is approximately zero for a dissociative mechanism.[121] For an associative mechanism on the other hand ΔV^* is large negative, due to the negative contribution from ΔV^*_{intr} (which arises from the bond formation) and only a minor contribution from ΔV^*_{solv}. Hence, a dissociative mechanism is indicated by small negative or positive ΔS^* (measured in J) and ΔV^* values, whereas large negative ΔS^* and ΔV^* values indicate an associative mechanism.

2.5. Cytotoxic studies

Since the initial discovery of the efficiency of the platinum(II) compound *cis*-$PtCl_2(NH_3)_2$ (cisplatin) as an anti-cancer drug,[122] the anti-proliferative activities of a wide variety of metal compounds have been investigated.[14, 123]

Titanocene derivatives and bis(β-diketonato)titanium(IV) appear to offer a different alternative for cancer chemotherapy. They do not follow the rationale and mechanism of action of the platinum complexes.[20]

Diacido titanium complexes of type Cp_2TiX_2, where X = carboxylates, phenolates, dithiolenes and thiophenolates have shown anti-proliferative action.[14] Other mono-substituted complexes of formula Cp_2TiClX, where X = 1,3,5-trichlorophenolate, 1-aminothiophenolate, 1-methylphenolate and selenophenolate, have also exhibited similar anti-tumour activity.[14, 124]

Attempts aimed at improving the anti-tumour activity of cyclopentadienyl metal or metallocenyl complexes included the replacement of H of $C_5H_5^-$ for R (R = CH_3, C_2H_5 and $N(CH_3)_2$) groups ranging from mono- to deca-substitution. This modification of the Cp ligand on $(C_5H_5)Ti^{2+}$ showed a dramatic reduction in the anti-tumour activity, as the degree of H substitution increases.[14] However, substitution on the cyclopentadienyl ring(s) with carbomethoxy has shown increased anti-tumour action.[15]

Several ionic titanocene complexes of general formula $[Cp_2TiXL]^+Y^-$ or $[Cp_2TiL_2]^{2+}[Y^-]_2$, where X is an anionic ligand and L is a neutral ligand, have been tested for anti-proliferative action. These species offer higher solubility in water than the neutral titanocene dihalides. Some representative examples of this type of complex are $[Cp_2Ti(bipy)][CF_3SO_3]_2$, $[Cp_2Ti(phen)][CF_3SO_3]_2$, $[Cp_2Ti[o\text{-}S(NHCH_3)C_6H_4]^+I^-$ and $[Cp_2Ti(Cl)NCCH_3]^+[FeCl_4]^-$.[14, 123, 125]

Budotitane (Figure 2.19) belongs to the class of bis(β-diketonato)metal complexes.[126] The M(β-diketonato)$_2X_2$ complexes are highly susceptible to hydrolysis and are relatively difficult to dissolve in water. Variation of the R groups (no. A-D) of the (β-diketonato) ligands in [M(β-diketonato)$_2X_2$] complexes can increase the anti-tumour activity; the anti-tumour activity is independent of the leaving group X (Table 2.12).[2]

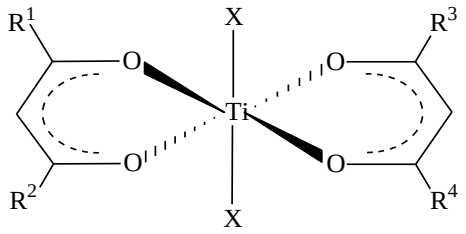

Variations of X, R^1, R^2, R^3 and R^4 are shown in Table 2.12.

Figure 2.19. Structure of budotitane.

Table 2.12. Anti-tumour activity of Ti(β-diketonato)$_2$X$_2$. T/C(%) = (median survival time of treated animal vs. median survival time of control animal) x 100.

Number	β-diketonato	X	T/C(%)
A	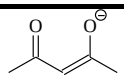	OEt	90-100
B	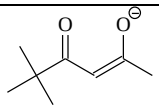	OEt	130-170
C	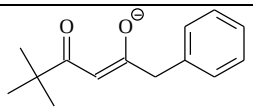	OEt	150-200
D	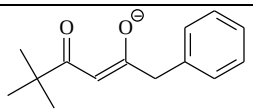	Cl	150-200
E	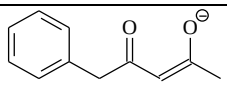	OEt	130-170
F	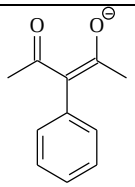	OEt	200-250
G	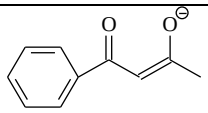	OEt	>300
H	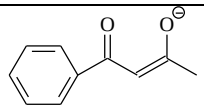	Cl	>300
I	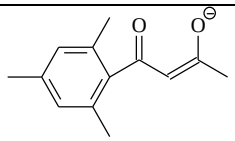	Cl	>300
J	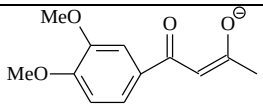	Cl	150-200
K	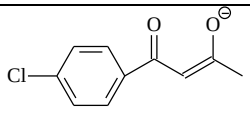	Cl	150-200
L	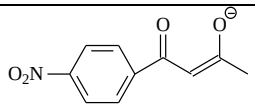	Cl	100-120

From the examination of the extent to which the aromatic groups (E-H) on the β-diketonato ligand in complexes of the type [M(β-diketonato)$_2$X$_2$] changes the anti-cancer efficiency of the complexes in mice, it is evident that when phenyl groups stand in direct

conjugation to the metal enolate pseudo-aromatic ring, the anti-tumour activity increase dramatically (G-H).

Variations on the phenyl ring (I-L) also affect the anti-tumour properties of the complexes. The introduction of methyl groups at the phenyl ring (I) does not alter anti-tumour activity, whereas methoxy, chlorine and nitro groups reduce anti-tumour activity (J-L).

Another parameter in changing the activity of the [M(β-diketonato)$_2$X$_2$] type of complexes is changing of the central metal atom of the complexes (Table 2.13).[2] In this case the titanium and zirconium derivatives with the benzoylacetonato ligand produces the highest activity, followed by a marked decrease in the order Hf > Mo > Sn > Ge for the other metals tested (Table 2.13).

Table 2.13. Anti-tumour activity of M(bzac)$_2$X$_2$.

M	T/C(%)
Ti	>300
Zr	>300
Hf	200-250
Mo	150-200
Sn	120-150
Ge	100-110

[1] P. Köpf-Maier, *Z. Naturforsch*., 1979, **34c**, 1174.

[2] B.K. Keppler and M.E. Heim, *Drugs of the Future*, 1988, **3,** 638.

[3] H. Köpf and P. Köpf-Maier, *Angew. Chem. Int. Ed. Engl.*, 1979, **18**, 477.

[4] A. Ravzavi and J. Ferrara, *J. Organomet. Chem.*, 1992, **435**, 299.

[5] F.H. Gorlitz, P.K. Gowik, T.M. Klapotke, D. Wang, R. Meier and J.V. Weltzen, *J. Organomet. Chem.*, 1991, **408**, 343.

[6] J.C. Green, M.L.H. Green and C.K. Prout, *J. Chem. Soc., Chem. Commun.*, 1972, 421.

[7] G.L. Soloveichik, T.M. Arkhireeva, V.K. Bel'skil and B.M. Bulychev, *Metalloorg. Khim.*, 1988, **1**, 226.

[8] T.S. Cameron, T.M. Klapotke, A. Schulz and J. Valkonen, *J. Chem. Soc., Dalton Trans.*, 1993, 659.

[9] G.H.W. Milburn and M.R. Truter, *J. Chem. Soc. (A)*, 1966, 1609.

[10] P. Köpf-Maier, M. Leitner and H. Köpf, *J. Inorg. Nucl. Chem.*, 1980, **42**, 1789.

[11] P. Köpf-Maier, B. Hesse and H. Köpf, *J. Cancer Res. Clin. Oncol.*, 1980, **96**, 43.

[12] S. Bradley, P.C. McGowan, K.A. Oughton, M. Thornton-Pett and M.E. Walsh, *J. Chem. Soc., Chem. Commun.*, 1999, 77.

[13] M.A.D. McGowan and P.C. McGowan, *Inorg. Chem. Commun.*, 2000, **3**, 337.

[14] P. Köpf-Maier and H. Köpf, *Struct. Bonding*, 1988, **70**, 103.

[15] J.R. Boyles, M.C. Baird, B.G. Campling and N. Jain, *J. Inorg. Biochem.*, 2001, **84**, 159.

[16] W.P. Hart, D. Shihua and M. D. Rausch, *J. Organomet. Chem.*, 1985, **282**, 111.

[17] M.D. Rausch, J.F. Lewison and W.P. Hart, *J. Organomet. Chem.*, 1988, **358**, 161.

[18] J.A. Smith, J.V. Seyerl, G. Hutter and H.H. Brintzinger, *J. Organomet. Chem.*, 1979, **173**, 175.

[19] P.J. Shapiro, *Coord. Chem. Rev.*, 2002, **231**, 67.

[20] E. Meléndez, *Crit. Rev. Oncol.*, 2002, **42**, 309.

[21] G. Wilkinson, Editor, *Comprehensive Organometallic Chemistry*, vol.3, Pergamon Press, Oxford, 1982, pp. 271-547 and references therein.

[22] J.M. Shreeve, Editor, *Inorganic Synthesis*, vol. 24, John Wiley & Sons, New York, p 147, 1986.

[23] R.T. Carlin and J. Fuller, *Inorg. Chim. Acta*, 1997, **225**, 189.

[24] H. Köpf and M. Smichmidt, *Z. Anorg. Allg. Chem.*, 1965, **340**, 139.

[25] S.A. Giddings, *Inorg. Chem.*, 1967, **6**, 849; R.B. King and C.A. Eggers, *Inorg. Chem.*, 1968, **7**, 340.

[26] G. Fachinetti and C. Floriani, *J. Chem. Soc., Dalton Trans.*, 1974, 2433.

[27] P.C Wailes, H. Weigold and A.P. Bell, *J. Organomet. Chem.*, 1971, **33**, 181.

[28] P.C. Bharara, *J. Organomet. Chem.*, 1976, **121**, 199.

[29] R. Choukroun and Gervais, *J. Chem. Soc., Dalton Trans.*, 1980, 1800.

[30] K. Andrä, *J. Organomet. Chem.*, 1968, **11**, 567.

[31] S.A. Shackelford, D.F. Shellhamer and V.L. Heasley, *Tetrahedron Lett.*, 1999, **40**, 6333.

[32] M.G. Meirim, E.W. Neuse, M. Rhemtula and S. Schmitt, *Trans. Met. Chem.*, 1988, **13**, 272.

[33] P.L. Timms and T.W. Turney, *Adv. Organomet. Chem.*, 1977, **15**, 53.

[34] G. Wilkinson, Editor, *Comprehensive Organometallic Chemistry*, vol. I and II, Pergamon Press, Oxford, 1982 and references therein.

[35] A.I. Vogel, *Practical Organic Chemistry including Qualitative Organic Analysis*, 3rd Edition, Longman, London, 1977, pp. 864-865.

[36] T.J. Pinnavalia and R.C. Fay, *Inorg. Chem.*, 1968, **7**, 502.

[37] D.A. White, *J. Inorg. Nucl. Chem.*, 1971, **33**, 691.

[38] R.S.P. Coutts and P.C. Wailes, *Aust. J. Chem.*, 1969, **22**, 1547.

[39] A.M. Bond, R. Colton, U. Englert, H. Hűgel and F. Merken, *Inorg. Chim. Acta*, 1995, **235**, 117.

[40] F. Bottomley, I.J.B. Lin and P.S. White, *J. Organomet. Chem.*, 1981, **212**, 341.

[41] H. Klein and U. Thewalt, *J. Organomet. Chem.*, 1980, **194**, 297.

[42] G. Doyle and R.S. Tobias, *Inorg. Chem.*, 1967, **6**, 1111.

[43] N.V. Alekseev and I.A. Ronova, *Zh. Strukt. Khim.*, 1966, **7**, 103.

[44] G. Doyle and R.S. Tobias, *Inorg. Chem.*, 1968, **7**, 2479.

[45] A.T. Kotchevar, P. Ghosh, D.D. DuMez and F.M. Uckun, *J. Inorg. Biochem.*, 2001, **83**, 151.

[46] A.K. Sharma and N.K. Kaushik, *Z. Naturforsch.*, 1984, **39b**, 604.

[47] U.B. Saxena, A.K. Rai, V.K. Mathur and R.C. Mehrotra, *J. Chem. Soc.*, 1970, 904.

[48] G. Doyle and R.S. Tobias, *Inorg. Chem.*, 1968, **7**, 2484.

[49] D.C. Bradley and C.E. Holloway, *J. Chem. Soc., Chem. Commun.*, 1965, 284.

[50] M.J. Frazer and W.E. Newton, *Inorg. Chem.*, 1971, **10**, 2137.

[51] H.J. Keller, B.K. Keppler and D. Schmähl, *A. Forsch.*, 1982, **32(8)**, 806.

[52] L. Wolf and C. Tröltzch, *J. Prakt. Chem.*, 1962, **17**, 78.

[53] U.B. Saxena, A.K. Rai, V.K. Mathur and R.C. Mehrotra, *J. Chem. Soc.*, 1970, 904.

[54] M.E. Silver, H.K. Chun and R.C. Fay, *Inorg. Chem.*, 1982, **21**, 3765.

[55] J.G. Leipolt, S.S. Basson and L.J. Botha, *Inorg. Chim. Acta*, 1990, **168**, 215.

[56] R. Abeywickrema, M.A. Bennett, K.J. Cavell. M. Kony, A.F. Masters and A.G. Webb, *J. Chem. Soc., Dalton Trans.*, 1993, 59.

[57] G. Bartoli, C. Cimarelli, G. Palmieri, M. Bosco and R. Dalpozzo, *Synthesis*, 1990, 895.

[58] S.I. Murahashi and Y. Tsumiyama, *Bull. Chem. Soc. Jpn.*, 1987, **60**, 3285.

[59] H.A. Stefani, I.M. Costa and D. de O. Silva, *Synthesis*, 2000, 1526.

[60] M. Cindric, V. Vrdoljak, T. Kajfez, P. Novak, A. Brbot-Saranovic, N. Strukan and B. Kamenar, *Inorg. Chim. Acta*, 2002, **328**, 23.

[61] J.G. Leipoldt, S.S. Basson, E.C. Grobler and A. Roodt, *Inorg. Chim. Acta*, 1985, **99**, 13.

[62] J.G. Leipoldt, S.S. Basson and C.R. Dennis, *Inorg. Chim. Acta*, 1981, **50**, 121.

[63] J.G. Leipoldt, G.J. Lamprecht and D.E. Graham, *Inorg. Chim. Acta*, 1985, **101**, 123.

[64] M. Niewenhyzen, R. Schobert, F. Hampel and S. Hoops, *Inorg. Chim. Acta*, 2000, **304**, 118.

[65] N. Kobayashi, A. Muranaka and K. Ishii, *Inorg. Chem.*, 2000, **39**, 2256.

[66] M. Barthel, D. Dini, S. Vagin and M. Hanack, *Eur. J. Org. Chem.*, 2002, 3756.

[67] T.A. James and J.A. McCleverty, *J. Chem. Soc.*, 1970, 3318.

[68] P. Köpf-Maier, E. Neuse, T. Klapötke and H. Köpf, *Cancer Chemother. Pharmacol.*, 1989, **24**, 23.

[69] L.E. Manzer, *J. Organomet. Chem.*, 1976, **110**, 291.

[70] M.L.H. Green and C.R. Lucas, *J. Chem. Soc., Dalton Trans.*, 1972, 1000.

[71] E.O. Fischer and R. Amtmann, *J. Organomet. Chem.*, 1967, **9**, 15.

[72] S. Gambarotta, C. Floriani, A. Chiesi-Villa and C. Guastini, *J. Am. Chem. Soc.*, 1982, **104**, 1918.

[73] G. Fachinetti, C. Floriani and H. Stoeckli-Evans, *J. Chem. Soc., Dalton Trans.*, 1977, 2297.

[74] C. Floriani and G. Floriani, *J. Chem. Soc., Chem. Comm.*, 1972, 790.

[75] G.A. Razuvaev, G.A. Domrachev, V.V. Sharutin and O.N. Suvorova, *J. Organomet. Chem.*, 1977, **141**, 313.

[76] M. Yongxiang, Z. Ying and W. Xin, *Polyhedron*, 1989, **8**, 929.

[77] P.T. Kissinger and W.R. Heineman, *J. Chem. Educ.*, 1983, **60**, 702.

[78] D.H. Evans, K.M. O'Connell, R.A. Peterson and M.J. Kelly, *J. Chem. Educ.*, 1983, **60**, 290.

[79] G.A. Mobbot, *J. Chem. Educ.*, 1983, **60**, 697.

[80] A.J. Bard and L.R. Faulknaer, *Electrochemical Methods: Fundamentals and Applications*, Wiley, New York, 1980, chapter 6.

[81] P.A. Christensen and A. Hamnett, *Techniques and Mechanisms in Electrochemistry*, Blackie Academic & Professional, London, 1994, pp. 55-67, 170-175.

[82] J.J. Van Benschoten, J.Y. Lewis, W.R. Heineman, D.A. Roston and P.T. Kissinger, *J. Chem. Educ.*, 1983, **60(9)**, 772.

[83] P.T. Kissinger and W.R. Heineman, *Laboratory Techniques in Electroanalytical Chemistry*, Dekker, New York, 1984, chapter 13.

[84] R.R. Gagné, C.A. Koval and G.C. Lisensky, *Inorg. Chem.*, 1980, **19**, 2855

[85] G. Gritzener and J. Kuta, *Pure and Appl. Chem.*, 1984, **56**, 461.

[86] H.M. Koepp, H. Wendt and H. Stehlow, *Z. Electrochem.*, 1960, **64**, 483.

[87] J. Conradie, Ph.D. Study, University of the Orange Free State, R.S.A., 1999.

[88] C. LaVanda, D.O. Cowan, C. Leitch and K. Bechgaard, *J. Amer. Chem. Soc.*, 1974, **96**, 6788.

[89] W.H. Morrison, Jr., S. Krogsrud and D.N. Hendrickson, *Inorg. Chem.*,1973, **12**, 1998.

[90] G.M. Brown, T.J. Meyer, D.O. Cowan, C. LeVanda, F. Kaufman, P.V. Roling and M.D. Rausch, *Inorg. Chem.*, 1975, **14**, 506.

[91] W.C. du Plessis, J.J.C. Erasmus, G.J. Lamprecht, J. Conradie, T.S. Cameron, M.A.S. Aquino and J.C. Swarts, *Can. J. Chem.*,1999, **77**, 378.

[92] W.C. du Plessis, T.G. Vosloo and J.C. Swarts, *J. Chem. Soc., Dalton Trans.*, 1998, 2507.

[93] J.E. Gorton, H.L. Lentzner and W.E. Watts, *Tetrahedron*, 1971, **27**, 4353.

[94] J. Langmaier, Z. Samec, V. Varga, M. Horacek, R. Choukroun and K. Mach, *J. Organomet. Chem.*, 1999, **584**, 323.

[95] G.V. Loukova and V.V. Strelets, *J. Organomet. Chem.*, 2000, **606**, 203.

[96] N. El Murr, A. Chaloyard and J. Tirouflet, *J. Chem. Soc. Chem. Comm.*, 1980, 446.

[97] M.A Vorotyntsev, M. Casalta, E. Pousson, L. Roullier, G. Boni and C. Moise, *Electrochim, Acta*, 2001, **46**, 4017.

[98] A. Vallat, R. Roulier and C. Bourdon, *J. Electroanal. Chem.*, 2003, **542**, 75.

[99] J. Langmaier, Z. Samec, V. Varga, M. Horacek, R. Choukroun and K. Mach, *J. Organomet. Chem.*, 1999, **579**, 348.

[100] G.V. Loukova and V.V. Strelets, *J. Organomet. Chem.*, 2000, **606**, 203.

[101] A. Antinolo, G.S. Bristow, G.K. Campbell, A.W. Duff, P.B. Hitchcock, R.A. Kamarudin, M.F. Lappert, R.J. Norton, N. Sarjudeen and D.J.W. Winterborn, *Polyhedron*, 1989, **8**, 1601.

[102] J. Langmaier, Z. Samec, V. Varga, M. Horacek, R. Choukroun and K. Mach, *J. Organomet. Chem.*, 1999, **584**, 323.

[103] P. Ghosh, S. Ghosh, C. Navara, R.K. Narla, A. Benyumov and F.M. Uckun, *J. Inorg. Biochem.*, 2001, **84**, 241.

[104] R.J. Cross, *Chem. Soc. Rev.*, 1985, **14**, 197.

[105] F. Mathey and A. Servin, *Molecular Chemistry of the Transition Elements*, John Wiley & Sons, Chichester, 1996, pp. 28-50.

[106] R.G. Wilkins, *Kinetics and Mechanisms of Reactions of Transition metal complexes*, 2nd Edition, VCH, Weinheim, 1991, pp. 103, 232-242.

[107] U. Belluco, L. Cattalini, F. Basolo, R.G. Pearson and A. Turco, *J. Am. Chem. Soc.*, 1995, **87**, 241.

[108] R.G. Pearson, H. Sobel and J. Songstad, *J. Am. Chem. Soc.*, 1968, **90**, 319.

[109] J.G. Leipolt, S.S. Basson, G.J. van Zyl and G.J.J. Steyn, *J. Organomet. Chem.*, 1991, **418**, 241.

[110] W. Robb and C.G. Nicholson, *S. Afr. J. Chem.*, 1978, **31**, 1.

[111] J.G. Leipoldt and E.C. Grobler, *Transition Met. Chem.*, 1986, **11**, 110.

[112] A. Werner, *Z. Anorg. Chem.*, 1893, **3**, 267.

[113] S.S. Zmdahl and R.S. Dargo, *J. Am. Chem. Soc.*, 1968, **90**, 6669.

[114] D.F Shriver, P. Atkins and C.H. Langford, *Inorganic Chemistry*, 2nd Edition, Freeman, New York, 1994, 467.

[115] F.Basolo, J. Chatt, H.B. Gray, R.G. Pearson and B.L. Shaw, *J. Chem. Soc.*, 1961, 2207.

[116] P. Köpf-Maier, E. Neuse, T. Klapötke and H. Köpf, *Cancer Chemother. Pharmacol.*, 1989, **24**, 23.

[117] L. Helm, MINSQ, Non-linear parameter estimation and model developement, least squares parameter optimisation V3.12, MicroMath Scientific Software, Salt Lake City, UT (1990).

[118] S.H. Maron and J.B. Lando, *Fundamentals of Physical Chemistry*, Macmillan Publishing Co. Inc., New York, 1974, p 677.

[119] S. H. Maron and J.B. Lando, *Fundamentals of Physical Chemistry*, Macmillan Publishing Co. Inc., New York, 1974, p 326.

[120] S. Arrhenius, *Z. Phys. Chem.*, 1889, **4**, 226.

[121] E. Whalley, *J. Chem. Phys.*, 1963, **38**, 1400.

[122] B. Rosenberg, L. VanCamp, J.E. Trosko and V.H. Mansour, *Nature*, 1969, **222**, 385.

[123] P. Köpf-Maier, *Eur. J. Clin. Pharmacol.*, 1994, **47**, 1.

[124] P. Köpf-Maier, T.P. Klapötke and H. Köpf, *Inorg. Chim. Acta*, 1988, **153**, 119.

[125] P.Köpf-Maier and H. Köpf, *Chem. Rev.*, 1987, **87**, 1137.

[126] M.J. Blandamer and J. Burgess, *Coord. Chem. Rev.*, 1980, **31**, 93.

Chapter 3

Results and Discussion

3.1. Introduction

The synthesis and characterization of a selection of new and known organometallic compounds of the type $[Mc(LL')]^{+}ClO_4^{-}$, [Mc(LL')] and $[M(Cp)(Cl)(LL')_2]$ with Mc = Tc (titanocenyl, $(C_5H_5)_2Ti^{2+}$), Zc (zirconocenyl, $(C_5H_5)_2Zr^{2+}$), Hc (hafnocenyl, $(C_5H_5)_2Hf^{2+}$) and Vc (vanadocenyl, $(C_5H_5)_2V^{2+}$), M = Ti, Zr, Hf and V and LL' = the bidentate ligands $acac^{-}$ (acetylacetonato), $bzac^{-}$ (benzoylacetonato), $tfaa^{-}$ (trifluoroacetylacetonato), fca^{-} (ferrocenoylacetonato), maa^{-} (methyl acetoacetonato), $Sacac^{-}$ (thioacetylacetonato), cat^{2-} (1,2-benzenediolato or catecholato), $Scat^{2-}$ (1,2-benzenedithiolato or thiocatecholato), $biphen^{2-}$ (2,2-biphenyldiolato) and Cp = cyclopentadienyl are described in this chapter, see Figure 3.1.

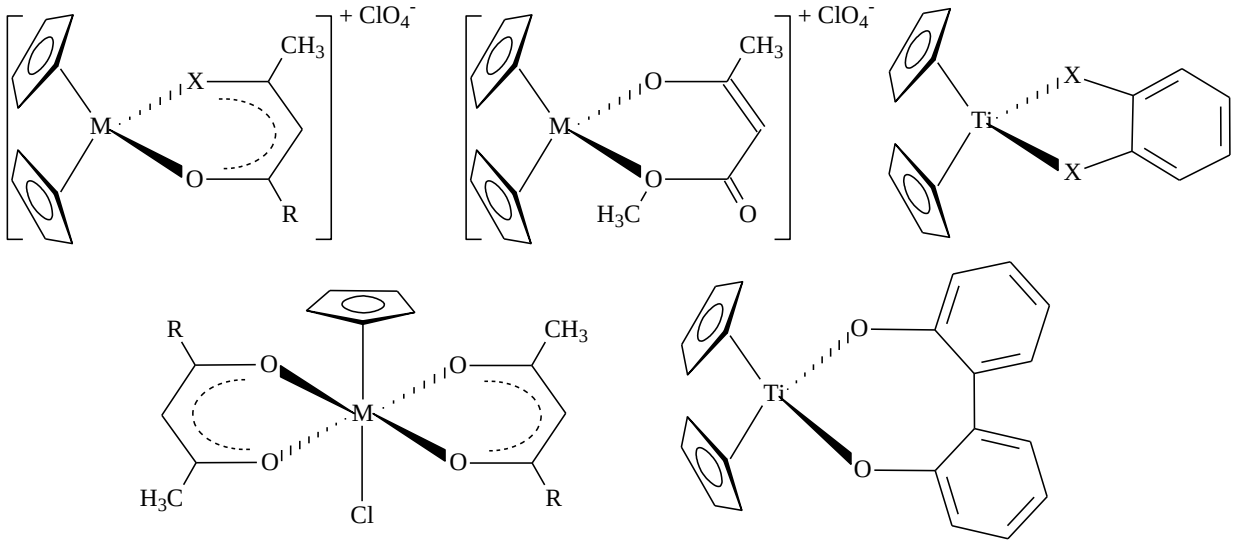

R = CH_3, CF_3, Ph and Fc

X = O, S

M = Ti, Zr, Hf and V

Figure 3.1. Structures of new and known organometallic compounds of the type $[Mc(LL')]^{+}ClO_4^{-}$, [Mc(LL')] and $[M(Cp)(Cl)(LL')_2]$.

RESULTS AND DISCUSSION

Spectroscopic characterization of these complexes was preformed by proton nuclear magnetic resonance (^{1}H NMR), infra red (IR) and ultra violet (UV) spectroscopy. New compounds were also subjected to elemental analysis.

Substitution kinetics of the cat^{2-}, $acac^-$ and $Sacac^-$ ligands with Hacac, HSacac and H_2biphen, as well as the cyclic voltammetry (CV) and bulk electrolysis (BE) of these complexes are described. The influences of the group electronegativity (χ_R) of the R groups on the β-diketonato ligand in the complexes of the kind $[Mc(CH_3COCHCOR)]^+ClO_4^-$ are correlated to the obtained formal reduction potentials.

The influence of the ring size *viz* five, six or seven-membered chelation rings on the substitution kinetics are described.

Some cytotoxic properties of selected compounds on cancer cells are also presented.

3.2. Synthesis

3.2.1. β-Diketonates and thio-β-diketonates

The β-diketone ferrocenoylacetone (Hfca) [40] was prepared by Claisen condensation of acetylferrocene and ethyl acetate in the presence of a base (Scheme 3.1).

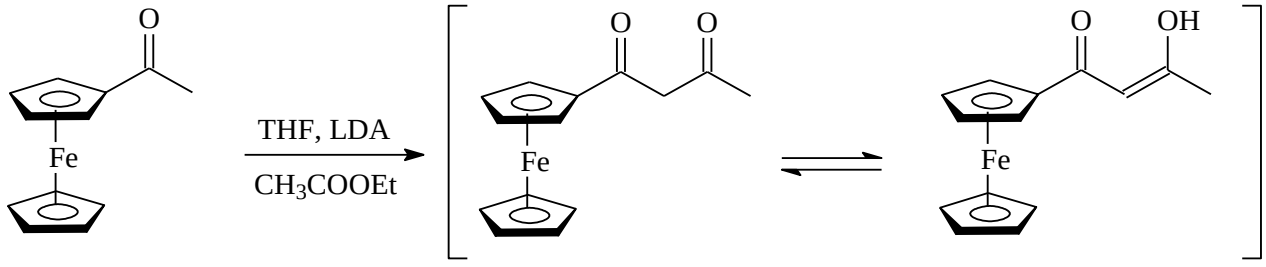

[40]

Scheme 3.1. Synthetic route utilized for preparation of [40].

β-Diketones exist in solution and in the vapour phase,[1] in equilibrium mixtures of keto and enol tautomers. A ^{1}H NMR study indicates, by comparing the relative intensities of the CH_2 (keto) and CH (enol) signals, that the enol form dominates in solution.[2]

Thioacetylacetone [26] was synthesised *via* a reaction between acetylacetone and H_2S under acidic conditions (Scheme 3.2).

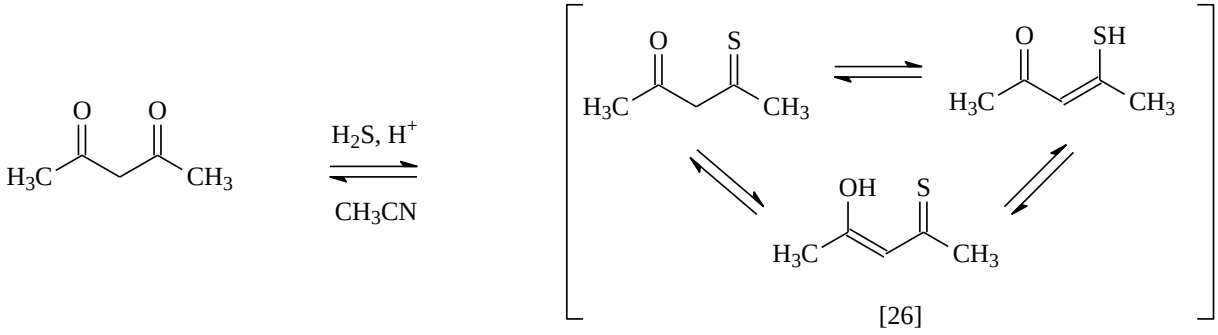

Scheme 3.2. Synthetic route utilized for preparation of [26].

The critical factors controlling the reaction are temperature and the nature of the solvent used. Treatment of acetylacetone with both H_2S gas and HCl gas at -40˚C leads to the complete and exclusive formation of thioacetylacetone within 6h. Decomposition takes place slowly at room temperature, but freshly prepared thioacetylacetone can be kept for months at -20˚C.

3.2.2. Titanium complexes

Tetrahedral mono-β-diketonate titanium(IV) complexes of the type [Tc(β-diketonato)]$^+ClO_4^-$; octahedral bis-β-diketonate titanium(IV) complexes of the type [Ti(Cp)(Cl)(β-diketonato)$_2$] and tetrahedral bi-chelating titanium(IV) complexes of the kind [Tc(bi-chelating ligand)] were synthesized.

3.2.2.1. Mono-β-diketonato titanocenyl complexes

A variety of [Tc(β-diketonato)]$^+ClO_4^-$ complexes (see Table 3.1) were synthesized according to the general procedure as described by Doyle and Tobias (Scheme 3.3).[3] The synthesis starts with the dissolving of $TcCl_2$ in water to give a cationic species. Next follows the replacement of the two Cl^- groups of the titanocene dichloride with perchlorate (ClO_4^-). This reaction is driven by the precipitation of silver chloride (AgCl). This replacement is made to enhance the next step of the synthesis. Seeing as ClO_4^- is a much better leaving group than Cl^-, the substitution of the β-diketonate ligand onto the titanium centre is promoted. The product that forms is an ionic species with ClO_4^- as the counter ion. A base or hydrogen acceptor is not

needed in this reaction due to the fact that the β-diketonate moiety has a keto-enol tautomere and the major form in solution is the enol form.[2]

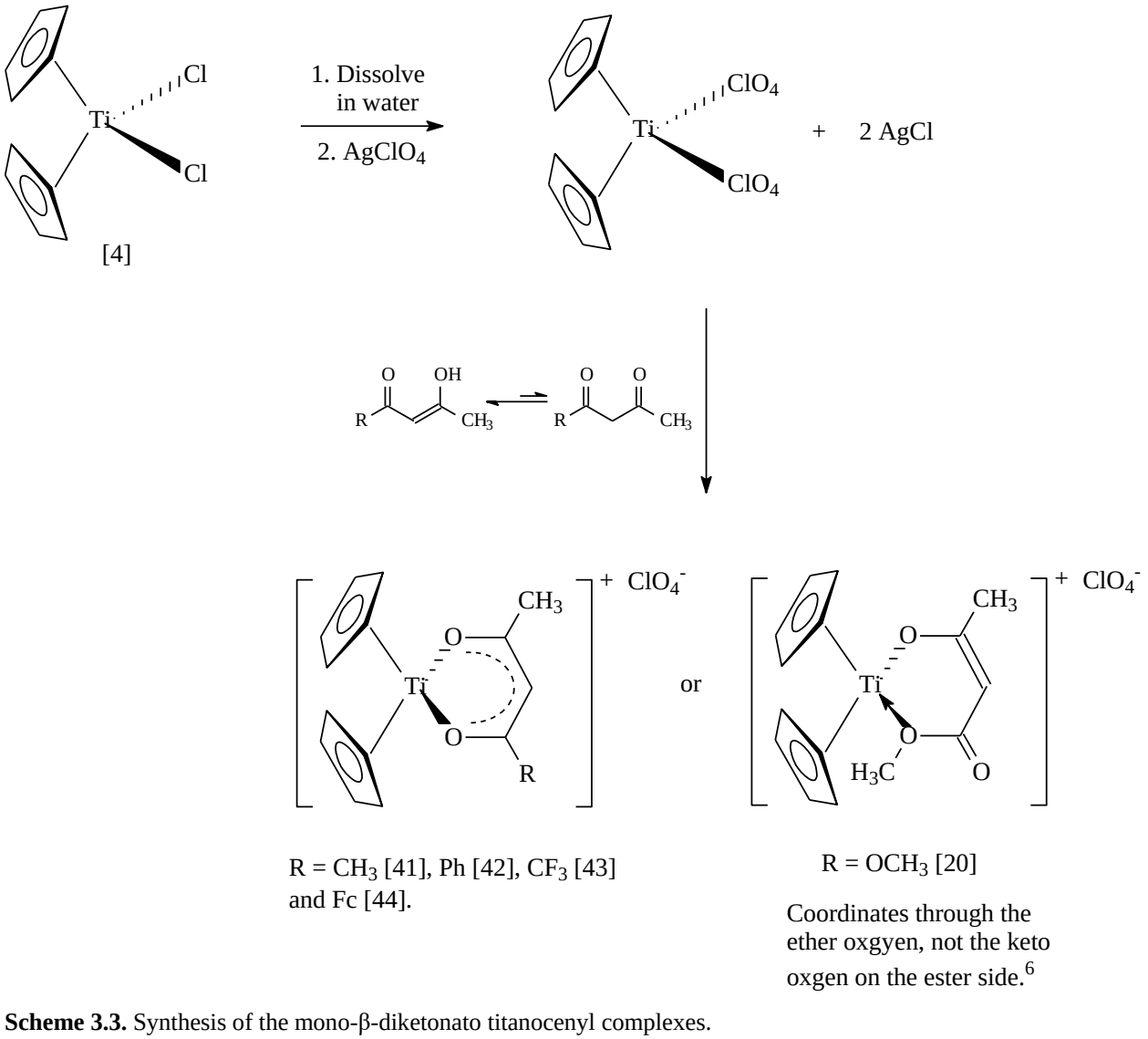

R = CH_3 [41], Ph [42], CF_3 [43] and Fc [44].

R = OCH_3 [20]

Coordinates through the ether oxgyen, not the keto oxgen on the ester side.[6]

Scheme 3.3. Synthesis of the mono-β-diketonato titanocenyl complexes.

Table 3.1. Different Mono-β-diketonato titanocenyl complexes

Tc complex	No.	Yield	Colour		Microanalysis for C and H			
					Cal. C	Found C	Cal. H	Found H
$[Tc(tfaa)]^+ClO_4^-$	[43]	16%	Light-brown	New	41.8%	42.1%	3.3%	3.5%
$[Tc(maa)]^+ClO_4^-$	[20]	48%	Yellow-brown	Known[4]	-	-	-	-
$[Tc(acac)]^+ClO_4^-$	[41]	86%	Grey-red	Known[3]	-	-	-	-
$[Tc(bzac)]^+ClO_4^-$	[42]	65%	Light-brown	Known[3]	-	-	-	-
$[Tc(fca)]^+ClO_4^-$	[44]	46%	Red-brown	New	52.7%	53.5%	4.2%	4.4%

These titanocenyl β-diketonato complexes are all insoluble in water, hexane and ether, but soluble in organic solvents such as chloroform, dichloromethane, acetone and ethanol. However, dissolving the product in ethanol causes decomposition of the product by the splitting off one of the cyclopentadienyl rings.[5]

The titanocenyl β-diketonato compounds of Table 3.1 have been found to be very stable and could be stored for up to two years. It is also stable in solution: after standing two days in acetone or acetonitrile no decomposition was detected.

The ^{1}H NMR spectra of chloroform-*d* (acetone-d_6 as well) solutions of all the mono-β-diketonato titanocenyl complexes $[(C_5H_5)_2Ti(CH_3COCHCOR)]^+ClO_4^-$ are simple and easily interpreted (Figure 3.2). All the spectra show three general signals: the cyclopentadienyl protons (counts for 10 protons) resonates at a low field (~6.9 ppm) due to the cyclopentadienyl aromatic system; secondly the methine proton (counts for 1 proton) which resonates at a slightly higher field (~6.1 ppm) but still in the aromatic region due to the pseudo aromatic system which is generated by the β-diketonato ligand coordinated to the Ti metal; and thirdly the signal at the aliphatic region which belongs to the methyl protons. The other signals that appear belong to the R groups (CH_3, Ph, CF_3, Fc, OCH_3) of the β-diketonato ligand $(CH_3COCHCOR)^-$, varied in position in the different complexes. The change in the R group causes shifts in the position of the three first described signals due to electronic communication through the C-C bonds *via* conjugation. Depending on the electron donation or electron withdrawing properties of the R group, the signals are moved either up or down field (Table 3.2).

Table 3.2. Difference in ^{1}H NMR shifts (in $CDCl_3$), carbonyl stretching frequency and synthesized yields of the mono-β-diketonato titanocenyl complexes of the type $[Tc(CH_3COCHCOR)]^+ClO_4^-$. Group electronegativity, χ_R, and the pK_a of the free β-diketones are also listed.

R group	^{1}H NMR position of the methine proton / ppm	ν_{CO} of the titanium complex / cm^{-1}	Yield	χ_R [a] / Gordy scale	pK_a of the free β-diketone
CF_3	5.96	1589	16%	3.01	6.30[6]
OCH_3	5.52	1678	48%	-	-
CH_3	6.14	1524	86%	2.34	8.95[6]
Ph	6.19	1565	65%	2.21	8.70[6]
Fc	6.65	1509	46%	1.87	10.01[2]

a) χ_R (Gordy scale)[2, 7] apparent group electronegativity values.

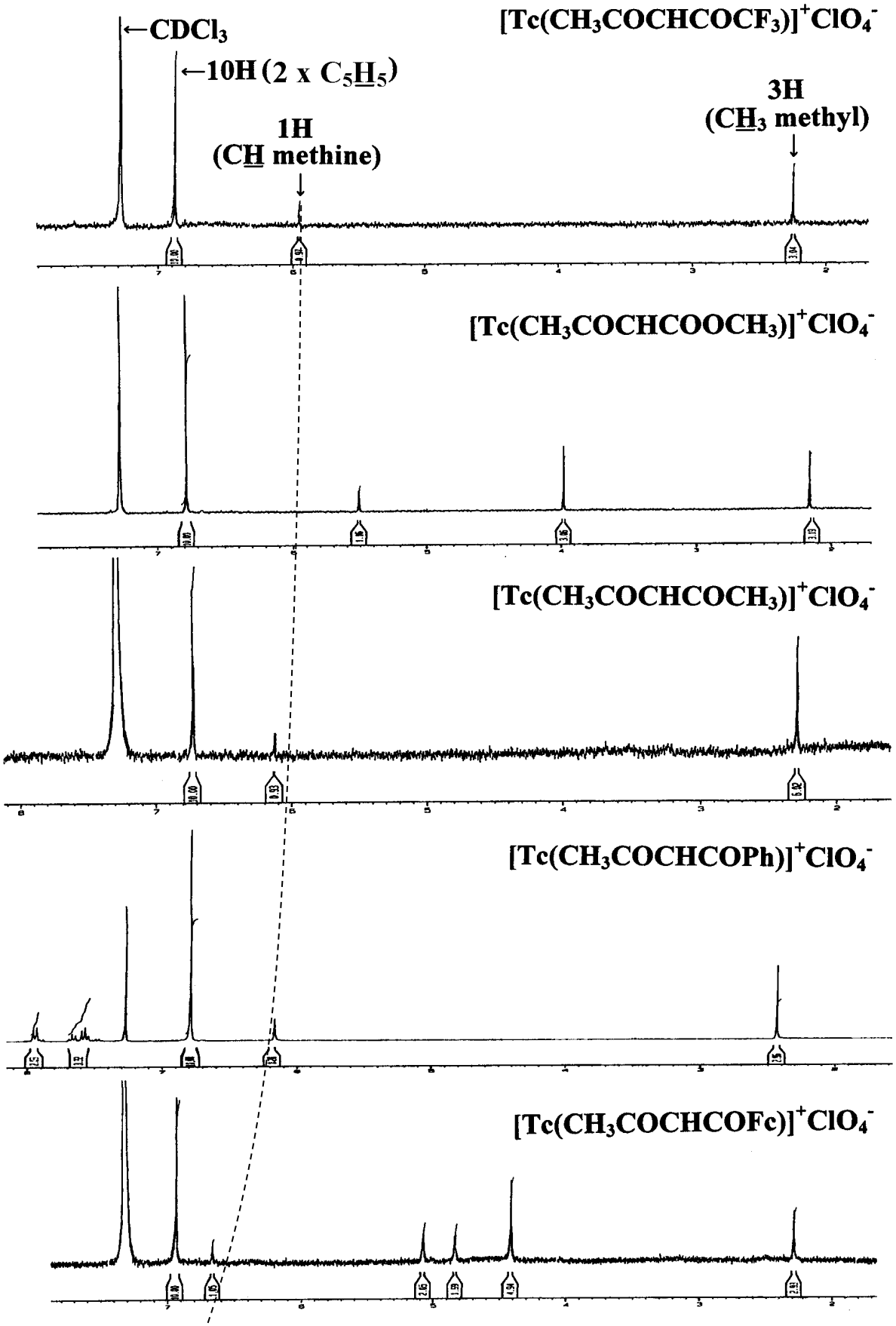

Figure 3.2. ^{1}H NMR's of $[Tc(CH_3COCHCOR)]^+ClO_4^-$ complexes, where R = CF_3, CH_3, Ph, Fc, OCH_3. From top to bottom: $[Tc(tfaa)]^+ClO_4^-$ [43], $[Tc(maa)]^+ClO_4^-$ [20] $[Tc(acac)]^+ClO_4^-$ [41], $[Tc(bzac)]^+ClO_4^-$ [42] and $[Tc(fca)]^+ClO_4^-$ [44].

Seeing as the keto ester complex [20] does not possess the same structural bonding as the other $[Tc(\beta\text{-diketonato})]^{+}ClO_4^{-}$ complexes (Scheme 3.3),[4] it will not be considered in the group electronegativity relationships.

Compound [43] has the lowest yield (Table 3.2). This poor yield of the CF_3 complex may be due to the fact that the Ti-F bond strength is so strong (569 kJ mol^{-1})[8], it is expected that some of the $[Tc(ClO_4)_2]$ will break the C-F bond (552 kJ mol^{-1})[8] of the β-diketone (Htfaa). This leads to decomposition of the β-diketone (Htfaa), i.e. low yields in the synthesis of [43].

An increase in the percentage yield of the $[Tc(\beta\text{-diketonato})]^{+}ClO_4^{-}$ complexes as the group electronegativity of the R groups of the β-diketonato ligand increases is observed, see Figure 3.3 Left (the CF_3 complex is not considered due to the reason explained above).

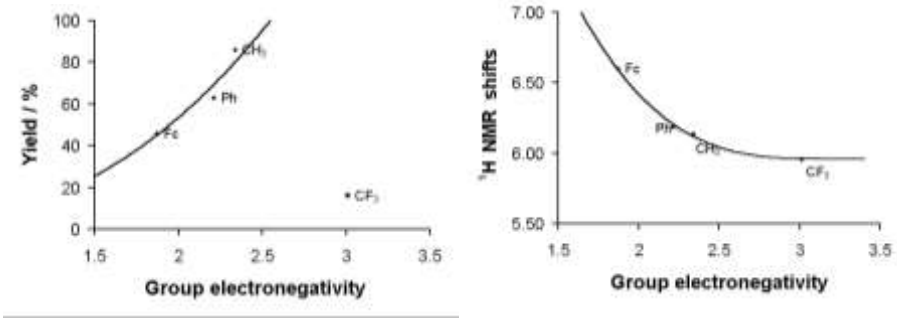

Figure 3.3. Left: Relationship between percentage yield (%) and the group electronegativities (Gordy scale) of the R-groups on the β-diketonato ligands. Right: Relationship between ^{1}H NMR shifts of the methine proton and the group electronegativities (Gordy scale) of the R-groups on the β-diketonato ligands

From Figure 3.3 (Right) it can be seen that with increasing group electronegativity of the R group on the β-diketonato ligand there is a decrease in ^{1}H NMR shift of the methine proton to a higher field. The methine signals are in the aromatic region. This is due to the pseudo-aromatic metallocyclic ring to which it is bounded.

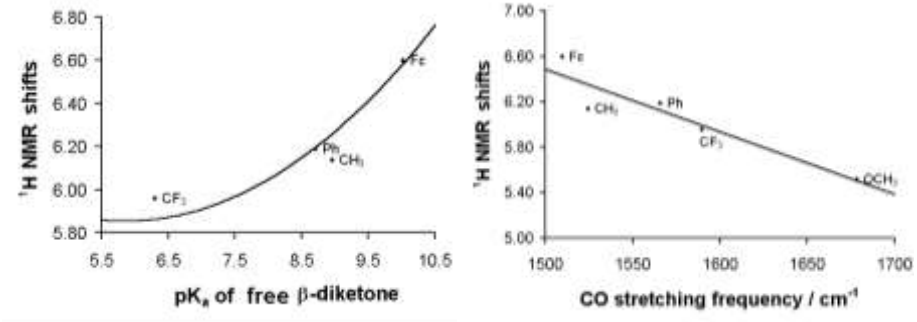

Figure 3.4. Left: Relationship between ^{1}H NMR shifts of the methine proton and pK_a of the free β-diketone. Right: Relationship between ^{1}H NMR shifts of the methine proton and the carbonyl stretching frequency of the titanocenyl complex.

It can also be seen from Figure 3.4 (Left) that as the pK_a of the free β-diketone increases there is an increase in ^1H NMR shift of the methine proton to a lower field.

Comparison of the yields of known complexes in this study with yields previously reported showed that repeated experiments led to higher yields. For [41] Doyle and Tobias obtained 70%,[3] the highest yield of this study was 86%. A different procedure by Bond yielded 95%.[9] For [42] Doyle and Tobias reported 51%,[3] this study gave 63%. A possible explanation for the higher yields obtained in this study is that in this study, preparation of the titanium perchlorate salt was done in a nitrogen atmosphere, whereas the procedure described by Doyle and Tobias was done in normal oxygen-containing atmosphere.

Synthesis of $[Tc(fca)]^+$ cation is difficult because of the insolubility of CH_3COCH_2COFc in water. Mixed solvent systems utilising H_2O as solvent for $[Tc(ClO_4)_2]$ species and THF, acetonitrile or chloroform for CH_3COCH_2COFc were tried. To make the β-diketonato ligand more compatible with the aqueous solvent of $[Tc(ClO_4)_2]$, attempts were made to complex the titanocenyl moiety with $[CH_3COCHCOFc]^-$, rather than allowing it to react with the free β-diketone. Conversion of CH_3COCH_2COFc to $[CH_3COCHCOFc]^-$ was achieved with NaOH and triethylamine. The anionic counter anion ClO_4^- also substituted with diethyl dithiocarbamate. It turns out that CH_3COCH_2COFc reacted best with $[Tc(ClO_4)_2]$ in a H_2O/THF mixture. Results of the different procedures are summarised in Table 3.3.

Table 3.3. Various procedures tried for the synthesis of $[Tc(fca)]^+$.

Procedure no	Counter ion	Medium used for dissolving Tc	Medium used for dissolving β-diketone	Yield
1	ClO_4^-	H_2O	THF	46%
2	ClO_4^-	H_2O	THF + NaOH	38%
3	ClO_4^-	H_2O	$CHCl_3$	12%
4	ClO_4^-	H_2O	CH_3CN	Reaction failed
5	ClO_4^-	CH_3CN	$CH_3CN + NEt_3$	Reaction failed
6	Diethyl dithiocarbamate	H_2O	THF	Reaction failed

3.2.2.2. Bis-β-diketonato titanium complexes

A variety of $[Ti(Cp)(Cl)(\beta\text{-diketonato})_2]$, β-diketonato = $acac^-$, $bzac^-$, $tfaa^-$ and fca^-, complexes (see Table 3.4) were synthesized according to the general procedure as described by Frazer and Newton (Scheme 3.4).[10] The general procedure involves the dissolving of the

β-diketone (2 mol) and triethylamine (1 mol) in acetonitrile. The triethylamine acts as a hydrogen acceptor, thus the β-diketone loses a proton to become the deprotonated β-diketonato anion, which is a good coordinating ligand. This mixture is added to titanocene dichloride (1 mol) also in acetonitrile. One of the Cl^- ligands and one of the cyclopentadienyl rings are replaced by two β-diketonato anions to form the product. The solvent is removed under reduced pressure and the dry residue is extracted with toluene to separate the desired neutral complex from the salt triethylammonium chloride. After removal of the toluene (under reduced pressure) the product is found as a crystalline solid. Seeing as these complexes are highly moisture sensitive they are stored under nitrogen.

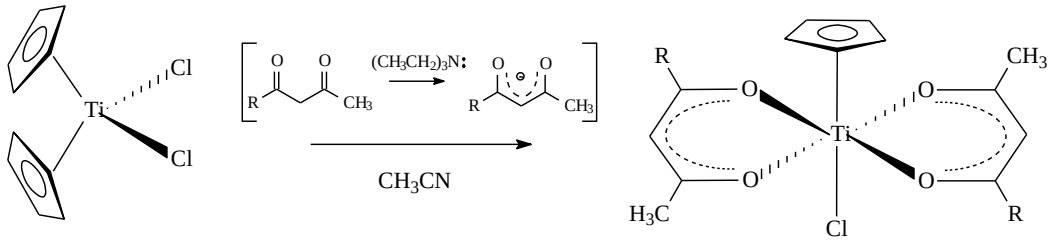

R = CH_3 [45], Ph [46], Fc [47] and CF_3 [48]

Scheme 3.4. Synthesis of the bis-β-diketonato titanium complexes.

Table 3.4. Different bis-β-diketonato titanium complexes

Tc complex	No.	Yield	Colour		Microanalysis of C and H			
					Cal. C	Found C	Cal. H	Found H
$[Ti(Cp)(Cl)(tfaa)_2]$	[48]	19%	Brown	New	39.6%	39.7%	2.9%	2.8%
$[Ti(Cp)(Cl)(acac)_2]$	[45]	43%	Orange	Known[10]	-	-	-	-
$[Ti(Cp)(Cl)(bzac)_2]$	[46]	53%	Orange	Known[10]	-	-	-	-
$[Ti(Cp)(Cl)(fca)_2]$	[47]	28%	Red	New	57.7%	57.6%	4.6%	4.5%

The procedure described by Frazer and Newton used acetonitrile as the reaction solvent.[10] In this study, however, it was found during the synthesis of the mono-β-diketonato fca complex, [44], (paragraph 3.2.2.1.) that acetonitrile was not a good reaction solvent. To find the best solvent for the bis-β-diketonato complex, two trial experiments were set up for Hbzac, the one in CH_3CN and the other in THF. It was found that the CH_3CN reaction (Frazer and Newton's procedure) worked well whereas the THF one did not work. This surprising result is in contrast to what was found for mono-β-diketonato complexation.

The ^1H NMR spectra of chloroform-d^1 solutions of all the bis-β-diketonato titanium complexes are not quite as simple and easily to interpret as the mono-β-diketonato titanocenyl complexes (Figure 3.5 and Appendix Spectra 8-11). The cyclopentadienyl protons' signal

(counts for 5) of these complexes becomes a multiplet and in both the acac and fca complexes the methine and methyl signals become multiplets. The signal for the cyclopentadienyl protons for these complexes resonates at a slightly higher field than their mono-β-diketonato counterparts. This is expected as the mono-β-diketonato complexes are cationic (and therefore electron deficient) whereas the bis-β-diketonato complexes are neutral (and therefore more electron rich).

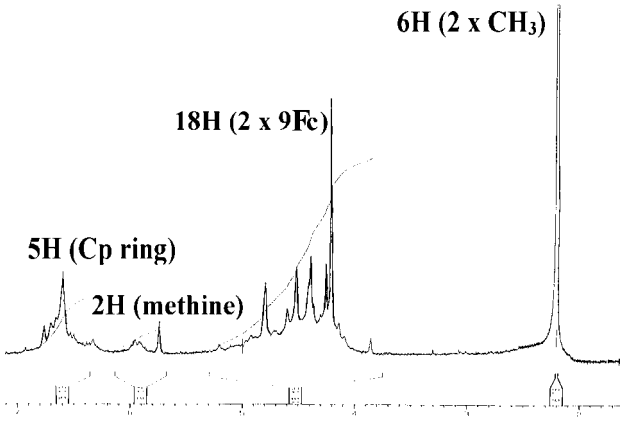

Figure 3.5. ^{1}H NMR of [47] in cholorform-d^{1}.

Interpretation of the ^{1}H NMR spectrum of [47] is very difficult; the signals for the Fc group cannot be assigned at all. At best, one can observe multiplet at 4-5.2 ppm that counts the correct number of protons, namely 18. The ferrocenyl based multiplet could be attributed to different possible isomers of the complexes (Figure 3.6). This causes different interactions through space. However, this mixed multiplet signal is integrated for the correct amount of protons.

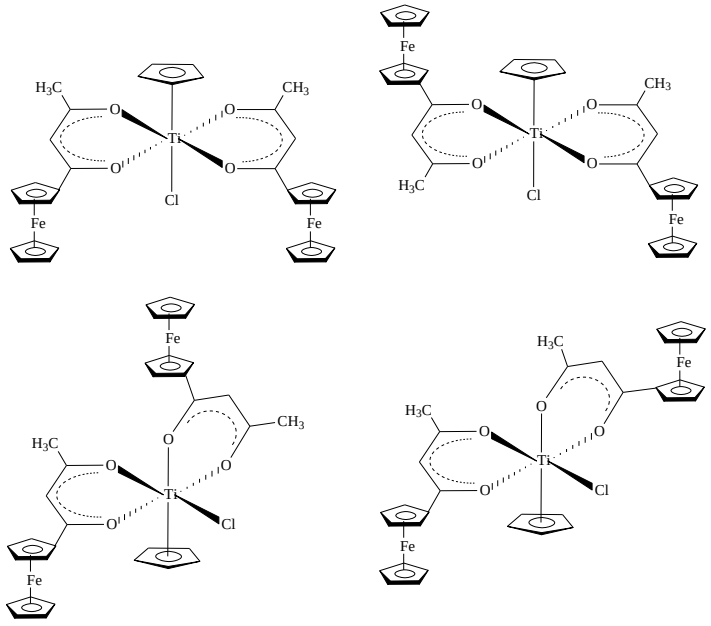

Figure 3.6. Four possible isomers of [47]. Many other isomers may also exist, including interchanging position of the $(C_5H_5)^-$ and Cl^- ligands and isomers where the direction of ferrocenyl protruding is reversed (i.e. up or down).

No apparent trend could be indentified for the relationship between the positions of the dominant $(C_5\underline{H}_5)^-$ (~6.6 ppm) or methine ^{1}H NMR signals and the group electronegativity of the R group on the β-diketonato ligands in the complexes of the type $[Ti(Cp)(Cl)(CH_3COCHCOR)_2]$ with R = CF_3, CH_3, Ph and Fc (Table 3.5).

Table 3.5. ^{1}H NMR shifts (in $CDCl_3$), carbonyl stretching frequency and yield of the bis-β-diketonato titanocium complexes $[Ti(Cp)(Cl)(CH_3COCHCOR)_2]$, group electronegativity of each R group and the pK_a of the free β-diketone.

R group	^{1}H NMR position of cyclopentadienyl protons[a]	ν_{CO} of the titanium complex	Yield	χ_R (Gordy scale)	pK_a of the β-diketone
CF_3	6.6	1533	19%	3.01	6.30[6]
CH_3	6.6	1528	43%	2.34	8.95[6]
Ph	6.6	1516	53%	2.21	8.70[6]
Fc	6.6	1512	28%	1.87	10.01[1]

a) position of the high intensity peak

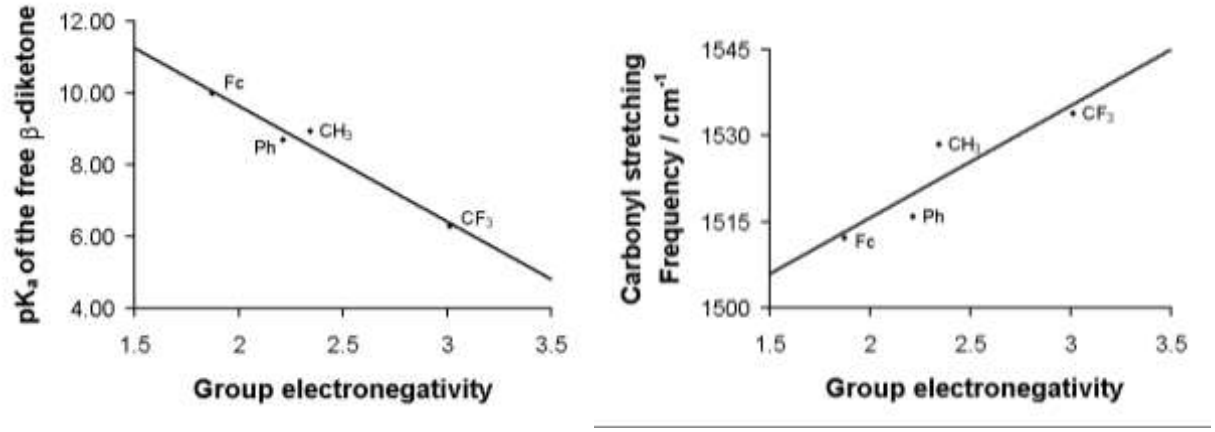

Figure 3.7. Left: Relationship between apparent group electronegativities of the R groups of the β-diketone and the pK_a of the free β-diketone. Right: Relationship between ν_{CO} of complexes $[Ti(Cp)(Cl)(CH_3COCHCOR)_2]$ and apparent group electronegativities of the R groups of the β-diketonato ligands.

Figure 3.7 presents the relationship between the pK_a of a β-diketone $[CH_3COCH_2COR]$ and the group electronegativity of the R group on the β-diketone. Groups with a high electronegativity (highly electron withdrawing) on the β-diketone backbone make it more acidic with resulting decrease in the pK_a of the β-diketone. Htfaa with the CF_3 group

(χ_{CF3} = 3.01), is the most acidic β-diketone with pK_a = 6.30. In contrast, on the other end of the scale, the pK_a of Hfca with the Fc group (χ_{Fc} = 1.87) is 10.01.

It can be seen from Figure 3.7 (Right) that with increasing electronegativity there is an increase in the carbonyl stretching frequency of the [Ti(Cp)(Cl)($CH_3COCHCOR)_2$]. With an increase in ν_{CO} the C-O (carbon-oxygen) bond order (bond strength) increases and the M-OC (metal-oxygen) bond order (bond strength) decreases. It can thus be concluded that in the complexes series [Ti(Cp)(Cl)($CH_3COCHCOR)_2$], the lower the group electronegativity of the R substituent is, the stronger the Ti-OC bond will be.

For the yield obtained, bis-β-diketones display a similar general trend as the mono-β-diketones (Table 3.5). The CF_3 complex has the lowest yield, and can again be attributed to the stability of Ti-F bonds (see section 3.2.2.1). The yield of the bis-β-diketonato titanium complexes are roughly two times smaller than that for the mono-β-diketonato titanocene counterparts and this could be explained by the fact that titanium is more inclined to form a four coordinated tetrahedral species than a six coordinated octahedral species.

3.2.2.3. Other bi-chelating titanocenyl complexes

A variety of other titanocenyl complexes were also synthesised (Figure 3.8). These were the cationic $[Tc(Sacac)]^+$ [49] and the neutral [Tc(cat)] [9], [Tc(Scat)] [50] and [Tc(biphen)] [51] with $Sacac^-$ = thioacetylacetonato, $biphen^{2-}$ = 2,2-biphenyldiolato, cat^{2-} = 1,2-benzenediolato and $Scat^{2-}$ = 1,2-benzenedithiolato (Figure 3.8 and Table 3.6).

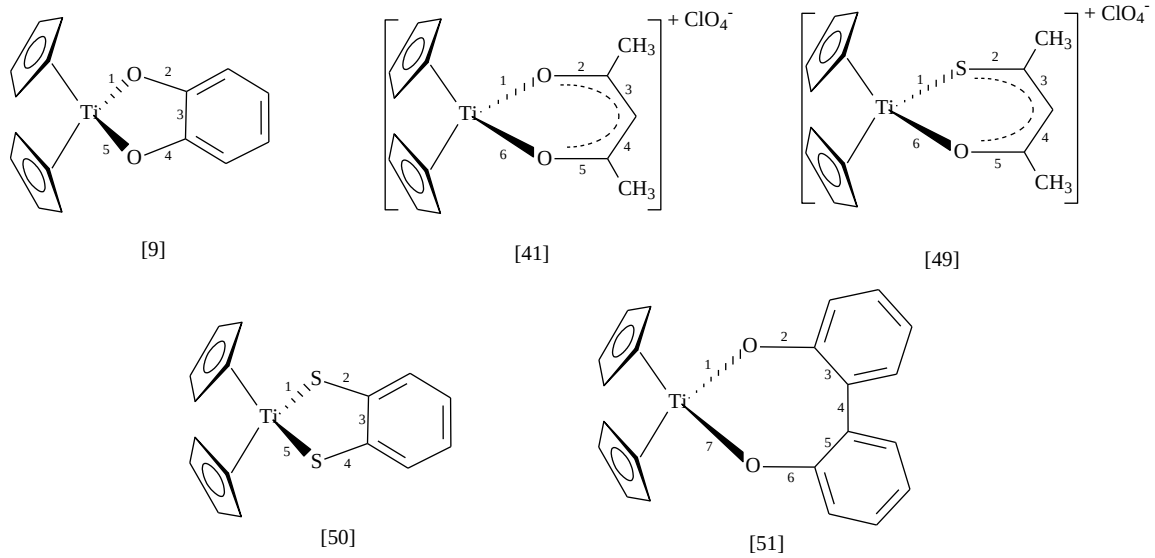

Figure 3.8. Structure of five-, six and seven-membered metallocyclic titanocenyl compounds, $[Tc(acac)]^+ClO_4^-$ [41] $[Tc(Sacac)]^+ClO_4^-$ [49] [Tc(biphen)] [51], [Tc(cat)] [9] an [Tc(Scat)] [50].

Table 3.6. Bi-chelating mono-ligand titanocenyl complexes

Tc complex	No.	Yield	Colour	Metallocyclic ring size	
$[Tc(Sacac)]^+ClO_4^-$	[49]	24%	Olive-green	6	New
[Tc(cat)]	[9]	98%	Bright red	5	Known[11]
[Tc(Scat)]	[50]	61%	Green-brown	5	Known[12]
[Tc(biphen)]	[51]	45%	Red-orange	7	Known[11]

A β-thioketonato titanocenyl complex, [49], was synthesized to compare the chemical and physical properties of the complex with one of the oxygen atoms in the β-diketonate ligand acetylacetonato, is replaced by a sulphur atom. The same procedure that was used to synthesize [41] was used to synthesize [49] (Scheme 3.3). The yield for the sulphur derivative was dramatically less than that for the oxygen analogous, 86% yield for [41] and 24% yield for [49]. The effect of S replacement of O on the ^{1}H NMR spectra is moderate. There is ± 1 ppm shift (relative to the acac complex) to a higher field for the methine proton peak position. The different colour of grey-red (acac complex) to olive-green (Sacac complex) caused a 20 nm wavelength increase to 575 nm for the maximum UV-absorption band.

All the β-diketonato and the Sacac titanocenyl complexes thus far described posses a six-membered pseudoaromatic core around the titanium nucleus. To compare reactivity and stability, five- and seven-membered metallocyclic titanocenyl complexes [9], [50] and [51] were synthesized (Figure 3.8).

The seven-membered metallocyclic titanocenyl complex, [51], was obtained by reacting 2,2-biphenyldiol with titanocene dichloride (Scheme 3.5). The synthetic route followed was the same as the procedure to bind 2,2-biphenyldiol to a titanium phthalocyanine.[13] It is quite a simple method where the reagents (titanocene dichloride and 2,2-biphenyldiol) are merely dissolved in dichloromethane and stirred for 2 hours at room temperature.[13] This method is more simple than that followed by Andrä.[11] The ^{1}H NMR in chloroform-*d*[1] shows the 10 cyclopentadienyl protons and two sets of quartets, which count for four each for the two phenyl rings, all in the aromatic region (Figure 3.9 and Appendix Spectrum 15). The UV-spectrum of the red-orange complex shows a maximum absorption at 520 nm.

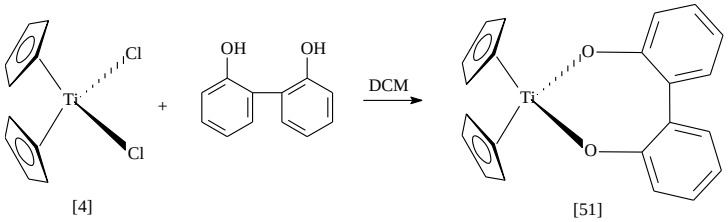

Scheme 3.5. Synthesis of the seven-membered metallocyclic titanocenyl complex, [Tc(biphen)], [51].

The five-membered metallocyclic titanocenyl complex, [9], was also obtained according to Scheme 3.5 (yield 98%), which is the same procedure used to synthesise [51] by using H_2cat instead of H_2biphen.[13] Other methods to obtain [9] with lower yields included:

a) the same procedure used for the β-diketonato titanocenyl complexes (Scheme 3.3), adjusted by the addition of a base as a hydrogen acceptor (36% yield),
b) a procedure used for the binding of 1,2-benzenediol to a titanium phthalocynine, which involves the refluxing of titanocene dichloride and 1,2-benzenediol in dichloromethane for an hour (15% yield)[14]

As with the seven-membered metallocyclic titanocenyl complex [51], the ^{1}H NMR spectra in chloroform-*d*[1] of the five-membered metallocyclic complex [9] is simple and easy to interpret (Figure 3.9 and Appendix Spectrum 13). It consists of a singulet for the 10 cyclopentadienyl protons and two sets of multiplets which count for two protons each. The UV-spectrum of the bright-red complex shows a maximum absorption at 515 nm.

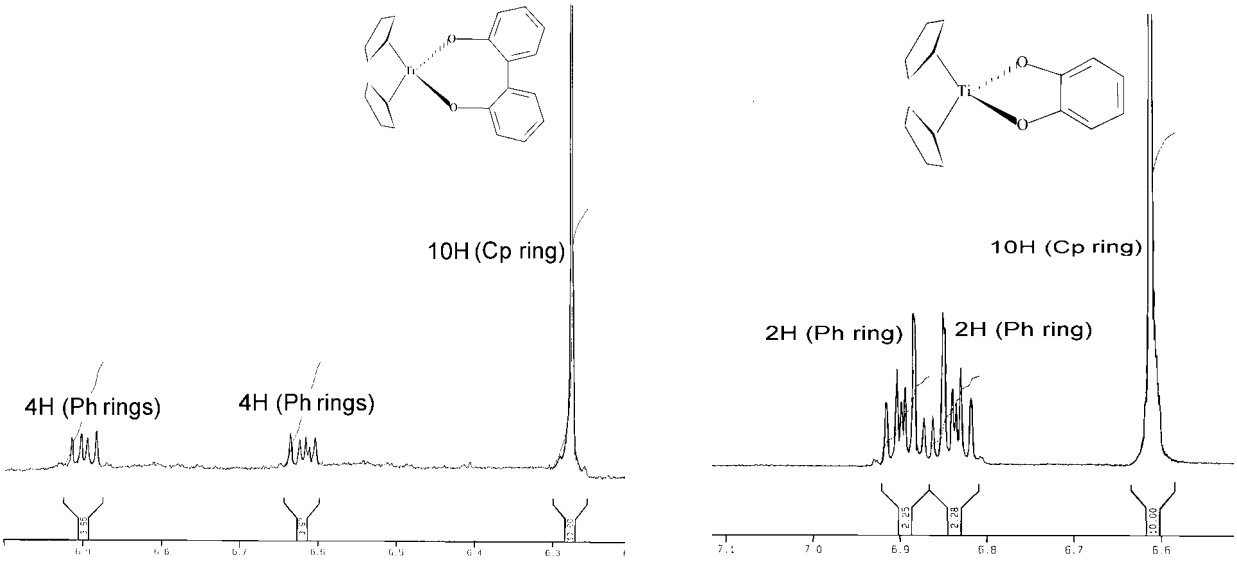

Figure 3.9. Left: ^{1}H NMR of [51] in $CDCl_3$. Right: ^{1}H NMR of [9] in $CDCl_3$.

An interesting observation was that upon synthesizing the five and seven-membered metallocyclic compounds in a Schlenk set-up (i.e. oxygen free conditions), coordination of 1,2-benzenediol and 2,2-biphenyldiol to the titanocenyl according to Scheme 3.5 failed. This may be interpreted that moisture acts as hydrogen acceptor.

Synthesis of [Tc(Scat)], [50], according to the method of synthesizing the oxygen counterpart [Tc(cat)] of [50] failed. The procedure similar to that of making [Tc{Scat(Cl_4)}] was tried (Scheme 3.6).[15] It involves the addition of 1,2-benzenedithiol and triethylamine in warm ethanol to a hot solution of titanocene dichloride in acetone and heating over a steambath till

precipitate forms. However, it seems like one Cp ring was split off and two $Scat^{2-}$ ligands binded in the presence of oxygen. This may be attributed to the fact that ethanol is known to split off one Cp ring, causing the binding of two $Scat^{2-}$ ligands. However, when this reaction was repeated under Schlenk conditions, the binding of the 1,2-benzenedithiol in one equivalent to the titanocenyl moiety proceeded effectively in 61% yield.

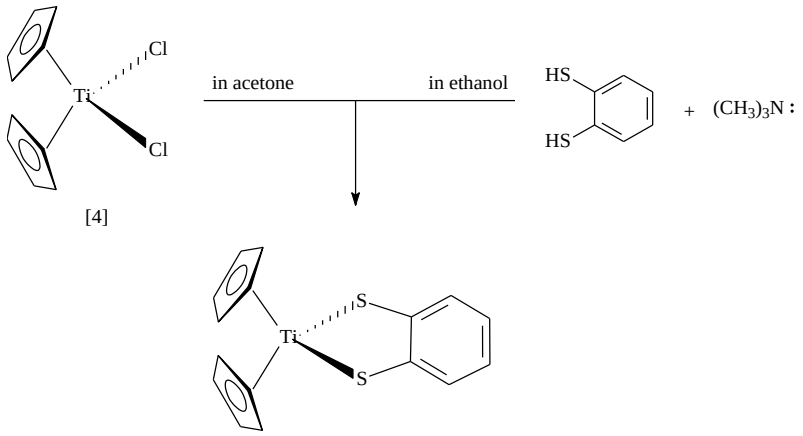

Scheme 3.6. Synthesis of the five-membered metallocyclic titanocenyl complex, [50].

3.2.3. Zirconium complexes

The synthesis of tetrahedral mono-β-diketonato zirconocenyl(IV) complexes of the type $[Zc(\beta\text{-diketonato})]^{+}ClO_4^{-}$ and octahedral bis-β-diketonato zirconium(IV) complexes of the type $[Zr(Cp)(Cl)(\beta\text{-diketonato})_2]$ are described in this section.

3.2.3.1. The Attempted synthesis of mono-β-diketonato zirconocenyl complexes

The synthesis of mono-β-diketonato zirconocenyl(IV) complexes was targeted in this study. The expected route for obtaining these complexes is shown in Scheme 3.7.

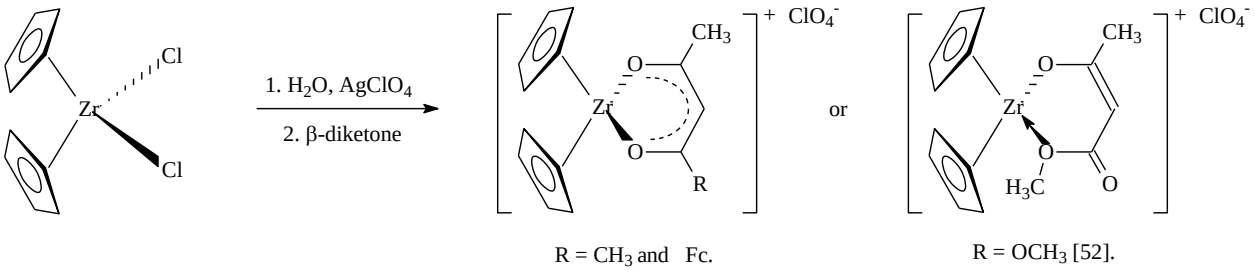

Scheme 3.7. Attempted synthesis of mono-β-diketonato zirconocenyl complexes.

Various methods to obtain mono-β-diketonato zirconocenyl complexes failed or were unsatisfactory. This observation could be attributed to zirconium's reluctance to form a four coordinated tetrahedral species, due to the presence of the 4*d*-orbitals. Zirconium appears to be more comfortable with a coordination sphere of five to eight ligands.

$[Zc(acac)]^+ClO_4^-$ was obtained in the crude reaction product *via* the similar procedure used for the titanium counter part [41],[3] according to Scheme 3.3 and 3.7. ^1H NMR showed that the desired species was present in the crude but there were large amount of reagents and other unidentified compounds present as well. After recrystallization, the crystals were lighter in colour but it was unable to dissolve in any solvent as polymerisation possibly occurred. $[Zc(acac)]^+ClO_4^-$ is a salt and hence cannot be cleaned on silicon columns

The ^1H NMR of $[Zc(fca)]^+ClO_4^-$ also confirmed the presence of the desired species in the crude reaction mixture, but there were also unwanted, unknown peaks present. After recrystallization, some of the reagents' peaks disappeared but unknown peaks were still present. Some of these could possibly be assigned to the coordination of the cyclopentadienyl of the ferrocenyl group to the zirconium to give zirconium a coordination sphere of five. This could however, not be confirmed.

Table 3.7. Different Mono-β-diketonato zirconocenyl complexes attempted to synthesize.

Zc complex	Yield	
$[Zc(acac)]^+ClO_4^-$	Very small impure quantities[a]	New
$[Zc(fca)]^+ClO_4^-$	Very small impure quantities[a]	New
$[Zc(acac)]^+[S_2CN(Et)_2]^-$	Very small impure quantities[a]	Known[16]
$[Zc(fca)]^+[S_2CN(Et)_2]^-$	Reaction failed completely	New
$[Zc(maa)]^+ClO_4^-$	26%	New

a) ^1H NMR shows the correct product is present in the crude reaction mixture, but it could not be cleaned or isolated.

Literature suggest in a single report,[16] that the targeted $[Zc(\beta\text{-diketonato})]^+$ cation may be isolated utilising diethyl dithiocarbamate as the counter anion. This report used acetylacetone as the coordinating ligand. All attempts to achieve isolation of the target complexes $[Zc(acac)]^+[S_2CN(Et)_2]^-$ and $[Zc(fca)]^+[S_2CN(Et)_2]^-$ failed. Again, as with the ClO_4^- counter anion, the ^1H NMR before recrystallization of the crude product confirms the presence of the desired complex together with large amounts of unreacted diethyl dithiocarbamate. After recrystallization the product became insoluble, suggesting polymerisation or that the formation of bridged zirconium species possibly took place.

The only zirconium four coordinated complex, which could be isolated in satisfactory yields, was the β-keto ester, derivative $[Zc(maa)]^{+}ClO_4^{-}$ [52] (Figure 3.10). This was synthesized like the titanium counterpart (Scheme 3.3) with fair yield.[4] The complex has a very distinct pink colour and its ^1H NMR was very much the same as the titanium's ^1H NMR (see Appendix Spectrum 16). No obvious reason could be found why the zirconocenyl keto-ester would behave different than the titanocenyl keto ester. The author concludes as with the titanocenyl analogue that the isolated product coordinates *via* the ether oxygen and not *via* the keto oxygen on the ester side of the ligand. This is shown in Figure 3.10.

Target compound, possibly not isolated

Possible product isolated

[52]

Figure 3.10. Possible structures of $[Zc(maa)]^{+}ClO_4^{-}$, Zr coordination through the keto oxygen on the ester side, (left) and Zr coordination through the ether oxygen (right).

To prove the structure of $[Zc(maa)]^{+}ClO_4^{-}$, a crystal structure of the $[Zc(maa)]^{+}ClO_4^{-}$ complex is required. To date no suitable crystals could be obtained.

3.2.3.2. Bis-β-diketonato zirconium complexes

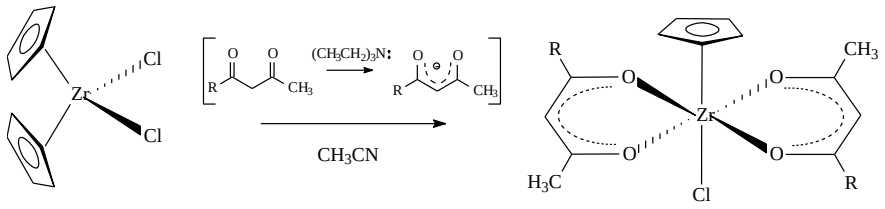

R = CH_3 [53], Ph [54], Fc [55]

Scheme 3.8. Synthesis of the bis-β-diketonato zirconium complexes.

The β-diketonato complexes were made the same way as the titanium analogues according to Scheme 3.8, by the procedure described by Frazer and Newton.[10] As was found for titanium complexes, the ^1H NMR is crowded and shows peaks of multiplicity. The integration count for each group of protons is, however, correct. The ^1H NMR of the known, [53] and [54] (see Appendix Spectra 17-18), was the same as that reported by Frazer and Newton, proving the correct product was obtained. With the exception of the acac complex [54] all the other's

cyclopentadienyl proton signals are multiplets. For all the complexes the methine and methyl signals are split into multiplets. The other signals in the spectrum come from the different R groups (CH_3 [53], Ph [54] and Fc [55]). The Fc signal, as was the case with the titanium, shows high multiplicity and could not be resolved, but again integrate for the correct amount of protons (18). The phenyl rings of the bzac zirconium complex's ^1H NMR signals were also unresolved but integrated for the correct amount of protons (10). Both these phenomena are expounded by the same explanation as was given for the titanium analogues, namely the existence of various isomers (paragraph 3.2.2.2). Yields of each complex are given in Table 3.8.

Table 3.8. Different bis-β-diketonato zirconium complexes

Zc complex	No.	Yield	Colour		Microanalysis of C and H			
					Cal. C	Found C	Cal. H	Found H
$[Zr(Cp)(Cl)(acac)_2]$	[53]	29%	White	Known[10]	-	-	-	-
$[Zr(Cp)(Cl)(bzac)_2]$	[54]	23%	Yellow	Known[10]	-	-	-	-
$[Zr(Cp)(Cl)(fca)_2]$	[55]	43%	Dark red	New	54.3%	54.1%	4.3%	4.6%

3.2.4. Hafnium and vanadium complexes

Tetrahedral mono-β-diketonato hafnocenyl(IV) and vanadocenyl(IV) complexes of the type $[Mc(\beta\text{-diketonato})]^+ClO_4^-$ and octahedral bis-β-diketonato hafnium(IV) and vanadium(IV) complexes of the type $[M(Cp)(Cl)(\beta\text{-diketonato})_2]$ were synthesized, Mc = $(C_5H_5)_2Hf^{2+}$ or $(C_5H_5)_2V^{2+}$; M = Hf or V.

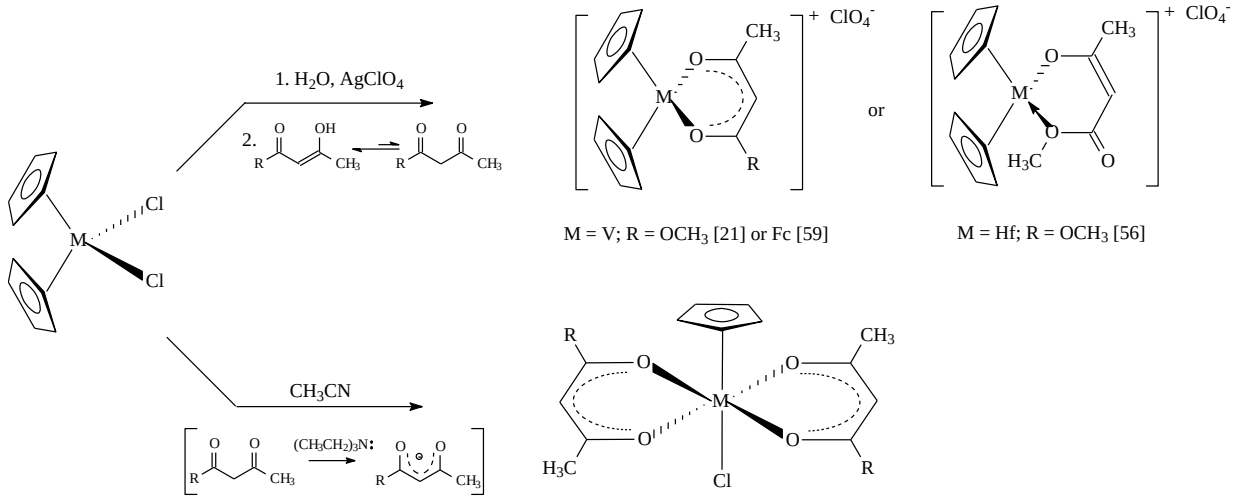

Scheme 3.9. Synthesis of $[Mc(\beta\text{-diketonato})]^+ClO_4^-$ and $[M(Cp)(Cl)(\beta\text{-diketonato})_2]$, Mc = $(C_5H_5)_2Hf^{2+}$ or $(C_5H_5)_2V^{2+}$; M = Hf or V.

The methyl acetylacetone mono-β-diketonato hafnocenyl complex [56] was synthesized according to the procedure used for the titanium and zirconium counterparts (Scheme 3.9).[4] The lower yields were attributed to the presence of 4*d*, 5*d* and 4*f*-orbitals, which would favour higher coordination numbers than four. The ^{1}H NMR is consistent with that of the target compound (see Appendix Spectrum 20). The ^{1}H NMR is also similar to that found for the titanocenyl and zirconocenyl analogues, and again no obvious reason could be found why the hafnocenyl β-keto-ester would behave different than the titanocenyl β-keto-ester. It can thus be concludes as with the titanocenyl and zirconocenyl analogue that the isolated product coordinates *via* the ether oxygen and not *via* the keto oxygen on the ester side of the ligand.

Vanadium and titanium are so closely related that it was not surprising that their chemical properties are also closely related.[17] All the vanadium and hafnium synthesis was done under the same reaction conditions as for titanium mono- and bis-β-diketonato complexes (Scheme 3.9). No ^{1}H NMR could be drawn seeing as vanadium(IV) is paramagnetic. Conformation of the correct products was obtained from microanalysis.

Table 3.9. Different β-diketonato hafnium and vanadium complexes

Hc complex	No.	Yield	Colour		Microanalysis of C and H			
					Cal. C	Found C	Cal. H	Found H
$[Hc(maa)]^+ClO_4^-$	[56]	5%	White	New	-	-	-	-
$[Hf(Cp)(Cl)(acac)_2]$	[57]	36%	Light yellow	New	-	-	-	-
$[Hf(Cp)(Cl)(fca)_2]$	[58]	9%	Dark red	New	48.5%	48.1%	3.8%	4.1%
$[Vc(fca)]^+ClO_4^-$	[59]	49%	Dark-green	New	52.4%	53.1%	4.2%	4.6%
$[Vc(maa)]^+ClO_4^-$	[21]	36%	Green	Known[4]	34.3%	34.0%	3.7%	3.6%
$[V(Cp)(Cl)(fca)_2]$	[60]	32%	Dark-green	New	57.5%	56.9%	4.5%	4.9%
$[V(Cp)(Cl)(acac)_2]$	[61]	17%	Green	New	51.5%	51.7%	5.5%	5.3%

The higher yields of the four-coordinated vanadium derivatives to the hafnium and zirconium derivatives are obvious (Table 3.9). This is consistent with our belief that the presence of the 4*d*, 5*d* and 4*f* orbitals in Zr and Hf favours higher coordination numbers than four. Vanadium has no 4*d*, 5*d* and 4*f* orbitals.

Longer reaction times of ± 10 h were needed to synthesize the bis-β-diketonato hafnium, [57] and [58], complexes than that used for their titanium and vanadium counterparts (Scheme 3.9).[10] The low yields of the six-coordinated hafnium derivatives (Table 3.9) could be attributed to the 4*d*, 5*d* and 4*f* orbitals of hafnium, which allows for easy side reactions.

3.3. Electrochemistry

3.3.1. Introduction

The formal reduction potential of all the redox active metal centres in all the synthesized titanium, zirconium, hafnium and vanadium complexes were determined. From the formal reduction potential an attempt was made to quantify the electronic influence of the different R substituents on the redox active metal centres of each of these compounds. The redox couples obtained were the M^{4+}/M^{3+} couple with M = Ti, Zr, Hf and V as well as the Fe^{3+}/Fe^{2+} couple in the ferrocenyl substituent.

3.3.2. Titanium complexes

3.3.2.1. Titanocene dichloride

Figure 3.11 shows the cyclic voltammograms of titanocene dichloride alone, titanocene dichloride in the presence of free ferrocene as an internal reference and free ferrocene at 200 mV s^{-1}. From Figure 3.11 it is observed that the addition of free ferrocene to titanocene dichloride does not influence the position of the free titanocene dichloride or ferrocene. Thus ferrocene as internal standard, and free ferrocene have the same formal reduction potential, *viz* 77 mV *vs* Ag/Ag^+.[18] Reduction potentials in this thesis are reported *vs* Ag/Ag^+, but can easily convert *vs* Fc/Fc^+ by subtracting 77 mV from the values reported. The cyclic voltammetry results of pure titanocene dichloride and free ferrocene are tabulated in Table 3.10.

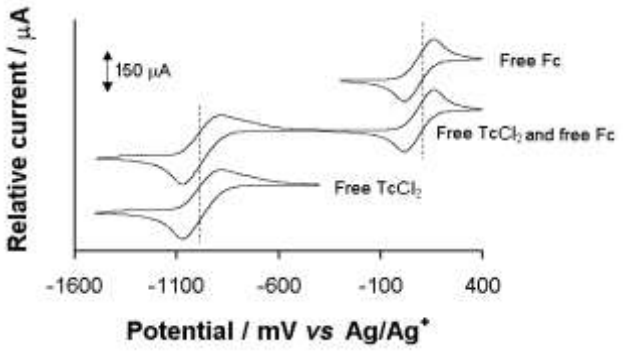

Figure 3.11. The cyclic voltammograms of a 3.0 mmol dm^{-3} titanocene dichloride, titanocene dichloride (3.0 mmol dm^{-3}) with free ferrocene (1.5 mmol dm^{-3}) added and free ferrocene (1.5 mmol dm^{-3}) in acetonitrile (supporting electrolyte is 0.1 mol dm^{-3} tetrabuthylammonium hexafluorophosphate) on a glassy carbon working electrode at 25˚C at scan rate 200 mV s^{-1}.

Table 3.10. The cyclic voltammetry data obtained from voltammograms (*vs* Ag/Ag^+) of titanocene dichloride and free ferrocene measured in 0.1 mol dm^{-3} tetrabuthylammonium hexafluorophosphate/CH_3CN with a glassy carbon working electrode at 25ºC. Scan rates, E_{pa} (anodic peak potential), ΔE_p (difference between the anodic and cathodic peak potentials), E^{01} (formal reduction potentials), i_{pa} (anodic peak current) and i_{pa}/i_{pc} (anodic/cathodic peak current relationship) are shown. The concentration of the titanocene dichloride was 3.0 mmol dm^{-3} and of ferrocene was 1.5 mmol dm^{-3}. $E^{01} = (E_{pa} + E_{pc})/2$.

v / mV s^{-1}	E_{pa} / mV	ΔE_p / mV	E^{01} / mV[a]	i_{pa} / μA	i_{pa}/i_{pc}
Titanocene dichloride					
50	-869	213	-976	93	0.93
100	-859	244	-981	110	0.96
150	-849	259	-979	132	0.91
200	-838	304	-990	154	0.92
Ferrocene					
50	109	68	75	96	1.00
100	112	71	76	118	1.00
150	114	73	77	145	1.01
200	115	76	77	167	1.01

a) Some author(s)* prefer to use $E_{1/2}$ instead of E^{01} for quasi-reversible processes. In this study, E^{01} will be used.

As can be seen from Table 3.10, even though titanocene dichloride displays a reduction as well as an oxidation peak with $i_{pa}/i_{pc} \approx 1$, it is electrochemically irreversible because the average ΔE value is 255 mV. This could be due to very slow electron transfer kinetics.

Electrochemical reversibility implies $i_{pa}/i_{pc} = 1$ and that the peak potential differences, ΔE_p of a one-electron process at 25ºC should theoretically be 59 mV, independent of the scan rate.[19] However, factors such as overvoltage and internal resistance cause ΔE_p values in acetonitrile to be somewhat larger. Since ferrocene is known to be reversible and ΔE_p for ferrocene was found to be 77 mV at a scan rate of 200 mV s^{-1}, in the contents of this study, any value of ΔE_p smaller than 90 (at a scanrate of 200 mV s^{-1}) is taken to imply electrochemical reversibility of the investigated redox couple.

3.3.2.2. Metallocenes

The cyclic voltammograms of various metallocene dichlorides (titanocene dichloride, zirconocene dichloride, hafnocene dichloride and vanadocene dichloride) were recorded and the comparative voltammograms are shown in Figure 3.12. The comparative electrochemical data for these voltammograms are summarised in Table 3.11.

* A.M. Bond, R. Colton, U. Englert, H. Hugel and F. Marken, *Inorg. Chim. Acta*, 1995, **235**, 117.

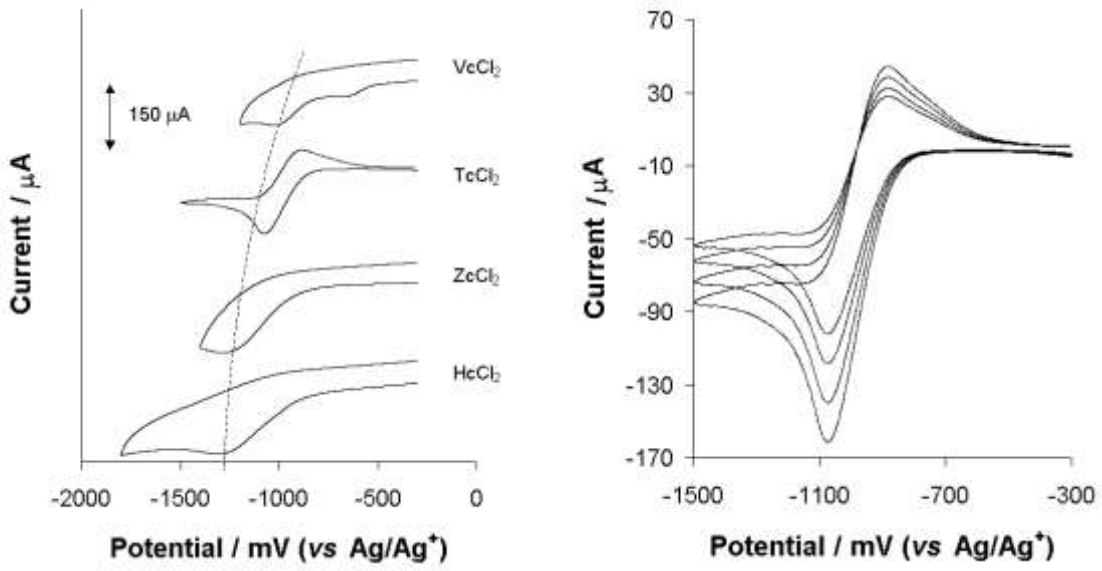

Figure 3.12. Left: The cyclic voltammograms of various 3.0 mmol dm^{-3} metallocene dichloride complexes (supporting electrolyte is 0.1 mol dm^{-3} tetrabuthylammonium hexafluorophosphate) in acetonitrile on a glassy carbon-working electrode at 25˚C and a scan rate of 200 mV s^{-1}. Vc = $(C_5H_5)_2V^{2+}$, Tc = $(C_5H_5)_2Ti^{2+}$, Zc = $(C_5H_5)_2Zr^{2+}$ and Hc = $(C_5H_5)_2Hf^{2+}$. Right: The cyclic voltammograms of a 3.0 mmol dm^{-3} titanocene dichloride (supporting electrolyte is 0.1 mol dm^{-3} tetrabuthylammonium hexafluorophosphate) in acetonitrile on a glassy carbon working electrode at 25˚C and at scan rates of 50-200 mV s^{-1} (50 mV increments).

Table 3.11. The cyclic voltammetry data obtained from voltammograms (*vs* Ag/Ag^+) of various metallocene dichlorides measured in 0.1 mol dm^{-3} tetrabuthylammonium hexafluorophosphate/CH_3CN with a glassy carbon working electrode at 25ºC and a scan rate of 200 mV s^{-1}. The concentration of the metallocene dichloride complexes was 3.0 mmol dm^{-3}. Atomic electronegativity of the metals, χ_M, is also shown.

Metallocene dichlorides	E_{pc} / mV	ΔE_p / mV	E^{01} / mV	i_{pc} / μA	i_{pa}/i_{pc}	χ_M
$V(Cp)_2(Cl)_2$	-1034	-	-	150	-	1.45
$Ti(Cp)_2(Cl)_2$	-1142	304	-990	154	0.92	1.32
$Zr(Cp)_2(Cl)_2$	-1314	-	-	145	-	1.21
$Hf(Cp)_2(Cl)_2$	-1326	-	-	130	-	1.23

Zirconocene dichloride, hafnocene dichloride and vanadocene dichloride were found to behave electrochemically and chemically irreversible. Titanocene dichloride has an anodic peak, but the peak potential difference ΔE = 304 mV is too big to be compatible with electrochemical reversibility or even quasi-reversibility. Since $i_{pa}/i_{pc} \approx 1$ for this complex, the Ti^{4+}/Ti^{3+} couple is chemically reversible. From a variable temperature study done in this laboratory on titanocene dichloride, chemical reversibility of the redox couple decreased as the temperature increases, the oxidation peak disappeared.

Comparison of the cathodic peak potentials (E_{pc}) of the various metallocene dichlorides in Figure 3.13 displays the relationship between the metals' peak cathodic potentials and their atomic electronegativity.[20] As the atomic electronegativity increases the peak cathodic potential accordingly increases. The more electronegative the metal the more difficult it will be reduced and thus the relatively more positive the peak cathodic potential becomes. Zirconocene dichloride and hafnocene dichloride have for al practical purposes the same atomic electronegativity. As expected they display peak cathodic potentials very close to each other.

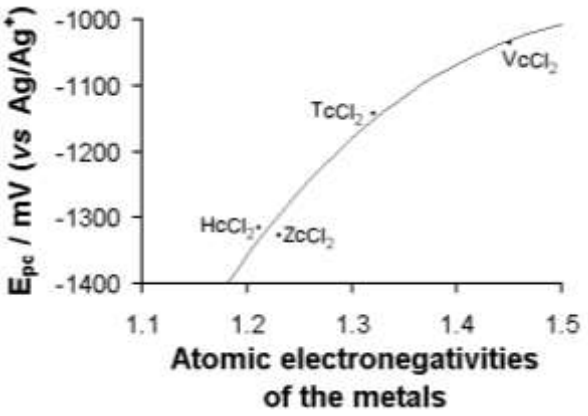

Figure 3.13. Relationship between the cathodic peak potential (E_{pc}) of the various metallocene dichlorides (titanocene, zirconocene, hafnocene and vanadocene) and their atomic electronegativities.[20]

It was found by many researchers that the cyclic voltammograms of titanocene dichloride and zirconocene dichloride in DCM and THF gave better reversibility than in CH_3CN.[21, 22, 23] These results were repeatable (Figure 3.14 and Table 3.12), during the course of this study.

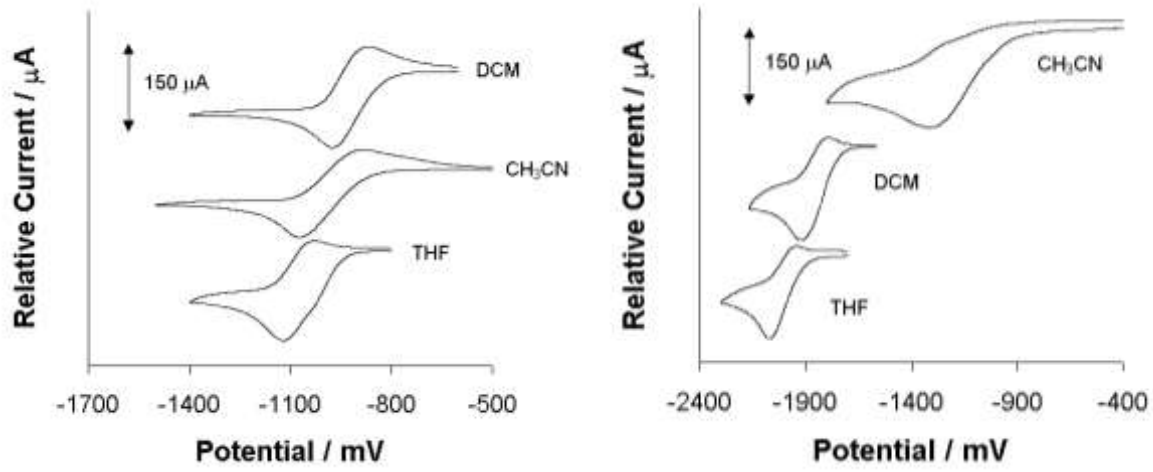

Figure 3.14. The cyclic voltammograms of 3.0 mmol dm^{-3} titanocene dichloride (Left) and zirconocene dichloride (Right) (supporting electrolyte is 0.2 mol dm^{-3} tetrabuthylammonium hexafluorophosphate) in DCM, THF and CH_3CN on a glassy carbon working electrode at 25˚C and a scan rate of 200 mV s^{-1}.

Table 3.12. The cyclic voltammetry data obtained from voltammograms (*vs* Ag/Ag^+ and Fc/Fc^+) of titanocene dichloride and zirconocene dichloride measured in 0.2 mol dm^{-3} tetrabuthylammonium hexafluorophosphate CH_3CN, DCM and THF solution with a glassy carbon working electrode at 25ºC at scan rate 200 mV s^{-1}. The concentration of titanocene dichloride and zirconocene dichloride was 3.0 mmol dm^{-3}

Mc	Solvent	E^{01} *vs* Ag/Ag^+ / mV	E^{01} *vs* Fc/Fc^+ / mV[a]	ΔE_p / mV	i_{pa}/i_{pc}	E^{01} *vs* Fc/Fc^+ / mV[b] [21, 22, 23, 24]
$TcCl_2$	DCM	-922	-1122	117	0.83	-1160
	THF	-1077	-1277	106	0.62	-1280
	CH_3CN	-990	-1190	304	0.92	-900
$ZcCl_2$	DCM	-1858	-2058	160	0.50	-2060
	THF	-2003	-2193	138	0.40	-2158
	CH_3CN	-1314	-1391	-	-	-

a) E^{01} values *vs* Fc/Fc^+ (as an internal standard).

b) Published E^{01} values.

The measured values and electrochemical behaviour were found to be markedly dependent on the solvent of the solution. Titanocene dichloride displayed electrochemical quasi-reversible behaviour in THF and DCM with ΔE_p values less than 150 mV at a scan rate of 200 mV s^{-1}. In CH_3CN, however, $TcCl_2$ demonstrates a drastic deviation from this quasi-reversible electrochemical behaviour with ΔE_p = 304 mV. The peak current ratio $i_{pa}/ i_{pc} \approx 1$ is in accordance with the expected chemical reversibility of this type of reaction. The observed electrochemical behaviour of $ZcCl_2$ can be described as electrochemical quasi-reversible in THF, electrochemically irreversible in DCM and complete chemical and electrochemical irreversible in CH_3CN since no oxidation peak was observed.

3.3.2.3. Mono-β-diketonato titanocenyl complexes

The cyclic voltammetry of all the mono-β-diketonato titanium complexes of the type $[Tc(\beta\text{-diketonato})]^+ClO_4^-$ with β-diketonato = trifluoroacetylacetonato ($tfaa^-$) [43], methyl acetoacetonato (maa^-) [20], acetylacetonato ($acac^-$) [41], benzoylacetonato ($bzac^-$) [42] and ferrocenoylacetonato (fca^-) [44] are shown in Figure 3.15 and the comparative data are shown in Table 3.13.

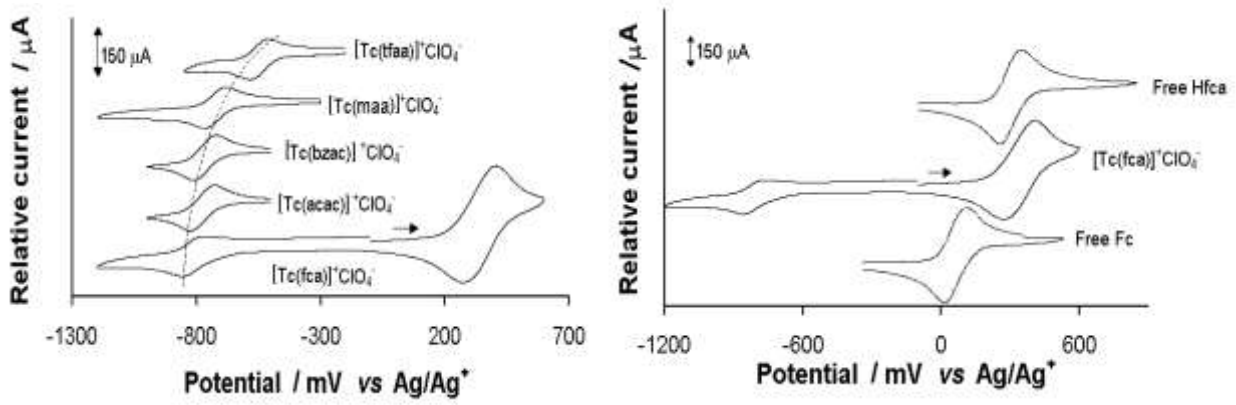

Figure 3.15. Left: The cyclic voltammograms of various 3.0 mmol dm^{-3} solutions of mono-β-diketonato titanocenyl complexes of the type $[Tc(\beta\text{-diketonato})]^+ClO_4^-$ with β-diketonato = $tfaa^-$ [43], maa^- [20], $acac^-$ [41], $bzac^-$ [42] and fca^- [44] (supporting electrolyte is 0.1 mol dm^{-3} tetrabuthylammonium hexafluorophosphate) in acetonitrile on a glassy carbon working electrode at 25˚C and a scan rate of 200 mV s^{-1}. Right: The comparative cyclic voltammograms of 3.0 mmol dm^{-3} $[Tc(fca)]^+ClO_4^-$, 3.0 mmol dm^{-3} free ferrocene and 3.0 mmol dm^{-3} free Hfca (supporting electrolyte is 0.1 mol dm^{-3} tetrabuthylammonium hexafluorophosphate) in acetonitrile on a glassy carbon working electrode at 25˚C and a scan rate of 200 mV s^{-1}.

Table 3.13. The cyclic voltammetry data obtained from voltammograms (*vs* Ag/Ag^+) of various mono-β-diketonato titanocenyl complexes of the type $[Tc(\beta\text{-diketonato})]^+ClO_4^-$ with β-diketonato = $tfaa^-$, maa^-,$acac^-$, $bzac^-$ and fca^-, Hfca and free frerocene measured in 0.1 mol dm^{-3} tetrabuthylammonium hexafluorophosphate/CH_3CN with a glassy carbon working electrode at 25ºC and a scan rate of 200mV s^{-1}. Data tabulated is of the Ti^{4+}/Ti^{3+} couple unless stated otherwise. The concentration of the all complexes was 3.0 mmol dm^{-3}.

Tc complex	No.	E_{pa} / mV	ΔE_p / mV	E^{01} / mV	i_{pa} / μA	i_{pa}/i_{pc}
$[Tc(CH_3COCHCOCF_3)]^+ ClO_4^-$	[43]	-502	78	-534	69	0.94
$[Tc(CH_3COCHCOOCH_3)]^+ ClO_4^-$	[20]	-674	78	-713	67	0.84
$[Tc(CH_3COCHCOC_6H_5)]^+ ClO_4^-$	[42]	-727	77	-766	70	0.81
$[Tc(CH_3COCHCOCH_3)]^+ ClO_4^-$	[41]	-735	84	-775	68	0.96
$[Tc(CH_3COCHCOFc)]^+ ClO_4^-$	[44]	-757	84	-813	72	0.85
Ferrocenyl fragment from above complex	-	389	96	341	324	1.05
Free Fc	-	115	76	77	332	1.03
Hfca	[40]	283	92	237	336	1.03

All the mono-β-diketonato titanium complexes were found to exhibit an electrochemical reversible Ti^{4+}/Ti^{3+} couple according to:

$$Ti^{IV} + e^- \rightleftharpoons Ti^{III}$$

with $\Delta E_p \leq 90$ mV for the one-electron transfer process involved. It is known that the Ti(III) β-diketonato complexes do exist and that this redox reaction does not change the coordination sphere of the complex. For example Coutts and Wailes made the Ti(III) titanocenyl acetylacetonate complex in 1969.[25] The overall reaction during the cyclic voltammetry experiment is therefore:

$$[(C_5H_5)_2Ti^{IV}(CH_3COCHCOR)]^+ + e^- \rightleftharpoons [(C_5H_5)_2\,Ti^{III}(CH_3COCHCOR)]$$

The $[Tc(fca)]^+ClO_4^-$ complex exhibits an additional quasi-reversible Fc/Fc^+ redox couple:

$$Fc^+ + e^- \rightleftharpoons Fc \quad \text{or} \quad [(C_5H_5)_2Fe^{III}]^+ + e^- \rightleftharpoons (C_5H_5)_2Fe^{II}$$

corresponding to the ferrocenyl ligand in the compound since $\Delta E = 96$ mV for this couple. The measured E^{01} value of the free Fc of 77 mV is the same as the published value (77 mV).[18]

In comparing the formal reduction potential for $[Tc(CH_3COCHCOR)]^+ClO_4^-$ complexes with R = CH_3 ($\chi_{CH3} = 2.34$); Ph ($\chi_{Ph} = 2.21$); CF_3 ($\chi_{CF3} = 3.01$) and Fc ($\chi_{Fc} = 1.87$), the titanium(IV) become increasingly more difficult to reduce as the group electronegativity, χ_R, of the R group increases, see Figure 3.16 (Left). This is expected, because the more electron withdrawing the R group, the more positive the titanium(IV) centre will be and accordingly the more difficult it will be to reduce it, Ti(IV) + e^- → Ti(III). Ferrocenyl is less electron withdrawing than CH_3, $\chi_{CH3} = 2.34$ *vs* $\chi_{Fc} = 1.87$. Therefore the titanium(IV) metal centre is more negative when bounded to the ferrocenyl β-diketonato ligand and thus easier to reduce. This explains the relatively more negative formal reduction potential of the fca complex over that observed for the acac complex.

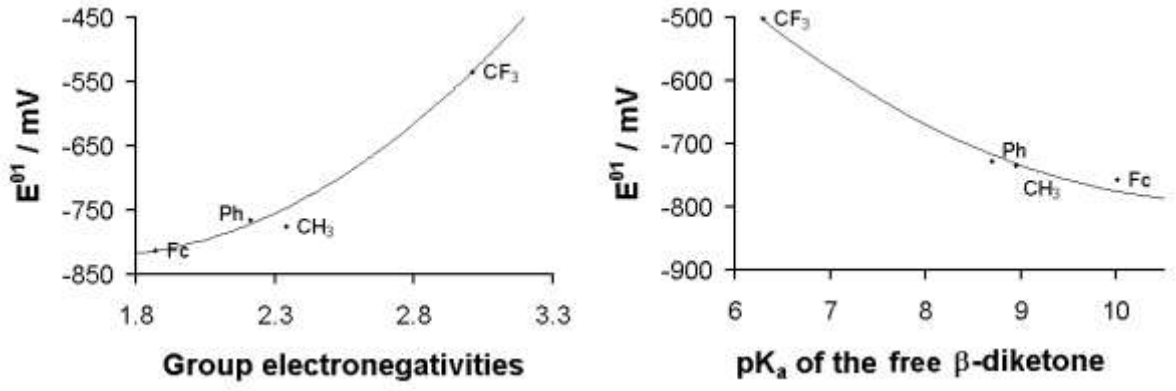

Figure 3.16. Graphs of the relationships of the formal reduction potential (E°) of the mono-β-diketonato titanocenyl complexes $[Tc(CH_3COCHCOR)]^+ClO_4^-$ with R = CH_3, Ph, CF_3 and Fc *vs* apparent group electronegativities of the R groups on the β-diketonato ligands (Left) and the pK_a of the β-diketone ligands (Right).

Although there are no linear relationship between the formal reduction potential of the mono-β-diketonato titanocene and the pK_a of the β-diketonato ligands (Table 3.2), a general trend is observed that with increasing pK_a there is a decrease in E^{01} (Figure 3.16).

The ratio $i_{pa}/i_{pc} \approx 1$ for both Ti^{4+}/Ti^{3+} and Fc/Fc^{+} redox couples of the studied complexes. This is indicative of good chemical reversibility, $i_{pa} \approx 70$ μA for all redox couples except for the oxidation of the ferrocenyl ligand of [44]. Comparison of i_{pa} values of this complex with the same concentration and the same scan rate of free ferrocene and ferrocenoylacetone (the free ferrocene β-diketone, Hfca) show that the peak anodic current for ferrocenyl of fca^{-} bounded to titanocenyl is the same as that found for the free ferrocene and ferrocenyl of the Hfca (Figure 3.15 and Table 3.13). The anodic peak current of the bounded ferrocenyl, however, is enhanced 4.5 times that of the titanium, even though in both instances a one electron transfer process is involved. This one electron transfer process is confirmed by bulk electrolysis, shown in Section 3.3.5. No explanation can be given for the large difference in peak currents for the Ti and Fc groups at present, further study is required.

Comparison of the data obtained for [41] and [42] during this study is mutually consistent with data published from Bond and co-workers.[9]

3.3.2.4. Bis-β-diketonato titanium complexes

The cyclic voltammetry of all the bis-β-diketonato titanium complexes [Ti(Cp)(Cl)(β-diketonato)$_2$] with β-diketonato = $tfaa^{-}$ [48], $acac^{-}$ [45], $bzac^{-}$ [46] and fca^{-} [47] (see Figure 3.17 and Table 3.14) exhibit an irreversible titanium reduction peak (i_{pa} not detected, $i_{pa} = 0$) according to

$$Ti^{IV} + e^{-} \longrightarrow Ti^{III}$$

except for the [47] complex for which the Ti^{4+}/Ti^{3+} couple were chemically reversible ($i_{pa}/i_{pc} \approx 1$) and electrochemically irreversible ($\Delta E = 244$ mV). The Fc/Fc^{+} couple for this complex is quasi-reversible according to

$$Fc^{+} + e^{-} \rightleftharpoons Fc$$

because $\Delta E \approx 95$ mV.

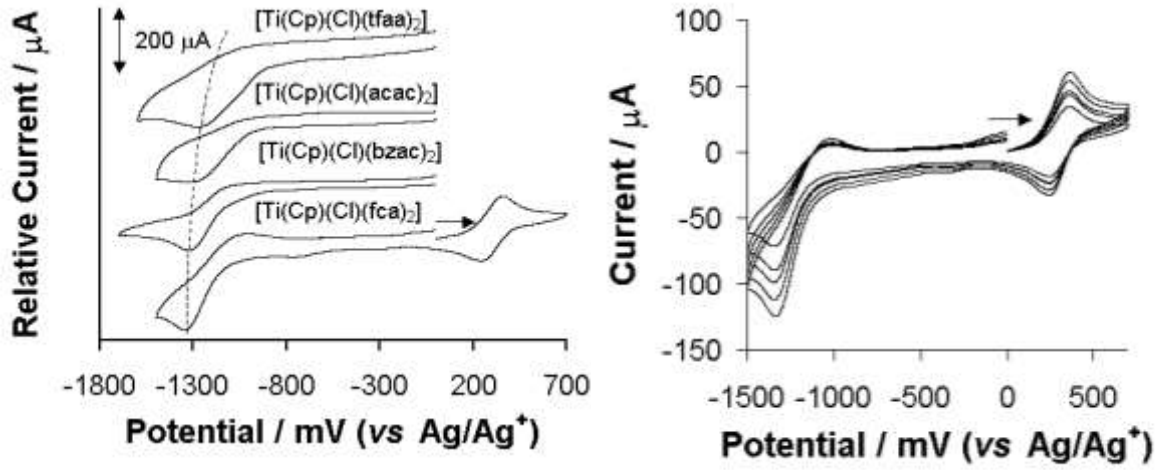

Figure 3.17. Left: The cyclic voltammograms of various 3.0 mmol dm^{-3} bis-β-diketonato titanium complexes of the type [Ti(Cp)(Cl)(β-diketonato)$_2$] with β-diketonato = $tfaa^-$, $acac^-$, $bzac^-$ and fca^- (supporting electrolyte is 0.1 mol dm^{-3} tetrabuthylammonium hexafluorophosphate), in acetonitrile with a glassy carbon working electrode at 25˚C and at a scan rate of 200 mV s^{-1}. Right: The cyclic voltammograms of a 3.0 mmol dm^{-3} [47] (supporting electrolyte is 0.1 mol dm^{-3} tetrabuthylammonium hexafluorophosphate) in acetonitrile with a glassy carbon working electrode at 25˚C and a scan rates of 50-250 mV s^{-1} (50 mV increments).

Table 3.14. The cyclic voltammetry data obtained from voltammograms (*vs* Ag/Ag^+) of various bis-β-diketonato titanium complexes of the type [Ti(Cp)(Cl)(β-diketonato)$_2$] with β-diketonato = $tfaa^-$, $acac^-$, $bzac^-$ and fca^- measured in 0.1 mol dm^{-3} tetrabuthylammonium hexafluorophosphate/CH_3CN with a glassy carbon working electrode at 25ºC and a scan rate of 200 mV s^{-1}. Data tabulated is of the Ti^{4+}/Ti^{3+} couple, unless stated otherwise. The concentration of the titanium complexes was 3.0 mmol dm^{-3}.

Tc complex	No.	E_{pc} / mV	ΔE_p / mV	E^{01} / mV	i_{pc} / µA	i_{pa}/i_{pc}
[Ti(Cp)(Cl)(tfaa)$_2$]	[48]	-1290	-	-	133	-
[Ti(Cp)(Cl)(acac)$_2$]	[45]	-1342	-	-	118	-
[Ti(Cp)(Cl)(bzac)$_2$]	[46]	-1347	-	-	128	-
[Ti(Cp)(Cl)(fca)$_2$]	[47]	-1361	244	-1163	155	0.94
Ferrocenyl fragment from above complex	-	255	95	302	56	0.97

The peak cathodic potentials for [Ti(Cp)(Cl)($CH_3COCHCOR$)$_2$] complexes was compared with the group electronegativity of the R groups of the β-diketonato ligands, with R = CH_3 (χ_{CH3} = 2.34); Ph (χ_{Ph} = 2.21); CF_3 (χ_{CF3} = 3.01) and Fc (χ_{Fc} = 1.87). It was found that, the titanium(IV) become increasingly more difficult to reduce as the group electronegativity, χ_R, of the R group increases in an almost linear fashion, see Figure 3.18.

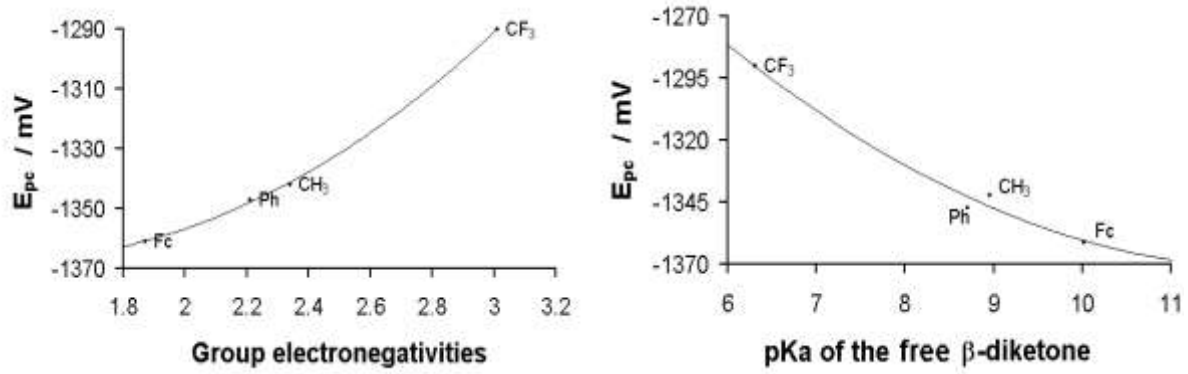

Figure 3.18. Graphs of the relationships of the peak cathodic potential of the bis-β-diketonato titanium complexes [Ti(Cp)(Cl)(β-diketonato)$_2$] with β-diketonato = tfaa$^-$, acac$^-$, bzac$^-$ and fca$^-$, measured in 0.1 mol dm^{-3} tetrabuthylammonium hexafluorophosphate/CH_3CN with a glassy carbon working electrode at 25ºC and a scan rate of 200 mV s^{-1} *vs* apparent group electronegativities of the R groups on the β-diketonato ligands (Left) and the pK_a of the free β-diketone (Right).

Although there is no linear relationship between the E_{pc} of the bis-β-diketonato titanium complex and the pK_a of the free β-diketone (Table 3.2), a general trend is observed that with increasing pK_a there is a decrease in the E_{pc} (Figure 3.18).

It should be mentioned here that for [47], only one oxidation and reduction peak is observed for both the ferrocene moieties (E^{01} = 312 mV, see Figure 3.17 Right). This is confirmed by the Oster Young square wave (OSWV) graph (Figure 3.19), which shows definitely only one peak at both slow and fast scan rates. The ΔE_p value of the Fc/Fc$^+$ couple for the bis-β-diketonato complexes [Ti(Cp)(Cl)(fca)$_2$] (96 mV) is the same as for the mono-β-diketonato complex [Tc(fca)]$^+ClO_4^-$ (95 mV), also implying that the two ferrocenyl moieties are reduced and oxidised simultaneously. A broadened peak would imply that the two ferrocenyl moieties are not reduced and oxidised at exactly the same potential but this was not found. Bulk electrolysis confirms that for the redox couple at 312 mV, two electrons are transferred (paragraph 3.3.5), one for each Fc moiety. This is in contrast to electrochemical studies done on diferrocenoylmethane (Hdfcm), [Rh(dfcm)(CO)$_2$] and [Ir(dfcm)(CO)$_2$], which revealed that there are two peaks (overlapping) for the Fc/Fc$^+$ couple.[26] This result indicates that the two fca$^-$ ligands in [47] are not in good communication with each other. They exist as two separate entities independent of each other even though they are coordinated to the same titanium nucleus. The complexes [M(Cp)(Cl)(fca)$_2$] with M = Zr, Hf and V (paragraph 3.3.4.1), also showed just one ferrocenyl wave.

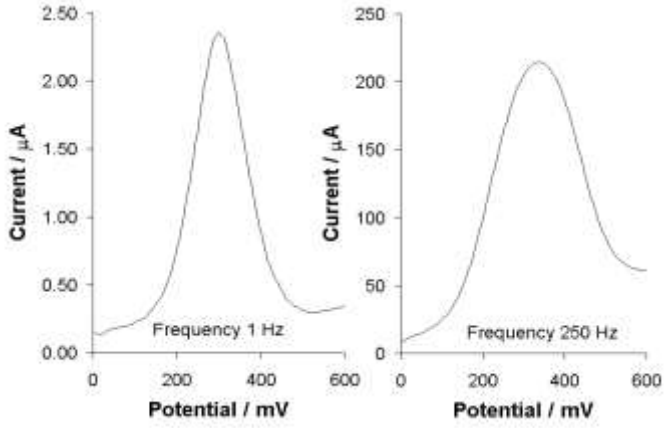

Figure 3.19. An Oster Young Square wave (OSWV) graph of $[Ti(Cp)(Cl)(fca)_2]$ between 0-600 mV, frequency 1 Hz (slow scan, left) and 250 Hz (fast scan, right).

When the bis-β-diketonato titanium complexes and the mono-β-diketonato titanium complexes are compared (Figure 3.20) the spread in E_{pc} when going from R = Fc to R = CF_3 for the bis-β-diketonato titanium complexes are smaller (-1361 mV to –1290 mV = 71 mV *vs* –757 mV to –502 mV = 255 mV) but the same directional trend is followed. The E_{pc} of the bis-β-diketonato titanium complexes are approximately two times lower, relative to Ag/Ag^+, than that for the mono-β-diketonato titanocenyl complexes. This implies that the titanium metal centre in the bis-β-diketonato titanium(IV) complexes are reduced more difficult relative to the titanium metal in the mono-β-diketonato titanocenyl(IV) complexes. However, in the Ti(III) form, the bis-β-diketonato titaniumcomplexes are oxidised more easily. The six-coordinated octahedral bis-β-diketonato titanium(IV) complex are coordinatively saturated, while the four coordinated tetrahedral mono-β-diketonato titanocenyl(IV) complex are not coordinatively saturated, saturation complexation is only a possible contributing factor.

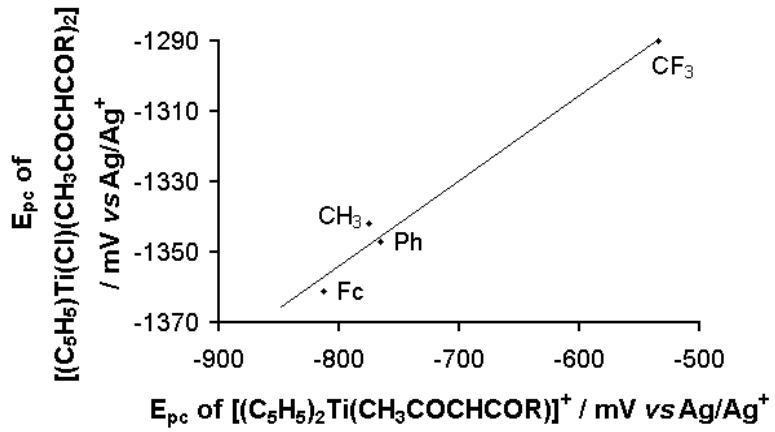

Figure 3.20. Relationship between the E_{pc} values of $[(C_5H_5)Ti(Cl)(CH_3COCHCOR)]$ and the E_{pc} values of the $[(C_5H_5)_2Ti(CH_3COCHCOR)]^+ClO_4^-$, R = CH_3, Ph, CF_3 and Fc.

3.3.2.5. Other bi-chelating titanocenyl complexes

The cyclic voltammograms of selected bi-chelating mono-ligand titanocenyl complexes of the types $[Tc(LL')]^+ClO_4^-$ with LL' = $Sacac^-$ [49] and [Tc(LL')], with LL' = $biphen^{2-}$ [51], cat^{2-} [9] and $Scat^{2-}$ [50] (see Figure 3.22), with metallocyclic ring sizes five to seven-membered are shown in Figure 3.21. The corresponding electrochemical data are shown in Table 3.15.

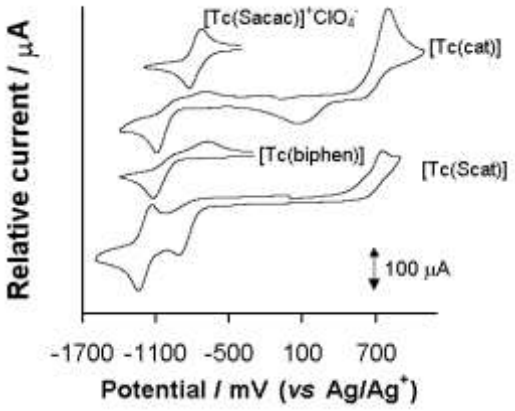

Figure 3.21. The cyclic voltammograms of 3.0 mmol dm^{-3} bi-chelating mono-ligand titanocenyl complexes of the types $[Tc(LL')]^+ClO_4^-$ with LL' = $Sacac^-$ [49] and [Tc(LL')] , with LL' = $biphen^{2-}$ [51], cat^{2-} [9] and $Scat^{2-}$ [50] (supporting electrolyte is 0.1 mol dm^{-3} tetrabuthylammonium hexafluorophosphate) in acetonitrile on a glassy carbon working electrode at 25˚C and a scan rate of 200 mV s^{-1}.

Table 3.15. The cyclic voltammetry data of the Ti^{4+}/Ti^{3+} couple of various bi-chelating mono-ligand titanocenyl complexes of the types $[Tc(LL')]^+ClO_4^-$ with LL' = $acac^-$, $Sacac^-$ and [Tc(LL')], with LL' = $biphen^{2-}$, cat^{2-} and $Scat^{2-}$, as obtained from voltammograms (*vs* Ag/Ag^+) measured in 0.1 mol dm^{-3} tetrabuthylammonium hexafluorophosphate/CH_3CN with a glassy carbon working electrode at 25ºC and a scan rate of 200mV s^{-1}. The concentration of the titanium complexes was 3.0 mmol dm^{-3}.

Tc complex	No.	E_{pc} / mV	ΔE_p / mV	E^{01} / mV	i_{pc} / μA	i_{pa}/i_{pc}	Metallocyclic ring size
$[Tc(acac)]^+ClO_4^-$	[41]	-735	84	-775	68	0.96	6
$[Tc(Sacac)]^+ClO_4^-$	[49]	-831	90	-780	71	0.97	6
[Tc(cat)]	[9]	-1111	439	-[a]	73	0.20	5
[Tc(biphen)]	[51]	-1119	323	-[a]	72	0.48	7
[Tc(Scat)]	[50]	-1262	147	-1188	70	0.98	5

a) Electrochemical irreversible process, E^{01} meaningless.

According to the i_{pa}/i_{pc} and ΔE_p values, the Ti^{IV}/Ti^{III} couple of [49] is chemically and electrochemically reversible ($i_{pa}/i_{pc} \approx 1$ and $\Delta E_p \leq 90$mV), [50] is electrochemically quasi-

reversible ($i_{pa}/i_{pc} \approx 1$ but $\Delta E_p > 90$ mV) while [9] and [51] are chemically and electrochemically irreversible ($i_{pa}/i_{pc} << 1$; $\Delta E_p > 150$ mV).

[49] is structurally the same as [41] (Figure 3.22), except for one oxygen which has been replaced by a sulphur. The similarities between these compounds can be seen from the electrochemical data: Firstly, the formal reduction potentials are essentially the same within experimental error (5 mV) E^{01} = -775 mV for [41] and E^{01} = -780 mV for [49]. In principle, this difference could also be attributed to higher electronegativity of oxygen (3.5) over sulphur (2.4),[20] but the difference is so small that no meaning is read into it. The second similarity is the ΔE values, ΔE = 84 mV for [41] and ΔE = 90 mV for [49], these small variations may be due to different heterogeneous electron transfer kinetic rates between compound and electrode but again, the difference is so small that it is not regarded as meaningful. Other similarities are peak potentials and peak currents which are both approximately the same for the two complexes (i_{pa} = 68 μA for [41] and i_{pa} = 71 μA for [49]).

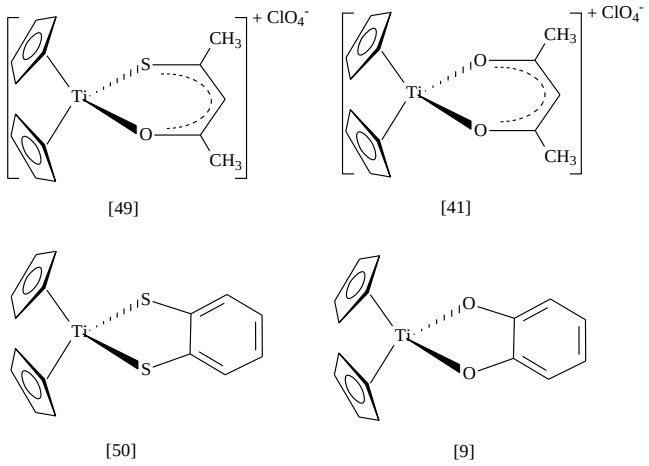

Figure 3.22. Structures of $[Tc(Sacac)]^+ClO_4^-$ [49], $[Tc(acac)]^+ClO_4^-$ [41], [Tc(Scat] [50] and [Tc(cat)] [9].

[50] is the sulphur version of [9] (see Figure 3.22), the electrochemical data obtained for these two complexes are, however, quite different. Since the 1,2-benzenediolato (cat) derivative shows irreversible electrochemistry, E_{pc} values are compared in this discussion. The E_{pc} of [50] (-1262 mV) is lower than that of [9] (-1111 mV) and this is consistent with the fact that sulphur is less electron withdrawing than the oxygen atom (χ_S = 2.4 and χ_O = 3.5). As a consequence the titanium centre will thus be more positive in [9] and will accordingly be easier to reduce. The conductivity was also experimentally measured during this study. The conductivity of [50] (5 mM in acetonitrile at 25˚C) is 1.15 x 10^{-5} S m^{-1}, which is about three times bigger than that for [9] (5 mM in acetonitrile at 25˚C) 3.7 x 10^{-6} S m^{-1}. The redox-couple of cat^{2-} and $Scat^{2-}$ in [9] and [50] will be discussed in paragraph 3.3.3.

The peaks at 814 mV and 39 mV on Figure 3.21 for [9], as well as at 775 mV and –927 mV for [50] is ligand centred electrochemical waves and will be understood after discussion of the ligand electrochemistry in the next section.

3.3.3. Electrochemistry in sulphuric acid on an activated glassy carbon electrode

It was found that activation of a glassy carbon electrode, by oxidation at +1.8 V in 0.1 M H_2SO_4/H_2O for 28 min, greatly increases the reversibility of 1,2-benzenediol (8 mM) in 0.1 M H_2SO_4/H_2O.[27] In this study reproducible electrochemical reversible behaviour for 1,2-benzenediol in 0.1 M H_2SO_4/H_2O were obtained. However, it was found that by changing solvent to acetonitrile 1,2-benzenediol displayed irreversible electrochemistry on an activated glassy carbon electrode (Figure 3.23). Comparative data is shown in Table 3.16.

The theoretical formal reduction potential of Fc *vs* the Ag/Ag^+ reference electrode, following the procedure shown in Figure 3.24, is 203 mV. It was experimentally determined in this study that when Fc was dissolved in a 10% acetonitrile, 90% 0.1 M H_2SO_4/H_2O solution (supporting electrode KCl) its formal reduction potential *vs* Ag/AgCl was 208 mV, which is for all practical purposes the same as 203 mV. The formal reduction potentials (E^{01} values) of 1,2-benzenediol in 0.1 M H_2SO_4 and in CH_3CN *vs* ferrocene as an internal standard (reference) are within 6.7%. Thus even though 1,2-benzenediol is irreversible in acetonitrile, the E^{01} values in different solvents *vs* the same internal reference, here ferrocene, are thus comparable.

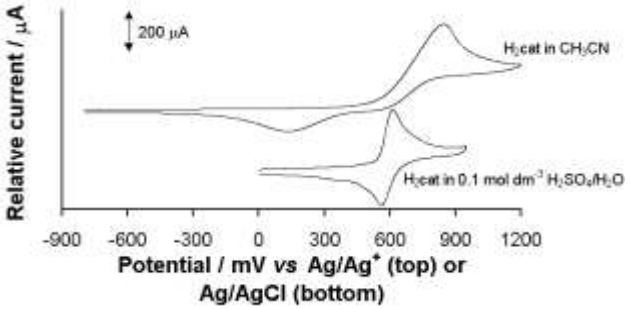

Figure 3.23. The cyclic voltammogram of 3.0 mmol dm^{-3} 1,2-benzenediol (H_2cat) (supporting electrolyte is 0.1 mol dm^{-3} tetrabuthylammonium hexafluorophosphate) in acetonitrile on an activated glassy carbon working electrode at 25˚C. The reference electrode is Ag/Ag^+ and scan rate 200 mV s^{-1} (top). Cyclic voltammogram of 3.0 mmol dm^{-3} 1,2-benzenediol (supporting electrolyte is 0.1 mol dm^{-3} KCl) in 0.1 M H_2SO_4 on an activated glassy carbon working electrode at 25˚C. The reference electrode is Ag/AgCl and scan rate 200 mV s^{-1} (bottom).

Table 3.16. The cyclic voltammetry data obtained from voltammograms of 1,2-benzenediol in

a) acetonitrile (*vs* Ag/Ag^+) at scan rate 200 mV s^{-1} and

b) 0.1 M H_2SO_4/H_2O (*vs* Ag/AgCl) at scan rate 200mV s^{-1}

The concentration of 1,2-benzenediol was 3.0 mmol dm^{-3}. $E^{01} = (E_{pa} + E_{pc})/2$.

1,2-Benzenediol in different solvents	E_{pa} / mV	ΔE_p / mV	E^{01} / mV *vs* Ag/AgCl	E^{01} / mV *vs* Fc/Fc^{+} [a]	E^{01} / mV *vs* Ag/Ag^+
CH_3CN	812	635	494[b]	417[b]	494[b]
0.1 M H_2SO_4/H_2O	621	59	592	389	466[c]

a) Fc/Fc^+ was used as an internal standard.

b) Strictly spoken, E^{01} is meaningless for an electrochemically irreversible process ($\Delta E_p > 150$ mV). Since the redox couple of 1,2-benzenediol displays electrochemical reversible behaviour in 0.1 M H_2SO_4/H_2O, as well as chemically reversible behaviour in 0.1 M H_2SO_4/H_2O ($i_{pa}/i_{pc} \approx 1$), E^{01} has been calculated for comparative purposes.

c) Calculate value according to Figure 3. 24.

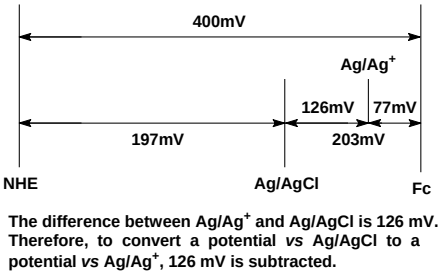

Figure 3.24. Illustration to show the conversion of potential *vs* Ag/AgCl to potential *vs* Ag/Ag^+ or Fc/Fc^+. Fc/Fc^+ *vs* Ag/Ag^+ = 77 mV,[18] Fc/Fc^+ *vs* NHE = 400 mV,[28] and Ag/AgCl *vs* NHE = 197 mV.[29]

There are a few possible explanations for the better electrochemical reversibility of 1,2-benzenediol in H_2SO_4 than in acetonitrile:

- Water has a higher dielectric constant (78.5) than acetonitrile (37.5); a higher dielectric constant means the solvent has a lower electric resistance.
- H_2SO_4 is itself an electrolyte, thus current is transferred even better than just with KCl (the electrolyte in water mixtures).
- Water has a lower specific resistance (8.94 ohm cm) than acetonitrile (37 ohm cm).[30]
- The measure conductance of 0.1 M H_2SO_4 was found to be 5.64 x 10^{-3} S m^{-1} whereas acetonitriles' was 1.03 x 10^{-6} S m^{-1} at 22˚C.
- Lastly and probably most important is that 1,2-benzenediols' redox reaction is pH dependent (Scheme 3.10) and the redox reaction would naturally be faster in acid medium, thus the peak anodic difference would be smaller.

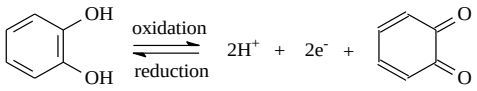

Scheme 3.10. The oxidation and reduction reaction of 1,2-benzenediol.

Seeing as 1,2-benzenediol gave such good results in 0.1 M H_2SO_4/H_2O, other compounds related to 1,2-benzenediol and used in this study were subjected to similar electrochemical conditions for comparative purposes. The cyclic voltammograms of 1,2-benzenediol, 1,2-benzenedithiol and 2,2-biphenyldiol were recorded and the comparative voltammograms are shown in Figure 3.25. The electrochemical data related to these voltammograms are shown in Table 3.17.

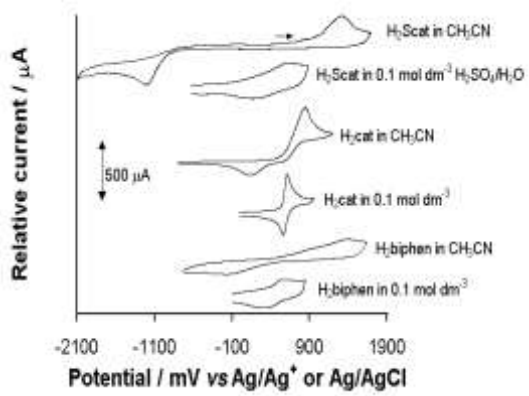

Figure 3.25. The cyclic voltammogram of 3.0 mmol dm^{-3} 1,2-benzenediol, 1,2-benzenedithiol and 2,2-biphenyldiol in different solvents with a glassy carbon working electrode at 25˚C and a scan rate of 200 mV s^{-1}:

a) 0.1 mol dm^{-3} tetrabuthylammonium hexafluorophosphate/CH_3CN (reference electrode is Ag/Ag^+) and

b) 0.1mol dm^{-3} KCl/0.1 M H_2SO_4 reference electrode is Ag/AgCl

Table 3.17. The electrochemical data obtained from voltammograms of 1,2-benzenediol, 1,2-benzenedithiol and 2,2-biphenyldiol in

a) acetonitrile (*vs* Ag/Ag^+) at scan rate 200 mV s^{-1} and

b) 0.1 M H_2SO_4 (*vs* Ag/AgCl) at scan rate 200 mV s^{-1}

The concentration of 1,2-benzenediol, 1,2-benzenedithiol and 2,2-biphenyldiol was 3.0 mmol dm^{-3}

	E_{pa} / mV	ΔE_p / mV	E^{01} / mV	E^{01} / mV *vs* Fc[a]	E^{01} / mV *vs* Ag/Ag^+
1,2-benzenediol, H_2cat, in different solvents					
CH_3CN	812	635	[b]	[b]	[b]
0.1M H_2SO_4/H_2O	621	59	592	389	466[c]
1,2-benzenedithiol, H_2Scat, in different solvents					
CH_3CN	1332	2551	[b]	[b]	[b]
0.1M H_2SO_4/H_2O	639	488	[b]	[b]	[b]
2,2-Biphenyldiol, H_2biphen, in different solvents					
CH_3CN	1200	1187	[b]	[b]	[b]
0.1M H_2SO_4/H_2O	548	259	[b]	[b]	[b]

a) Internal standard.

b) E^{01} calculation not meaningful because $\Delta E_p > 90$ mV (i.e. not reversible electrochemistry).

c) Calculate value according to Figure 3. 24.

With 1,2-benzenediol there was a 90% improvement for the difference in peak potentials ΔE_p when the solvent was changed from acetonitrile to 0.1 M H_2SO_4/H_2O. Improvement for the ΔE_p values for 1,2-benzenedithiol and 2,2-biphenyldiol was also observed when the solvent was changed, (80.1% and 78.2% respectively), but the redox reaction for 1,2-benzenedithiol and 2,2-biphenyldiol is still totally electrochemically irreversible.

The peaks at 814 mV and 39 mV on Figure 3.21 for [9], as well as at 775 mV and –927 mV for [50] are descended from the ligands cat^{2-} and $Scat^{2-}$ respectively. See the voltammograms of free ligands H_2cat and H_2Scat in Figure 3.25.

3.3.4. Early transition metals (titanium group metals)

3.3.4.1. Bis-β-diketonato complexes of early transition metals

Replacement of one cyclopentadienyl ring and one Cl^- group in the metallocene dichlorides $TcCl_2$, $ZcCl_2$, $HcCl_2$ and $VcCl_2$ with two acetylacetonato ligands, changes the coordination sphere of the metals (Ti, Zr, Hf, V) from four to six. The cyclic voltammograms of these bis-acetylacetonato metal complexes of the type $[M(Cp)(Cl)(acac)_2]$ where M = Ti [45], Zr [53], Hf [57] and V [60] were taken and the comparative graphs are shown in Figure 3.26 and the comparative data are tabulated in Table 3.18. From this data, the influence of the metal centre on the electrochemical behaviour can be probed.

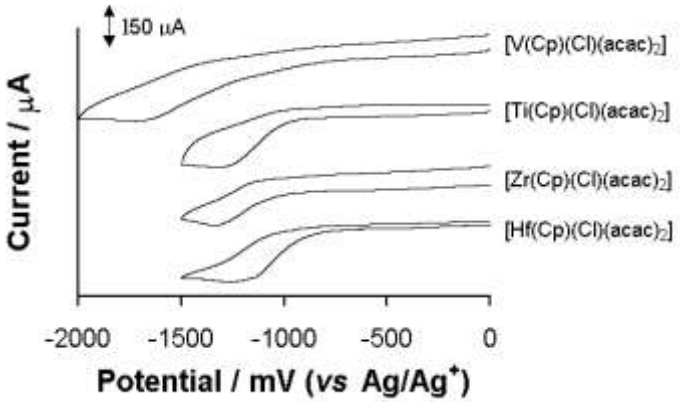

Figure 3.26. The cyclic voltammograms of various 3.0 mmol dm^{-3} bis-acetylacetonato metal complexes of the type $[M(Cp)(Cl)(acac)_2]$ where M = Ti [45], Zr [53], Hf [57] and V [60] (supporting electrolyte is 0.1 mol dm^{-3} tetrabuthylammonium hexafluorophosphate) in acetonitrile on a glassy carbon working electrode at 25˚C and a scan rate of 200 mV s^{-1}.

Table 3.18. The cyclic voltammetry data obtained from voltammograms (*vs* Ag/Ag^{+}) of various metal complexes measured in 0.1 mol dm^{-3} tetrabuthylammonium hexafluorophosphate/CH_3CN with a glassy carbon working electrode at 25ºC and a scan rate of 200 mV s^{-1}. The concentration of the metal complexes was 3.0 mmol dm^{-3}.

Metallocene	No.	E_{pc} / mV[a]	i_{pc} / μA
$[V(Cp)(Cl)(acac)_2]$	[60]	-1726	150
$[Ti(Cp)(Cl)(acac)_2]$	[45]	-1342	154
$[Zr(Cp)(Cl)(acac)_2]$	[53]	-1350	145
$[Hf(Cp)(Cl)(acac)_2]$	[57]	-1258	130
$[Ti(Cp)(Cl)(bzac)_2]$	[46]	-1347	135
$[Zr(Cp)(Cl)(bzac)_2]$	[54]	-1376	126

a) No anodic peak was observed.

The cyclic voltammograms of the $[M(Cp)(Cl)(acac)_2]$ complexes of Table 3.18 and Figure 3.26 show complete chemical and electrochemical irreversibility with no oxidation peaks. Complexes of the type $[M(Cp)(Cl)(bzac)_2]$ with M = Ti and Zr behave similarly. Results are summarised in Table 3.18.

The influence of the ferrocenyl group on the electrochemistry of this kind of bis-β-diketonato complexes of the early transition elements, can be seen on the cyclic voltammogram of the $[M(Cp)(Cl)(fca)_2]$ complexes with M = Ti [47], Zr [55], Hf [58] and V [61]. See Figure 3.27 and Table 3.19.

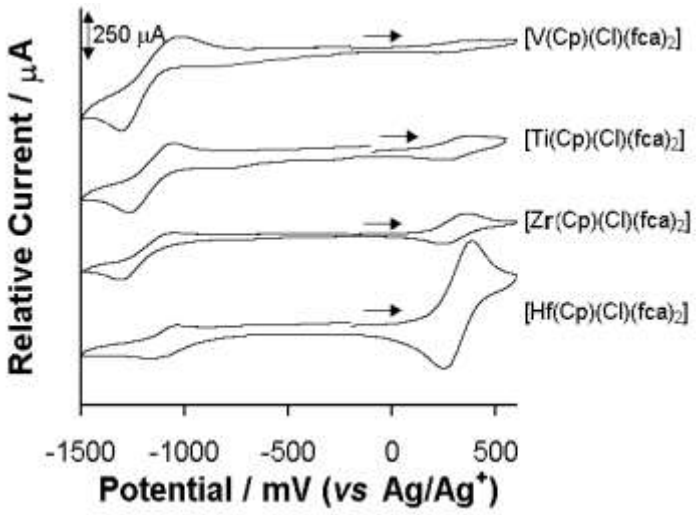

Figure 3.27. The cyclic voltammograms of various 3.0 mmol dm^{-3} bis-ferrocenoylacetonato metal complexes of the type $[M(Cp)(Cl)(fca)_2]$ where M = Ti [47], Zr [55], Hf [58] and V [61] (supporting electrolyte is 0.1 mol dm^{-3} tetrabuthylammonium hexafluorophosphate) in acetonitrile with a glassy carbon working electrode at 25˚C and a scan rate of 200 mV s^{-1}.

Table 3.19. The cyclic voltammetry data obtained from voltammograms (*vs* Ag/Ag^+) of various bis-ferrocenoylacetonato metal complexes (Ti, Zr, Hf, V) measured in 0.1 mol dm^{-3} tetrabuthylammonium hexafluorophosphate/CH_3CN with a glassy carbon working electrode at 25ºC and a scan rate of 200 mV s^{-1}. The concentration of the metal complexes was 3.0 mmol dm^{-3}.

Metal complex	Ionic radii of metal / Å	E_{pa} / mV [a]	ΔE_p / mV	i_{pa} / µA	i_{pa}/i_{pc}	E_{pa} / mV [a]	ΔE_p / mV	i_{pa} / µA	i_{pa}/i_{pc}	Period [b]
		Ti^{4+}/Ti^{3+} couple				Fc/Fc^+ couple				
$[V(Cp)(Cl)(fca)_2]$	0.63	-1010	312	152	0.68	423	218	28	0.86	4
$[Ti(Cp)(Cl)(fca)_2]$	0.68	-1041	244	155	0.94	349	95	56	0.97	3
$[Zr(Cp)(Cl)(fca)_2]$	0.79	-1041	281	114	0.96	370	144	70	0.92	3
$[Hf(Cp)(Cl)(fca)_2]$	0.78	-1031	150	84	0.93	371	142	224	0.95	5

a) Only E_{pa} reported, E^{01} calculated not meaningful since $\Delta E > 90$ mV.

b) Period in the periodic table.

The presence of the ferrocenyl group on the β-diketonato ligand, does have a different influence on the electrochemistry of the V, Ti, Zr and Hf metal centres than does the metal-free ligand, acetylacetonato. Even though the redox active ferrocene-containing ligand (fca^-) coordinated to the complex does cause the appearance of oxidation peaks for the metals Ti, Zr, Hf and V, hereby indicating a degree of chemical reversibility, the electrochemical process associated with V, Ti, Zr and Hf is still irreversible due to $\Delta E_p > 150$ mV.

The Fc/Fc^+ couple of the $[M(Cp)(Cl)(fca)_2]$ complexes showed chemical reversibility ($i_{pa}/i_{pc} \approx 1$), but is electrochemically quasi-revesible (90 mV < ΔE_p < 150 mV) for M = Ti, Zr, Hf and electrochemically irreversible ($\Delta E_p > 150$ mV) for M = V. No relationship between the E_{pa}, period in the periodic table, ionic radii or atomic electronegativity of the metal could be found.

i_{pa} of the M^{4+}/M^{3+} (M = Ti, Zr, Hf and V) couple of Ti and V, both of the fourth period of the periodic table were similar, about 150 µA. This current decreased upon going to the fifth period, (114 µA). Going to the sixth period, (84 µA). i_{pa} of Fc/Fc^+ couple however, showed the opposite trend. The ferrocenyl peak current ratios increased as ionic radii of the central coordinating metal cation decreased.

3.3.5. Bulk electrolysis

Bulk electrolysis was preformed on selected complexes representing each of the different classes of compounds, which were studied electrochemically. The reduction step of the Ti and the oxidation step of the Fc were subjected to bulk electrolysis. As an example the graph of the

current-time and charge-time of the oxidation of the ferrocenyl ligand coordinated to titanium in $[Tc(fca)]^+ClO_4^-$ [44] and $[Ti(Cp)(Cl)(fca)_2]$ [47] is shown in Figure 3.28. The bulk electrolysis data and results of all the compounds investigated are summarised in Table 3.20.

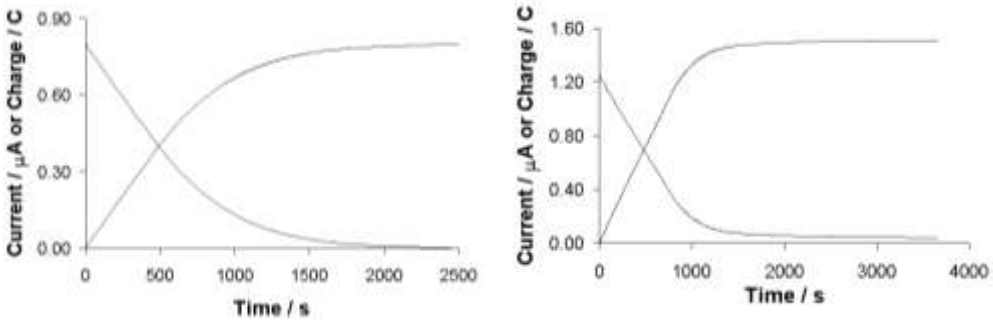

Figure 3.28. Current-time and charge-time response for the oxidation of Fc in $[Ti(Cp)(Cl)(fca)_2]$ [47] (Left) at E_{exp} = 700 mV and $[Tc(fca)]^+ClO_4^-$ [44] (Right) at E_{exp} = 600 mV.

Table 3.20. Results from bulk electrolysis. Electrolysis was preformed on N mol of the indicated complex in 0.1 mol dm^{-3} tetrabuthylammonium hexafluorophosphate/CH_3CN at 15.1˚C, using a carbon plate working electrode. Q = total charge collected and n = electrons transferred per molecule. E_{exp} indicate the position at which the oxidation of the ferrocenyl ligand or the reduction of the Ti in the complexes indicated, was performed.

Complex	Mass / mg	10^5 N / mol	Q / C	Q/NF	n	E_{exp} / mV
$[Tc(fca)]^+ClO_4^-$, [44]						
Ti	8.5	1.54	1.497	1.04	1	-1200
Fc	8.5	1.54	1.511	1.05	1	600
$[Ti(Cp)(Cl)(fca)_2]$, [47]						
Ti	10.7	1.55	0.801	1.08	1	-1500
Fc	10.7	1.55	1.498	2.02	2	700
cat						
cat	1.6	1.45	2.798	1.99	2	1100
[Tc(cat)], [9]						
Ti	6.2	1.60	1.506	0.98	1	-1400
cat	6.2	1.60	3.126	2.02	2	1100

The expected amount of electrons, were transferred in all cases (Table 3.20). For complex [44], both the Ti and Fe are involved in one electron transfer processes (Figure 3.29) for complex [47], the number of electrons transferred for the Fc group was twice that of Ti (Figure 3.29), because two Fc-groups are present. As for the ligand 1,2-benzenediol, the two-electron transfer process was confirmed. In the complex [9], the 1,2-benzenediolato transfers two electrons and the Ti core just one (Figure 3.29).

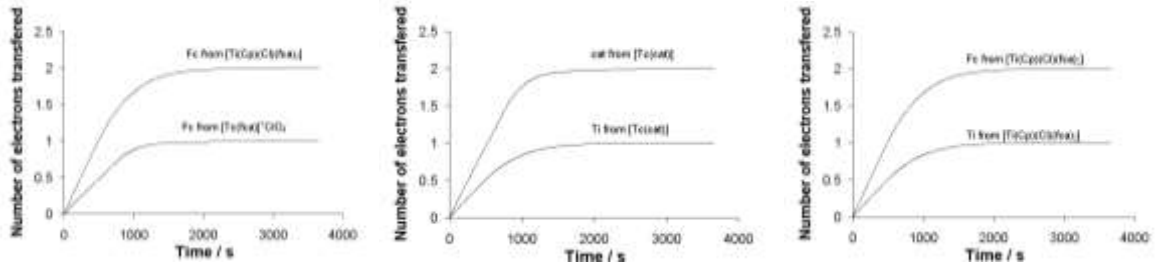

Figure 3.29. Left: Graph of number of electrons transferred *vs* time for the oxidation of Fc in [44] at E_{exp} = 600 mV and [47] at E_{exp} = 700 mV. Middel: Coulometry experiment of [9] indicate the overall amount of electrons that flow during oxidation of the 1,2-benzenediolato ligand or during the reduction of the titanium(IV) metal. Right: Coulometry experiment of [47] indicate the overall amount of electrons that flow during oxidation of the ferrocenyl ligand or during the reduction of the titanium(IV) metal.

3.4 Substitution kinetics of various titanium bidentate complexes

3.4.1 Introduction

The substitution reactions investigated in this kinetic study, involves the five-, six- and seven-membered metallocyclic complexes of titanocenyl; [Tc(cat)] [9], $[Tc(acac)]^+ClO_4^-$ [41], $[Tc(Sacac)]^+ClO_4^-$ [49] and [Tc(biphen)] [51] with Hacac, Hsacac and H_2biphen.

The general rate law applicable to the substitution reaction between titanocenyl complexes of the type $[Tc(L_1L_2)]^x$ (x = 0, +1) and an incoming ligand L_3L_4 (L_1L_2 and L_3L_4 both bidentate ligands such as 1,2-benzenediolato, acetylacetonato, thioacetylacetonato and 2,2-biphenyldiolato) according to Scheme 3.11, is given by equation 3.1.

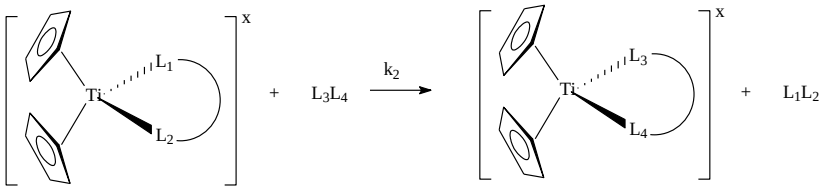

Scheme 3.11. General reaction scheme of the substitution reaction of titanocenyl complexes with a bidentate ligand, x = 0, +1, the charge of the titanocenyl complex.

Equation 3.1.

$$\text{Rate} = \{k_s + k_2[L_3L_4]\}[[Tc(L_1L_2)]^x]$$

with x = 0, +1, the charge of the titanocenyl complex. If $[L_3L_4] >> [[Tc(L_1L_2)]^x]$ then this rate simplifies to:

$$Rate = k_{obs}[[Tc(L_1L_2)]^x]$$

with the pseudo first-order rate constant $k_{obs} = k_s + k_2[L_3L_4]$.

3.4.2 A kinetic study of substitution reactions between 2,2-biphenyldiol and different sized metallocyclic titanocenyl complexes

In this section the results of the substitution of the bidentate ligands $L_1L_2 = cat^{2-}$, $acac^-$ and $Sacac^-$ from $[Tc(L_1L_2)]^x$ (x = 0, +1; the charge of the complex) with 2,2-biphenyldiol according to Scheme 3.12 is reported.

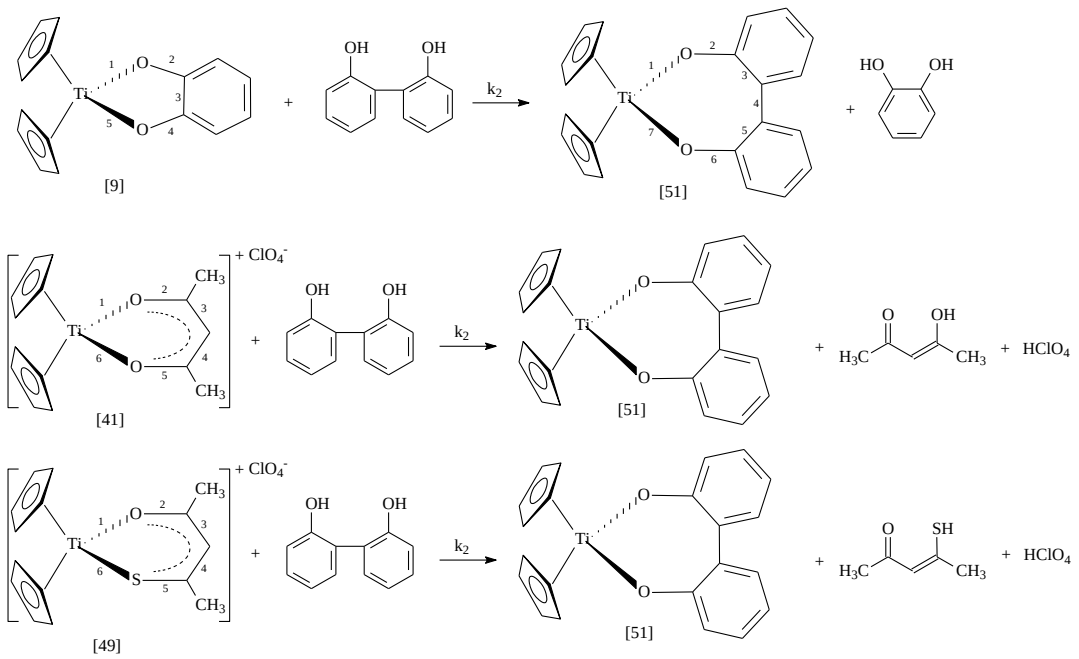

Scheme 3.12. Substitution reactions between 2,2-biphenyldiol and 5 or 6-membered metallocyclic titanocenyl complexes to give the seven-membered pseudo-aromatic product [Tc(biphen)].

Figure 3.30 shows the UV-spectra of [Tc(cat)] [9], $[Tc(acac)]^+ClO_4^-$ [41], $[Tc(Sacac)]^+ClO_4^-$ [49] and [Tc(biphen)] [51], the spectral data are summarized in Table 3.21.

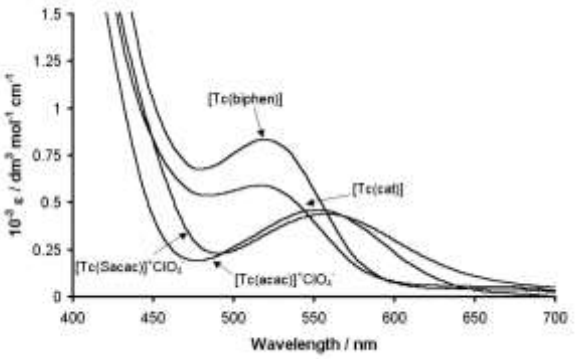

Figure 3.30. UV Spectra of [9], [41], [49] and [50] at 25˚C in acetone.

Table 3.21. Molecular extinction coefficients (ε) of the titanocenyl complexes at 25˚C in acetone ($\lambda_{exp} = \lambda_{maks}$).

Ti-complex	No.	λ_{exp} / nm	ε / $dm^3\ mol^{-1}\ cm^{-1}$
[Tc(cat)]	[9]	515	5891
$[Tc(acac)]^+ClO_4^-$	[41]	550	4597
$[Tc(Sacac)]^+ClO_4^-$	[49]	558	4372
[Tc(biphen)]	[51]	520	8337

The linear relationship (Figure 3.31) that exists between the absorbance values and different concentrations (from 0.0001 mol dm^{-3} to 0.005 mol dm^{-3}) of the titanium complexes [9], [41], [49] and [51] in acetone, illustrates that these four complexes obey the Beer-Lambert law, $A = \varepsilon c\ell$ with A = absorbance, ε = extinction coefficient, c = concentration and ℓ = path length.

The pseudo first-order reaction rate constants k_{obs} were obtained by following the formation of [51] at the indicated wavelength (Table 3.21). The product of the substitution had the same UV spectrum than [51], confirming the reaction Scheme 3.13 for the substitution of the bidentate ligands L_1L_2 = cat^{2-}, $acac^-$ and $Sacac^-$ from $[Tc(L_1L_2)]^x$ (x = 0, +1) with 2,2-biphenyldiol.

The reactions were carried out under pseudo first-order reaction conditions, [ligand] >> [Ti-complex]. A linear relationship was obtained for ln C (measured as ln V {V = potential difference measured in V}, where V ∞ C) *vs* time for every substitution reaction, and showed that the reaction is first-order in the titanocenyl complex. This linear relationship was found for at least two to three half-lives.

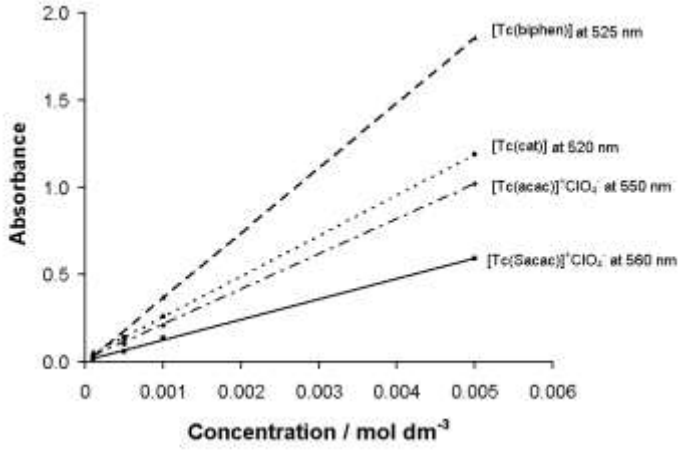

Figure 3.31. Graph of absorbance *vs* concentration of [9], [41], [49] and [51], in acetone at 25˚C taken at λ_{exp} as indicated.

All the graphs of k_{obs} vs [2,2-biphenyldiol] for each titanocenyl complex (Figure 3.32-3.34) are straight lines through the origin, which implies a first-order dependence on

[2,2-biphenyldiol], with the second order rate constant given by the slope (Table 3.22). Further, the zero intercept indicated, as expected, that the solvent does not contribute meaningful to the mechanism of substitution.

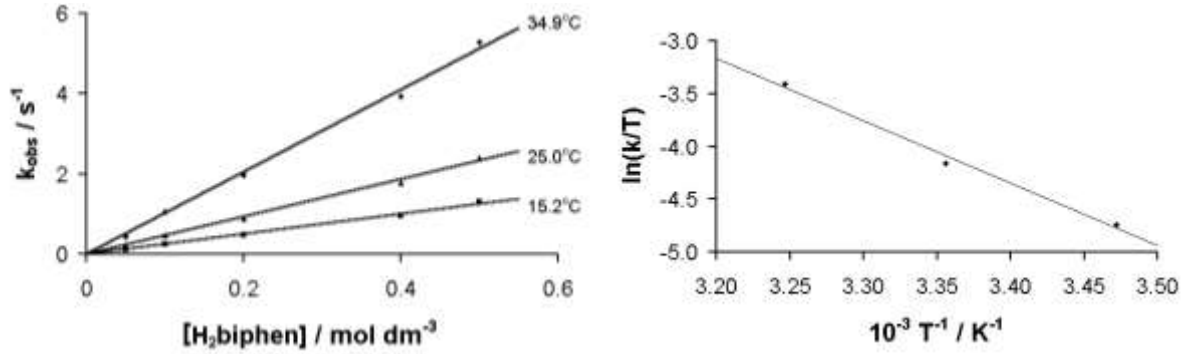

Figure 3.32. Graph of k_{obs} vs [2,2-biphenyldiol] (left) and *ln* (k_2/T) vs 1/T (right) for the substitution of 1,2-benzenediolato from [9)] with 2,2-biphenyldiol at T = 15.2˚C, 25.0˚C and 34.9˚C. [Ti-complex] = 0.002 mol dm^{-3}.

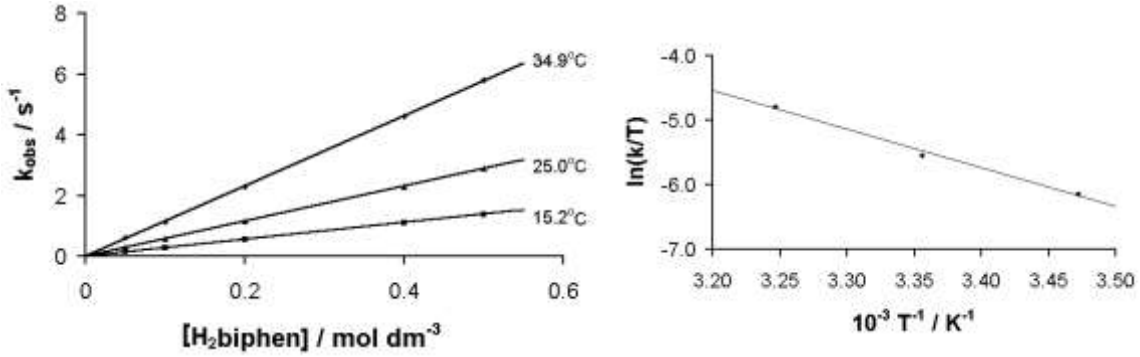

Figure 3.33. Graph of k_{obs} vs [2,2-biphenyldiol] (left) and *ln* (k_2/T) vs 1/T (right) for the substitution of $acac^-$ from [41] with 2,2-biphenyldiol at T = 15.2˚C, 25.0˚C and 34.9˚C. [Ti-complex] = 0.002 mol dm^{-3}.

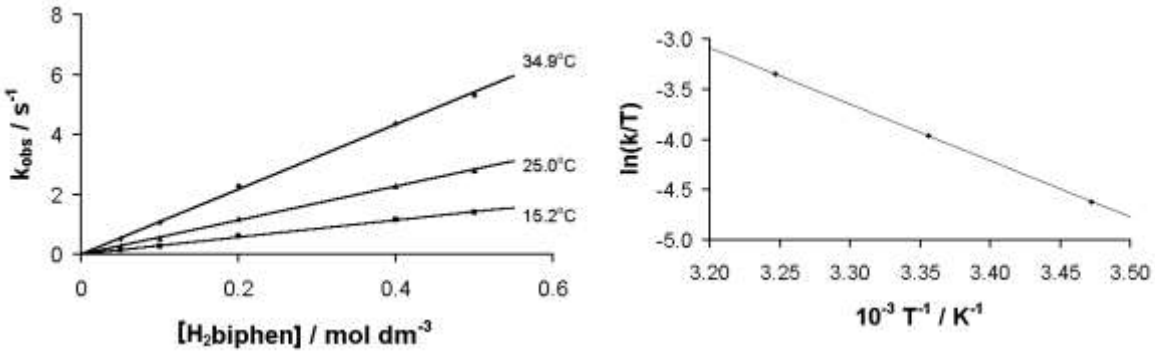

Figure 3.34. Graph of k_{obs} vs [2,2-biphenyldiol] (left) and *ln* (k_2/T) vs 1/T (right) for the substitution of $Sacac^-$ from [49] with 2,2-biphenyldiol at T = 15.2˚C, 25.0˚C and 34.9˚C. [Ti-complex] = 0.002 mol dm^{-3}.

The values of the second order rate constants at three different temperatures, as well as the activation parameters for each titanocenyl complex were calculated and summarised in Table 3.22.

Table 3.22. The second order rate constants (k_2) at three different temperatures and the activation parameters for substitution reactions between 2,2-biphenyldiol and different sized metallocyclic titanocenyl complexes. Standard deviations are given in brackets.

Titanocenyl complex	T / ˚C	k_2 / $dm^3\ mol^{-1}\ s^{-1}$	ΔH^* / kJ mol^{-1}	ΔS^* / J $K^{-1}\ mol^{-1}$	ΔG^* / kJ mol^{-1}	E^{01} / mV
[Tc(cat)]	15.2	2.5(3)	49.19(2)	-516.8(2)	203.21(5)	-891
	25.0	4.6(9)				
	34.9	10.2(3)				
$[Tc(acac)]^+ClO_4^-$	15.2	2.7(5)	49.79(8)	-528.2(1)	207.18(7)	-775
	25.0	5.7(8)				
	34.9	11.5(5)				
$[Tc(Sacac)]^+ClO_4^-$	15.2	2.8(2)	46.75(6)	-525.7(9)	203.40(4)	-780
	25.0	5.7(1)				
	34.9	10.8(1)				

The k_2 values for the substitution reaction between 2,2-biphenyldiol and the different titanocenyl complexes are for all practical purposes the same, indicating that E^{01} of Ti^{4+}/Ti^{3+} does not influence the rate of substitution.

There is for all practical purposes no difference in the activation parameters for the different titanocenyl complexes, due to the fact that they are structurally all very closely related. However, one would have expected that the five-membered metallocyclic catecholato complex would react at a different rate than the two six-membered metallocyclic β-diketonato complexes. In practice this was not observed.

The big negative activation entropy suggests that the mechanism of substitution is associative of nature. A schematic representation of this associative substitution mechanism could be described by either Scheme 3.13 A or 3.13 B (the substitution of [9] with 2,2-biphenodiol is shown as an example in Scheme 3.13). Kinetically Scheme 3.13 A and B are indistinguishable from a mechanism where step 1 is slow and step 2 is fast or step 1 is fast and step 2 is slow.

Scheme 3.13. A

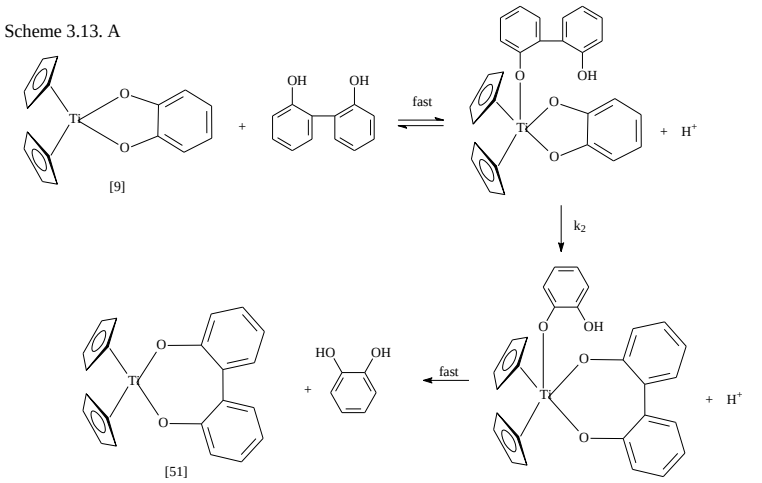

[51]

Scheme 3.13. B

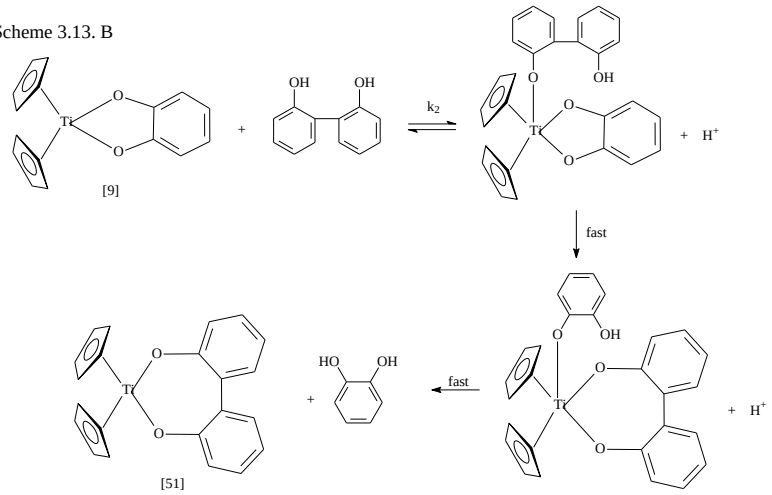

[51]

Scheme 3.13. A schematic representation of the two possible paths of the associative mechanism where the incoming ligand 2,2-biphenodiol displaces 1,2-benzenediolato from [9]. Kinetically mechanism 3.14 A and B are instinguisable from a mechanism where step 1 is slow and step 2 is fast or step 1 is fast and step 2 is slow.

3.4.3 A kinetic study of substitution reactions between (1,2-benzenediolato)biscyclopentadienyl titanium(IV) and acetylacetone, thioacetylacetone and 2,2-biphenyldiol

In this section the results of the substitution of the bidentate ligands cat^{2-} from [Tc(cat)], [9], with acetylacetone, thioacetylacetone and 2,2-biphenyldiol according to Scheme 3.14 is reported.

All the graphs for [9] of k_{obs} of the substitution reaction *vs* concentration of the substitution ligands (acetylacetone, thioacetylacetone and 2,2-biphenyldiol) are straight lines through the origin (Figure 3.35-3.37), which implies a first-order dependence on the substitution ligands. Further, the zero point shows that the rate law is a single term rate equation. The solvent

does not contribute meaningful to these reactions. Confirmation of the product of the substitution reaction was obtained by UV spectra.

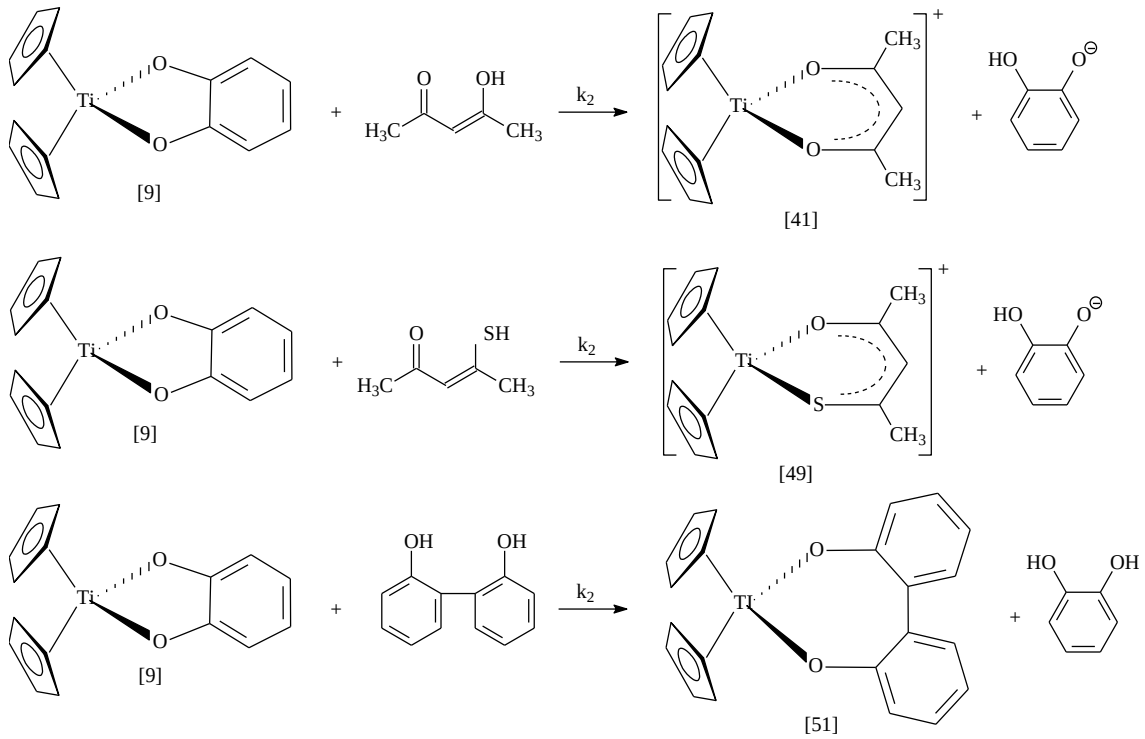

Scheme 3.14. Substitution reactions between [9] and the incoming ligand acetylacetone, thioacetylacetone and 2,2-biphenyldiol.

The linear relationship for the graph of ln (k_2/T) vs 1/T of the second order rate constants at different temperatures was determined for each substitution reaction, and is shown in Figure 3.35-3.37. The second order rate constant, activation enthalpy (ΔH^*), activation entropy (ΔS^*) and activation of free energy (ΔG^*) of the substitution reactions of [9] with acetylacetone, thioacetylacetone and 2,2-biphenyldiol are summarised in Table 3.23.

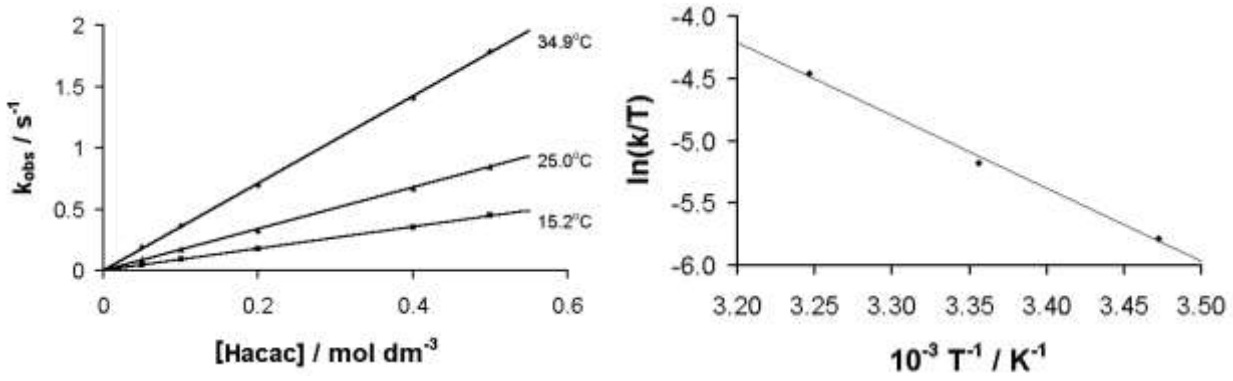

Figure 3.35. Graph of k_{obs} vs [acetylacetone] (left) and *ln* (k_2/T) vs 1/T (right) for the substitution of 1,2-benzenediol from [9] with acetylacetone at T = 15.2˚C, 25.0˚C and 34.9˚C. [Ti-complex] = 0.002 mol dm^{-3}.

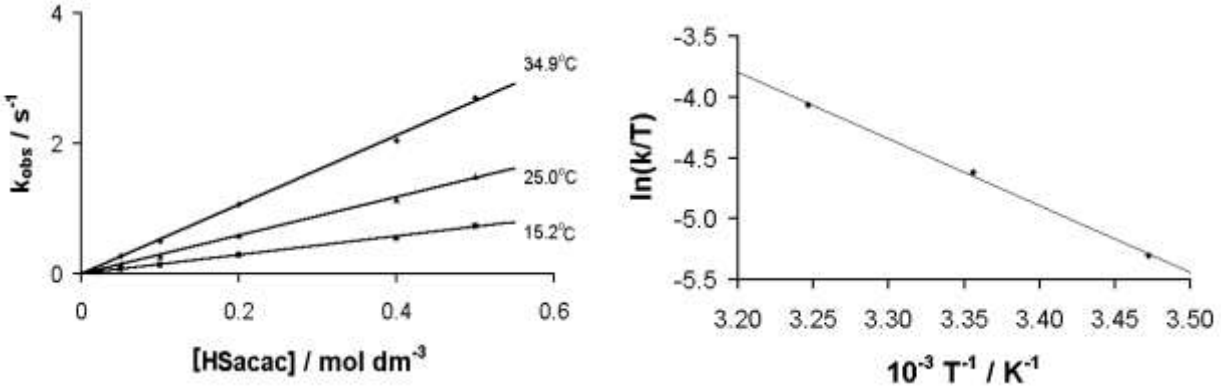

Figure 3.36. Graph of k_{obs} vs [thioacetylacetone] (left) and *ln* (k_2/T) vs 1/T (right) for the substitution of 1,2-benzenediol from [9] with thioacetylacetone at T = 15.2˚C, 25.0˚C and 34.9˚C. [Ti-complex] = 0.002 mol dm^{-3}.

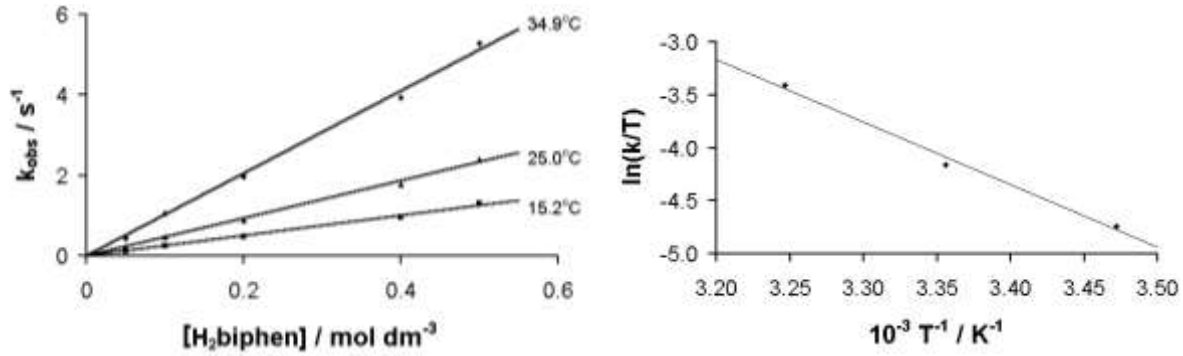

Figure 3.37. Graph of k_{obs} vs [2,2-biphenyldiol] (left) and *ln* (k_2/T) vs 1/T (right) for the substitution of 1,2-benzenediol from [9] with 2,2-biphenyldiol at T = 15.2˚C, 25.0˚C and 34.9˚C. [Ti-complex] = 0.002 mol dm^{-3}.

Table 3.23. The second order rate constants (k_2) at three different temperatures and the activation parameters for substitution reactions of 1,2-benzenediolato from [9] with acetylacetone, 2,2-biphenyldiol and thioacetylacetone. Standard deviations are given in brackets.

Incoming ligand	T / ˚C	k_2 / dm^3 mol^{-1} s^{-1}	ΔH^* / kJ mol^{-1}	ΔS^* / J K^{-1} mol^{-1}	ΔG^* / kJ mol^{-1}
Hacac	15.2	0.8(3)	48.6(1)	-518.7(2)	154.6(1)
	25.0	1.6(4)			
	34.9	3.5(5)			
HSacac	15.2	1.4(1)	45.7(7)	-529.4(9)	157.8(8)
	25.0	2.9(1)			
	34.9	5.3(2)			
H_2biphen	15.2	2.8(2)	49.1(2)	-516.5(1)	154.1(1)
	25.0	5.7(1)			
	34.9	10.8(1)			

With reference to the different second order rate constants (although practically quite similar) for the substitution of 1,2-benzenediolato from [9] with acetylacetone, 2,2-biphenyldiol and thioacetylacetone, a reactivity sequence for [9] can be arranged:

(most reactive) H_2biphen > HSacac > Hacac (least reactive)

Displacing the five-membered metallocycle to form the seven-membered metallocycle (Scheme 3.14. bottom) occurs faster than the displacement of five-membered metallocycle to form six-membered metallocycle (Scheme 3.14. top and middle).

There is little difference between the activation parameters for the different incoming ligands, due to the fact that they are all very closely related.

The big negative activation entropy implies that the mechanism of substitution is associative of nature.

3.4.4 A kinetic study of substitution reactions between (acetylacetonato)biscyclopentadienyl titanium(IV) perchlorate and thioacetylacetone

In this section the results of the substitution of acetylacetonato from $[Tc(acac)]^+ClO_4^-$, [41], with thioacetylacetone according to Scheme 3.15 is reported.

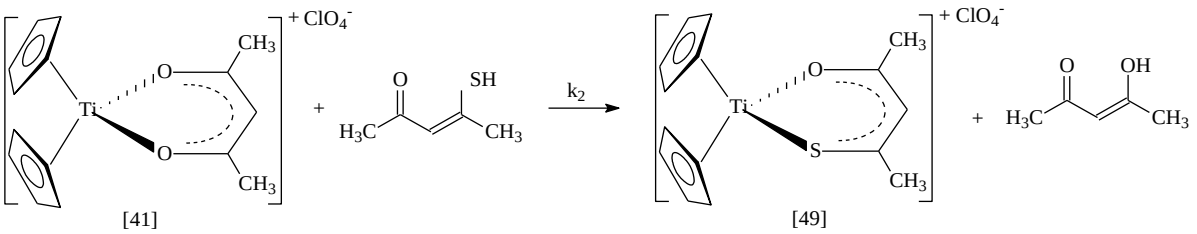

Scheme 3.15. Substitution reactions of $acac^-$ from [41] with thioacetylacetone.

The graph of k_{obs} for the substitution reaction between thioacetylacetone and [41] *vs* [thioacetylacetone] yields a straight line through the origin (Figure 3.38), which implies a first-order dependence on the thioacetylacetone.

The linear relationship for the graph of *ln* (k_2/T) vs 1/T of the second order rate constants at different temperatures of the substitution reaction of acetylacetonato from [41] with thioacetylacetone is shown in Figure 3.38. The second order rate constant at different temperatures, activation enthalpy (ΔH^*), activation entropy (ΔS^*) and activation of free energy

(ΔG^*) of the substitution reactions of acetylacetonato from [41] with thioacetylacetone in acetone are summarised in Table 3.24.

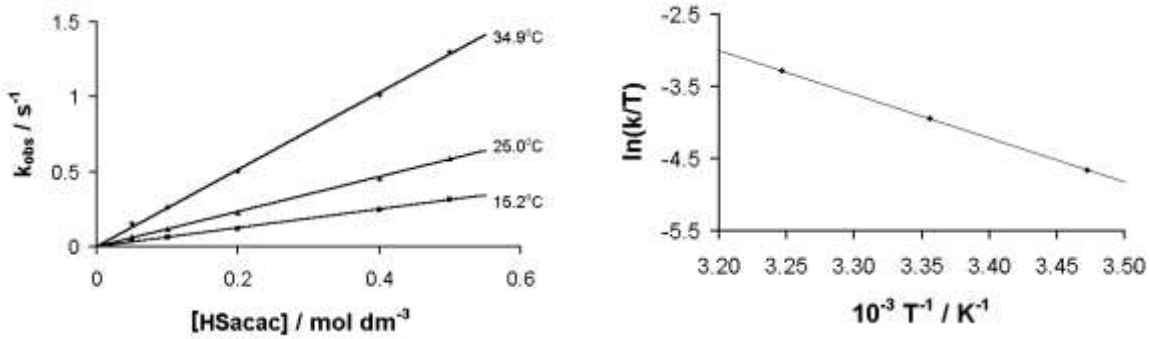

Figure 3.38. Graph of k_{obs} vs [thioacetylacetone] (left) and *ln* (k_2/T) vs 1/T (right) for the substitution of acetylacetonato from [41] with thioacetylacetone at T = 15.2˚C, 25.0˚C and 34.9˚C. [Ti-complex] = 0.002 mol dm^{-3}.

Table 3.24. The second order rate constants (k_2) at three different temperatures and the activation parameters for substitution reaction of acetylacetonato from [41] with thioacetylacetone. Standard deviations are given in brackets.

Incoming ligand	T / ˚C	k_2 / dm^3 mol^{-1} s^{-1}	ΔH^* / kJ mol^{-1}	ΔS^* / J K^{-1} mol^{-1}	ΔG^* / kJ mol^{-1}
HSacac	15.2	0.62(1)	50.4(1)	-499.9(2)	149.0(1)
	25.0	1.1(8)			
	34.9	2.5(9)			

The second order rate constant is small. This is understandable because the incoming ligand and the displaced ligand differs only by one oxygen, which is sulphur in the thioacetylacetone. The revers reaction, the substitution reaction of thioacetylacetonato from [49] with acetylacetone was not observed even in the presence of a hundred-fold excess of acetylacetone over [49]. Displacement of acetylacetonato from [41] by thioacetylacetone is thus due to the slightly higher atomic electronegativity (Allred, Rochow) of oxygen (3.5) over sulphur (2.4).[20] With the higher atomic electronegativity of the acetylacetonato ligand the titanium centre is relatively more positive than with the thioacetylacetonato ligand. Seeing as thioacetylacetone is not as electronegative as acetylacetone, it is a better nucleophile and would thus attack the relatively more positive titanium centre of [41].

Activation entropy is a large negative value, which implies an associative mechanism as explained in paragraph 3.4.2 and 3.4.3.

3.4.5. Relative stability of the different sized metallocyclic titanocenyl complexes

The stability of the complexes is determined by the order by which bounded ligands are displaced by the free ligands. From data obtained and discussed in paragraphs 3.4.1-3.4.4 the following series of stability can be deduced:

{most stable} [Tc(biphen)] (7-membered ring) > $[Tc(Sacac)]^+$ (6-membered ring) > $[Tc(acac)]^+$ (6-membered ring) > [Tc(cat)] (5-membered ring) {least stable}

It is known that the angle between two ligands (L-M-L) in a tetrahedral coordination sphere is 109.5º.[31] Comparing this tetrahedral angle to that found for $[Tc(acac)]^+ClO_4^-$ (O-Ti-O = 84.3º),[9] a compound related to [Tc(biphen)], (1,1'-bi-naphtholato-O,O)-(1,2-bis(η^5-3-t-butyl-cyclopentadienyl)-1,1,2,2-tetramethylethane)-titanium hexane solvate (O-Ti-O = 94.09º),[32] and a compound related to [Tc(cat)], [Tc(diethyl diazomalonate)] (O-Ti-O = 70.6˚),[33] it can be seen that the O-Ti-O tetrahedral angle of [Tc(biphen)] of 94.09(6)º is near to the 109.5º ideal. This could explain why [Tc(biphen)] is the most stable compound. The ideal tetrahedral angle is the least distorted in the seven-membered metallocycle and therefore there is less steric strained.

3.5. Cytotoxicity evaluation

The purpose of the synthesis of all these complexes of this study was to investigate their physical properties, and also to investigate their application possibilities in terms of anticancer activity. The latter was probed by determining the cyctoxicity of selected compounds against cancer cells. The types of cancer cells that were used in this investigation were CoLo (a human colorectral cell line) and HeLa (a human cervix epitheloid cancer cell line). Prof. C.E.J. Medlen from the Department of Pharmacology at the University of Pretoria is acknowledged for performing these tests and for constructing the survival curves of the obtained results. Survival curves indicate percentage cell survival, plotted as a function of drug dose with concentration expressed in μmol dm^{-3}. IC_{50} values (drug dose required for 50% cell death) were estimated by extrapolation.

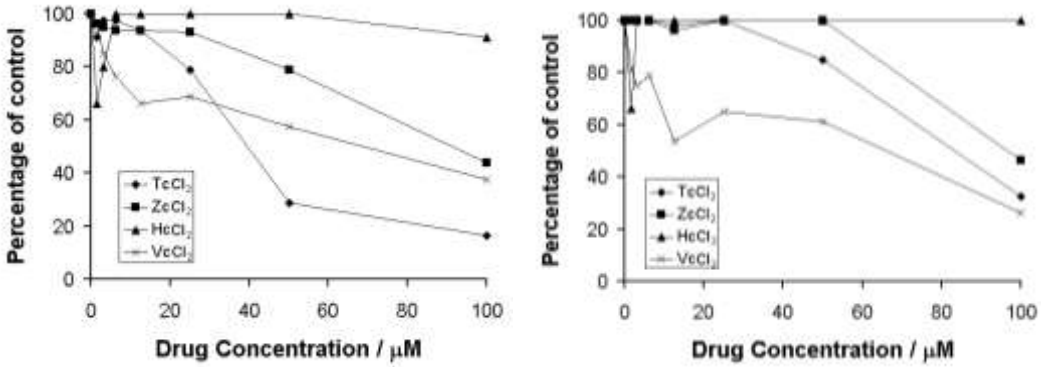

Figure 3.39. Plots of percentage survival CoLo (left) and HeLa cells (right) against concentration (μmol dm^{-3}) of $TcCl_2$, $ZcCl_2$, $HcCl_2$ and $VcCl_2$.

Table 3.25. IC_{50} values for CoLo and HeLa cell lines after treatment with $TcCl_2$, $ZcCl_2$, $HcCl_2$ and $VcCl_2$. Metal electronegativity, χ_M, and peak cathodic potential Epa (see paragraph 3.3.2.2.) are also listed.

Drug	IC_{50} value for CoLo cell line / μmol dm^{-3}	IC_{50} value for HeLa cell line / μmol dm^{-3}	Electronegativity of the metal[20]	E_{pc} / mV *vs* Ag/Ag^+	Period in the periodic table	Group in the periodic table
$[Ti(Cp)_2(Cl)_2]$	39.37	84.51	1.32	-1142	4	ivB
$[Zr(Cp)_2(Cl)_2]$	87.87	>100	1.22	-1314	5	ivB
$[Hf(Cp)_2(Cl)_2]$	>100	>100	1.23	-1326	6	ivB
$[V(Cp)_2(Cl)_2]$	64.3	63.30	1.45	-1034	4	vB

At first the cancer cells were treated with metallocene dichlorides investigated in this essay (Figure 3.39 and Table 3.25). From the survival curves it was observed that hafnocene dichloride is completely unreactive (had no cytotoxic properties) and zirconocene dichloride only very weakly active. Vanadocene and titanocene dichloride (already in clinical trials) both showed good reactivity towards the destruction of the cancer cells. The cytotoxic properties of these four compounds are in accordance with published results.[34] However, based on the chemical study that was described in the earlier part of this thesis, an explanation for the observed cytotoxic trend can be proposed.

The first general trend that can be observed is that there is an increase in cytotoxicity for the CoLo cell line with an increase in electronegativity of the metal centre (Table 3.25). This can be seen most prominently when going down in the group on the periodic table. The HeLa cells also showed this trend when going from left to right in the periodic table. However, going to the right in the period there is a decrease in activity with increasing electronegativity when CoLo cells are considered. Secondly, upon comparing the activity of $[M(Cp)_2Cl_2]$ with M = Ti, Zr, Hf and V, with peak anodic potentials, Table 3.25, it is observed that the most reactive species,

vanadocene and titanocene dichloride also have the most positive peak cathodic potentials. The mechanism of these drugs induce electron transfer, thus it means that Zr and Hf derivatives are too difficult to reduce in a biological environment. However, even at –1142 and –1034 mV, the Ti and V derivatives are very difficult to reduce. This casts doubt on an electron transfer mechanism. It implies that where good leaving ligands are employed, these complexes may involve substitution processes on DNA. This possibility requires further investigation. Thirdly, since we have observed that the 4*d* orbitals of Zr and the 5*d* and 4*f* orbitals of Hf induce substitution processes that lead to compound destruction *via* coordination-sphere changes, it is possible that the kinetic lability of Zr and Hf towards substitution destroys the cytotoxic capabilities of these compounds.

In an effort to increase the reactivity of metallocene derivatives, the chloride ligands in metallocene dichlorides were replaced by various substituents. For further testing only titanium derivatives were used seeing as it displayed good overall cytotoxic activity and because of the ease of synthesis.

The substitution of the chloride ligands in $TcCl_2$ with various β-diketonates to give $[Tc(\beta\text{-diketonato})]^+ClO_4^-$ derivatives, increased the cytotoxic reactivity of the titanocene complexes approximately three times for the CoLo cells and approximately two times for the HeLa cells (Table 3.26 and Figure 3.40-41). In the best cases, by substituting the chloride anions in $TcCl_2$ with either an fca^- or a $tfaa^-$ β-diketonato ligand, the IC_{50} values decreased from 39.37 for $TcCl_2$ to 10.71 or 8.06 μmol dm^{-3} for CoLo cells. The higher cytotoxicity of $[Tc(\beta\text{-diketonato})]^+$ complexes was not due to the ClO_4^- counter anion, because separate tests using $NaClO_4$ as cytotoxic agent, showed that $NaClO_4$ has IC_{50} values substantially higher than the titanocenyl derivatives (Table 3.26, $IC_{50,\ NaClO4}$ > 100 μmol dm^{-3}). The Scat derivative lowered the IC_{50} values to 6.71 μmol dm^{-3} for the CoLo cell line. Improvements on the IC_{50} values of HeLa cells followed the same tendency as for the CoLo cell line.

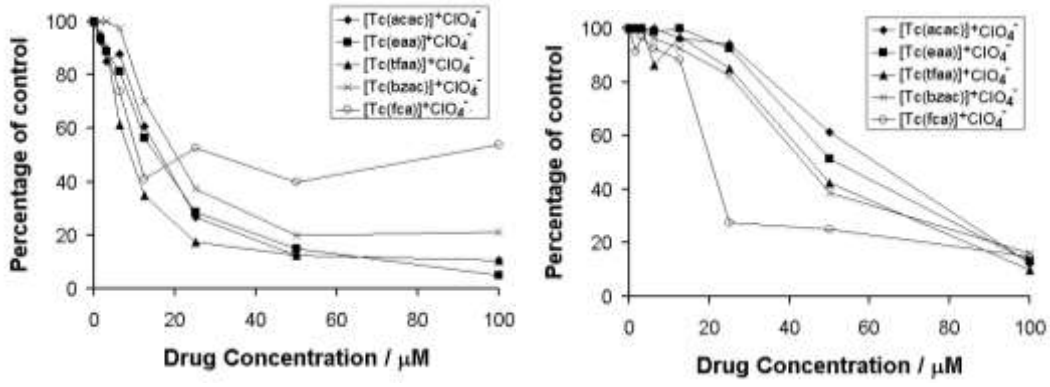

Figure 3.40. Plots of percentage survival of cells for CoLo (left) and HeLa (right) against concentration (μmol dm^{-3}) of different titanocenyl β-diketonato complexes.

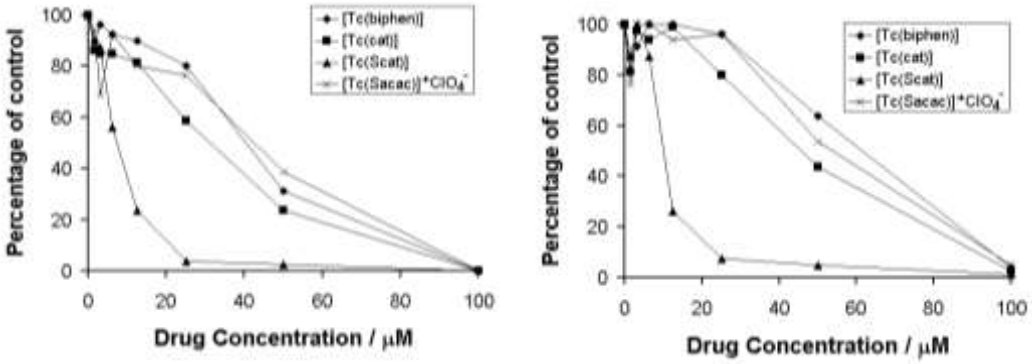

Figure 3.41. Plots of percentage survival of cells for CoLo (left) and HeLa (right) against concentration (μmol dm^{-3}) of titanocenyl complexes with bi-chelating ligands, 2,2-biphenyldiolato, 1,2-benzenediolato, 1,2-benzenedithiolato and thioacetylacetonato.

Table 3.26. IC_{50} values for CoLo and HeLa cell lines for different titanocenyl complexes, group electronegativity (χ_R) of the R-groups on the β-diketonate and the formal reduction potentials of the Ti^{4+}/Ti^{3+} couple of the titanocenyl derivatives are also shown.

Drug	Ti^{4+}/Ti^{3+} E^{01} / mV *vs* Ag/Ag^+	IC_{50} value for CoLo cell line / μmol dm^{-3}	IC_{50} value for HeLa cell line / μmol dm^{-3}	χ_R [2, 7]
$NaClO_4$		>100	>100	-
$[Tc(acac)]^+ClO_4^-$	-775	11.27	58.06	2.34
$[Tc(bzac)]^+ClO_4^-$	-766	17.54	43.74	2.21
$[Tc(tfaa)]^+ClO_4^-$	-534	8.06	44.42	3.01
$[Tc(fca)]^+ClO_4^-$	-813	10.71	21.27	1.87
$[Tc(maa)]^+ClO_4^-$	-713	14.39	51.24	-
$[Tc(Sacac)]^+ClO_4^-$	-780	42.24	52.47	-
[Tc(biphen)]	-957[a]	40.52	59.08	-
[Tc(cat)]	-891[a]	30.04	42.81	-
[Tc(Scat)]	-1188[a]	6.71	9.86	-

a) Not true E^{01} values as ΔE_p > 90 mV, see Table 3.15.

Since no clear trend between IC_{50} values for CoLo and HeLa cells and E^{01} values for the Ti^{4+}/Ti^{3+} couple could be identified in complexes of the type $[Tc(\beta\text{-diketonato})]^+ClO_4^-$ (Table 3.26), doubt exists as to whether an electron transfer mechanism is very dominant in the mechanism of action of these particular complexes. It is more likely that the leaving capabilities of the β-diketonato ligand is so much better than that of the Cl^- ligands in $TcCl_2$, that the β-diketonato complexes may operate at least in part by a substitution mechanism with DNA. This possibility is currently under investigation in this laboratory. No clear relationship between the group electronegativity of the R groups in complexes of the type $[Ti(Cp)_2(CH_3COCHCOR)]^+ClO_4^-$ could be found either (Figure 3.42).

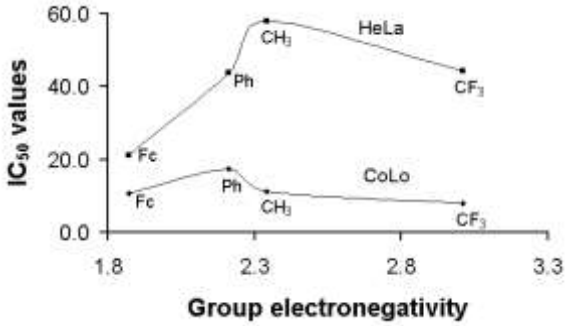

Figure 3.42. Graph of IC_{50} values of CoLo and HeLa cells *vs* group electronegativity of the R groups of the β-diketonato ligand in $[Ti(Cp)_2(CH_3COCHCOR)]^+ClO_4^-$, R = Fc, Ph, CH_3, OCH_3 and CF_3.

The high cytotoxicity that the complexes $[Tc(fca)]^+ClO_4^-$ and $[Tc(tfaa)]^+ClO_4^-$ have, could not be traced to E^{01} or group electronegativities of the R group of the β-diketonate ligands of the CF_3 or Fc side groups. It may, however, be simply because these two molecules have two cytotoxic moieties in them: the titanocenyl group,[35] and the Fc,[36] or CF_3,[37] from the β-diketonato ligands fca^- and $tfaa^-$ respectively. It follows that the high cytotoxicity of these two complexes are probably the result of synergistic effects between the two cytotoxic moieties of each molecule.

Seeing as some of these β-diketonato titanium complexes display such good reactivity, it was thought that the coordination of two β-diketonate ligands onto a titanium core might increase the complexes' cytotoxicity even more. Thus the bis-β-diketonato titanium complexes listed in Table 3.27 were tested on CoLo and HeLa cells (Figure 3.43 and Table 3.27).

By comparing IC_{50} values in Table 3.26 and 3.27, the bis-β-diketonato complexes $[Ti(Cp)(Cl)(bzac)_2]$ and $[Ti(Cp)(Cl)(tfaa)_2]$ were indeed found to be slightly more cytotoxic than the corresponding mono-β-diketonato complexes $[Tc(bzac)]^+ClO_4^-$ and $[Tc(tfaa)]^+ClO_4^-$. The complex $[Ti(Cp)(Cl)(fca)_2]$ exhibited almost the same IC_{50} values than $[Tc(fca)]^+ClO_4^-$, while the bis-β-diketonato acac derivative was less cytotoxic than its mono-β-diketonato counterpart $[Tc(acac)]^+ClO_4^-$.

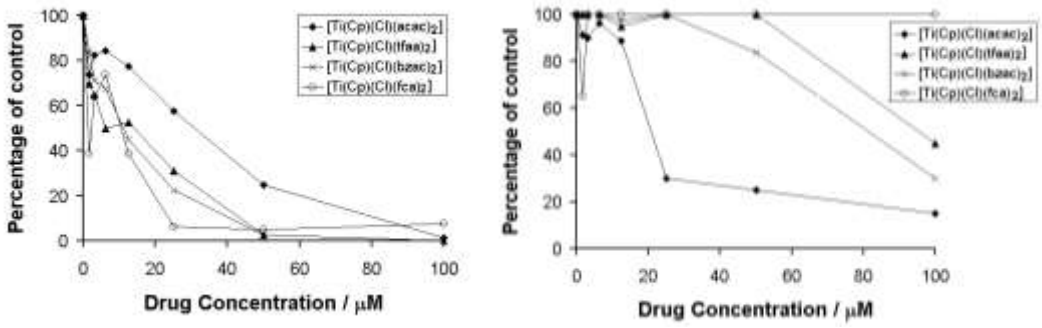

Figure 3.43. Plots of percentage survival of cells for CoLo (left) and HeLa (right) against concentration (μmol dm^{-3}) of different bis-β-diketonato titanium complexes.

Table 3.27. IC_{50} values for HeLa and CoLo cell line of bis-β-diketonato titanium complexes. Group electronegativity of the R-groups on the β-diketonato, χ_R, (Gordy scale)[2, 7] and E_{pc} values of titanium complexes are also given.

Drug	IC_{50} value for CoLo cell line / μmol dm^{-3}	IC_{50} value for HeLa cell line / μmol dm^{-3}	χ_R (Gordy scale)	E_{pc} / mV
$[Ti(Cp)(Cl)(fca)_2]$	10.99	16.50	1.87	-1361
$[Ti(Cp)(Cl)(bzac)_2]$	11.44	19.99	2.21	-1347
$[Ti(Cp)(Cl)(acac)_2]$	30.82	65.46	2.34	-1342
$[Ti(Cp)(Cl)(tfaa)_2]$	6.52	29.27	3.01	-1290

As can be seen from Table 3.27, there is no apparent correlation between IC_{50} values and the physical properties E^{01} or group electronegativities of the R group of the β-diketones. As was the case with the mono-β-diketonato titanium(IV) complexes, the ferrocenoylacetonato titanium(IV) complex showed the overall highest cytotoxicity. This is probably due to the synergistic effect made possible by combination of the two anti-tumour active species, titanocenyl and ferrocenyl, within the same compound.

The overall good cytotoxic results of the bis-β-diketonato complexes of Table 3.27 correlate good with that found for budotitane (T/C(%)[#] > 300), which also contains the bis-benzoylacetonato ligand.

[1] A.H. Lowrey, P.D. D'Antonio and J. Karle, *J. Am. Chem. Soc.*, 1971, **93**, 6399.

[2] W.C. du Plessis, T.G. Vosloo and J.C. Swarts, *J. Chem. Soc., Dalton Trans.*, 1998, 2507.

[3] G. Doyle and R.S. Tobias, *Inorg. Chem.*, 1967, **6**, 1111.

[4] G. Doyle and R.S. Tobias, *Inorg. Chem.*, 1968, **7**, 2484.

[5] P.C. Bharara, *J. Organomet. Chem.*, 1976, **121**, 199.

[6] J. Stary, *The solvent extraction of metal chelates*, MacMillan Company, New York, 1964, p. 196-202.

[7] R.E. Kagarise, *J. Am. Chem. Soc.*, 1955, **77**, 1377.

[8] R.C. Weast, Editor, *Handbook of Chemistry and Physics*, 65th Edition, CRC Press, Boca Raton, Florida, 1984, p F-176.

[9] A.M. Bond, R. Colton, U. Englert, H. Hugel and F. Marken, *Inorg. Chim. Acta*, 1995, **235**, 117.

[10] M.J. Frazer and W.E. Newton, *Inorg. Chem.*, 1971, **10**, 2137.

[11] K. Andrä, *J. Organomet. Chem.*, 1968, **11**, 567.

[12] H. Köpf and M. Schmidt, *J. Organomet. Chem.*, 1965, **4**, 426.

[13] N. Kobayashi, A. Muranaka and K. Ishii, *Inorg. Chem.*, 2000, **39**, 2256.

[#] T/C(%) = (median survival time of treated animal vs. median survival time of control animal) x 100.

[14] M. Barthel, D. Dini, S. Vagin and M. Hanack, *Eur. J. Org. Chem.*, 2002, 3756.

[15] T.A. James and J.A. McCleverty, *J. Chem. Soc. (A)*, 1970, 3318.

[16] A.K. Sharma and N.K. Kaushik, *Z. Naturforsch.*, 1984, **39b**, 604.

[17] G. Doyle and R.S. Tobias, *Inorg. Chem*., 1968, **7**, 2479.

[18] W.C. du Plessis, J.C. Erasmus, G.J. Lamprecht, J. Conradie, M.A.S. Aquino and J.C. Swarts, *Can. J. Chem.*, 1999, **77**, 378.

[19] P.T. Kissinger and W.R. Heinemen, *J. Chem. Educ.*, 1983, **60**, 702.

[20] A.L. Allered and E.G. Rochow, *J. Inorg. Nucl. Chem.*, 1958, **5**, 264.

[21] J. Langmaier, Z. Samec, V. Varga, M. Horacek, R. Choukroun and K. Mach, *J. Organomet. Chem.*, 1999, **584**, 323.

[22] G.V. Loukova and V.V. Strelets, *J. Organomet. Chem.*, 2000, **606**, 203.

[23] N. El Murr, A. Chaloyard and J. Tirouflet, *J. Chem. Soc., Chem. Comm.*, 1980, 446.

[24] M.A. Vorotyntsev, M. Casalta, E. Pousson, L. Roullier, G. Boni and C. Moise, *Electrochim. Acta*, 2001, **46**, 4017.

[25] R.S.P. Coutts and P.C. Wailes, *Aust. J. Chem.*, 1969, **22**, 1547.

[26] J. Conradie, Ph.D. Study, University of the Orange Free State, R.S.A., 1999.

[27] H. Holden Thorp, *J. Educ. Chem.*, 1992, **69**, 250.

[28] H.M. Koepp, H. Wendt and H. Strehlow, *Z. Elektrochem.*, 1960, 483.

[29] User manual, Metrohm AG 9101 Herisau.

[30] R.T. Sawyer and L.J. Roberts, Jr., *Experimental Electrochemistry for Chemists*, Wiley, New York, 1974, p 188.

[31] J. McMurry, *Organic Chemistry*, 4th Edition, Brooks/Cole Publishing Co., Pacific Grove, 1995, p 20.

[32] M.S. Erikson, F.R. Fronczek and M.L. McLaughlin, *J. Organomet. Chem.*, 1991, **415**, 75.

[33] S. Gambarotta, C. Floriani, A. Chiesi-Villa and C. Guastini, *J. Am. Chem. Soc.*,1982, **104**, 1918.

[34] P. Köpf-Maier, M. Leitner and H. Köpf, *J. Inorg. Nucl. Chem.*, 1980, **42**, 1789.

[35] J.R. Boyles, M.C. Baird, B.G. Campling and N. Jain, *J. Inorg. Biochem.*, 2001, **84**, 159.

[36] D. Osella, M. Ferrali, P. Zanello, F. Laschi, M. Fontani, C. Nervi and G. Cavigiolio, *Inorg. Chim. Acta*, 2000, **306**, 42.

[37] M. Kawase, A. Shah, H. Gaveriya, N. Motohasi, H. Sakagami, A. Varga and J. Molnar, *Bioorg. Medi. Chem.*, 2002, **10**, 1051.

Chapter 4

Experimental

4.1. Introduction

In this chapter all experimental procedures, reaction conditions and techniques are described.

4.2. Materials

Solid reagents (Merck, Aldrich) employed in preparations were used without further purification. Liquid reagents were purchased from Aldrich and used without further purification. Solvents were distilled prior to use and water was double distilled. Organic solvents were dried according to published methods.[1] Melting points (m.p.) were determined with a Reichert Thermopan microscope with a Koffler hot-stage and are uncorrected. Canadian Microanalytical Service, Canada, preformed element analysis.

4.3. Spectroscopic and conductivity measurements

^{1}H NMR measurements at 289 K were recorded on a Bruker Advance DPX 300 NMR spectrometer. The chemical shifts were reported relative to $SiMe_4$ at 0.00 ppm. IR spectra were recorded on a Digilab FTS 2000 Fourier transform spectrometer utilizing a He-Ne laser at 632.6 nm, and UV spectra were recorded in a Cary 50 Probe UV/Visible spectrophotometer. Conductivity measurements were recorded with a Metrohm Herisau Konduktometer E 527 conductivity meter.

4.4. Synthesis

4.4.1. β-Diketonates and thio-β-diketonates

4.4.1.1. 1-Ferrocenoyl-1,3-butanedione, Hfca [40]

Acetylferrocene (2 g, 8.7 mmol) was degassed for 1 h. Dry THF (7 ml) was added and the solution was stirred for a few minutes. Lithium diisopropylamide (4 ml) was added slowly, while the solution was kept cool in an ice-bath and stirred for a further 30 min at room temperature. Dry ethyl acetate (1 ml) was added and the solution was left to stir overnight. Ether was added to precipitate the salt, which was filtered off and washed with ether. The solid was dissolved in HCl (0.5 M, 200 ml) and stirred until all the solid dissolved. Ether was added and the layers were separated. The ether layer was washed with water, dried with sodium sulphate and the solvent removed under reduced pressure to yield red crystals as the product. Yield 29% (681 mg). ν (C=O)/cm^{-1} = 1620. δ_H (300MHz, $CDCl_3$)/ppm: 2.10 (s; 3H; CH_3 enol); 2.34(s; 3H; CH_3 keto); 3.85 (s; 2H; CH_2 keto); 4.21 (s; 5H; C_5H_5 enol); 4.27 (s; 5H; C_5H_5 keto); 4.51 (t; 2H; 0.5 x C_5H_4 enol); 4.60 (t; 2H; 0.5 x C_5H_4 keto); 4.79 (t; 2H; 0.5 x C_5H_4 enol); 4.81 (t; 2H; 0.5 x C_5H_4 keto); 5.74 (s; 1H; CH enol).

4.4.1.2. 4-Thioxopentan-2-one, HSacac [26]

A solution of acetylacetone (35 g) in 300 ml acetonitrile was cooled to -50˚C, a stream of H_2S gas was passed through for 2 h during which the temperature was allowed to rise to -40˚C. Then HCl gas was passed through the solution for 1.5 h at -40˚C. Another stream of H_2S gas was passed through for 3 h at -40˚C. The solution was poured into a mixture of 500 ml ice water, 300 ml pentane and 100 ml ether under manual stirring. The layer was separated and the water layer washed with pentane/ether (3:1). The combined organic layer was washed with water, dried with sodium sulphate and the solvent removed under reduced pressure, yielding a yellow liquid. Yield 48% (20 g). ν (C=O)/cm^{-1} = 1607. δ_H (300MHz, $CDCl_3$)/ppm: 2.05 (s; 6H; 2 x CH_3 enol); 2.18 (s; 3H; CO-C$\underline{H}_3$ thioenol); 2.28 (s; 6H; 2 x CH_3 keto); 2.39 (s; 3H; CS-C$\underline{H}_3$ thioenol); 3.62 (s; 2H; CH_2 keto); 5.52 (s; 1H; CH enol); 5.35 (s; 1H; CH thioenol).

4.4.2. Titanium complexes

4.4.2.1. 2,4-Pentanedionato-κ^2O,O'-bis(η^5-cyclopentadienyl)titanium(IV) perchlorate, $[Tc(acac)]^+ClO_4^-$ [41]

Dichlorobiscyclopentadienyltitanium(IV) (titanocene dichloride) (120 mg, 0.48 mmol) was suspended in 3 ml water and stirred under nitrogen. Silver perchlorate (199 mg, 0.96 mmol) was added and the mixture was stirred for about an hour under nitrogen. Silver chloride (white precipitate) was filtered off and washed with 2 ml water. The filtrate was cooled on an ice-bath and 2 ml cold acetylacetone (c.a. 4˚C) was added dropwise while stirring. A grey-purple precipitate formed immediately, which was filtered off and washed with water and ether. Yield 86% (155 mg). Melting point >230˚C. ν (C=O)/cm^{-1} = 1524. δ_H (300MHz, $CDCl_3$)/ppm: 2.29 (s; 6H; 2 x CH_3); 6.14 (s; 1H; CH); 6.73 (s; 10H; 2 x C_5H_5). δ_H (300MHz, d-acetone)/ppm: 2.32 (s; 6H; 2 x CH_3); 6.38 (s; 1H; CH); 6.92 (s; 10H; 2 x C_5H_5).

4.4.2.2. 1-Phenyl-1,3-butanedionato-κ^2O,O'-bis(η^5-cyclopentadienyl) titanium(IV) perchlorate, $[Tc(bzac)]^+ClO_4^-$ [42]

Titanocene dichloride (200 mg, 0.79 mmol) was suspended in 5 ml water and stirred under nitrogen. Silver perchlorate (330 mg, 1.59 mmol) was added and the mixture was stirred for about an hour under nitrogen. Silver chloride (white precipitate) was filtered off and washed with 2 ml water. The filtrate was cooled on an ice-bath and benzoylacetone (128 mg, 0.79 mmol) dissolved in 1.5 ml cold THF (c.a. 4˚C) was added dropwise while stirring. A grey-brown precipitate formed immediately, which was filtered off and washed with water and ether. Yield 65% (225 mg). Melting point 189-194˚C. ν (C=O) /cm^{-1} = 1565. δ_H (300MHz, $CDCl_3$)/ppm: 2.44 (s; 3H; CH_3); 6.19 (s; 1H; CH); 6.79 (s; 10H; 2 x C_5H_5); 7.62 (m; 3H; C_6H_5); 7.95 (m; 2H; C_6H_5).

4.4.2.3. 1,1,1-Trifluoro-2,4-pentanedionato-κ^2O,O'-bis(η^5-cyclopentadienyl) titanium(IV) perchlorate, $[Tc(tfaa)]^+ClO_4^-$ [43]

Titanocene dichloride (250 mg, 1.0 mmol) was suspended in 6 ml water and stirred under nitrogen. Silver perchlorate (414 mg, 2.0 mmol) was added and the mixture was stirred for about

an hour under nitrogen. Silver chloride (white precipitate) was filtered off and washed with 2 ml water. The filtrate was cooled on an ice-bath and trifluoroacetylacetone (154 mg, 1.0 mmol) dissolved in 1.5 ml cold THF (c.a. 4˚C) was added dropwise while stirring. A light brown precipitate formed immediately, which was filtered off and washed with water and ether. Yield 16% (69 mg). Melting point >230˚C. ν (C=O)/cm^{-1} = 1589. δ_H (300MHz, $CDCl_3$)/ppm: 2.25 (s; 3H; CH_3); 5.96 (s; 1H; CH); 6.89 (s; 10H; 2 x C_5H_5). Microanalysis calculated C, 41.8%, H 3.3% and found C, 42.1%, H 3.5%.

4.4.2.4. 1-Ferrocenoyl-1,3-butanedionato-κ^{2}O,O'-bis(η^5-cyclopentadienyl) titanium(IV) perchlorate, [Tc(fca)]$^+$ClO$_4^-$ [44]

Titanocene dichloride (180 mg, 0.717 mmol) was suspended in 6 ml water and stirred under nitrogen. Silver perchlorate (297 mg, 1.43 mmol) was added and the mixture was stirred for about an hour under nitrogen. Silver chloride (white precipitate) was filtered off and washed with 2 ml water. The filtrate was cooled on an ice-bath and ferrocenoylacetone (150 mg, 0.717 mmol) dissolved in 1.5 ml cold THF (c.a. 4˚C) was added dropwise while stirring. A red-brown precipitate formed immediately, which was filtered off and washed with water and ether. Yield 46% (149 mg). Melting point 86-89˚C. ν (C=O)/cm^{-1} = 1509. δ_H (300MHz, $CDCl_3$)/ppm: 2.25 (s; 3H; CH_3); 4.41 (s; 5H; C_5H_5 from Fc); 4.84 (s; 2H; C_5H_4 from Fc); 5.06 (s; 2H; C_5H_4 from Fc); 6.65 (s; 1H; CH); 6.96 (s; 10H; 2 x C_5H_5). Microanalysis calculated C, 52.7%, H 4.2% and found C, 53.5%, H 4.4%.

4.4.2.5. 1-Methoxy-1,3-butanedionato-κ^{2}O,O'-bis(η^5-cyclopentadienyl) titanium(IV) perchlorate, [Tc(maa)]$^+$ClO$_4^-$ [20]

Titanocene dichloride (120 mg, 0.48 mmol) was suspended in 3 ml water and stirred under nitrogen for a few minutes. Silver perchlorate (199 mg, 0.96 mmol) was added and the mixture was stirred for about an hour under nitrogen. Silver chloride (white precipitate) was filtered off and washed with 2 ml water. The filtrate was cooled on an ice-bath and 2 ml cold ethyl acetoacetone (c.a. 4˚C) was added dropwise while stirring. A grey-brown precipitate formed immediately, which was filtered off and washed with water and ether. Yield 48% (90 mg). Melting point >230˚C. ν (C=O)/cm^{-1} = 1678. δ_H (300MHz, $CDCl_3$)/ppm: 2.11 (s; 3H; CH_3); 3.98 (s; 3H; OCH_3); 5.52 (s; 1H; CH); 6.79 (s; 10H; 2 x C_5H_5).

4.4.2.6. Chloro(η^5-cyclopentadienyl)bis(2,4-pentanedionato-κ^2O,O') titanium(IV), [Ti(Cp)(Cl)(acac)$_2$] [45]

To a solution of titanocene dichloride (125 mg, 0.5 mmol) dissolved in 10 ml acetonitrile, was added acetylacetone (100 mg, 1.0 mmol) and triethyl amine (50.5 mg, 0.5 mmol) in 2.5 ml acetonitrile. The solution was stirred for several hours at room temperature under nitrogen. The solvent was removed under reduced pressure and the resulting white-orange precipitate was shaken with toluene to dissolve the product. The unwanted white precipitate was filtered off and from the filtrate the solvent was removed under reduced pressure to obtain the product. The product was recrystallized from acetone and hexane. Seeing as this complex is highly moisture sensitive it is stored under nitrogen. Yield 43% (75 mg). Melting point >230˚C. ν (C=O)/cm^{-1} = 1528. δ_H (300MHz, $CDCl_3$)/ppm: 1.8-2.4 (m; 12H; 4 x CH_3); 5.68 and 5.75 (2 x s; 2H; 2 x CH); 6.6 (m; 5H; C_5H_5).

4.4.2.7. Chloro(η^5-cyclopentadienyl)bis(1-phenyl-1,3-butanedionato-κ^2O,O') titanium(IV), [Ti(Cp)(Cl)(bzac)$_2$] [46]

To a solution of titanocene dichloride (125 mg, 0.5 mmol) dissolved in 10 ml acetonitrile, was added benzoylacetone (165 mg, 1.0 mmol) and triethylamine (50.5 mg, 0.5 mmol) in 2.5 ml acetonitrile. The solution was stirred for several hours at room temperature under nitrogen. The solvent was removed under reduced pressure and the resulting white-orange precipitate was shaken with toluene to dissolve the product. The unwanted precipitate was filtered off and from the filtrate the solvent was removed under reduced pressure to obtain the product. The product was recrystallized from acetone and hexane. Seeing as this complex is highly moisture sensitive it is stored under nitrogen. Yield 53% (78 mg). Melting point 142-145˚C. ν (C=O)/cm^{-1} = 1516. δ_H (300MHz, $CDCl_3$)/ppm: 2.0-2.4 (m; 6H; 2 x CH_3); 6.30-6.45 (m; 2H; 2 x CH); 6.6 (m; 5H; C_5H_5); 7.2-8.3 (m; 10H; 2 x C_6H_5).

4.4.2.8. Chloro(η^5-cyclopentadienyl)bis(1-ferrocenoyl-1,3-butanedionato-κ^2O,O')titanium(IV), [Ti(Cp)(Cl)(fca)$_2$] [47]

To titanocene dichloride (39 mg, 0.27 mmol) dissolved in 10 ml acetonitrile, was added ferrocenoylacetone (150 mg, 0.55 mmol) and triethyl amine (27 mg, 0.27 mmol) in 2.5 ml acetonitrile. The solution was stirred for several hours at room

temperature under nitrogen. The solvent was removed under reduced pressure and the resulting red-brown precipitate was shaken with toluene to dissolve the product. The unwanted precipitate was filtered off and from the filtrate the solvent was removed under reduced pressure to obtain the product. The product was recrystallized from acetone and hexane. Seeing as this complex is highly moisture sensitive it is stored under nitrogen. Yield 28% (44 mg). Melting point 93-94˚C. ν (C=O)/cm^{-1} = 1512. δ_H (300MHz, $CDCl_3$)/ppm: 2.20 (s; 6H; 2 x CH_3); 3.9-5.1 (m; 18H; 2 x C_5H_5, 2 x C_5H_4 from Fc); 5.7-6.1 (m; 2H; 2 x CH); 6.30-6.85 (m with high intensity peak at ± 6.6; 5H; C_5H_5). Microanalysis calculated C, 57.7%, H 4.6% and found C, 55.4%, H 4.9%.

4.4.2.9. Chloro(η^5-cyclopentadienyl)bis(1,1,1-trifluoro-2,4-pentanedionato-κ^2O,O')titanium(IV), [Ti(Cp)(Cl)(tfaa)$_2$] [48]

To a solution of titanocene dichloride (500 mg, 2 mmol) dissolved in 15 ml acetonitrile, was added trifluoroacetylacetone (616 mg, 4 mmol) and triethyl amine (202 mg, 2 mmol) in 5 ml acetonitrile. The solution was stirred for several hours at room temperature under nitrogen. The solvent was removed under reduced pressure and the resulting white orange-brown precipitate was shaken with toluene to dissolve the product. The unwanted precipitate was filtered off and from the filtrate the solvent was removed under reduced pressure to obtain the product. The product was recrystallized from acetone and hexane. Seeing as this complex is highly moisture sensitive it is stored under nitrogen. Yield 19% (173 mg). Melting point 82-85˚C. ν (C=O)/cm^{-1} = 1533. δ_H (300MHz, $CDCl_3$)/ppm: 2.0-2.5 (m; 6H; 2 x CH_3); 5.9-6.0 (2 x s; 2H; 2 x CH); 6.2-6.7 (with high intensity peak at ± 6.6; 5H; C_5H_5). Microanalysis calculated C, 39.6%, H 2.9% and found C, 39.7%, H 1.9%.

4.4.2.10. 4-Thio-2-pentanone-κ^2O,O'-bis(η^5-cyclopentadienyl)titanium(IV) perchlorate, [Tc(Sacac)]$^+ClO_4^-$ [49]

Titanocene dichloride (250 mg, 1 mmol) was suspended in 10 ml water and stirred under nitrogen. Silver perchlorate (408 mg, 2 mmol) was added and the mixture was stirred for about an hour under nitrogen. Silver chloride (white precipitate) was filtered off and washed with 2 ml water. The filtrate was cooled on an ice-bath and cold thioacetylacetone (116 mg, 1 mmol) in 2 ml cold THF was added dropwise while stirring. A green-brown precipitate formed immediately, which was filtered off and washed with water and ether. Yield 24% (94 mg).

Melting point >230˚C. ν (C=O)/cm^{-1} = 1522. δ_H (300MHz, $CDCl_3$)/ppm: 2.29 (s; 6H; 2 x CH_3); 6.03 (s; 1H; CH); 6.75 (s; 10H; 2 x C_5H_5).

4.4.2.11. (1,2-Benzenediolato)biscyclopentadienyl titanium(IV), [Tc(cat)] [9]

Titanocene dichloride (250 mg, 1 mmol) and 1,2-benzenediol (110 mg, 1.03 mmol) was dissolved in 5 ml DCM and stirred for 2 h at room temperature. The solvent was removed under reduced pressure and the precipitate was washed with ether. Yield 98% (324 mg). Melting point 100-103˚C. δ_H (300MHz, $CDCl_3$)/ppm: 6.61 (s; 10H; 2 x C_5H_5); 6.84 (m; 2H; C_6H_4); 6.89 (m; 2H; C_6H_4).

4.4.2.12. (1,2-Benzenedithiolato)biscyclopentadienyl titanium(IV), [Tc(Scat)] [50]

To a hot acetone solution (20 ml) of titanocene dichloride (125 mg, 0.5 mmol) was added, over a period of 5 min, a warm solution of 1,2-benzenedithiolate (75 mg, 0.5 mmol) in ethanol containing triethyl amine (0.5 ml). The solution was warmed on a steam-bath for 5 min, the solvent was removed under reduced pressure and the precipitate was washed with isopropanol and pentane. Yield 61% (103 mg). Melting point 150-152˚C. δ_H (300MHz, $CDCl_3$)/ppm: 6.60 (s; 10H; 2 x C_5H_5); 7.15 (m; 2H; C_6H_4); 7.49 (m; 2H; C_6H_4).

4.4.2.13. (2,2-Biphenyldiolato)biscyclopentadienyl titanium(IV), [Tc(biphen)] [51]

Titanocene dichloride (250 mg, 1 mmol) and 2,2-biphenyldiol (194 mg, 1.03 mmol) was dissolved in 5 ml DCM and stirred for 2 h at room temperature. The solvent was removed under reduced pressure and the precipitate was washed with ether. Yield 45% (184 mg). Melting point 208-211˚C. δ_H (300MHz, $CDCl_3$)/ppm: 6.28 (s; 10H; 2 x C_5H_5); 6.62 (m; 4H; C_6H_4); 6.90 (m; 4H; C_6H_4).

4.4.3. Zirconium Complexes

4.4.3.1. 2,4-Pentanedionato-κ^2O,O'-bis(η^5-cyclopentadienyl)zirconium(IV) diethyl dithiocarbamate

Dichlorobiscyclopentadienylzirconium(IV) (zirconocene dichloride) (300 mg, 1.03 mmol) was suspended in 4 ml water and stirred for a few minutes, acetylacetone (140 mg, 1.4 mmol) was added dropwise. The resulting solution was stirred overnight and any unwanted precipitate that formed was filtered off. The filtrate was added to a concentrated solution of diethyldithiocarbamate while shaking. The solution was centrifuged and the resulting precipitate was digested in hot water (60-70ºC) for 2 h. The precipitate was filtered off and the product was recrystallized from DCM and petroleum ether. Yield 0.6% (2.9 mg). Melting point >230˚C. ν (C=O)/cm^{-1} = 1625. δ_H (300MHz, $CDCl_3$)/ppm: 2.11 (s; 6H; 2 x CH_3); 5.56 (s; 1H; CH); 6.13 (s; 10H; 2 x C_5H_5).

4.4.3.2. 1-Methoxy-1,3-butanedionato-κ^2O,O'-bis(η^5-cyclopentadienyl) zirconium(IV) perchlorate, $[Zc(maa)]^+ClO_4^-$ [52]

Zirconocene dichloride (200 mg, 0.68 mmol) was suspended in 3 ml water and stirred under nitrogen for a few minutes. Silver perchlorate (284 mg, 1.37 mmol) was added and the mixture was stirred for about an hour under nitrogen. Silver chloride (white precipitate) was filtered off and washed with 2 ml water. The filtrate was cooled on an ice-bath and 2 ml cold ethyl acetylacetone (c.a. 4˚C) was added dropwise while stirring. The solvent was removed and to the resulting oil was added hexane and sodium perchlorate. The mixture was left overnight in the fridge and the resulting pink precipitate was filtered and washed with water and ether. Yield 36% (107 mg). Melting point >230˚C. ν (C=O)/cm^{-1} = 1732. δ_H (300MHz, $CDCl_3$)/ppm: 2.30 (s; 3H; CH_3); 3.44 (s; 3H; OCH_3); 5.45 (s; 1H; CH); 6.41 (s; 10H; 2 x C_5H_5).

4.4.3.3. Chloro(η^5-cyclopentadienyl)bis(2,4-pentanedionato-κ^2O,O') zirconium(IV), $[Zr(Cp)(Cl)(acac)_2]$ [53]

To a solution of zirconocene dichloride (146 mg, 0.5 mmol) dissolved in 10 ml acetonitrile, was added acetylacetone (100 mg, 1.0 mmol) and triethyl amine (50.5 mg, 0.5 mmol) in 2.5 ml acetonitrile. The solution was stirred overnight at room temperature under

nitrogen. The solvent was removed under reduced pressure and the resulting white precipitate was shaken with toluene to dissolve the product. The unwanted precipitate was filtered off and from the filtrate the solvent was removed under reduced pressure to obtain the product. The product was recrystallized from acetone and hexane. Seeing as this complex is highly moisture sensitive it is stored under nitrogen. Yield 29% (57 mg). Melting point 181-183˚C. ν (C=O)/cm^{-1} = 1625. δ_H (300MHz, $CDCl_3$)/ppm: 1.8-2.0 (m; 12H; 4 x CH_3); 5.6-5.8 (d; 2H; 2 x CH); 6.33 (s; 5H; C_5H_5).

4.4.3.4. Chloro(η^5-cyclopentadienyl)bis(1-phenyl-1,3-butanedionato-κ^2O,O') zirconium(IV), [Zr(Cp)(Cl)(bzac)$_2$] [54]

To a solution of zirconocene dichloride (146 mg, 0.5 mmol) dissolved in 10 ml acetonitrile, was added benzoylacetone (165 mg, 1.0 mmol) and triethylamine (50.5 mg, 0.5 mmol) in 2.5 ml acetonitrile. The solution was stirred overnight at room temperature under nitrogen. The solvent was removed under reduced pressure and the resulting white precipitate was shaken with toluene to dissolve the product. The unwanted precipitate was filtered off and from the filtrate the solvent was removed under reduced pressure to obtain the product. The product was recrystallized from acetone and hexane. Seeing as this complex is highly moisture sensitive it is stored under nitrogen. Yield 26% (59 mg). Melting point 146-148˚C. ν (C=O)/cm^{-1} = 1515. δ_H (300MHz, $CDCl_3$)/ppm: 1.9-2.4 (m; 6H; 2 x CH_3); 6.25 (2 x s; 2H; 2 x CH); 6.55 (m; 5H; C_5H_5); 7.3-8.1 (m; 10H; 2 x C_6H_5).

4.4.3.5. Chloro(η^5-cyclopentadienyl)bis(1-ferrocenoyl-1,3-butanedionato-κ^2O,O')zirconium(IV), [Zr(Cp)(Cl)(fca)$_2$] [55]

To zirconocene dichloride (50 mg, 0.17 mmol) dissolved in 10 ml acetonitrile, was added ferrocenoylacetone (93 mg, 0.34 mmol) and triethyl amine (18 mg, 0.17 mmol) in 2.5 ml acetonitrile. The solution was stirred overnight at room temperature under nitrogen. The solvent was removed under reduced pressure and the resulting red-brown precipitate was shaken with toluene to dissolve the product. The unwanted precipitate was filtered off and from the filtrate the solvent was removed under reduced pressure to obtain the product. The product was recrystallized from acetone and hexane. Seeing as this complex is highly moisture sensitive it is stored under nitrogen. Yield 43% (45 mg). Melting point >230˚C. ν (C=O)/cm^{-1} = 1517. δ_H (300MHz, $CDCl_3$)/ppm: 1.9-2.2 (m; 6H; 2 x CH_3); 4.0-5.1 (m; 18H; 2 x C_5H_5, 2 x C_5H_4 from

Fc); 5.7-5.9 (m; 2H; 2 x CH); 6.51 (m; 5H; C_5H_5). Microanalysis calculated C, 54.3%, H 4.3% and found C, 54.1%, H 4.6%.

4.4.4. Hafnium Complexes

4.4.4.1. 1-Methoxy-1,3-butanedionato-κ^2O,O'-bis(η^5-cyclopentadienyl) hafnium(IV) perchlorate, $[Hc(maa)]^+ClO_4^-$ [56]

Dichlorobiscyclopentadienylhafnium(IV) (hafnocene dichloride) (200 mg, 0.68 mmol) was suspended in 3 ml water and stirred under nitrogen for a few minutes. Silver perchlorate (284 mg, 1.37 mmol) was added and the mixture was stirred for about an hour under nitrogen. Silver chloride (white precipitate) was filtered off and washed with 2 ml water. The filtrate was cooled on an ice-bath and 2 ml cold ethyl acetylacetone (c.a. 4˚C) was added dropwise while stirring. The solvent was removed and to the resulting oil was added hexane and sodium perchlorate. The mixture was left overnight in the fridge and the resulting white precipitate was filtered and washed with water and ether. Yield 5% (18 mg). Melting point >230˚C. ν (C=O)/cm^{-1} = 1629. δ_H (300MHz, $CDCl_3$)/ppm: 2.14 (s; 3H; CH_3); 3.93 (s; 3H; OCH_3); 5.51 (s; 1H; CH); 6.78 (s; 10H; 2 x C_5H_5).

4.4.4.2. Chloro(η^5-cyclopentadienyl)bis(2,4-pentanedionato-κ^2O,O') hafnium(IV), $[Hf(Cp)(Cl)(acac)_2]$ [57]

To a solution of hafnocene dichloride (189.5 mg, 0.5 mmol) dissolved in 10 ml acetonitrile, was added acetylacetone (100 mg, 1.0 mmol) and triethyl amine (50.5 mg, 0.5 mmol) in 2.5 ml acetonitrile. The solution was stirred overnight at room temperature under nitrogen. The solvent was removed under reduced pressure and the resulting white precipitate was shaken with toluene to dissolve the product. The unwanted precipitate was filtered off and from the filtrate the solvent was removed under reduced pressure to obtain the product. The product was recrystallized from acetone and hexane. Seeing as this complex is highly moisture sensitive it is stored under nitrogen. Yield 36% (86 mg). Melting point 164-166˚C. ν (C=O)/cm^{-1} = 1520. δ_H (300MHz, $CDCl_3$)/ppm: 1.8-2.1 (m; 12H; 4 x CH_3); 5.55 (d; 2H; 2 x CH); 6.42 (s; 5H; C_5H_5).

4.4.4.3. Chloro(η^5-cyclopentadienyl)bis(1-ferrocenoyl-1,3-butanedionato-κ^2O,O')hafnium(IV), [Hf(Cp)(Cl)(fca)$_2$] [58]

To hafnocene dichloride (94 mg, 0.25 mmol) dissolved in 10 ml acetonitrile, was added ferrocenoylacetone (136 mg, 0.5 mmol) and triethyl amine (25 mg, 0.25 mmol) in 2.5 ml acetonitrile. The solution was stirred overnight at room temperature under nitrogen. The solvent was removed under reduced pressure and the resulting red-brown precipitate was shaken with toluene to dissolve the product. The unwanted precipitate was filtered off and from the filtrate the solvent was removed under reduced pressure to obtain the product. The product was recrystallized from acetone and hexane. Seeing as this complex is highly moisture sensitive it is stored under nitrogen. Yield 9% (16 mg). Melting point 78-80˚C. ν (C=O)/cm^{-1} = 1514. δ_H (300MHz, $CDCl_3$)/ppm: 2.2-2.5 (m; 6H; 2 x CH_3); 3.9-5.2 (m; 18H; 2 x C_5H_5, 2 x C_5H_4 from Fc) 5.6-5.8 (m; 2H; 2 x CH); 6.1-6.4 (m; 5H; C_5H_5). Microanalysis calculated C, 48.5%, H 3.8% and found C, 46.1%, H 4.1%.

4.4.5. Vanadium Complexes

Note: As vanadium(IV) is paramagnetic, no ^{1}H NMR's could be recorded.

4.4.5.1. 1-Ferrocenoyl-1,3-butanedionato-κ^2O,O'-bis(η^5-cyclopentadienyl) vanadium(IV) perchlorate, [Vc(fca)]$^+$ClO$_4^-$ [59]

Dichlorobiscyclopentadienylvanadium(IV) (vanadocene dichloride) (150 mg, 0.588 mmol) was suspended in 5 ml water and stirred under nitrogen for a few minutes. Silver perchlorate (245 mg, 1.18 mmol) was added and the mixture was stirred for about an hour under nitrogen. Silver chloride (white precipitate) was filtered off and washed with 2 ml water. The filtrate was cooled on an ice-bath and ferrocenoylacetone (159 mg, 0.588 mmol) dissolved in 1.5 ml cold THF (c.a. 4˚C) was added dropwise while stirring. A dark-green precipitate formed immediately, which was filtered off and washed with water and ether. Yield 49% (158 mg). Melting point 178-180˚C. ν (C=O)/cm^{-1} = 1674. Microanalysis calculated C, 52.4%, H 4.2% and found C, 54.1%, H 4.6%.

4.4.5.2. 1-Methoxy-1,3-butanedionato-κ^2O,O'-bis(η^5-cyclopentadienyl) vanadium(IV) perchlorate, $[Vc(maa)]^+ClO_4^-$ [21]

Vanadocene dichloride (120 mg, 0.47 mmol) was suspended in 3 ml water and stirred under nitrogen for a few minutes. Silver perchlorate (199 mg, 0.96 mmol) was added and the mixture was stirred for about an hour under nitrogen. Silver chloride (white precipitate) was filtered off and washed with 2 ml water. The filtrate was cooled on an ice-bath and 2 ml cold ethyl acetylacetone (c.a. 4˚C) was added dropwise while stirring. A grey-green precipitate formed immediately, which was filtered off and washed with water and ether. Yield 36% (67 mg). Melting point >230˚C. ν (C=O)/cm^{-1} = 1629. Microanalysis calculated C, 34.3%, H 3.7% and found C, 34.0%, H 3.6%.

4.4.5.3. Chloro(η^5-cyclopentadienyl)bis(2,4-pentanedionato-κ^2O,O') vanadium(IV), $[V(Cp)(Cl)(acac)_2]$ [57] [60]

To vanadocene dichloride (25 mg, 0.19 mmol) dissolved in 3 ml acetonitrile, was added acetylacetone (19 mg, 0.38 mmol) and triethyl amine (9.5 mg, 0.19 mmol) in 0.5 ml acetonitrile. The solution was stirred for several hours at room temperature under nitrogen. The solvent was removed under reduced pressure and the resulting green precipitate was shaken with toluene to dissolve the product. The unwanted precipitate was filtered off and from the filtrate the solvent was removed under reduced pressure to obtain the product. The product was recrystallized from acetone and hexane. Seeing as this complex is highly moisture sensitive it is stored under nitrogen. Yield 17% (11 mg). Melting point >230˚C. ν (C=O)/cm^{-1} = 1532. Microanalysis calculated C, 51.5%, H 5.5% and found C, 51.7%, H 5.3%.

4.4.5.4. Chloro(η^5-cyclopentadienyl)bis(1-ferrocenoyl-1,3-butanedionato-κ^2O,O')vanadium(IV), $[V(Cp)(Cl)(fca)_2]$ [61]

To vanadocene dichloride (64 mg, 0.25 mmol) dissolved in 10 ml acetonitrile, was added ferrocenoylacetone (136 mg, 0.5 mmol) and triethyl amine (25 mg, 0.25 mmol) in 2.5 ml acetonitrile. The solution was stirred for several hours at room temperature under nitrogen. The solvent was removed under reduced pressure and the resulting red-brown precipitate was shaken with toluene to dissolve the product. The unwanted precipitate was filtered off and from the filtrate the solvent was removed under reduced pressure to obtain the product. The product was recrystallized from acetone and hexane. Seeing as this complex is highly moisture sensitive it is

stored under nitrogen. Yield 32% (46 mg). Melting point >230˚C. ν (C=O)/cm^{-1} = 1517. Microanalysis calculated C, 57.5%, H 4.5% and found C, 56.4%, H 4.9%.

4.5. Electrochemistry

Measurements on ca. 3.0 mmol dm^{-3} solutions of the complexes in acetonitrile containing 0.10 mmol dm^{-3} tetra-*n*-butylammonium hexafluorophosphate (Fluka, electrochemical grade) as supporting electrolyte were conducted under a blanket of purified argon at 25.0˚C utilizing a BAS 100 B/W electrochemical workstation interfaced with a personal computer. A three electrode cell, which utilized a Pt auxiliary electrode, a glassy carbon (surface area 0.0707 cm^2) working electrode and an Ag/Ag$^+$ (0.010 mol dm^{-3} $AgNO_3$) reference electrode[2] mounted on a Luggin capillary was used.[3, 4] All temperatures were kept constant to within 0.5˚C. Successive experiments under the same experimental conditions, showed that all formal reduction and oxidation potentials were reproducible within 5 mV.

For the experiments done in 0.1 mol dm^{-3} H_2SO_4/H_2O, measurements on ca. 3.0 mmol dm^{-3} solutions of the complexes in 0.1 mol dm^{-3} H_2SO_4/H_2O containing 0.1 mol dm^{-3} KCl (Fluka, electrochemical grade) as supporting electrolyte were conducted under a blanket of purified argon at 25.0˚C. A three electrode cell, which utilized a Pt auxiliary electrode, a glassy carbon (surface area 0.0707 cm^2) working electrode and an Ag/AgCl reference electrode using a salt bridge containing 0.10 mol dm^{-3} KCl/H_2O.

Bulk electrolysis was carried out on the BAS 100 B/W voltammograph at 25.0˚C. A three electrode cell, which utilized a Pt wire auxiliary electrode (isolated from the sample by means of a salt bridge with 0.10 mol dm^{-3} $TBAPF_6/CH_3CN$), a glassy carbon working electrode (electro-active area 3 cm^2) and an Ag/Ag$^+$ (0.010 mol dm^{-3}, $AgNO_3$ in 0.10 mol dm^{-3} $TBAPF_6/CH_3CN$) reference electrode mounted on a Luggin capillary was employed. Current reading and the integrated current (C) were recorded automatically by using BAS 100 W Windows software.

4.6. Substitution kinetic measurements

The Beer-Lambert law, $A = \varepsilon c \ell$ with A = UV/Vis absorbance, ε = molar extinction coefficient, c = concentration and ℓ = path length = 1 cm, was found to be valid for all complexes in the concentration range (from 0.0001 mol dm^{-3} to 0.005 mol dm^{-3}) utilised for the kinetic studies. Pseudo first order rate constants, k_{obs}, were determined by monitoring the disappearance of the $[Tc(L_1L_2)]^+$ or $[Tc(L_1L_2)]$ complexes (paragraph 3.4, ([Tc(cat)], $[Tc(acac)]^+ClO_4^-$, $[Tc(Sacac)]^+ClO_4^-$) at the indicated wavelengths, λ_{exp}, on a 05-109 pbp Spectrakinetic stopped

flow spectrometer. The incoming ligands' (paragraph 3.4, acetylacetone, thioacetylacetone and 2,2-biphenyldiol) concentrations were 25, 50, 100, 200 and 250 times that of the $[Tc(L_1L_2)]^+$ or $[Tc(L_1L_2)]$ complexes (0.002 mol dm^{-3}). Voltage-time data was collected and k_{obs} values were determined from a linear fit of data according to:

$$\ln (A_0 - A_\infty / A_t - A_\infty) = k_{obs}t$$

A_0 indicates initial absorbance, A_t is the absorbance at time t and A_∞ is the absorbance at infinity. The second order rate constant, k_2, was determined (slope) from the relationship between the k_{obs} and the different incoming ligand concentrations according to the following equation:

$$k_{obs} = k_2[\text{incoming ligand}] + k_s$$

It was found that $k_s = 0$ for all complexes. The activation parameters ΔH^* (activation enthalpy), ΔS^* (activation entropy) and ΔG^* (Free energy of activation) for the substitution reactions were determined from the least square fits of the reaction rate constants *vs* temperature data according to the Arrhenius equation:

$$k = (RT/Nh)e^{(-\Delta H^*/RT)}e^{(\Delta S^*/R)}$$

which can be rewritten in a linear form:

$$\ln (k/T) = (-\Delta H^*/RT) + (\Delta S^*/R) + \ln(R/Nh)$$

h = Planck constant = 6.625×10^{-3} J s, N = Avogadro's number = 6.023×10^{23} mol^{-1}, R = Gas constant = 8.314 J mol^{-1} K^{-1}.

The activation free energy was calculated from:

$$\Delta G^* = \Delta H^* - T\,\Delta S^*$$

4.7. Cytotoxic tests

The author acknowledges Prof. C.E.J. Medlen from the Department of Pharmacology, University of Pretoria, for performing these experiments and for compilation of the survival curves.

4.7.1. Sample preparation

Metallocenes dichlorides (Ti, Zr, Hf and V), titanocene complexes (40-44) and titanium complexes (45-51) were dissolved in DMSO to give stock concentration of 10 mg cm^{-3} and diluted in the appropriate growth medium supplemented with fetal calf serum (FCS) to give final DMSO concentrations not exceeding 0.5% and drug concentration of 1-3000 μg cm^{-3} prior to cell experiments.

4.7.2. Cell cultures

Human colorectral cell line, CoLo DM320 (ATCC CCL-220), was grown as a suspended culture in RPMI 1640. The human cervix epitheloid cancer cell line, HeLa (ATCC CCl-2), was grown as a monolayer culture in MEM. Growth media was incubated at 37˚C under 5% CO_2 and fortified with 10% FCS and 1% penicillin and streptomycin. Appropriate solvent control systems were included. Cells were seeded at 2000 cells/well for 24 h incubation experiments and 400 cells/well for 7 days incubation experiments in 96 well microtiter plates in a final volume of 200 μl of growth medium in the presence or absence of different concentrations of experimental drugs. Wells without cells and with cells but without drugs were included as controls. After incubation at 37˚C for 1 day or 7 days, cell survival was measured by means of the colometric 3-(4,5-dimethylthiazol-2-yl)-diphenyltetra sodium bromide (MMT) assay.

---

[1] B.S. Furniss, A.J. Hannaford, P.W.G. Smith and A.R. Tatchell, *Vogel's Textbook of Practical Organic Chemistry*, 4th Edition, Longman, New York, p 264-318.

[2] D.T. Sawyer and J.L. (Jr) Roberts, *Experimental electrochemistry for chemists*, Wiley, New York, 1974, p 54.

[3] D.H. Evans, K.M. O'Connell, R.A. Peterson and M.J. Kelly, *J. Chem. Educ.*, 1983, **60**, 291.

[4] G.A. Mabbott, *J. Chem. Educ.*, 1983, **60**, 697.

Chapter 5

Summary, Conclusions and Future Perspectives

In this study, 13 new and 11 known complexes of the metals Ti, Zr, Hf and V with different bi-chelating ligands were synthesised. These complexes were all characterised by several techniques, including infra red, ^{1}H NMR and microanalysis, in order to differentiate their activities such as formal reduction potentials and kinetic rate constants and compare their physical properties.

A variety of tetrahedral mono-β-diketonato titanocenyl(IV) complexes of the form $[Tc(CH_3COCHCOR)]^+ClO_4^-$ (see Figure 5.1), where Tc = $(C_5H_5)_2Ti^{2+}$ and R = CH_3, Ph, CF_3 (new), Fc (new) and OCH_3, were synthesised. The same type of metallocene complexes, namely $[Vc(CH_3COCHCOFc)]^+ClO_4^-$ (new) and $[Mc(CH_3COCHCOOCH_3)]^+ClO_4^-$ with Mc = $(C_5H_5)_2V^{2+}$, $(C_5H_5)_2Zr^{2+}$ (new) and $(C_5H_5)_2Hf^{2+}$ (new) were also prepared successfully.

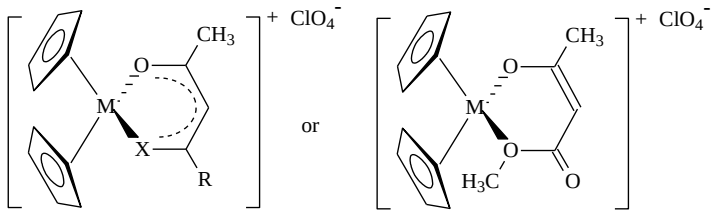

R = CH_3 , Ph, CF_3 and Fc
M = Ti, V, Zr or Hf
X = O or S

R = OCH_3.

Figure 5.1. Structures of tetrahedral mono-β-diketonato metallocenyl(IV) complexes.

For titanium(IV), a β-thioxoketonato titanocenyl(IV) complex (new) {$[Tc(CH_3CSCHCOCH_3)]^+ClO_4^-$} (see Figure 5.1) was prepared for comparison with $[Tc(CH_3COCHCOCH_3)]^+ClO_4^-$, *via* the same procedure. Since the mono-β-diketonato titanocenyl(IV) complexes all contain a six-membered metallocyclic ring, five- and seven-membered metallocyclic titanocenyl(IV) complexes were synthesised for comparison. The five membered titanocenyl(IV) complexes were prepared by complexing titanocenyl(IV) with bidentate ligands 1,2-benzenediol and its sulphur counterpart 1,2-benzenedithiol to give $[Tc(OC_6H_4O)]$ and $[Tc(SC_6H_4S)]$ (see Figure 5.2). The seven membered titanocenyl(IV) complexes were prepared by complexing titanocenyl(IV) with the bidentate ligand 2,2-biphenyldiol to give $[Tc(OC_6H_4C_6H_4O)]$ (see Figure 5.2).

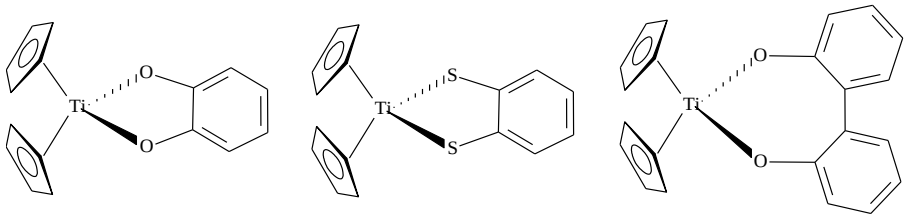

Figure 5.2. Structures of 5- and 7-membered metallocyclic titanocenyl(IV) complexes.

A series of 7 new and 4 known octahedral bis-β-diketonato metal(IV) complexes of the form $[M(Cp)(Cl)(CH_3COCHCOR)_2]$ (see Figure 5.3), where M = Ti, Zr, Hf and V and R = CH_3, Ph, CF_3 and Fc, were prepared. From ^1H NMR studies on the bis-β-diketonato complexes it was revealed that these compounds exist as more than one isomer.

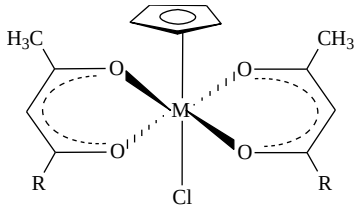

Figure 5.3. Structure of octahedral bis-β-diketonato metal(IV) complexes.

Electrochemical studies in CH_3CN, utilising cyclic voltammetry, was preformed on all synthesised complexes. The mono-β-diketonato titanocenyl(IV) complexes all revealed chemical and electrochemical reversible Ti^{4+}/Ti^{3+} couples, with the Fc/Fc^+ couple of the $[Tc(CH_3COCHCOFc)]^+ClO_4^-$ complex electrochemically quasi-reversible. The formal reduction potential of the Ti^{4+}/Ti^{3+} couple is influenced by the group electronegativity of the R group of the β-diketonato ligand. With an increase in group electronegativity of the R group of the β-diketonato ligand, there is an increase in formal reduction potential of the Ti^{4+}/Ti^{3+} couple. This is expected, because the more electron withdrawing the R group, the more positive the titanium(IV) centre will be and accordingly the more difficult it will be to reduce it, $Ti(IV) + e^- \rightarrow Ti(III)$.

The thioacetylacetonato titanocenyl(IV) complex, $[Tc(CH_3CSCHCOCH_3)]^+ClO_4^-$, revealed chemical and electrochemical reversibility for the Ti^{4+}/Ti^{3+} couple. Electrochemical data of the other bi-chelating ligand titanocenyl(IV) complexes (bi-chelating ligand = 1,2-benzenediolato, 1,2-benzenedithiolato and 2,2-biphenyldiolato) revealed chemical and electrochemical irreversibility for the Ti^{4+}/Ti^{3+} couple.

For the bis-β-diketonato titanium(IV) complexes, the Ti^{4+}/Ti^{3+} couple is chemically irreversible except for $[Ti(Cp)(Cl)(CH_3COCHCOFc)_2]$ where Ti^{4+}/Ti^{3+} couple is chemically reversible and electrochemically irreversible with the Fc/Fc^+ couple displaying electrochemical

quasi-reversibility. The reduction of Ti metal centre is still influenced by the electronegativity of the R group on the β-diketonato ligand.

Electrochemical data for the metallocene dichlorides of Zr, Hf and V, al showed chemical irreversibility, Ti showed chemical reversibility and electrochemical irrevesibility, with E_{pc} dependent on the metals' atomic electronegativity. The bis-acetylacetonato metal(IV) complexes, $[M(Cp)(Cl)(CH_3COCHCOCH_3)_2]$ with M = Ti, Zr, Hf and V displayed the same chemical irreversible character as the metallocene dichlorides. In contrast with the bis-acetylacetonato metal(IV) complexes, the bis-ferrocenoylacetonato metal(IV) complexes, $[M(Cp)(Cl)(CH_3COCHCOFc)_2]$ with M = Ti, Zr, Hf and V showed chemical reversibility but not electrochemical reversibility for the M^{4+}/M^{3+} couple, the Fc/Fc^+ couples displayed electrochemical quasi-reversibility except for the V complex.

Bulk electrolysis preformed on selected complexes $[Tc(CH_3COCHCOFc)]^+ClO_4^-$, $[Tc(OC_6H_4O)]$ and $[Ti(Cp)(Cl)(CH_3COCHCOFc)_2]$ showed that 1 electron was transferred in the Ti^{4+}/Ti^{3+} couple, 1 electron in the Fc/Fc^+ couple (the bis-complex showed 2 electrons transferred one for each Fc) and 2 electrons in the redox process of the 1,2-benzenediolato ligand.

The substitution reactions investigated in this kinetic study, involved the five-, six- and seven membered metallocyclic titanocenyl complexes: $[Tc(OC_6H_4O)]$, $[Tc(CH_3COCHCOCH_3)]^+ClO_4^-$, $[Tc(CH_3COCHCSCH_3)]^+ClO_4^-$ and $[Tc(OC_6H_4C_6H_4O)]$.

The general rate law applicable to the substitution reaction between the titanocenyl complexes of the type $[Tc(L_1L_2)]^x$ (x = 0, +1) and an incoming ligand L_3L_4 (L_1L_2 and L_3L_4 both bidentate ligands such as 1,2-benzenediol, acetylacetone, thioacetylacetone and 2,2-biphenyldiol) according to Scheme 5.1 is given by Equation 5.1.

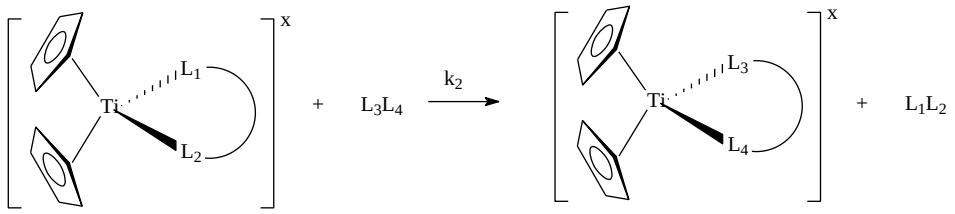

Scheme 5.1. General reaction scheme of the substitution reaction of titanocenyl complexes with a bidentate ligand, x = 0, +1, the charge of the titanocenyl complex.

Equation 5.1

$$\text{Rate} = \{k_s + k_2[L_3L_4]\}[[Tc(L_1L_2)]^x]$$

with x = 0, +1, the charge of the titanocenyl complex. If $[L_3L_4] >> [[Tc(L_1L_2)]^x]$ then this rate simplifies to:

$$Rate = k_{obs}[[Tc(L_1L_2)]^x]$$

with the pseudo first order rate constant $k_{obs} = k_s + k_2[L_3L_4]$, k_2 is the second order rate constant for the substitution process and k_s is the rate constant associated with the solvent (in this case acetone) taking part in the reaction. For the reactions studied, the plot of k_{obs} *vs* $[L_3L_4]$ passes through the origin, suggesting $k_s << k_2$ for acetone as the solvent. The large negative activation entropy ΔS^* found for all substitution reactions, implied that the mechanism of substitution is associative in nature.

For the substitution with 2,2-biphenyldiol of 1,2-benzenediolato, acetylacetonato, thioacetylacetonato from $[Tc(OC_6H_4O)]$, $[Tc(CH_3COCHCOCH_3)]^+ClO_4^-$ or $[Tc(CH_3COCHCSCH_3)]^+ClO_4^-$, it was found that the second order rate constant k_2 ($dm^3\ mol^{-1}\ s^{-1}$) were approximately the same (at 25.0˚C $[Tc(OC_6H_4O)]$ $k_2 = 4.6(9)\ dm^3\ mol^{-1}\ s^{-1}$, $[Tc(CH_3COCHCOCH_3)]^+ClO_4^-$ $k_2 = 5.7(8)\ dm^3\ mol^{-1}\ s^{-1}$, $[Tc(CH_3COCHCSCH_3)]^+ClO_4^-$ $k_2 = 5.7(1)\ dm^3\ mol^{-1}\ s^{-1}$), with the activation parameters (ΔH^*, ΔS^* and ΔG^*) displaying similarities.

The substitution of the bidentate ligand 1,2-benzenediolato from $[Tc(OC_6H_4O)]$ with acetylacetone, thioacetylacetone and 2,2-biphenyldiol revealed a small increase in the second order rate constant k_2 ($dm^3\ mol^{-1}\ s^{-1}$) when going from the six- to the seven-membered ring (acetylacetone, thioacetylacetone to 2,2-biphenyldiol). The second order rate constant k_2 for acetylacetone (at 25.0˚C $k_2 = 1.6(4)\ dm^3\ mol^{-1}\ s^{-1}$) are slightly smaller than that found for thioacetylacetone (at 25.0˚C $k_2 = 2.9(1)\ dm^3\ mol^{-1}\ s^{-1}$) probably due to the change in electronegativity and nucleophilicity in going from oxygen to sulphur. The second order rate constant k_2 for 2,2-biphenyldiol (at 25.0˚C $k_2 = 5.7(1)\ dm^3\ mol^{-1}\ s^{-1}$) is approximately twice that found for thioacetylacetone (at 25.0˚C $k_2 = 2.9(1)\ dm^3\ mol^{-1}\ s^{-1}$). Again, the activation parameters (ΔH^*, ΔS^* and ΔG^*) are nearly identical.

Substitution of acetylacetonato from $[Tc(CH_3COCHCOCH_3)]^+ClO_4^-$ with thioacetylacetone showed a small second order rate constant $k_2 = 1.1(8)\ dm^3\ mol^{-1}\ s^{-1}$, while the reverse reaction, the displacement of thioacetylacetonato from $[Tc(CH_3COCHCSCH_3)]^+ClO_4^-$ with acetylacetone was not observed.

From the kinetic data the following stability series for the different sized metallocyclic complexes was established:

{most stable} [Tc(biphen)] (7 membered ring) > $[Tc(Sacac)]^+$ (6 membered ring) > $[Tc(acac)]^+$ (6 membered ring) > [Tc(cat)] (5 membered ring) {least stable}

The cytotoxic properties in terms of potential anti-cancer application of the titanium(IV) complexes were studied. Human colorectral cell line (CoLo) and human cervix epitheloid cancer cell line (HeLa) cell lines were utilised to determine the cytotoxicity of the complexes. The complexes containing more than one antineoplastic moiety, $[Tc(CH_3COCHCOFc)]^+ClO_4^-$, and $[Ti(Cp)(Cl)(CH_3COCHCOFc)_2]$, gave better results than titanocene dichloride (currently in clinical trial phase II)[1] for the CoLo and HeLa cell lines, probably due to a synergistic effect of the ferrocenyl ligand and the titanocenyl moiety. $[Tc(SC_6H_4S)]$ showed the highest cytotoxic properties of all the titanium(IV) complexes synthesised in this study. All the titanium(IV) complexes tested display better IC_{50} values against the CoLo and HeLa cell lines than titanocene dichloride, which is currently in clinical phase II trials.[1]

Future perspectives from this study are vast. In this study a series of mono-β-diketonato, $[Tc(\beta\text{-diketonato})]^+ClO_4^-$, and bis-β-diketonato, $[Ti(Cp)(Cl)(\beta\text{-diketonato})_2]$, Ti(IV) complexes were synthesized and subjected to cyclic voltammetry and substitution kinetics. Similar studies on Zr, Hf, V, Nb and Mo should be done. Quantification of trends within a group (Ti, Zr and Hf complexes) or a certain period (Ti and V; Zr, Nb and Mo complexes) of the periodic table must be made. Applications of these new and known complexes synthesised in this study in terms of catalysis should be addressed. This would include polymerisation catalysis similar to Ziegler-Natta types of catalysts.[2]

A series of new titanocene-containing β-diketones can possibly be made. A study involving the R group on this titanocene-containing-β-diketone, including pK_a, electronegativity, electrochemistry and keto-enol kinetics can be done. The titanocene-containing-β-diketone can also be complexed to transition metal such as rhodium to find possible synergistic antineoplastic effects as well as catalytic properties.

[1] J.R. Boyles, M.C. Baird, B.G. Campling and N. Jain, *J. Inorg. Biochem.*, 2001, **84**, 159.

[2] F.A. Cotton, G. Wilkenson and P.L. Gaus, *Basic Inorganic Chemstry*, Wiley, New York, 1995, pp. 719-720.

Appendix

^{1}H NMR Spectra

Spectrum 1: 1-Ferrocenoyl-1,3-butanediol, Hfca [40]

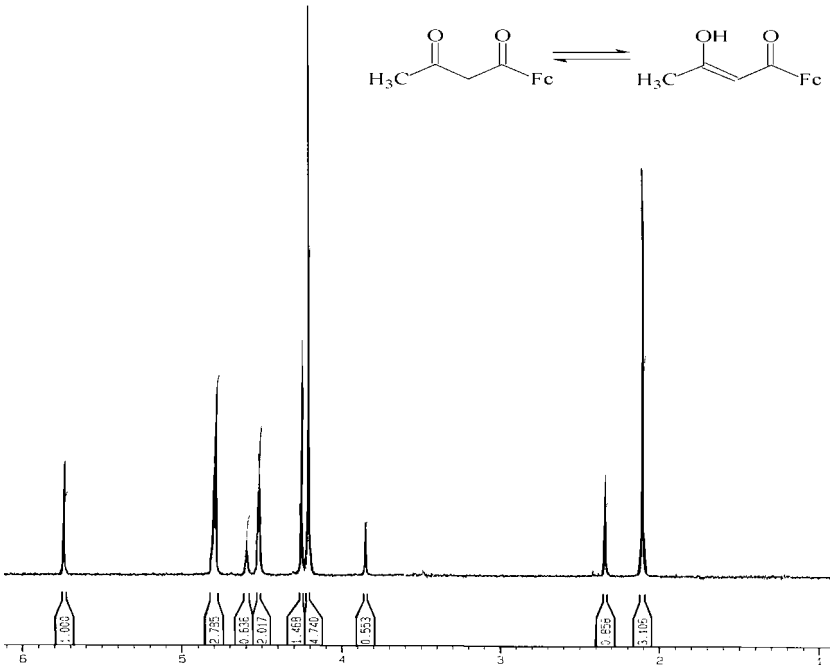

Spectrum 2: 4-Thioxopentan-2-one, HSacac [26]

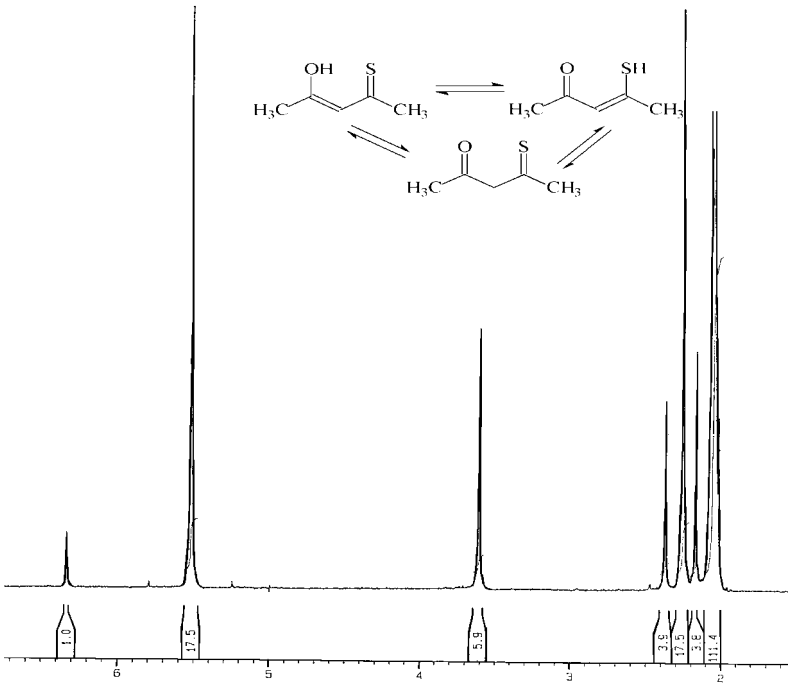

Spectrum 3: 2,4-Pentanedionato-κ^2O,O'-bis(η^5-cyclopentadienyl) titanium(IV) perchlorate, $[Tc(acac)]^+ClO_4^-$ [41]

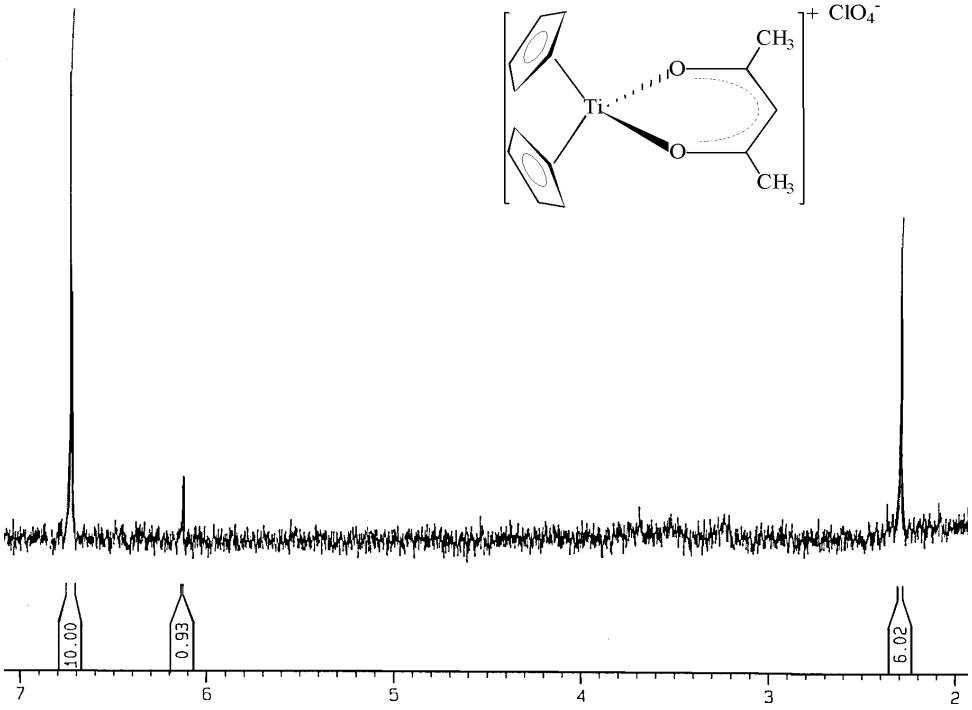

Spectrum 4: 1-Phenyl-1,3-butanedionato-κ^2O,O'-bis(η^5-cyclopentadienyl)titanium(IV) perchlorate, $[Tc(bzac)]^+ClO_4^-$ [42]

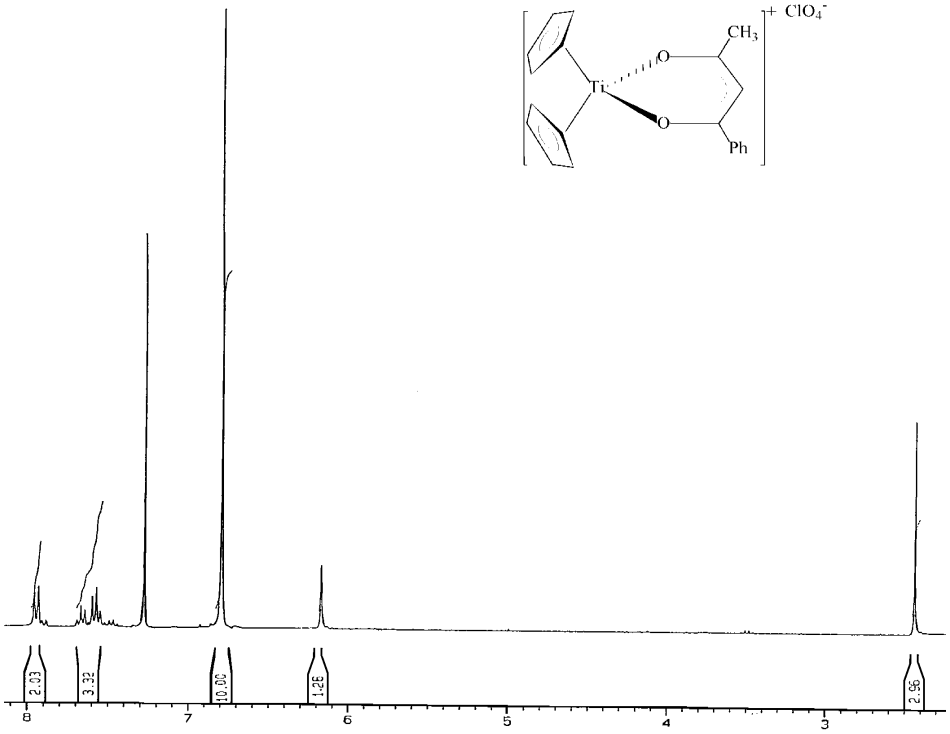

Spectrum 5: 1,1,1-Trifluoro-2,4-pentanedionato-κ^2O,O'-bis(η^5-cyclopentadienyl)titanium(IV) perchlorate, $[Tc(tfaa)]^+ClO_4^-$ [43]

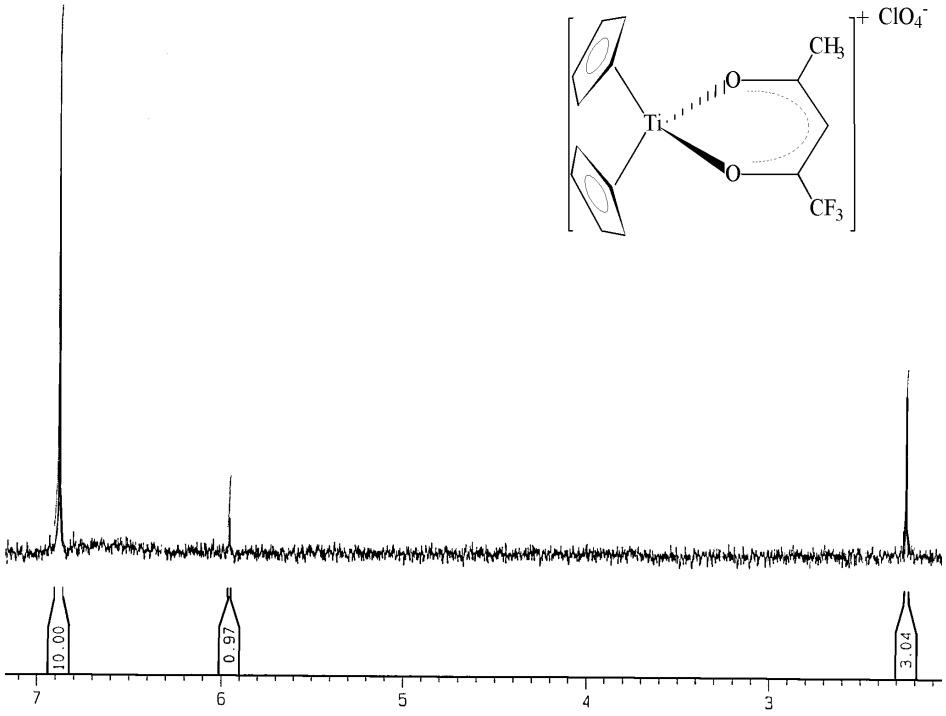

Spectrum 6: 1-Ferrocenoyl-1,3-butanedionato-κ^2O,O'-bis(η^5-cyclopentadienyl)titanium(IV) perchlorate, $[Tc(fca)]^+ClO_4^-$ [44]

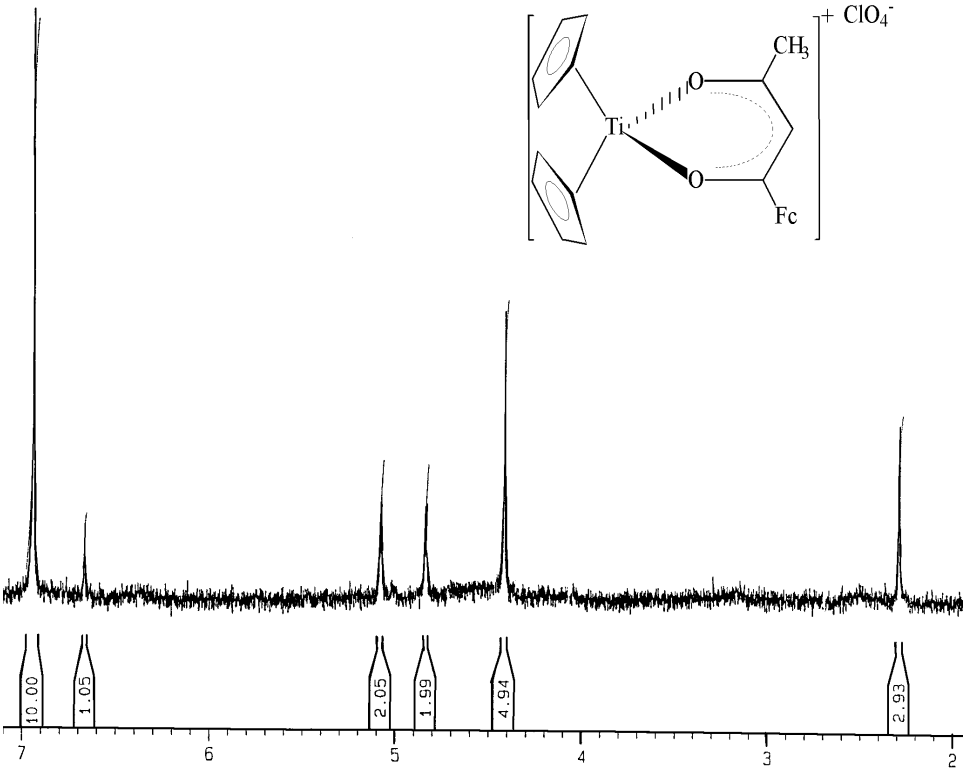

Spectrum 7: 1-Methoxy-1,3-butanedionato-κ^2O,O'-bis(η^5-cyclopentadienyl)titanium(IV) perchlorate, [Tc(maa)]$^+$ClO$_4^-$ [20]

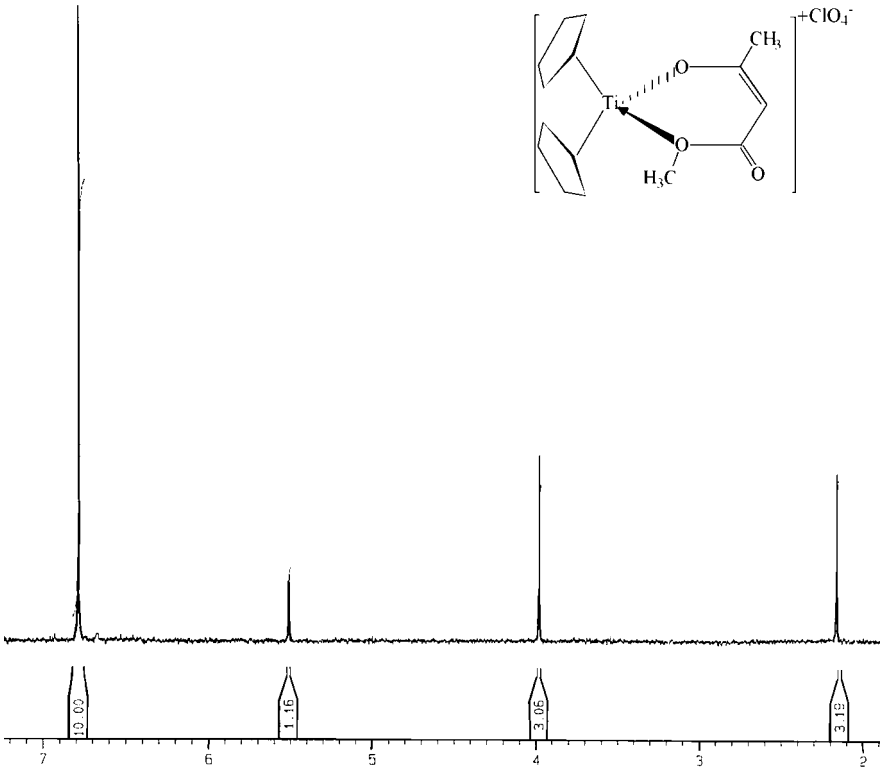

Spectrum 8: Chloro(η^5-cyclopentadienyl)bis(2,4-pentanedionato-κ^2O,O')titanium(IV), [Ti(Cp)(Cl)(acac)$_2$] [45]

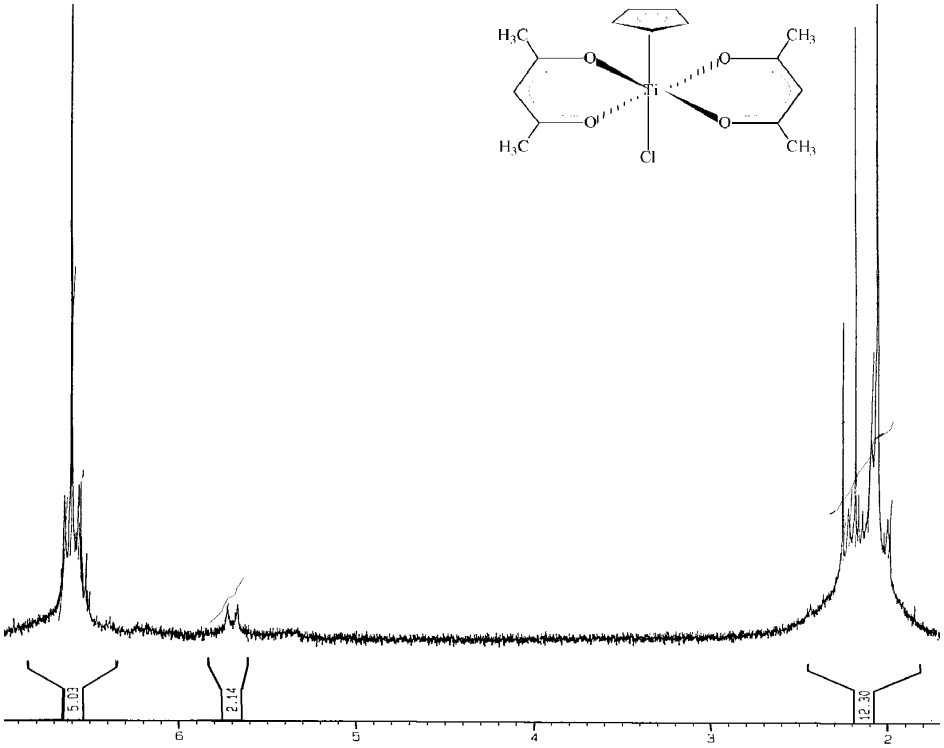

Spectrum 9: Chloro(η^5-cyclopentadienyl)bis(1-phenyl-1,3-butanedionato-κ^2O,O')titanium(IV), [Ti(Cp)(Cl)(bzac)$_2$] [46]

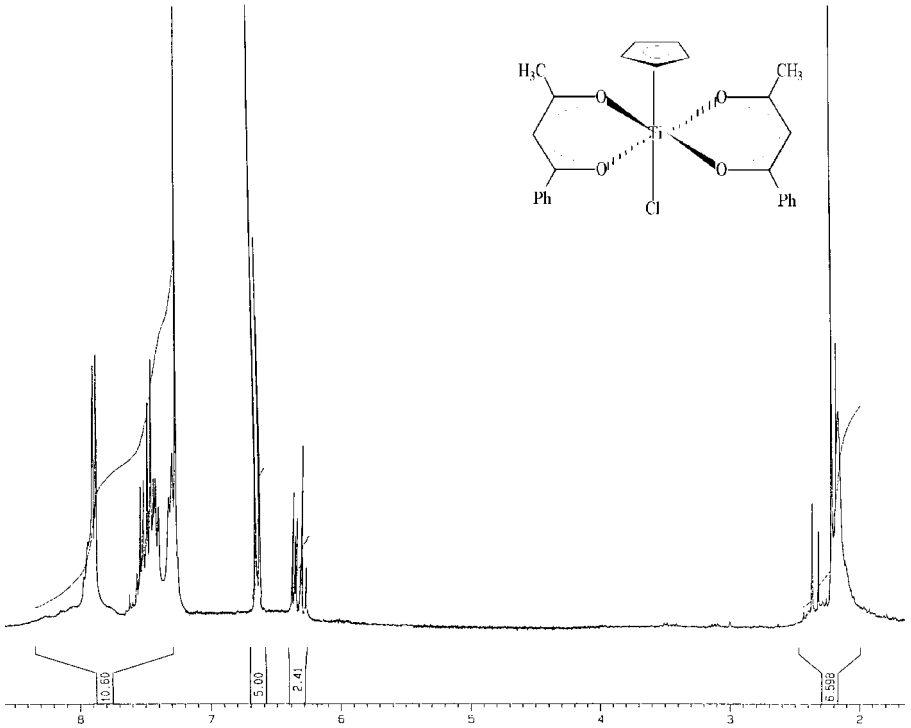

Spectrum 10: Chloro(η^5-cyclopentadienyl)bis(1-ferrocenoyl-1,3-butanedionato-κ^2O,O')titanium(IV), [Ti(Cp)(Cl)(fca)$_2$] [47]

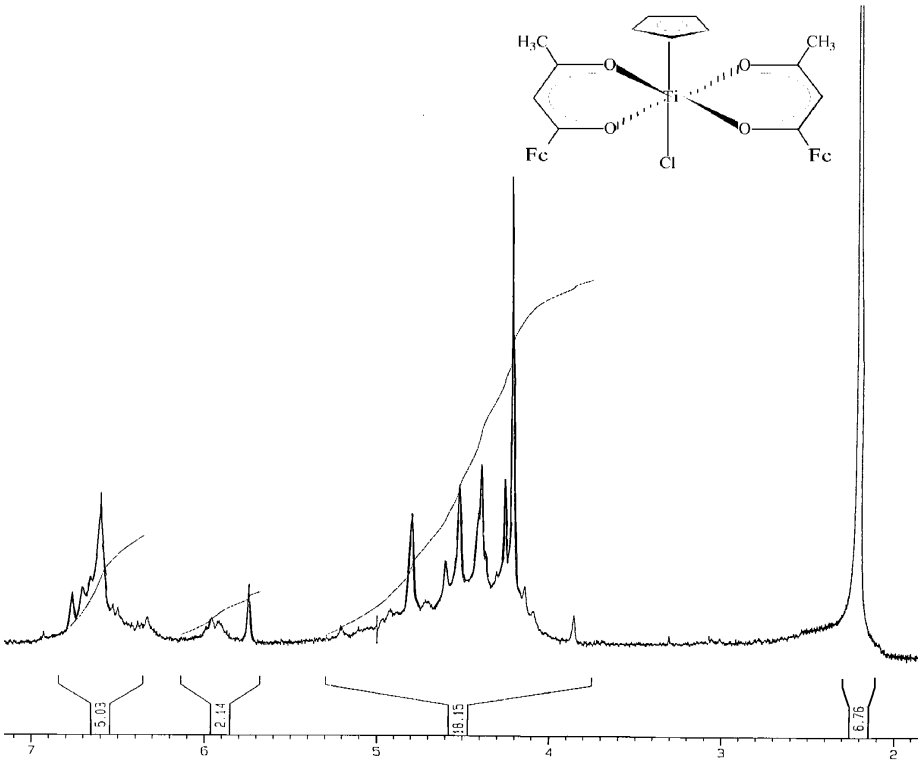

Spectrum 11: Chloro(η^5-cyclopentadienyl)bis(1,1,1-trifluoro-2,4-pentanedionato-κ^2O,O')titanium(IV), [Ti(Cp)(Cl)(tfaa)$_2$] [48]

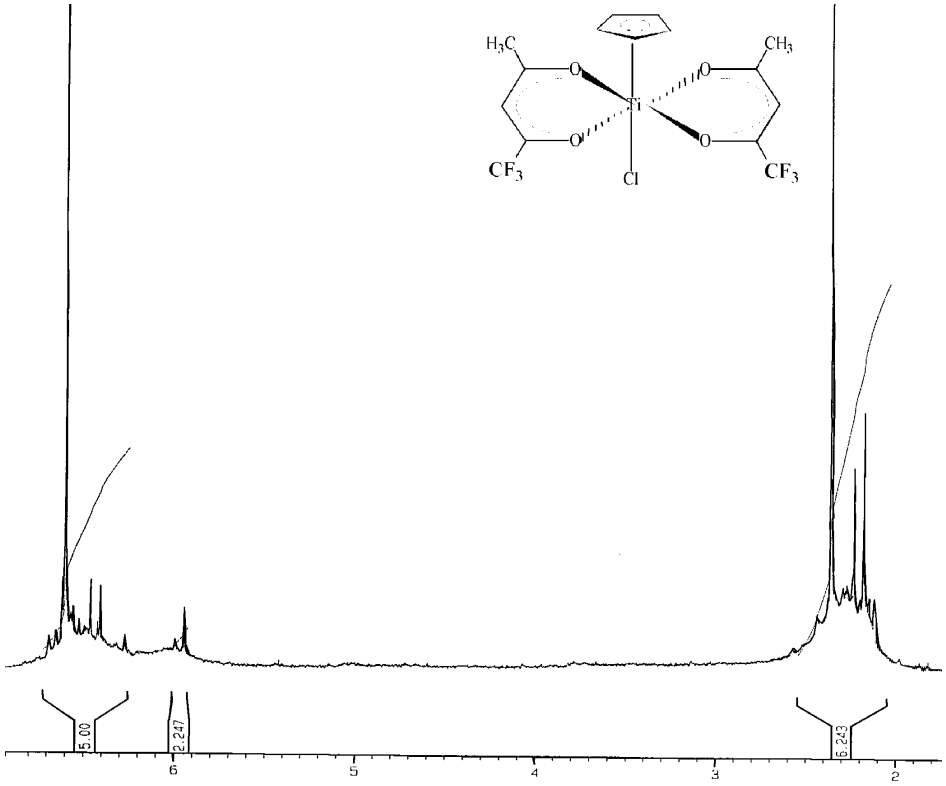

Spectrum 12: 4-Thio-2-pentanone-κ^2O,O'-bis(η^5-cyclopentadienyl) titanium(IV) perchlorate, [Tc(Sacac)]$^+$ClO$_4^-$ [49]

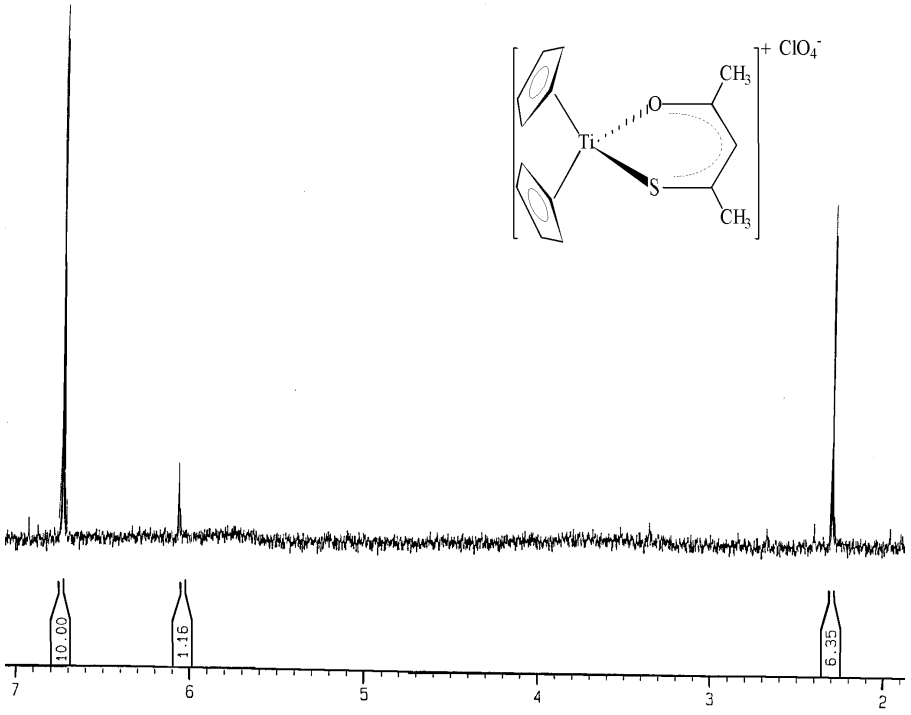

Spectrum 13: (1,2-Benzenediolato)biscyclopentadienyl titanium(IV), [Tc(cat)] [9]

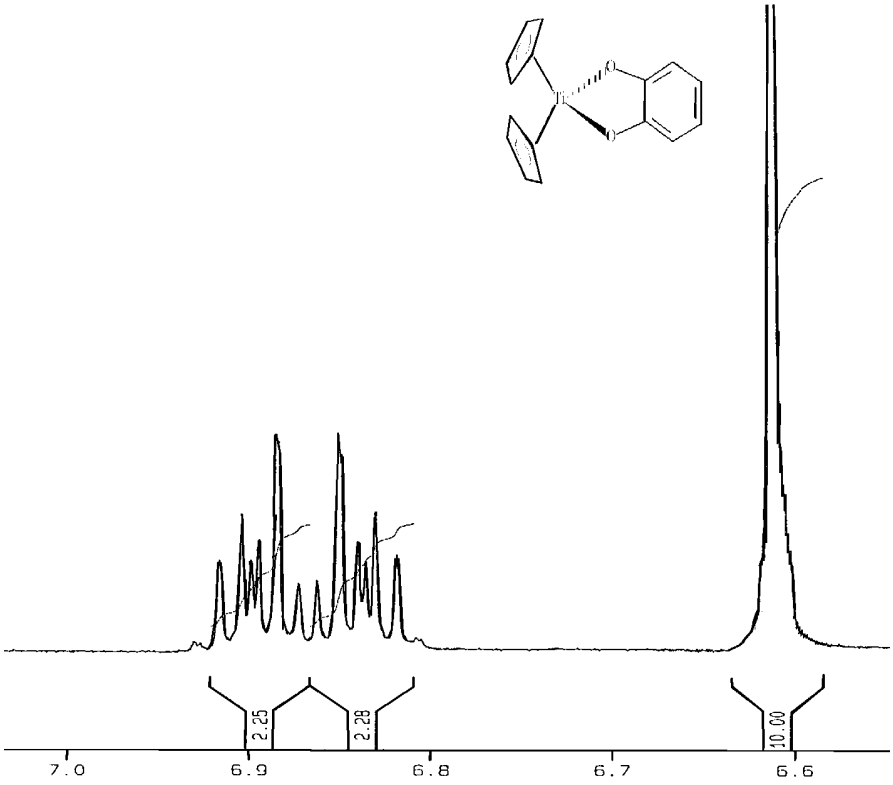

Spectrum 14: (1,2-Benzenedithiolato)biscyclopentadienyl titanium(IV), [Tc(Scat)] [50]

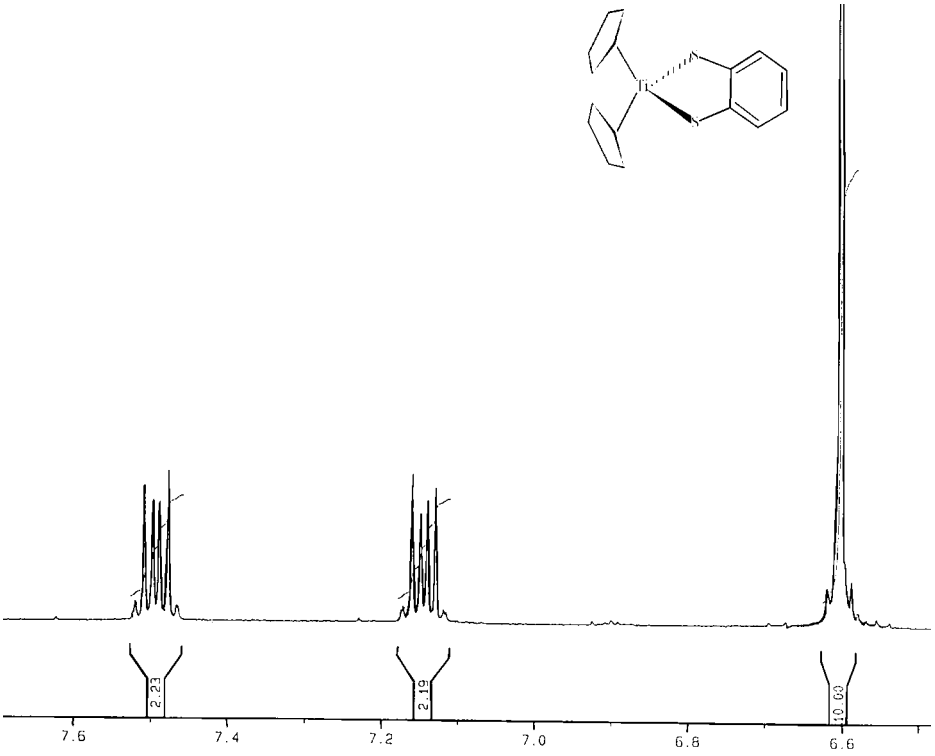

Spectrum 15: (2,2-Biphenyldiolato)biscyclopentadienyl titanium(IV), [Tc(biphen)] [51]

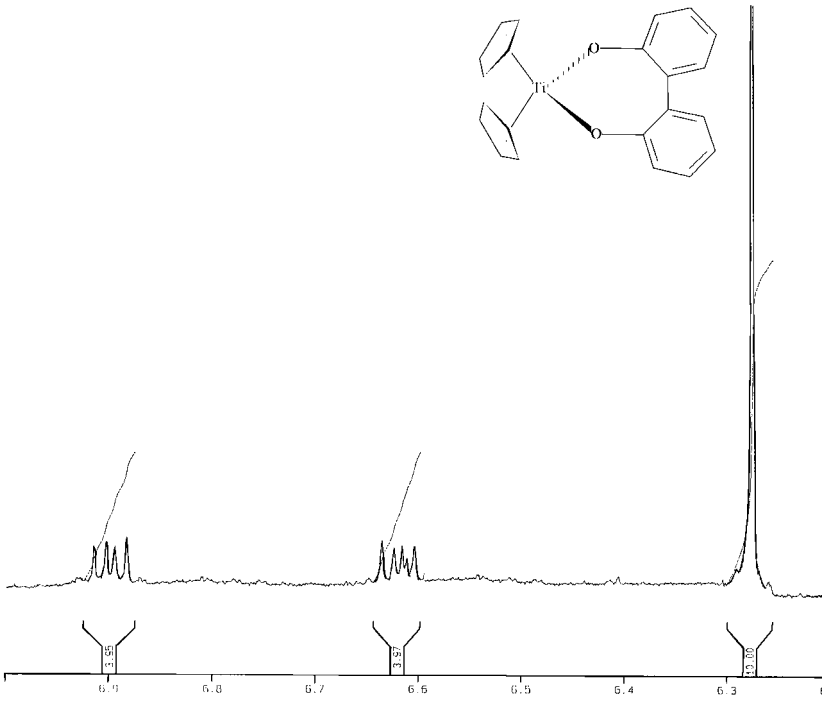

Spectrum 16: 1-Methoxy-1,3-butanedionato-κ^2O,O'-bis(η^5-cyclopentadienyl)zirconium(IV) perchlorate, [Zc(maa)]$^+$ClO$_4^-$ [52]

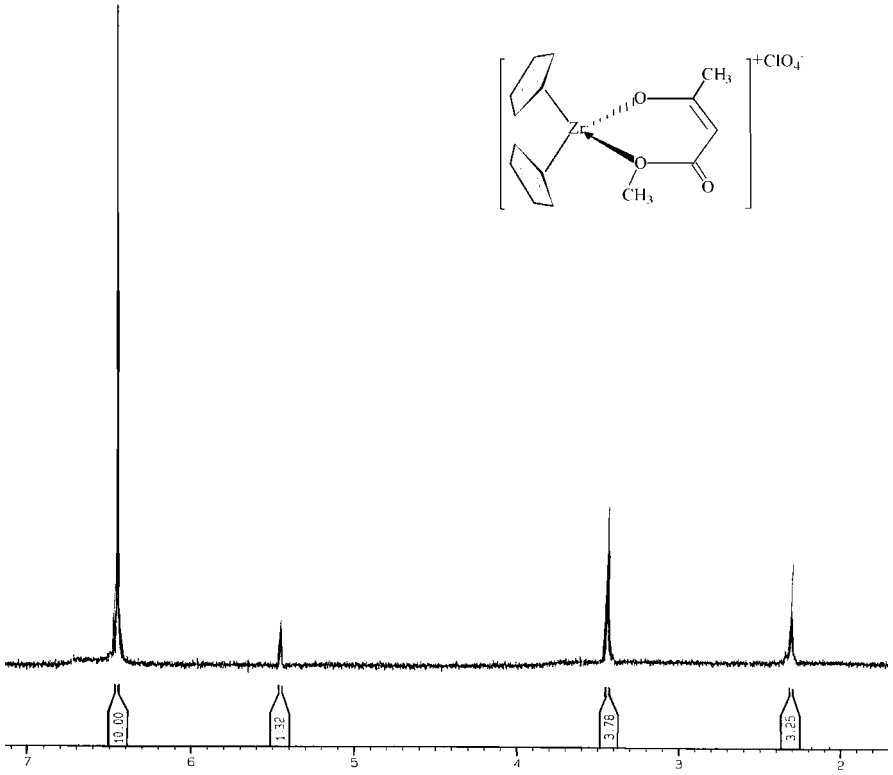

Spectrum 17: Chloro(η^5-cyclopentadienyl)bis(2,4-pentanedionato-κ^2O,O')zirconium(IV), [Zr(Cp)(Cl)(acac)$_2$] [53]

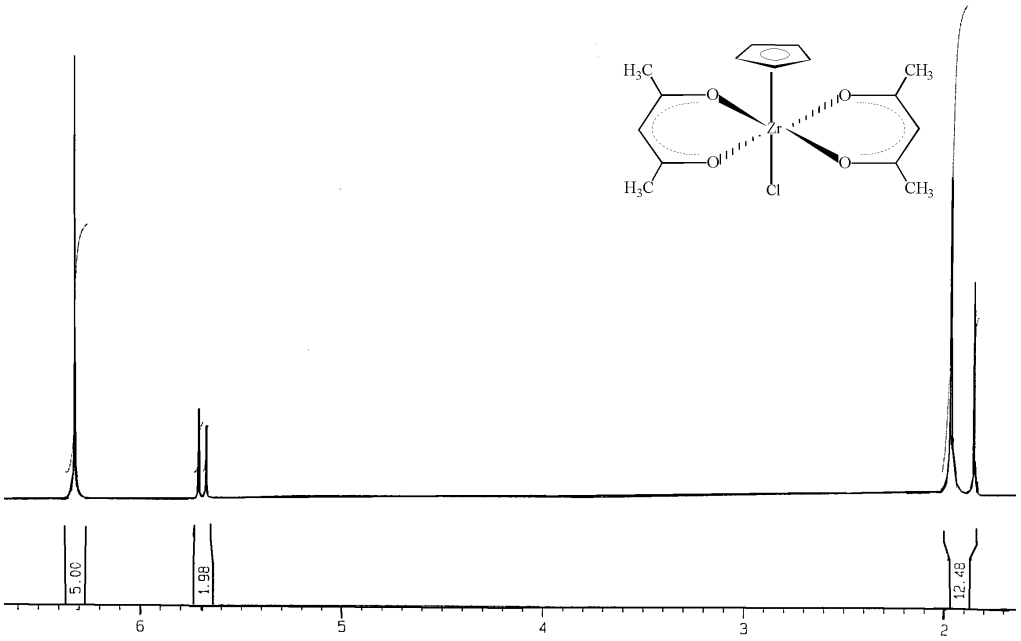

Spectrum 18: Chloro(η^5-cyclopentadienyl)bis(1-phenyl-1,3-butanedionato-κ^2O,O')zirconium(IV), [Zr(Cp)(Cl)(bzac)$_2$] [54]

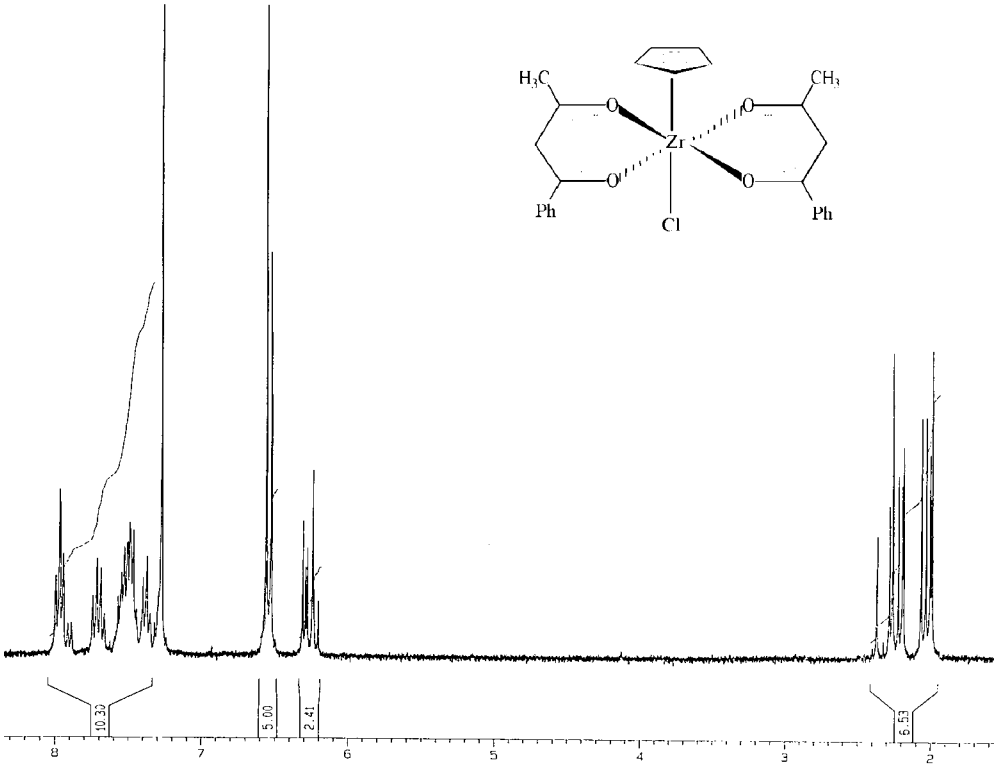

Spectrum 19: Chloro(η^5-cyclopentadienyl)bis(1-ferrocenoyl-1,3-butanedionato-κ^2O,O')zirconium(IV), [Zr(Cp)(Cl)(fca)$_2$] [55]

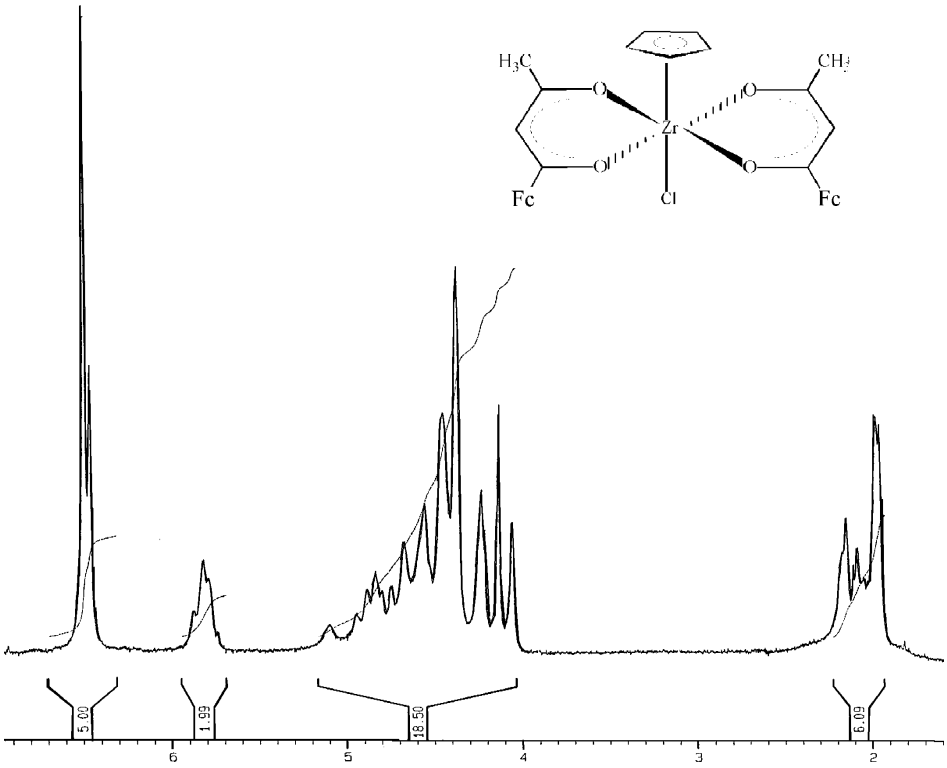

Spectrum 20: 1-Methoxy-1,3-butanedionato-κ^2O,O'-bis(η^5-cyclopentadienyl)hafnium(IV) perchlorate, [Hc(maa)]$^+$ClO$_4^-$ [56]

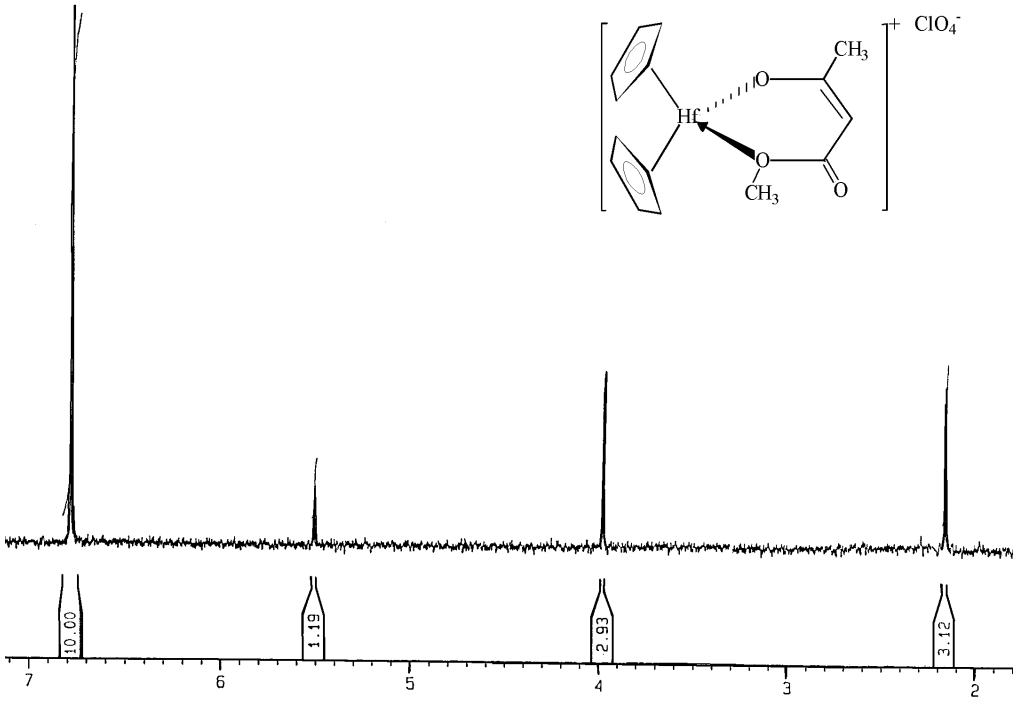

Spectrum 21: Chloro(η^5-cyclopentadienyl)bis(2,4-pentanedionato-κ^2O,O')hafnium(IV), [Hf(Cp)(Cl)(acac)$_2$] [57]

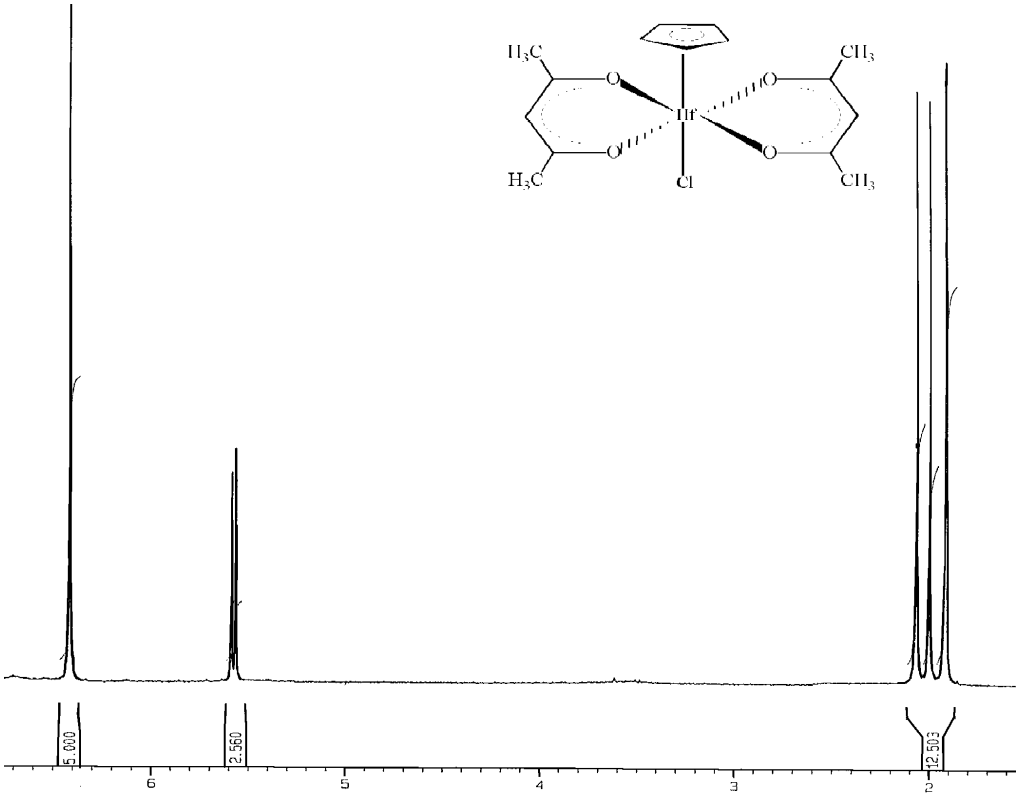

Spectrum 22: Chloro(η^5-cyclopentadienyl)bis(1-ferrocenoyl-1,3-butanedionato-κ^2O,O')hafnium(IV), [Hf(Cp)(Cl)(fca)$_2$] [58]

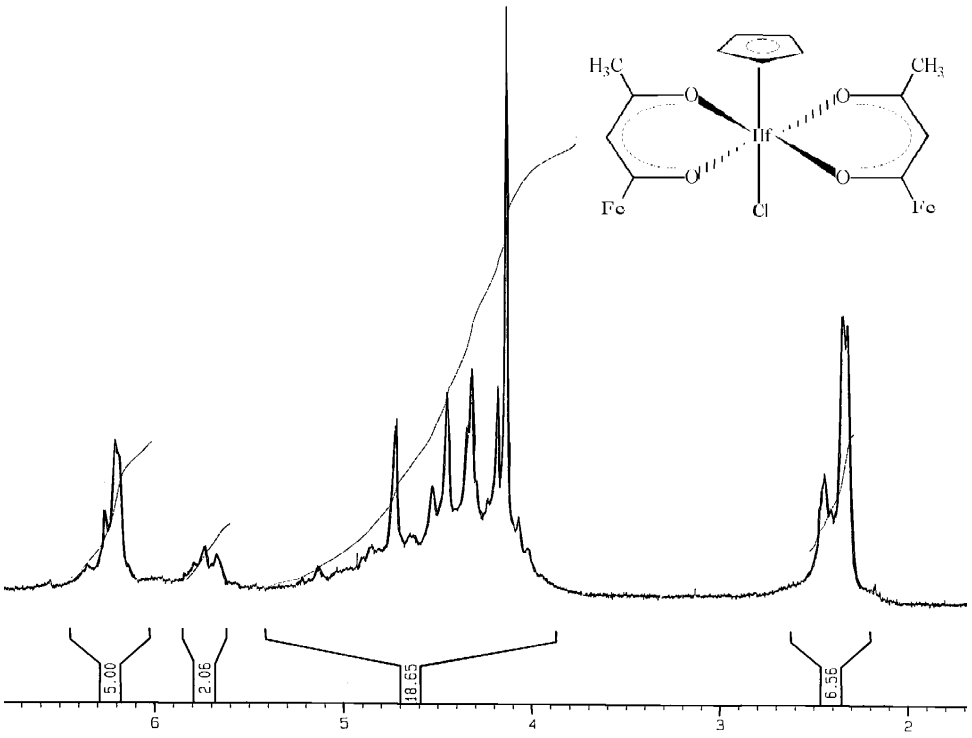

Abstract

Synthetic routes to prepare 13 new and 11 known complexes of the metals Ti, Zr, Hf and V with one bi-chelating ligands have been developed and optimised. A variety bi-chelating titanocenyl(IV) complexes of the form $[Tc(CH_3CXCHCOR)]^+ClO_4^-$ {Tc = $(C_5H_5)_2Ti^{2+}$, X = O, S and R = CH_3, Ph, CF_3, Fc and OCH_3} and [Tc(LL')] {LL' = 1,2-benzenediolato, 1,2-benzenedithiolato and 2,2-biphenyldiolato} were synthesised. Similar metallocene complexes, namely $[Vc(CH_3COCHCOFc)]^+ClO_4^-$ and $[Mc(CH_3COCHCOOCH_3)]^+ClO_4^-$ with Mc = $(C_5H_5)_2V^{2+}$, $(C_5H_5)_2Zr^{2+}$ and $(C_5H_5)_2Hf^{2+}$ were also successfully prepared. A series of 7 new and 4 known bis-β-diketonato metal complexes of the form $[M(Cp)(Cl)(CH_3COCHCOR)_2]$, where M = Ti, Zr, Hf and V and R = CH_3, Ph, CF_3 and Fc were also prepared.

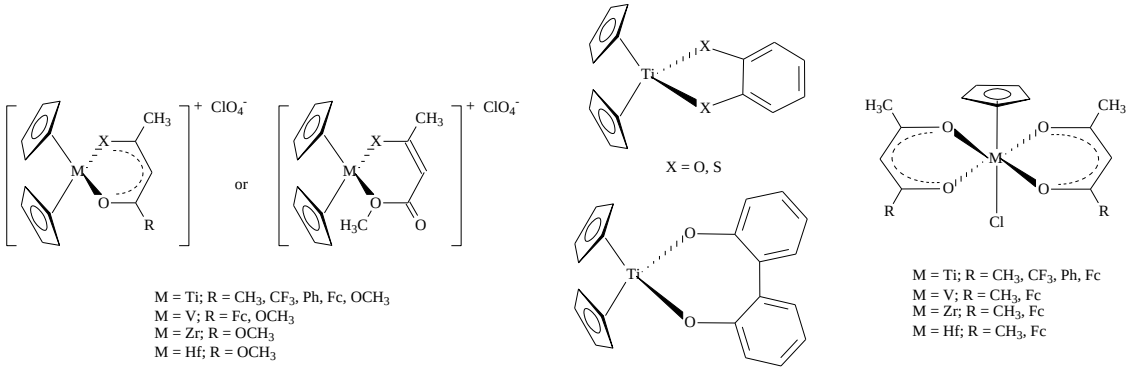

Electrochemical studies in CH_3CN on the mono-β-diketonato titanocenyl(IV) complexes all revealed chemical and electrochemical reversible Ti^{4+}/Ti^{3+} couples, with the Fc/Fc^+ couple of the $[Tc(CH_3COCHCOFc)]^+ClO_4^-$ complex electrochemically quasi-reversible. The formal reduction potential of the Ti^{4+}/Ti^{3+} couple increased with an increase in group electronegativity of the R group of the β-diketonato ligand. Electrochemical studies in CH_3CN on for the metallocene dichlorides of Zr, Hf and V, all showed chemical irreversibility, Ti showed chemical reversibility but electrochemical irreversibile with E_{pc} dependent on the metals' atomic electronegativity. The M^{4+}/M^{3+} couple of the bis-acetylacetonato metal(IV) complexes, $[M(Cp)(Cl)(CH_3COCHCOCH_3)_2]$ with M = Ti, Zr, Hf and V all displayed a chemical irreversible character in contrast to the bis-ferrocenylacetone metal(IV) complexes, $[M(Cp)(Cl)(CH_3COCHCOFc)_2]$ with M = Ti, Zr, Hf and V, showed chemical reversibility, but electrochemical irreversibility for the M^{4+}/M^{3+} couple. The Fc/Fc^+ couples display electrochemical quasi-reversibility except for the V-complex.

Substitution kinetics involving substitution of the bidentate ligand from $[Tc(OC_6H_4O)]$, $[Tc(CH_3COCHCOCH_3)]^+ClO_4^-$, $[Tc(CH_3CSCHCOCH_3)]^+ClO_4^-$ and $[Tc(OC_6H_4C_6H_4O)]$ with either acetylacetone, thioacetylacetone and 2,2-biphenyldiol showed the following stability series:

{most stable} $[Tc(OC_6H_4C_6H_4O)]$ (7 membered ring) > $[Tc(CH_3CSCHCOCH_3)]^+$ (6 membered ring) > $[Tc(CH_3COCHCOCH_3)]^+$ (6 membered ring) > $[Tc(OC_6H_4O)]$ (5 membered ring) {least stable}

Large negative activation entropy ΔS^* found for all substitution reactions, indicated towards an associative mechanism of substitution.

Cytotoxic studies revealed that complexes containing more than one antineoplastic moiety, $[Tc(CH_3COCHCOFc)]^+ClO_4^-$, and $[Ti(Cp)(Cl)(CH_3COCHCOFc)_2]$, showed better cytotoxicity than $TcCl_2$ (currently in clinical trial phase II) for the CoLo and HeLa cell lines, probably due to a synergistic effect of the ferrocenyl ligand and the titanocenyl moiety.

***Keywords*:** Metallocenes, β-diketones, cyclic voltammetry, substitution kinetics and cytotoxicity.

Opsomming

Sintetiese metodes om 13 nuwe en 11 bekende komplekse van die metale Ti, Zr, Hf en V met een bi-cheleerende ligande te sintetiseer is ontwikkel en geoptimiseer. ‘n Verskeidenheid bi-cheleerende titanoseniel (IV) komplekse met die vorm $[Tc(CH_3COCHCXR)]^+ClO_4^-$ {Tc = $(C_5H_5)_2Ti^{2+}$, X = O, S en R = CH_3, Ph, CF_3, Fc en OCH_3} en [Tc(LL’)] {LL’ = 1,2-benzeendiolato, 1,2-benzeenditiolato en 2,2-bifenieldiolato} is gesintetiseer. Soortgelyke komplekse, naamlik $[Vc(CH_3COCHCOFc)]^+ClO_4^-$ en $[Mc(CH_3COCHCOOCH_3)]^+ClO_4^-$ met Mc = $(C_5H_5)_2V^{2+}$, $(C_5H_5)_2Zr^{2+}$ en $(C_5H_5)_2Hf^{2+}$ is ook suksesvol gesintetiseer. ‘n Reeks van 7 nuwe en 4 bekende bis-β-diketonato metaal komplekse met die vorm $[M(Cp)(Cl)(CH_3COCHCOR)_2]$, waar M = Ti, Zr, Hf en V asook R = CH_3, Ph, CF_3 en Fc, is ook gesintetiseer.

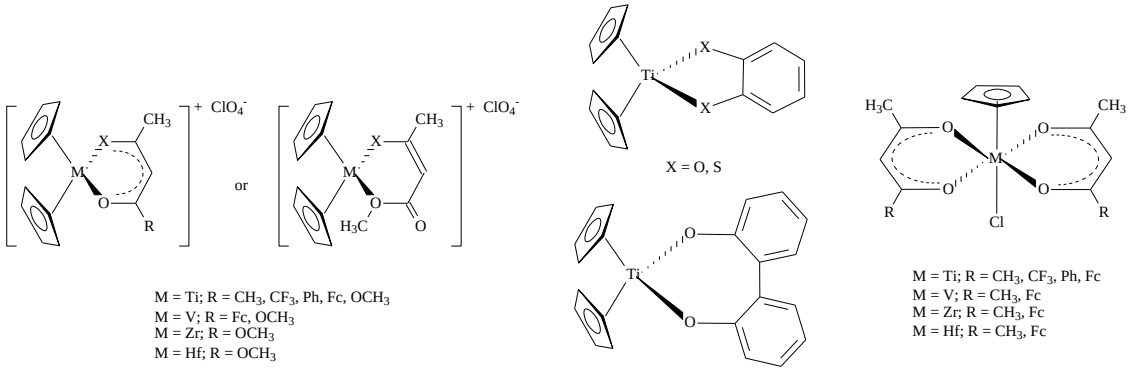

M = Ti; R = CH_3, CF_3, Ph, Fc, OCH_3
M = V; R = Fc, OCH_3
M = Zr; R = OCH_3
M = Hf; R = OCH_3

M = Ti; R = CH_3, CF_3, Ph, Fc
M = V; R = CH_3, Fc
M = Zr; R = CH_3, Fc
M = Hf; R = CH_3, Fc

Elektrochemiese studies in CH_3CN op die titanoseniel(IV) mono-β-diketonato komplekse het almal chemies en elektrochemiese omkeerbaarheid getoon vir die Ti^{4+}/Ti^{3+} koppels, met die Fc/Fc^+ koppel van die $[Tc(CH_3COCHCOFc)]^+ClO_4^-$ kompleks elektrochemiese quasi-omkeerbaar. Die formele reduksie potensiaal van die Ti^{4+}/Ti^{3+} koppels neem toe soos daar ‘n toename is in die groep elektronegatiwiteit van die R groep van die β-diketonato ligand. Elektrochemiese data vir die metalloseen dichloriede van Zr, Hf en V het almal chemiese onomkeerbaarheid getoon, Ti is chemies omkeerbaar en elektrochemies onomkeerbaar, met die E_{pc} waardes wat deur die metaal se atomiese elektronegatiwiteit beïnvloed word. Die M^{4+}/M^{3+} koppel van die bis-asetielasetonato metaal(IV) kompleks, $[M(Cp)(Cl)(CH_3COCHCOCH_3)_2]$ waar M = Ti, Zr, Hf en V het chemiese onomkeerbare gedrag getoon, in kontras met die bis-ferrosenielasetonato metaal(IV) komplekse, $[M(Cp)(Cl)(CH_3COCHCOFc)_2]$ waar M = Ti, Zr, Hf en V, wat chemiese omkeerbaarheid en elektrochemies onomkeerbaarheid getoon het vir die M^{4+}/M^{3+} koppel. Die Fc/Fc^+ koppels het elektrochemiese quasi-omkeerbaarheid getoon behalwe vir die V-kompleks.

Substitusie kinetika behels die substitusie van die bi-cheleerende ligande vanaf $[Tc(OC_6H_4O)]$, $[Tc(CH_3COCHCOCH_3)]^+ClO_4^-$, $[Tc(CH_3CSCHCOCH_3)]^+ClO_4^-$ of $[Tc(OC_6H_4C_6H_4O)]$ met asetielasetoon, tioasetielasetoon of 2,2-bifenieldiol het die volgende stabiliteits reeks gelewer:

{mees stabiel} $[Tc(OC_6H_4C_6H_4O)]$ (7 lid ring) > $[Tc(CH_3CSCHCOCH_3)]^+$ (6 lid ring) > $[Tc(CH_3COCHCOCH_3)]^+$ (6 lid ring) > $[Tc(OC_6H_4O)]$ (5 lid ring) {minste stabiel}

Die groot negatiewe entropie van aktiveering ΔS^* vir al die substitusie reaksies, het ‘n assiosatiewe meganisme van substitusie aandui.

Sitotoksiese studies het gewys dat komplekse wat meer as een antineoplastiese eenheid besit, $[Tc(CH_3COCHCOFc)]^+ClO_4^-$ en $[Ti(Cp)(Cl)(CH_3COCHCOFc)_2]$, het beter sitotoksisiteit getoon as $TcCl_2$ (wat tans in kliniese toets fase II is) teen die CoLo en HeLa sel lyne, waarskynlik as gevolg van die sinergistiese effek van die ferroseniel ligand en die titanoseniel eenheid.